UNIVERSITY OF SOUTHAMPTON

FACULTY OF ENGINEERING, SCIENCE AND MATHEMATICS
School of Ocean and Earth Science

The Effect of Phytoplankton Growth on Nitrogen Cycling in a non-Turbid Estuary, Southampton Water, UK

By

Sinhué Torres Valdés

Thesis for the Degree of Doctor of Phylosophy

October 2004

Graduate School of the Southampton Oceanography Centre

This PhD Dissertation by

Sinhué Torres Valdés

has been produced under the supervision of the following persons

Supervisor

Dr. Duncan A. Purdie

Chair of Advisory Panel

Prof. Patrick M. Holligan

Member of Advisory Panel

Dr. Richard Sanders

UNIVERSITY OF SOUTHAMPTON

ABSTRACT

FACULTY OF ENGEENERING, SCIENCE AND MATHEMATICS
SCHOOL OF OCEAN AND EARTH SCIENCE

Doctor of Philosophy

THE EFFECT OF PHYTOPLANKTON GROWTH ON NITROGEN CYCLING IN A NON-TURBID ESTUARY, SOUTHAMPTON WATER, UK

by Sinhué Torres-Valdés

Stable isotope tracer incubation techniques were used to estimate the uptake of nitrogen by phytoplankton growth in the Southampton Water estuarine system over the productive spring–summer period in 2001 and 2002. Nutrient uptake experiments were carried out at approximately 2 week intervals with water samples collected from three stations in the estuary, representative of coastal waters of the Solent, the mid-estuary and brackish waters of the system. In 2001, separate subsamples were incubated with ^{13}C-HCO_3 and ^{15}N-NO_3^-, ^{15}N-NH_4^+, and ^{15}N-urea, and were deployed *in situ* at 4 photic depths plus a dark incubation. In 2002, separated subsamples were incubated with ^{15}N-NO_3^- and ^{15}N-NH_4^+, and were deployed at 2 photic depths. In addition, in 2002 the release of DON and the regeneration of NH_4^+ were also quantified. Vertical profiles of temperature, salinity and irradiance were made at each station, and water samples from 5 depths were collected for later analysis of nutrients (nitrate, ammonium, urea, and silicate) and chlorophyll *a*. Chlorophyll *a* concentrations of up to 64 μg L^{-1} were measured, and generally increased from the coastal waters towards the upper estuary. Nutrient concentration were also higher in the inner estuary and appear to be affected by the seasonal cycle of phytoplankton growth, showing lower concentrations during the summer months. Uptake rates of nitrogen within the Southampton Water estuary were comparable with values reported in the literature for other similar estuaries and coastal systems, and showed that during extensive phytoplankton blooms within these systems comparatively elevated uptake rates can be reached. In general, the temporal variation in the uptake of N-nutrients was consistent with the seasonal variations in the Chl-*a* levels, showing higher rates between April/May to August during the two years investigated. Uptake rates during both years were higher in the inner estuary relative to the coastal waters of the system. Results showed that ammonium was the dominant source of nitrogen, contributing on average >60% to the total nitrogen uptake. Nitrate and urea however, showed dominant contributions on some occasions. The ^{15}N-tracer experiments carried out during this investigation demonstrated that phytoplankton activity can remove nitrate, ammonium and urea from the euphotic water column at rates of up to ~9, 28 and 51% h^{-1} of the ambient levels, and can potentially increase by threefold during periods of high water slack. ^{15}N-incubation experiments showed that an average of 74±32% of the nitrate taken up by phytoplankton was released as DON, and that ammonium uptake rates without correction for isotope dilution represented an average of 31±9% of those corrected. Results thus demonstrated that the impact of phytoplankton growth on the nitrogen levels can be underestimated if the gross uptake of nitrate and ammonium are not taken into account. With a water residence time estimated to be between 5 and 10 days for this estuary, the estimated turn over times of nitrate of more than 50 days imply that most of the nitrate is either exported from the estuary or removed by denitrification, whereas reduced forms of nitrogen are likely recycled within the system. The factors which are likely to control the uptake of nitrogen, as well as differences found between the two years studied are also discussed.

To the best person I have ever met,

even though I did not notice it during

the first few years.....

.....My Mother, Imelda Torres.

DECLARATION OF AUTHORSHIP

I, **Sinhué Torres-Valdés**, declare that the thesis entitled **"The Effect of Phytoplankton Growth on Nitrogen Cycling in a non-Turbid Estuary, Southampton Water, UK"** and the work presented in it are my own. I confirm that:

- this work was done wholly or mainly while in candidature for a research degree at this University;
- where any part of this thesis has previously been submitted for a degree or any other qualification at this University or any other institution, this has been clearly stated;
- where I have consulted the published work of others, this is always clearly attributed;
- where I have quoted from the work of others, the source is always given. With the exception of such quotations, this thesis is entirely my own work;
- I have acknowledged all main sources of help;
- where the thesis is based on work done by myself jointly with others, I have made clear what was done by others and what I have contributed myself;
- none of this work has has been published before submission.

Signed: [redacted] Sinhué Torres-Valdés

Date: OCTOBER 2004

Acknowledgements

- First and above all, to who ever understood when I deserted or disappointed them.
- I am very grateful to the National Council of Science and Technology (CONACYT), Mexico, for awarding me with a scholarship to pursue a PhD degree (Reg. 117672).
- I have never experienced so much patience towards my ignorance and never such a great support at all times. I am most grateful to my supervisor Dr. Duncan Purdie for his guidance and encouragement throughtout my PhD.
- I want to express my most sincere gratitude to Prof. Patrick Holligan and to Dr. Richard Sanders for their support, concern and advise during my advisory panel meetings.
- I am very grateful to Prof. Alan Kemp and Prof. Andrew Roberts for their support.
- Many thanks for their help and support to my dear friends and colleagues at the Microbiology Lab; Dr. Silvia N. Nascimento, Dr. Elham Ali (Eli), Dr. Arantza Iriarte, Dr. David Crawford, Angela Landolfi and..... A very special thanks to my great friend Judith Homewood for her interest in my work, support and help throughout the PhD.
- I am very grateful to Dr. Keith Weston (University of East Anglia) for his help and encouragement during my work with ^{15}N.
- I am also very grateful to Mike Bolshaw for his superb help when working at the IRMS lab of the SOES/SOC. Many thanks also to Prof. Eelco J. Rholing, Dr. Paul Wilson and Stuart Painter for their support and help while working at the IRMS lab.
- I am grateful to all the people who have helped me at some point through the PhD: Dr. Joanna Waniek, Dr. Peter J. Statham, Mr. Stephen Hayward, Diane Buckley, Dave Buck, Mike Doswell, Matt O'Shaughnessy and Graeme Leggatt, Ibrahim Al-Tesan, Sue Hartman, Dr. David Hydes, Paul Gooddy, the *Bill Conway* crew and Gillian Taylor (University of Newcastle).
- Life is never enjoyable without the presence of a good friend; great people who made you feel as special as they are. Thousand thanks to Agostino Merico, Susanne Ufermann, Hans Fangohr, James Harle, BanAnita-H (aka Ana Hilario), David Lambkin, Cesar Riveiro, Ulrike Riemenschneider, Laura Font, Steffen Dransfeld, Silvia Lucato, Marisa Motta, Luciano Pezzi, Babette Hoogakker, Alex Poulton, Mr. Oliver Nicolas Ross, Juan Larrasoaña, Paolo Cipollini, Maria Aboim, Manu Bassoi, Marie Le Goff, Adriana Huerta, Ben Rabe, Francisco Solis, Francisco Benitez and Julia Dias, Ivo Grigorov, Taro Hosoe and Ale Salvin, Philip Sexton, Iain Pitcairn, Ana Paula Teles, Herve Fache, Luciane Veek, Nico Caltabiano, Alice Stuart-Menteth, Erik Muxagata, Zoë Bond, Xana Aranda, Andrey Akhmetzhanov, Sarah Glynn and Naoise O'Reilly.
- I am hypermegasupergrateful to my Mother Imelda, to sister Selene and to my family in México, for their continuous support and encouragement.
- I am indebted and more than grateful to Sarah Comelli for her interest in my work, for her patience, her support, for cheering me up during difficult moments and for her beautiful smile.
- Muchas gracias perronas to my always supporting and dream-sharing friends from Perrones Inc., Pedro Medina Rosas and Jorge Fonseca Madrigal.
- Many thanks also to my excellent friends Alejandro Balbuena Hernandez, Carmina Torres[2], Carlos Peynador and to Camila.
- To the superb SOC FC.
- Finally, to Jah musical men, for dem riddim kept I in good spirits.

¡Carnaval toda la vida!

Contents

Appendices

List of Figures

List of Tables

Glossary of terms

Symbol	Definition
Chl-a	Chlorophyll a
NO_3^-	Nitrate
NH_4^+	Ammonium
$CO(NH_2)_2$	Urea
N_2	Molecular nitrogen
DIN	Dissolved inorganic nitrogen
DON	Dissolved organic nitrogen
PON	Particulate organic nitrogen
POC	Particulate organic carbon
PP	Primary production
E_0	Incident irradiance
PAR	Photosynthetically active radiation
k	Irradiance attenuation coefficient
ΔChl-a	Increase in Chl-a concentration over the incubation period (4 h)
$\rho\ NO_3^-$	Nitrate net uptake rate
$\rho_G\ NO_3^-$	Nitrate gross uptake rate
DON_{REL}	Dissolved organic nitrogen release rate
$\rho\ NH_4^+$	Ammonium net uptake rate
$P\ NH_4^+$	Ammonium uptake rate corrected for isotope dilution
$\rho_G\ NH_4^+$	Ammonium gross uptake rate
NH_{4REG}^+	Ammonium regeneration rate

Chapter 1

Introduction

1.1 General overview

The flux of riverine derived nutrients through estuaries is known to be greatly modified by organic cycling and retention processes (Seitzinger & Sanders, 1997; Herman & Heip, 1999; Josefson & Rasmussen, 2000; Middelburg & Nieuwenhuize, 2000a,b; Mortazavi *et al.*, 2000b,a). The amount of these materials that would otherwise reach the adjacent sea is thus reduced in some proportion. In non-turbid estuaries, the occurrence of extensive phytoplankton blooms can be a large sink for inorganic nutrients during productive periods (*e.g.* Humborg, 1997). The effect of this removal however, has rarely been investigated from direct measurements of nutrient uptake by estuarine phytoplankton.

The quality and quantity of nutrient inputs to marine systems have been greatly altered during recent decades (Nixon, 1995; Rendell *et al.*, 1997; Jickells, 1998; Herbert, 1999), and disturbances such as shifts in planktonic, pelagic and benthic species dominance have been observed as a consequence (Conley *et al.*, 1991; Rendell *et al.*, 1997; Jickells, 1998; Shalovenkov, 2000). The nitrogen cycle among other nutrients (*e.g.* C, P, and Si) is the most perturbed. Human activities such as energy production, fertiliser production and cultivation of crops fix $\approx$140 Tg N yr^{-1}, while estimated preindustrial biological fixation in the continents amounts to 90-130 Tg N yr^{-1} (Galloway *et al.*, 1995). About 41 Tg N yr^{-1} of the nitrogen fixed by human activities is transported to the coastal ocean by rivers (Galloway *et al.*, 1995). In addition, sewage effluent and wastewater inputs can represent up to 34% of the total nitrogen input in some regions (Howarth *et al.*, 1996). Nonetheless, about a half of this nitrogen input is consumed within estuaries (Nixon *et al.*, 1996).

In the Southampton Water estuarine system nitrate is known to show conservative dilution like behaviour even during more productive periods of the year, although complete removal by phytoplankton has been observed at high salinities (Hydes & Wright, 1999).

The effect of phytoplankton growth on nutrient concentration produces an annual cycle, with lower concentrations in summer (Kifle & Purdie, 1993; Hydes & Wright, 1999). Southampton Water presents a bimodal phytoplankton biomass cycle (Cebrián & Valiela, 1999), with highest chlorophyll peaks occurring usually between the months of March-May, and June-September (*e.g.* Leakey *et al.*, 1992; Kifle & Purdie, 1993; Iriarte & Purdie, 1994; Howard *et al.*, 1995). During this period, chlorophyll concentrations >15 μg L^{-1} and up to 70 μg L^{-1} have been measured in the coastal waters and the mid estuary respectively (*e.g.* Leakey *et al.*, 1992; Kifle & Purdie, 1993; Iriarte & Purdie, 1994; Howard *et al.*, 1995). The above information suggests that the potential of nitrogen removal by phytoplankton may be significant in this system, however, direct measurements of nitrogen uptake have not been carried out in Southampton Water. Thus, in the present study ^{15}N labelled tracer techniques were used to estimate the effect of phytoplankton growth on nitrogen fluxes through this estuary over the productive spring–summer periods in 2001 and 2002.

In the following sections, brief reviews concerning the nitrogen cycle and its study through the use of ^{15}N tracer techniques are presented. The first review includes a description of *i)* the biological reactivity of nitrogen, *ii)* the global nitrogen cycle, *iii)* the human impact on the nitrogen cycle and *iv)* the general effects of excess nitrogen in coastal systems. The reviews are followed first, by a brief historical description of the ^{15}N-tracer technique, improvements made to it and research achievements by the application of this method. Recent findings regarding the uptake of nitrogen by phytoplankton in estuaries and other marine systems are presented, and a brief description of the Southampton Water estuary and the research objectives of this study are given.

1.2 The nitrogen biogeochemical cycle

1.2.1 Biogeochemical cycles

Life on Earth is fuelled by solar energy and is based on the metabolism of key elements (*e.g.* C, N, P, H, O, S) that combined constitute the structure of living tissue and biofunctional molecules such as ATP, proteins or nucleic acids. These key elements are present in major reservoirs of the planet (*i.e.* the atmosphere, lithosphere and hydrosphere) in the form of inorganic compounds that are continuously transformed and transported from one reservoir to another by a number of natural processes (*e.g.* weathering, runoff, precipitation). Only photosynthetic organisms are capable of using solar energy and inorganic compounds to build organic matter (*i.e.* primary production) and therefore they are the base of the trophic chain. In this way, the fixed/assimilated compounds are transferred to higher trophic levels through heterotrophy. Once in the biosphere, the elements es-

sential for life are also transported between reservoirs in the form of organic or inorganic (*i.e.* through remineralization of organic matter) compounds. The continuous transport of these elements and their systematic transformations mediated by physical, chemical and biological processes are thus known as the biogeochemical cycle.

1.2.2 Biological reactivity of nitrogen

Due to its chemical diversity, nitrogen is involved in major processes governing the Earth as a system. Having an electronic configuration $1s^2\ 2s^2\ p^3$ (Fluck & Heumann, 2002), it has 5 electrons (e^-) on its external shell that are available to exchange[1]. Because of this, nitrogen is present at the oxidation states shown in **Fig. 1.1**. This figure is a simplified version of the nitrogen cycle, where the frame represents any system or reservoir with operating sources (inputs) and sinks (outputs). Within it, the nitrogen undergoes transformations mediated by biological, physical and chemical factors. However, key transformations of the nitrogen cycle are mediated mainly by microbiological processes. As can be appreciated from Fig. 1.1, the nitrogen biogeochemical cycle is composed of the following series of reactions.

Nitrogen fixation,

$$N_2 + 8H^+ + e^- \rightarrow 2NH_4^+ \rightarrow Organic\ Nitrogen \tag{1.1}$$

Ammonium assimilation and regeneration,

$$NH_4^+ \Leftrightarrow Organic\ Nitrogen \tag{1.2}$$

Dissolved organic nitrogen uptake and release,

$$DON \Leftrightarrow PON \tag{1.3}$$

Assimilatory nitrate reduction,

$$NO_3^- + 2H^+ + e^- \rightarrow NO_2^- + H_2O \tag{1.4}$$

$$NO_2^- + 8H^+ + e^- \rightarrow NH_4^+ + H_2O \tag{1.5}$$

Nitrification,

$$2NH_4^+ + 3O_2 \rightarrow 2NO_2^- + 4H^+ + 2H_2O \tag{1.6}$$

$$2NO_2^- + O_2 \rightarrow 2NO_3^- \tag{1.7}$$

[1]Source of information; http://www.webelements.com and http://www.shef.ac.uk/chemistry /orbitron/index.html (December 2003, Mark Winter, The University of Sheffield and WebElements Ltd, UK), and http://environmentalchemistry.com/yogi/periodic/index.html (December 2003).

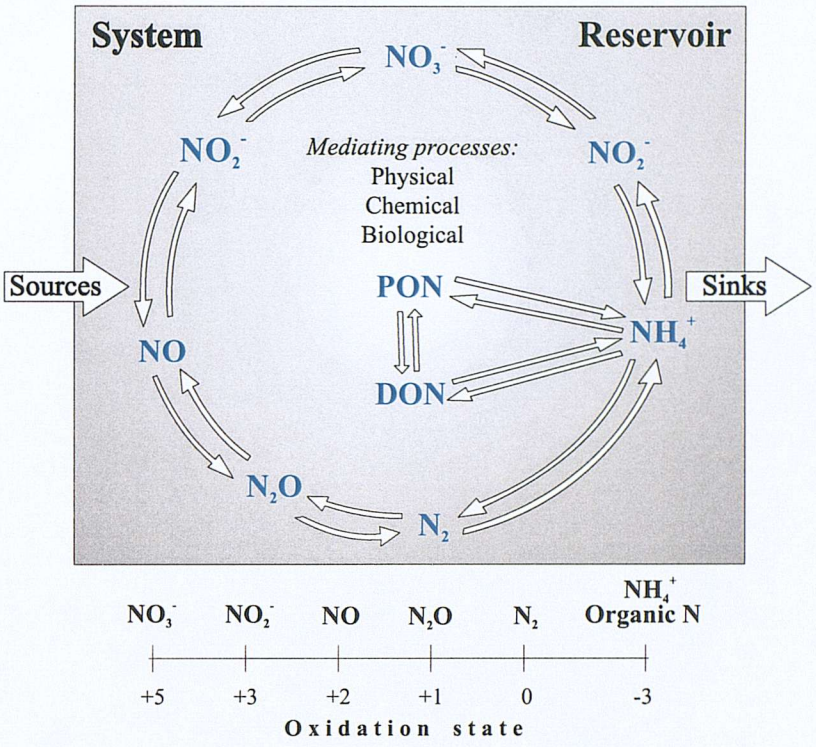

Figure 1.1: **Schematic representation of the nitrogen biogeochemical cycle.** The oxidation state of different nitrogen species is shown (organic N stands for both, particulate and dissolved organic nitrogen, PON and DON respectively). Based on http://www.sws.uiuc.edu/nitro/biogeo.asp (2003), and adapted from Libes (1992), Jaffe (1992), Herbert (1999), Karl & Michaels (2001) and http://www.sws.uiuc.edu/nitro/biogeo.asp (2003).

and denitrification (dissimilatory nitrate reduction),

$$5CH_2O + 4NO_3^- + 4H^+ \rightarrow 5CO_2 + 2N_2 + 7H_2O \tag{1.8}$$

where CH_2O is a generic representation of organic matter. Nitrous oxide (N_2O) and nitric oxide (NO), which are important compounds of the nitrogen biogeochemical cycle too (see subsection 1.2.4), are intermediate products of the nitrification and denitrification reactions. However, these compounds are also indirectly produced by humans during the combustion of fossil fuels and burning of biomass (*e.g.* Galloway *et al.*, 1995; Vitousek *et al.*, 1997a).

The reactions above determine the path nitrogen follows within the atmosphere, land and ocean, as well as the interaction between these environments (*i.e.* inputs and outputs). The microbiological transformations of nitrogen are linked together and are also linked with other essential elements such as silica or phosphorus. In this way, alterations to these reactions can potentially disturb not only the cycling of nitrogen, but also the cycling of other nutrients (*e.g.* Galloway & Cowling, 2002).

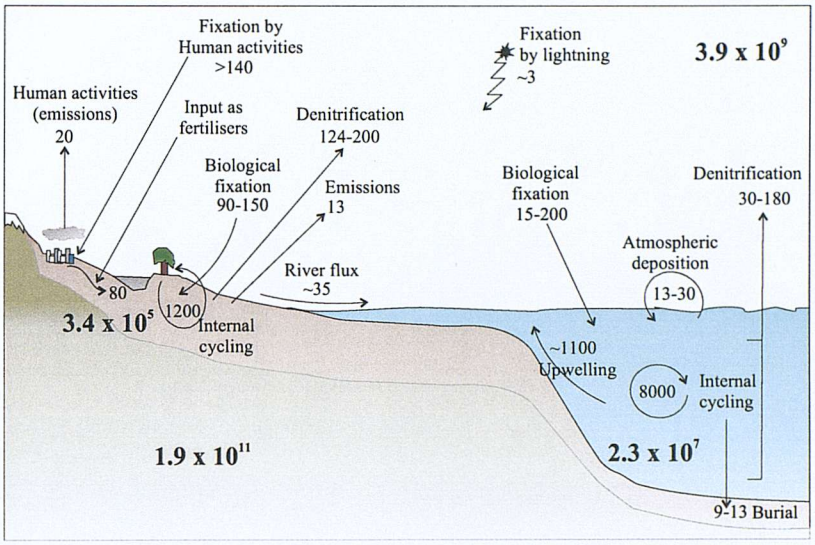

Figure 1.2: **Conceptual model of the global nitrogen cycle.** Large size numbers represent the terrestrial, crustal, atmospheric and oceanic nitrogen reservoirs in Tg N. Small size numbers and arrows represent nitrogen fluxes in Tg N yr^{-1} (1 Tg = 10^{12} g = 10^6 metric tons). Based on Schlesinger (1997), and adapted from Meybeck (1982), Libes (1992), Jaffe (1992), Galloway *et al.* (1995), Schlesinger (1997), Vitousek *et al.* (1997b), Galloway *et al.* (2002) and Galloway & Cowling (2002).

1.2.3 The global nitrogen cycle

Nitrogen plays an important role in the functioning, diversity and dynamics of terrestrial, freshwater and marine systems because its availability regulates the levels of productivity within them (Vitousek, 1994; Vitousek *et al.*, 1997a; Zehr & Ward, 2002). Since nitrogen is required for primary production, its cycle is strongly linked to the biogeochemical cycles of carbon, phosphorus and silica (*e.g.* Conley *et al.*, 1991; Falkowski *et al.*, 2000; Zehr & Ward, 2002).

Primary production (**PP**) in the ocean is $\sim 50 \times 10^3$ Tg C yr^{-1} (50 Gt C yr^{-1}) and $\sim 60 \times 10^3$ Tg C yr^{-1} (60 Gt C yr^{-1}) on land (Raven, 2001; Tyrrell, 2001). Assuming the Redfield ratio of C_{106}:N_{16} for the oceanic PP, and a C:N ratio of 50 for the net PP on land (Schlesinger, 1997), a supply of about 7500 and 1200 Tg N yr^{-1} are respectively required to support PP in both environments.

A conceptual model of the global nitrogen cycle including major reservoirs and fluxes of nitrogen in the Earth system is presented in **Fig. 1.2** (values reported are ranges taken from the reviews cited in the caption of the figure). 78% of the atmosphere is composed of nitrogen in its molecular form (Jaffe, 1992; Galloway *et al.*, 1995; Schlesinger, 1997), which also accounts for more than 95% of the nitrogen species dissolved in the ocean (Jaffe, 1992; Karl & Michaels, 2001). In spite of its abundance, $\mathbf{N_2}$ is not readily available for most organisms (Galloway *et al.*, 1995). Only diazotrophic cyanobacteria in the oceans

(Capone *et al.*, 1997; Mulholland & Capone, 2000; Zehr *et al.*, 1998, 2000, 2001) and a few terrestrial plants with symbiotic N-fixing microbiota (Schlesinger, 1997; Vitousek *et al.*, 1997a) are able to break the strong triple bond of N_2 (N≡N). Upon fixation however, the nitrogen is made available to other organisms in the form of particulate, dissolved organic and/or dissolved inorganic nitrogen. Globally, about 15-200 Tg N yr^{-1} and 90-150 Tg N yr^{-1} are fixed through diazotrophic activity in the ocean and on land respectively (*e.g.* Jaffe, 1992; Galloway *et al.*, 1995; Schlesinger, 1997). Lightning, the only natural N-fixing process apart from biological fixation, contributes <3 Tg N yr^{-1} as deposited N oxides, NO_x (Galloway *et al.*, 1995; Schlesinger, 1997). In this way, nitrogen fixation supplies <3% and ~12% of the nitrogen requirements for primary producers in the oceanic and terrestrial ecosystems respectively. Nonetheless, N-fixation is considered as the first point of the nitrogen biogeochemical cycle since it is the only natural means by which molecular nitrogen is transformed into biologically reactive species.

It is estimated that most of the nitrogen required by primary producers on land is obtained from recycling *in situ* and remineralization of organic matter in the soil (Schlesinger, 1997). In the open ocean, atmospheric deposition of the NH_3 volatised from the sea contributes <0.5% (see Fig. 1.2), whereas in the surface ocean where nutrients are usually scarce, upwelling and mainly recycling in the water column are major supplies of nitrogen to support primary production (see Fig. 1.2). In the coastal ocean, river inputs are a significant source, supplying ~35 Tg N yr^{-1} (Meybeck, 1982). Riverine input is particularly important because it supports primary producers in coastal systems such as estuaries, where increases in the nitrogen loading may significantly enhance phytoplankton activity.

As can be appreciated from Fig. 1.2, most of the nitrogen fixed each year in both realms (*i.e.* land and ocean) is returned back to the atmosphere through denitrification. In fact, estimations of preindustrial nitrogen fiuxes suggest that the nitrogen fixation and denitrification processes were in approximate balance in both environments (Galloway *et al.*, 1995). Only a proportion of the nitrogen fixed in the ocean was emitted to the atmosphere (and deposited back) and another proportion buried (see Fig. 1.2), while on land about 4.8 Tg N yr^{-1} and 8.1 Tg N yr^{-1} were emitted to the atmosphere as NO and NH_X respectively (Galloway *et al.*, 1995).

1.2.4 Human impact on the nitrogen cycle

Fixation and mobilisation of nitrogen by human activities have considerably altered the nitrogen biogeochemical cycle (*e.g.* Vitousek, 1994; Vitousek *et al.*, 1997a,b; Howarth, 1998; Herbert, 1999; Smith *et al.*, 1999; Falkowski *et al.*, 2000), and as a consequence it is the most perturbed among other nutrient cycles (*e.g.* C, P, and Si). Human activities such as production of fertilisers, food (mainly cultivation of crops) and energy, fix nitrogen

at a similar rate to that of biological fixation in the continents (Galloway *et al.*, 1995, 2002; Galloway & Cowling, 2002). Approximately 80 Tg of nitrogen are fixed anually through the Haber process (see Eqs., 1.9 to 1.11) mainly for the manufacture of fertilisers (Jaffe, 1992; Galloway *et al.*, 1995; Schlesinger, 1997; Vitousek *et al.*, 1997a), although a proportion of the nitrogen fixed is also used for the production of nitric acid and explosives (Jaffe, 1992). Moreover, since the Haber process is achieved at a pressure and temperature of 250 atm and 400°C respectively, there is great interest in the potential use of the nitrogenase enzyme, which dyazotrophic organisms use to fix nitrogen at 0.8 atm and 20°C (Jaffe, 1992). The fixation of N_2 for fertiliser production has increased from <10 to ~80 Tg N yr^{-1} beteween 1950 and 1990, and it is estimated to increase to >135 by the year of 2030 (Vitousek *et al.*, 1997b).

$$3CH_4 + 6H_2O \rightarrow 3CO_2 + 12H_2 \tag{1.9}$$

$$+ \qquad 4N_2 + 12H_2 \rightarrow 8NH_3 \tag{1.10}$$

$$= 3CH_4 + 6H_2O + 4N_2 \rightarrow 3CO_2 + 8NH_3 \tag{1.11}$$

Cultivation of crops (mainly legumes and forages) enhances the rate of biological fixation due to their symbiotic relationship with dyazotrophic microorganisms. Approximately 40 Tg N yr^{-1} are fixed through cultivation of crops (Vitousek *et al.*, 1997a,b), with a range of 32 to 53 Tg N yr^{-1} as estimated for the year of 1990 (Galloway *et al.*, 1995). Production of energy by combustion of fossil fuels transfers nitrogen from long-term geological reservoirs to the atmosphere (Vitousek *et al.*, 1997a), and unreactive N_2 is oxidised to reactive NO. More than 20 Tg N yr^{-1} are emited to the atmosphere in this way (Galloway *et al.*, 1995; Vitousek *et al.*, 1997b). In addition, biomass burning, land clearing and conversion, and drainage of wetlands with the eventual oxidation of their organic soils also mobilise nitrogen from long-term storage pools (Vitousek, 1994), mobilising >40, 20, and 10 Tg N yr^{-1} respectively (Vitousek *et al.*, 1997a).

As a result of the nitrogen fixed by human activities, there has also been an increase in the emssion of N to the atmosphere, nitrogen deposition and nitrogen mobilisation between different reservoirs. N_2O emissions are of particular interest due to its stratospheric-ozone-destructive and greenhouse properties (Jaffe, 1992). It is worth noting that the greenhouse effect per molecule of nitrous oxide is about 300x relative to each molecule of CO_2 (Schlesinger, 1997). While natural sources (in oceans and continents) emit about 10 Tg N yr^{-1} as N_2O, known anthropogenic sources deliver 15.7 Tg N yr^{-1} (Schlesinger, 1997). NO (or rather NO_x) emissions are of concern because these play an

important role in the chemistry of the atmosphere and participate in the photochemical production of tropospheric ozone (O_3), a pollutant that affects plant productivity and damages human health (Butcher, 1992; Galloway *et al.*, 1995; Vitousek *et al.*, 1997a). The oxidation of NO to HNO_3 in the atmosphere also contributes to the formation of acid rain. In addition to the >20 Tg N yr^{-1} emited to the atmosphere as NO through the combustion of fossil fuels, ~8 Tg N yr^{-1} more are added through biomass burning and another 5-20 Tg N yr^{-1} are emited from fertilised soils (Vitousek *et al.*, 1997a). Emissions of the reactive N-species NH_3 are also cosiderable, with 32 Tg N yr^{-1} derived from animal farming (*i.e.* domestic animal wastes), 10 Tg N yr^{-1} from fertilised fields, 7 Tg N yr^{-1} from biomass burning and coal combustion (5 and 2 Tg N yr^{-1} respectively), 4 Tg N yr^{-1} from human excretions and 0.2 Tg N yr^{-1} from automobiles (Galloway *et al.*, 1995; Schlesinger, 1997; Vitousek *et al.*, 1997a). Of the NO and NH_3 emited anually to the atmosphere, about 70% and 80% respectively are deposited back to terrestrial ecosystems (Galloway *et al.*, 1995) as NO_y and NH_x. The remaining percentage of NO and NH_3 (*i.e.* ~18 Tg N yr^{-1}) is transported to the oceanic atmosphere and deposited at sea (Galloway *et al.*, 1995). Although terrestrial ecosystems (*e.g.* forest, soils) are potential sinks for anthropogenic nitrogen, not all of it is stored in long term reservoirs (Vitousek *et al.*, 1997a; Howarth, 1998), with nitrogen loss to streams, groundwater and atmosphere occurring upon saturation in the soils (Galloway *et al.*, 2002). As a result, eutrophication of soils, streams, freshwater and coastal marine systems has been enhanced (Galloway *et al.*, 1995). The excess nitrogen favors N-limited primary producers, thus increasing competition between species and promoting the loss of biodiversity (Vitousek, 1994; Galloway *et al.*, 1995; Vitousek *et al.*, 1997a). In addition, it may indirectly affect the cycling of other nutrients by changing the relative nutrient ratios; *e.g.* N:P:Si (*e.g.* Conley *et al.*, 1991). Nitrogen delivered to rivers from fertilised fields and atmospheric deposition is an important source of reactive N to the coastal marine environment (Howarth, 1998), suppling about 41 Tg N yr^{-1} of the nitrogen fixed by human activities, and affecting estuaries, nearshore benthic ecosystems and coastal seas (Galloway *et al.*, 1995). In this way, the total input of nitrogen to coastal ocean via river-estuarine systems has been increased from ~35 Tg N yr^{-1} estimated for preindustrial times (see Fig. 1.2) to 76 Tg N yr^{-1}.

1.2.5 Nitrogen cycling in coastal marine systems

The global annual plant production on land is estimated to be of similar magnitude to that in the ocean surface. The biomass responsible for that production in the ocean however, is >100 times smaller than the terrestrial biomass. Approximately 60×10^3 Tg of carbon (10^3 Tg C = 1 Gt C) are fixed annually on land by a biomass of 550×10^3 Tg C, whereas about 50×10^3 Tg C yr^{-1} are fixed by a biomass of 4×10^3 Tg C in the ocean (Tyrrell, 2001). Moreover, ~46×10^3 Tg C yr^{-1} of the total oceanic PP is due to marine phytoplankton

(Raven, 2001); *i.e.* excluding PP by macroalgae and aquatic vascular plants. The contrast in the PP:biomass ratio in both environments is because considerable amounts of carbon are stored in long term reservoirs on land (*e.g.* lignin), whereas in the ocean the nature of the phytoplankton life cycle (from few days to a week) represents a relatively short term carbon storage (Tyrrell, 2001). The latter is of importance for biogeochemical cycles since the short lifespan of phytoplankton implies a comparatively faster recycling of nutrients in the marine environment.

The coastal ocean is particularly dynamic because it receives large quantities of organic and inorganic nutrients from the continents (Jickells, 1998) and exchanges matter and energy with the open ocean (Gattuso *et al.*, 1998). In spite of its small area (8.5%) relative to the global ocean surface, the coastal ocean accounts for 14-30% of the oceanic primary production (Pernetta & Milliman, 1995; Gattuso *et al.*, 1998). In an attempt to assess the value of ecosystems, the coastal ocean has been considered to be one of the most valuables on Earth due to the cycling of nutrients, with an important proportion due to nutrient cycling in estuaries (Costanza *et al.*, 1997). The natural cycling of nutrients however, has been largely altered by humans. Humans have exploited the coastal ocean for fishing (accounting for 90% of the world fish catch), generation of energy, transport, extraction of renewable and nonrenewable resources, waste disposal and for recreation (Holligan & de Boois, 1993; Pernetta & Milliman, 1995; Gattuso *et al.*, 1998; Jickells, 1998). About 37% (2.07 billion) of the global human population (5.62 billion as estimated for 1994) live within 100 km of the coast line (Cohen *et al.*, 1997). In this way, human activities have put the coastal ocean under increasing pressure.

A direct result of human activities during the last few decades, has been the alteration of the quality and quantity of nutrient inputs to coastal marine systems (Nixon, 1995; Rendell *et al.*, 1997; Howarth, 1998; Jickells, 1998). The consequences of these disturbances range from shifts in planktonic, pelagic and benthic species dominance (*e.g.* Conley *et al.*, 1991; Rendell *et al.*, 1997; Jickells, 1998; McClelland & Valiela, 1998a,b; Herbert, 1999; Shalovenkov, 2000) to nearly complete loss of some coastal marine ecosystems (Smith *et al.*, 1999; Cloern, 2001). As pointed out in the previous section (§ 1.2.4), the nitrogen cycle is the most altered of all nutrients as a result of human influence. The rate at which humans fix nitrogen equals that of preindustrial biological fixation on land and of the total nitrogen fixed by human activities, about 41 Tg N yr^{-1} are transported to the coastal ocean by rivers and estuaries, *i.e.* in addition to the preindustrial 35 Tg N yr^{-1} (see fig. Fig. 1.2). Nitrogen derived from fertilisers for example, is the major anthropogenic source of this nutrient in most of the drainage basins discharging water to the North Atlantic ocean (Howarth *et al.*, 1996). In addition, sewage effluents and waste water inputs to estuaries represent up to 34% of the total nitrogen input in some regions (*e.g.* Howarth *et al.*, 1996). The generation of reactive nitrogen by human activities will

continue to increase as population grows and it is estimated that if the present rate of reactive nitrogen production per capita is maintained, the total rate of reactive nitrogen generation will be ~900 Tg N yr^{-1} by the year 2050 (Galloway & Cowling, 2002). This information suggests that the inputs of reactive nitrogen to coastal systems are also likely to increase.

The excess nitrogen inputs to coastal marine systems are of concern because their effect is to promote primary production (Herbert, 1999; Meyer-Reil & Köster, 2000). The effects of enhancing primary production are variable and complex; detailed reviews regarding the cycling of nitrogen and the effects of the excess reactive nitrogen in coastal marine and other ecosystems can be found in Galloway *et al.* (1995), Richardson & Jorgensen (1996), Vitousek *et al.* (1997a,b), Smith *et al.* (1999), Herbert (1999), Anderson (2001), Cloern (2001), Galloway *et al.* (2002), and Galloway & Cowling (2002). Overall, the stimulation of phytoplankton growth can result in a decline of benthic photosynthesis due to the increased turbidity produced by the accumulation of phytoplankton cells in the water column (Richardson & Jorgensen, 1996; Herbert, 1999; Smith *et al.*, 1999; Meyer-Reil & Köster, 2000; Cloern, 2001). In addition, decomposition of benthic primary producers or sedimented cells after a bloom event generates large O_2 demands (*e.g.* Grenz *et al.*, 2000). This in turn can lead to hypoxic or anoxic conditions (Richardson & Jorgensen, 1996; Jickells, 1998; Meyer-Reil & Köster, 2000; Cloern, 2001) with concomitant death of pelagic organisms (Herbert, 1999). The increase in the occurrence of toxic phytoplankton species or excessive growth of macroalgae are among other problems associated with the increase of nitrogen loads (Richardson & Jorgensen, 1996; Herbert, 1999; Smith *et al.*, 1999; Anderson, 2001). Toxic blooms can kill wild and cultured commercial species, affecting thus important regional fisheries (Anderson, 2001). Some other species produce the so called 'nuisance' phytoplankton blooms, which are characterised by the production and accumulation of foam-like material which deteriorate the aesthetic values of recreational marine environments such as beaches. The growth of specific phytoplankton species, including toxic and nuisance organisms, is favoured by the change in nutrient ratios. The excess abundance of nitrogen implies other nutrients (*e.g.* P or Si) may become limiting for some primary producers (*e.g.* Conley *et al.*, 1991; Meyer-Reil & Köster, 2000). Del Amo *et al.* (1997) for example, found that the spring diatom bloom in the Bay of Brest (France) was limited mainly by silicate and pointed out that fifteen years earlier nitrogen was the main limiting nutrient. Nitrogen loads to the Bay of Brest had largely increased during the years prior to their study (Del Amo *et al.*, 1997). Other examples of affected areas are the Bodden (Southern Baltic Sea) and the Black Sea, where the dominance of diatoms has been lost and 'replaced' by cyanobacteria or coccoliths and flagellates (Jickells, 1998; Meyer-Reil & Köster, 2000). Similar trends have been found in many fresh water and marine systems (*e.g.* Conley *et al.*, 1991). In general, because of

the link between primary and secondary producers, the effect of increasing nitrogen loads (nitrogen eutrophication) can have considerable effects on the structure of food webs with not only ecological implications, but also with consequent social and economic impacts (Richardson & Jorgensen, 1996; McClelland & Valiela, 1998a; Anderson, 2001).

Diagenetic processes can also be influenced by increasing nitrogen loads. The rates of ammonification, nitrification and denitrification in the sediments of coastal systems are stimulated by increases in the organic matter supplied from the water column (Herbert, 1999; Grenz *et al.*, 2000). Ammonification in the sediments represents a source of regenerated nitrogen to the overlying waters. A proportion of the regenerated nitrogen however, is used during the nitrification process (*e.g.* Middelburg *et al.*, 1995). In turn, since the nitrification and denitrification processes are tightly coupled, the oxidised nitrogen (*i.e.* NO_3^-) is eventually reduced to N_2 and N_2O which are lost to the atmosphere. Thus, denitrification represents a loss of nitrogen from the system (Herbert, 1999). It is actually thought, that denitrification is a major sink of nitrogen in the coastal ocean (Nixon *et al.*, 1996; Herbert, 1999; Dong *et al.*, 2000). In estuarine systems, Nixon *et al.* (1996) estimated that estuarine processes retain and remove 30 to 65% of the total nitrogen received that would otherwise be transported to the adjacent sea. Of the nitrogen removed within estuaries, 40 to 50% is accounted for by denitrification (Seitzinger, 1988). The extent of nitrogen removal in estuaries is related to the water exchange (Nixon *et al.*, 1996), with the proportion of total nitrogen inputs lost through denitrification increasing with increased water residence time (Nixon *et al.*, 1996). Thus, denitrification in estuarine sediments represents a sink for the excess nitrogen that estuaries receive. However, although primary production is directly affected by the increase in supply of reactive nitrogen, little is known about the ability of phytoplankton to remove it from the water column; a process that can be potentially significant during productive periods.

In summary, increasing the supply of reactive nitrogen to estuaries and in general to coastal marine ecosystems can have profound impacts in their natural functioning. Furthermore, since humans largely exploit natural resources such as fisheries or even the aesthetic values of ecosystems (*e.g.* for recreational purposes), deleterious effects of nitrogen loads can have social and economic impacts. Therefore if nitrogen loads are to continue to increase and if serious effects to the ecosystems are to be avoided, it is necessary to understand the way ecosystems respond to the excess nitrogen supply. Nonetheless, despite that primary production is an important process which supports secondary production and which is directly affected by the excess of reactive nitrogen, little has been done to evaluate the effect of phytoplankton growth on nitrogen fluxes through estuaries.

1.3 The ^{15}N-tracer technique

Research on N-nutrient cycling has been carried out through the use of mass balance approaches (*e.g.* Nixon *et al.*, 1995; Grelowski *et al.*, 2000; Mortazavi *et al.*, 2000a) and also with the use of mixing diagrams in the particular case of estuaries (*e.g.* Morris *et al.*, 1995; Balls, 1994; Balls *et al.*, 1996; Rendell *et al.*, 1997; Herman & Heip, 1999). However, the study of the marine nitrogen cycle has been largely improved by the application of ^{15}N-tracer techniques. This is because as compared for example, with measurements of change in a N-nutrient concentration over a given incubation period, the ^{15}N-tracer technique is much more sensitive. A detail description of the fundamentals of this technique is presented in the following chapter. In the next few paragraphs, brief comments concerning improvements of the technique and relevant findings in the study of nitrogen cycling by its application are presented in chronological order.

Early uses of this technique involved the study of nitrogen fixation by plants and soil microorganisms (*e.g.* Burris & Miller, 1941). The technique was later adapted for studies on nitrogen fixation in lakes (Dugdale *et al.*, 1959) and further applications were carrried out in oceanic oligotrophic systems such as the Sargasso Sea (Dugdale *et al.*, 1961). Nees *et al.* (1962) presented the first detailed description of a ^{15}N method to measure nitrogen fixation in lakes. Briefly, the method consisted in removing the nitrogen dissolved in a natural-water sample and replacing it with ^{15}N-enriched N_2. After an incubation period, the total nitrogen was quantified after its removal from solution using the Kjeldahl technique. The ammonia evolved was oxidised to N_2, which was then either pumped to a gas-sample bulb connected to the sample-inlet of a mass spectrometer or sealed into glass tubing for later mass spectrometric analysis.

In the case of ammonium and urea uptake for example, the application of the technique has been extended to also estimate the regeneration rates of these two nutrients (Blackburn, 1979; Caperon *et al.*, 1979; Glibert, 1982; Glibert & Capone, 1993). Since ammonium and urea can be regenerated in the water column due to processes such as grazing or excretion by zooplankton, the isotope added (*i.e.* ^{15}N-tracer) at the beginning of an experiment is diluted over the incubation time (Glibert, 1982; Glibert & Capone, 1993). The dilution can be accounted for by measuring the change in the ^{15}N atom percent enrichment over the incubation time. This allows not only the estimation of regeneration rates but also to improve the measurements of net uptake rates by taking into account the dilution of the tracer (Glibert, 1982; Glibert & Capone, 1993).

Adaptations have been made to facilitate the use of the technique and increase its sensitivity. Preston & Owens (1983) for example interfaced an automatic elemental analyser (EA) with an isotope ratio mass spectrometer (IRMS); *i.e.* continuous flow coupled

EA-IRMS. This particular arrangement of instruments has the advantage of using a single sample for the measurement of total nitrogen and ^{15}N , and allows the analysis of several samples in relatively short periods of time (Preston & Owens, 1983). The automation of the technique has facilitated its use for shipboard ^{15}N analysis (Owens, 1988) and the sensitivity has been largely improved for analysis of sub-microgram levels of nitrogen (Owens & Rees, 1989).

The ^{15}N-tracer technique has become an important tool in biological oceanography and new concepts have been developed from its application. For example, Dugdale & Goering (1967) remarked that the nitrogen available for primary production (PP) in the surface ocean was supplied by two main sources. In this way, these authors proposed the concepts of 'new production' and 'regenerated production' to make a distinction between the PP fuelled by allochthonous (*i.e.* N_2 and NO_3^-) and the PP fuelled by autochthonous nitrogen (*i.e.* NH_4^+ and DON). The so called 'f' ratio, put forward by Eppley & Peterson (1979), is widely used in estimations of new production by relating the dominant nitrogen species taken up by phytoplankton to measured rates of PP. Although in many investigations NO_3^- and NH_4^+ are the main N-nutrients considered; *i.e.* $f = \frac{\rho NO_3^-}{\rho NO_3^- + \rho NH_4^+}$ (*e.g.* Eppley *et al.*, 1979), recent estimations also include organic nitrogen sources such as urea; *i.e.* $f = \frac{\rho NO_3^-}{\rho NO_3^- + \rho NH_4^+ + \rho CO(NH_2)_2}$ (*e.g.* Bury *et al.*, 1995; Watts & Owens, 1999; Tremblay *et al.*, 2000). These two concepts became relevant for instance, in studies addressing the export of carbon from the surface ocean as a means to reduce the elevated CO_2 levels in the atmosphere (*e.g.* Tremblay *et al.*, 2000; Bury *et al.*, 2001).

Bronk & Glibert (1991) developed a ^{15}N method for the measurement of dissolved organic nitrogen (DON) release by phytoplankton and found that the release rates of DON can account for a significant proportion of the nitrogen taken up. These authors later applied this method to study the uptake of DON (Bronk & Glibert, 1993a) and showed that the uptake of DON sometimes exceeded the uptake rates of ammonium and nitrate combined. Bronk *et al.* (1994) argued that the release of DON represents an important flux of nitrogen and pointed out that the usual measurements of nitrogen uptake underestimate the total nitrogen taken up. In this way, these authors made a distinction between the **net** nitrogen uptake and **gross** nitrogen uptake rates. The latter being the sum of the former and the release rate of DON. In their work, Bronk *et al.* (1994) argued that the measurement of new and regenerated production can be underestimated by up to 74% and 50% respectively by not including the amount of nitrogen taken up that has been released as DON in the commonly determined f ratio. These authors thus proposed a more complete conceptual model of the traditional view of new *versus* regenerated production. Briefly, the traditional view of new production established that the rate of export of particulate nitrogen from the surface to the deep ocean is more or less in balance with the upward flux of nitrate from bottom layers that is taken up by

phytoplankton. The revised conceptual model considers that the upward flux of nitrate plus nitrification plus N atmospheric deposition equals the rate of net nitrate uptake plus the release of DON, and that over appropriate scales of time and space, the net uptake rate plus the incorporation of DON into bacterial or autotrophic biomass equals the downward flux of PN plus the downward advection of DON (Bronk *et al.*, 1994).

The above information are only a few examples of the potential of ^{15}N-tracer techniques, which have proved to provide a powerful tool for biological oceanographic studies. The use of the technique to measure nitrogen fluxes in a broad range of ecosystems has increased with the development of new mass spectrometric instrumentation such as the continuous flow coupled EA-IRMS. However, despite its capabilities, the technique has scarcely been applied in order to evaluate the effect of phytoplankton growth on nitrogen fluxes through estuaries.

1.4 Nitrogen sources to phytoplankton and nitrogen removal

The contribution of various nitrogen sources to total nitrogen uptake by phytoplankton has been observed to be highly variable in open ocean, coastal and estuarine systems (*e.g.* Dortch, 1990; Bury *et al.*, 1995; Bronk *et al.*, 1998; Kudela & Dugdale, 2000; Tremblay *et al.*, 2000). The preference for a particular N source may be related to environmental factors such as nutrient availability/concentration (*e.g.* Dortch, 1990; Kudela & Dugdale, 2000) and/or light conditions (*e.g.* L'Helguen *et al.*, 1996; Berg *et al.*, 1997; Shaw *et al.*, 1998b), also to phytoplankton species, size structure, and biomass (*e.g.* Kudela & Dugdale, 2000; Tremblay *et al.*, 2000; Bury *et al.*, 2001), and therefore to time of year (Bronk *et al.*, 1998; Kudela & Dugdale, 2000). During a phytoplankton bloom in the North Atlantic, Bury *et al.* (2001) for example, recorded a change of the preference in the nitrogen source utilised. In their study through a phytoplankton bloom event (three-week period) nitrate uptake dominated over ammonium, however this changed towards the end of their study period to a regenerated based productivity apparently due to depletion of nitrate. In a study carried out in the Humber estuary (mouth and plume), Shaw *et al.* (1998b) found that the major contribution to N uptake shifted from nitrate to ammonium as the total nitrogen uptake decreased downstream. These authors also observed that in the region of the Humber plume uptake of reduced forms of nitrogen (ammonium and urea) were higher than nitrate uptake in April 1995, whereas uptake of nitrate was higher than reduced forms during June 1995. Bronk *et al.* (1998) found that in Chesapeake Bay in May, ammonium, nitrate and urea contributed roughly equal proportions to total nitrogen uptake, while in August and October the contribution of ammonium exceeded that of all the other substrates combined. Bronk *et al.* (1998) pointed out that these

results together with DON release and ammonium regeneration marked the change of an autotrophic system fuelled by river nitrate-supply during spring, to a heterotrophic system fuelled by regenerated reduced forms of nitrogen during summer and fall. It has also been observed that ammonium can be the dominant source of nitrogen over an annual cycle. Maguer *et al.* (1996) found that ammonium uptake contributed 54% to the annual total N uptake in the Western English Channel, which was mainly fuelled by regenerated nitrogen in the water column and to a lesser extent by regeneration from sediments. In general however, it appears from reports in the literature, that ammonium is the form of nitrogen most often taken up by phytoplankton (*e.g.* L'Helguen *et al.*, 1996; Bronk & Ward, 1999; Maguer *et al.*, 2000; Ward & Bronk, 2001; Weston *et al.*, 2004).

Most studies of nutrient inputs to rivers and estuaries have concentrated on determining the flux of inorganic forms of nitrogen (DIN) such as nitrate and ammonium (*e.g.* Balls, 1994; Humborg, 1997; Pakulski *et al.*, 2000), as these are rapidly assimilated and contribute to the eutrophication of receiving waters. However, recent research has demonstrated that a fraction of the dissolved organic nitrogen (DON) can also be rapidly assimilated (Bronk & Glibert, 1993a; Bronk *et al.*, 1994; Berg *et al.*, 1997), and therefore also contributes to eutrophication. In some regions, DON can account for up to 90% of the total nitrogen inputs to marine systems (*e.g.* Jorgensen *et al.*, 1999a). For example, Tremblay *et al.* (2000) found that urea dominated (69-93%) total N at all sampling sites in the Gulf of St. Lawrence in autumn. More over, uptake of organic nitrogen can be comparable to that of inorganic nitrogen sources in estuarine systems (*e.g.* Bronk *et al.*, 1998), or even higher (Berg *et al.*, 1997). Turnover times for the labile DON pool have been demonstrated to be short in estuaries (4 days) as compared with oceanic and coastal waters (10 ± 1 and 18 ± 14 days respectively) (Bronk *et al.*, 1994). Thus, non-conservative removal of DIN and DON by phytoplankton can potentially influence the seaward flux of nitrogen through an estuary. It has been observed that although planktonic uptake rates may be low in some estuaries, the nitrogen flux through the estuary can be reduced by up to 22% (*e.g.* the Tweed Estuary, Shaw *et al.*, 1998). However, the seasonal changes in relative levels of both DON and DIN have rarely been measured in estuaries, and their relative contributions to phytoplankton growth over time and space is not known in most systems. Therefore, within the present research it was aimed to quantify and evaluate the influence of planktonic biological removal of dissolved inorganic and organic nitrogen, to determine the relative contributions of these nitrogen sources to phytoplankton growth and to estimate the rates at which dissolved organic nitrogen is released and ammonium regenerated.

1.5 The Southampton Water estuarine system

Description of the system

The Southampton Water estuary (SW) is located on the south coast of the UK, forming part of the north-west extension of the Solent system (Lauria *et al.*, 1999) and being surrounded by the city of Southampton in its upper reaches (Hydes & Wright, 1999). The length of the estuary is about 10 km and it has a maximum width of 2.5 km. It also has an active central shipping channel which is dredged to a depth of about 15 m. The surrounding area is highly urbanised and there are large industrial complexes along its length. The SW is a partially mixed and macrotidal estuary, with a tidal range between 1.5 and 5 m and a tidal excursion of 2.5 km (Hydes & Wright, 1999). The estuary is characterised by a double high water that can last up to 3 hours (Dyer, 1997). The SW is mainly fed by the Test and Itchen rivers (draining mostly agricultural land), with combined average discharge of 1.54×10^6 m^3 d^{-1} (Hydes & Wright, 1999). The rivers Test and Itchen in turn, are fed from catchment basins with areas of 1260 and 400 km^2 respectively (Hydes, 2000). In addition to the freshwater supplied by the rivers, the system receives a sewage discharge of about 0.1×10^6 m^3 d^{-1}, which can contribute up to 25% of the flow when the river discharge is low (Hydes, 2000). Estimated flushing rates for spring and neap tides are ~26 and 76 h respectively (Wright *et al.*, 1997).

Phytoplankton in the Southampton Water estuary

Southampton Water presents a bimodal phytoplankton biomass cycle (Cebrián & Valiela, 1999), with highest chlorophyll peaks occurring usually between the months of March-May, and June-September (*e.g.* Leakey *et al.*, 1992; Kifle & Purdie, 1993; Iriarte & Purdie, 1994; Howard *et al.*, 1995). During this period, chlorophyll concentrations up to 15 μg L^{-1} and 70 μg L^{-1} have been measured in the coastal waters and the mid estuary respectively (*e.g.* Leakey *et al.*, 1992; Iriarte & Purdie, 1994; Howard *et al.*, 1995). Phytoplankton blooms in the system are of short duration and commonly last for about two weeks (*e.g.* Iriarte & Purdie, 1994; Crawford *et al.*, 1997). The composition of the phytoplankton populations in Southampton Water varies seasonaly and spatialy (*e.g.* Leakey *et al.*, 1992; Kifle & Purdie, 1993; Howard *et al.*, 1995; Ali, 2003). It is characterised by a spring and a summer bloom in the inner estuary, with only a spring bloom in the Solent. Blooms tend to start early in spring in the coastal waters and develop later in the inner estuary (*e.g.* Iriarte & Purdie, 1994). The spring bloom is commonly dominated by diatoms, and the summer bloom mainly dinoflagellates and flagellates (Leakey *et al.*, 1992; Kifle & Purdie, 1993; Howard *et al.*, 1995; Ali, 2003). Another characteristic organism of the planktonic population in the system is the phototrophic ciliate *Mesodinium rubrum*, which tends to bloom and develop 'red tides' during the summer months; mainly in the inner estuary (Crawford, 1992; Leakey *et al.*, 1992; Garcia *et al.*, 1993; Kifle & Purdie, 1993;

Iriarte & Purdie, 1994; Crawford *et al.*, 1997). The spacial distribution of phytoplankton species seems to be dominated by diatoms and flagellates in coastal waters, diatoms and dinoflagellates in the mid estuary; with dinoflagellates dominating mainly during summer. In the upper estuary, diatoms have been reported to be more abundant in June, flagellates in July and, diatoms, dinoflagellates and ciliates in August. The contribution to biomass however appears to be dominated by diatoms, dinoflagellates and ciliates (Ali, 2003). Phytoplankton growth in the estuary has been shown to be limited by light availability, although silicate and phosphorus limitation has been also suggested specially after bloom events (Ali, 2003).

Contribution of phytoplankton groups to biomass

In the most recent work in the Southampton Water estuary, Ali (2003) found that during the 1999 spring bloom (May) diatoms accounted for up to 70% of the total biomass (~370 μg C L^{-1}) and that during the summer bloom (July) dinoflagellates contributed up to 92% (~950 μg C L^{-1}). Flagellates are usually abundant and may exceed dinoflagellates in number (*e.g.* Howard *et al.*, 1995; Ali, 2003), but their contribution to the total biomass has been shown to be low (Ali, 2003). Ali (2003), found that flagellates contributed from ~40 to 90% of the total cell counts in a treansect all along the estuary on 15-Aug 2000, but their contribution to total biomass was <30%. *Mesodinium rubrum* has been reported to account for >50% of the total biomass on some occasions, although this has been observed when the levels of total biomass are relatively low; <300 and generally ~50 μg C L^{-1} (Ali, 2003).

Nutrients in the Southampton Water estuary

Southampton Water is considered to be a hypernutrifled estuary (Hydes & Wright, 1999; Hydes, 2000; Holley & Hydes, 2002). The mean concentration of nitrate in the two main rivers feeding the SW estuary have increased between 1974 and 1997, from 342 to 422 μmol L^{-1}, and from 308 to 393 μmol L^{-1} in the Test and Itchen respectively (Hydes, 2000). Nitrate typically contributes up to 97% of the total dissolved nitrogen pool in the estuary (Hydes & Wright, 1999). As compared with nitrate, nitrite in the system is present in relatively low levels, with a mean concentration of 4 μmol L^{-1} (Hydes & Wright, 1999). The Southampton Water estuary receives a number of effluent discharges from domestic and industrial sources that can account for up to 10% of the freshwater inputs to the system (Soulsby *et al.*, 1985, cited by Kifle & Purdie, 1993). Furthermore, sewage effluents dominate the inputs of ammonium, urea and phosphorus into the estuary (Hydes & Wright, 1999). Ammonium concentrations in the system can represent up to 30% of the dissolved nitrogen pool, although the mean concentration has been estimated to be 7 μmol L^{-1} (Hydes & Wright, 1999). The spatial distribution of urea has been shown to present a non conservative behaviour, and measured concentrations within the system are generally <2 μmol L^{-1} (Ashe, 1996). Urea as a proportion of dissolved nitrogen

(DIN) species (urea, nitrite, nitrate, and ammonium) has been reported within the range 0.8-16.4% and 0.1-9.9% in the mid estuary and coastal waters, respectively (Ashe, 1996).

In spite of the high nutrient concentrations in the system, nitrate is known to show conservative dilution-like behaviour even during more productive periods of the year, although complete removal by phytoplankton has been observed at high salinities; *i.e.* in the coastal waters of the system (Hydes & Wright, 1999). The effect of phytoplankton growth on the nutrient levels produces an annual cycle, characterised by lower concentrations in summer (Kifle & Purdie, 1993; Hydes & Wright, 1999; Hydes, 2000). However, the concentrations of nitrate within the system are related to the river flow. That is, higher concentrations have been measured during winter months when the precipitation rates are maximum and therefore lower levels are found during summer time when the river discharge is low (*e.g.* Hydes & Wright, 1999). The removal of nitrate in the system has been inferred with the use of mixing diagrams (*e.g.* Hydes & Wright, 1999; Hydes, 2000). This approach however, can not be applied to the study of ammonium or urea removal for instance, since both of these nutrients do not show conservative-like behaviour. In spite of the limitation of using mixing diagrams to evaluate nitrogen removal, direct uptake of nitrogen by phytoplankton has not been measured in this system. Furthermore, high Chl-*a* concentrations have been also measured in the inner estuary and removal of nitrogen is therefore likely to occur at this site as well. ^{15}N-tracer techniques represent a useful tool to evaluate the removal of nitrogen in a system like Southampton Water, where the high Chl-*a* concentrations (of up to 70 μg L^{-1}) that have been measured, suggest a significant potential for nitrogen removal from the water column. Besides, the fact that the Southampton Water estuary is surrounded by one of the most densely populated areas in the south coast of England make the system specially susceptible to human impact. Thus, research on the way the system respond to the nitrogen supply would provide useful information for managements purposes.

The following generalising points regarding nutrients and phytoplankton within Southampton Water estuary can be drawn from the information above:

- Sewage effluents dominate ammonium, urea and phosphate inputs to the estuary.
- High nutrient concentrations (*e.g.* >60 μmol L^{-1} NO_3^-, Iriarte & Purdie, 1994) can be measured in the inner estuary.
- An increase in nitrate concentrations from 342 to 422 μmol L^{-1}, and from 308 to 393 μmol L^{-1} has been recorded during the last few decades in the Test and Itchen rivers respectively (Hydes, 2000).
- High chlorophyll *a* levels (>20 μg L^{-1}) have been shown to be common between

March and September in the estuary.

- Nutrients within the system show an annual cycle, with lower concentrations over the productive period.

From these last two points a simple hypothesis can be stated;

'Phytoplankton play an important role in modifying N-nutrient forms through non-turbid estuaries'

1.6 Objectives

In order to test the above hypothesis, the objectives of this study were:

1. To quantify and evaluate the influence of biological removal of dissolved inorganic nitrogen forms (NO_3^- and NH_4^+), and $CO(NH_2)_2$ (as representative of the dissolved organic nitrogen pool) on nitrogen fluxes through a non-turbid temperate estuarine system during the productive spring-summer period.

2. To estimate the relative contributions of nitrate, ammonium, and urea to phytoplankton growth in a temperate macrotidal estuary.

3. To quantify the release of dissolved organic nitrogen and regeneration of ammonium from the uptake of dissolved inorganic nitrogen forms.

4. To investigate the influence of isotope dilution, ammonium regeneration and DON release on nitrogen cycling.

1.7 Thesis structure

A series of sampling surveys were carried out during the productive spring-summer period in 2001 and 2002. Water samples were collected from three selected stations along the estuary in order to measure the irradiance, salinity, temperature and concentration of nutrients and chlorophyll *a* throughout the water column. Water collected from the three sites was used to carry out incubations using ^{15}N techniques in order to measure the uptake of nitrate, ammonium and urea during the productive period in 2001. Incubations with three different ^{15}N-labelled nutrients were carried out *in situ* at 4 light levels and in the dark. The uptake of nitrate was complemented with simultaneous measurements of ^{13}C-bicarbonate uptake. In addition to the measurements carried out through out the water column at the three selected stations and based in part on the results obtained during 2001, during the productive period in 2002 ^{15}N-tracer incubations were carried out only with nitrate and ammonium at two light levels. In addition, during 2002 release rates

of dissolved organic nitrogen from nitrate and ammonium, and ammonium regeneration from ammonium uptake were also measured at one representative sampling station. In Chapter 2, the sampling strategy and the analytical methods used during this research are described in detail. Results from analytical tests are also presented in this chapter. In Chapter 3, the results obtained during the productive spring-summer period in 2001 are presented and discussed. Results from the second year of experiments, 2002, are presented and discussed in Chapter 4. In Chapter 5 a comparison is made between surface uptake rates in the two consecutive productive periods surveyed. Finally in Chapter 6, a summary of the research is presented and the main conclusions listed. Information additional to Chapters 2 to 5 is included in a number of appendices.

Chapter 2

Methods

In this chapter, the field work and sample processing protocols followed for chemical analyses and other variable determinations (*e.g.* Alkalinity) are described and results from analytical tests are presented. Additional information concerning the calibration of analytical techniques is presented in Appendix A.

2.1 Sampling Surveys in 2001

A series of sampling surveys were undertaken along the Southampton Water estuarine system during the productive spring-summer period in 2001 (**Fig. 2.1**). Water samples were collected every 2 weeks (spring tides) over the high water period, from three stations in the estuary representative of coastal waters of the Solent (Calshot buoy), the mid-estuary (NW Netley buoy) and brackish waters of the system; upper estuary (Eling buoy). The three sampling stations correspond to the position of navigation buoys (named between parenthesis) where previous research has been done (*e.g.* Kifle & Purdie, 1993; Iriarte & Purdie, 1994; Howard *et al.*, 1995; Lauria *et al.*, 1999; Hydes & Wright, 1999; Ali, 2003). The first three sampling surveys were carried out on board the SOC research vessel Bill Conway, but most surveys were carried out using a SOC R.I.B., which allowed the sampling to be carried out in $\leqslant$3 hours (*i.e.* the period of high water stand during spring tides). Sampling survey dates and stations are summarised in **Table 2.1**. In order to account for the spatial and temporal variability in the system, vertical profiles of **temperature**, **salinity** and **photosynthetically active radiation (PAR)** were measured at each station, and samples were collected from 5 depths throughout the water column for later analysis of **inorganic nutrients** (NO_3^-, NH_4^+, PO_4^{3-}, $Si(OH)_4$), **urea**, and **chlorophyll *a***. Salinity and temperature profiles were measured and data logged, at 0.5 sec intervals by deploying a YSI multi-probe (Model 6600-D), from surface down to 10 m depth. On a few occasions when the YSI was not available, a T/S probe (Tetra-Con 325) was used and data recorded at 1 m intervals. A LI-COR profiler (Model LI-1000)

was used to measure surface incident and downwelling PAR at 1 m intervals from surface down to 10 m depth. Water samples were collected from five depths using a 2 L Niskin bottle. Water collected from 1, 4, 7 and 9 m depth was placed into 500 mL polycarbonate bottles, which were then stored in coolboxes for later processing in the lab. Water collected from 2 m was placed into 10 L polycarbonate carboys, which were stored in thick black plastic bags for transportation to the lab. The samples collected from 2 m depth were used to carry out ^{15}N and ^{13}C-tracer incubation experiments.

Table 2.1: Dates on which water samples were collected from the 3 sampling stations in 2001. Dates during which incubation experiments were carried out are also shown.

Station / **Date (Julian day)**	*Coastal waters* Calshot[a]	*Mid estuary* NW Netley[a]	*Upper estuary* Eling[a]
20/04/01 (110)	☒	✓	✓
08/05/01 (128)	✓	✓	☒
21/05/01 (141)	✓ *	✓ *	☒
05/06/01 (156)	✓ *	✓ *	✓ *
19/06/01 (170)	✓ *	✓ *	✓ *
04/07/01 (185)	✓ *	✓ *	✓ *
20/07/01 (201)	✓ *	✓ *	✓ *
01/08/01 (213)	✓ *	✓ *	✓ *
16/08/01 (228)	✓ *	✓ *	✓ *
30/08/01 (242)	✓ *	✓ *	✓ *
17/09/01 (260)	✓ *	✓ *	✓ *
01/10/01 (274)	✓ *	✓ *	✓ *
15/10/01 (288)	✓ *	✓ *	✓ *
31/10/01 (304)	✓ *	✓ *	✓ *

✓ Water samples collected.
☒ Samples not collected.
* Tracer experiment.
[a] Name of navigation buoy.

2.2 Sampling Surveys in 2002

Sampling surveys in 2002 were undertaken from the same three stations as in 2001 representative of coastal waters, mid and upper estuary (**Fig. 2.1**). Dates on which sampling surveys and experiments were carried out are summarised in **Table 2.2**. Samples were also collected during spring tides and over high water period (every 2 weeks). Vertical profiles of temperature, salinity and PAR were measured at each station as in 2001. In 2002 however, water samples were collected from only 3 depths, as previous results generally showed no marked differences in nutrient and chlorophyll concentration between 4 and 9 m depth. Thus, water samples from 1, 2 and 9 m depth were collected for analysis of inorganic nutrients (NO_3^-, NH_4^+, PO_4^{3-}, $Si(OH)_4$), total dissolved nitrogen (TDN),

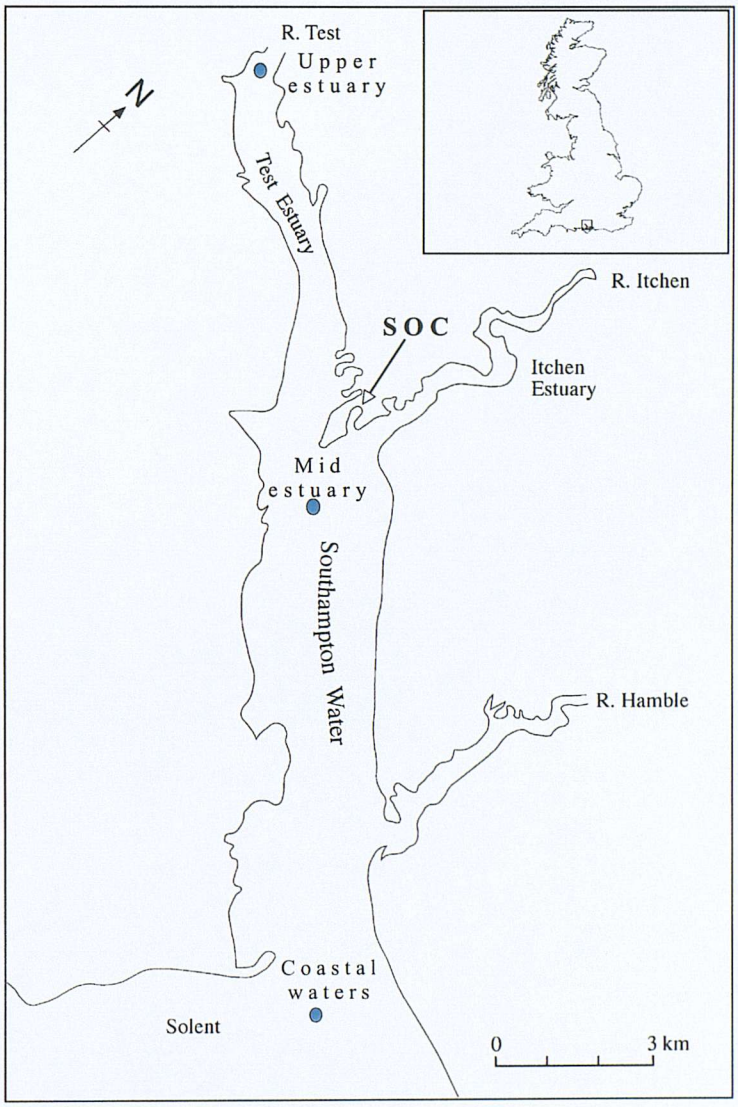

Figure 2.1: **Sampling stations within the Southampton Water estuary** (blue dots); upper estuary, mid estuary and coastal waters.

Table 2.2: Dates on which water samples were collected from the 3 samplings stations in 2002. Dates during which incubation experiments were carried out are also shown.

Station / **Date (Julian day)**	*Coastal waters* Calshot[a]	*Mid estuary* NW Netley[a]	*Upper estuary* Eling[a]
25/04/02 (115)	✓ *	✓ *	✓ *
09/05/02 (129)	✓ *	✓ *	✓ *
23/05/02 (143)	✓ *	✓ *	✓ *
10/06/02 (161)	☒	✓ *	✓ *
24/06/02 (175)	✓ *	✓ *	✓ *
09/07/02 (190)	☒	✓ *	✓ *
23/07/02 (204)	✓ *	✓ *	✓ *
07/08/02 (219)	✓ *	✓ *	✓ *
20/08/02 (232)	✓ *	✓ *	✓ *
06/09/02 (249)	✓ *	✓ *	✓ *
19/09/02 (262)	✓ *	✓ *	✓ *
03/10/02 (276)	✓ *	✓ *	✓ *
17/10/02 (290)	✓ *	✓ *	✓ *

✓ Water samples collected.
☒ Samples not collected.
* Tracer experiment.
[a] Navigation buoys.

and chlorophyll *a*. Water from 2 and 9 m depth was placed into 500 mL polycarbonate bottles and stored in coolboxes for later processing in the lab. Water collected from 1 m depth was place into 10 L polycarbonate carboys and stored in thick black plastic bags for transportation to the lab. The samples collected from 1 m depth were used to carry out ^{15}N-tracer incubation experiments.

2.3 Sample processing (2001 and 2002).

Cleaning protocol. Previous to each survey, all polycarbonate bottles and glassware used during the sampling or used for sample processing were *i)* washed with phosphate-free liquid detergent and tap water, *ii)* rinsed with 10% HCl, *iii*) rinsed with deionised water, *iv)* and finally rinsed with Milli-Q water. Thus, from each sample bottle and carboy:

A) 50 mL of water was filtered in duplicate through a 25 mm diameter GF/F filter using in-line syringe filtering units (Millipore Swynnex-25);

1. 50 mL of filtrate were collected directly into a 50 mL brown glass bottle containing 2 mL of phenol solution (Parsons *et al.*, 1984). These bottles were stored in a fridge for later ammonium analysis.

2. 25 mL of filtrate was poured into a plastic vial and kept frozen for later analysis of nitrate and phosphate.

3. The remaining 25 mL of filtrate was collected in a plastic vial and kept unfrozen in the dark for later silicate analysis.

4. The duplicate filters were folded in half, placed in plastic bags, and stored frozen for later determination of chlorophyll *a*.

B) 50 mL of water was collected in precombusted (550°C, 4 h) brown-glass bottles after filtering sample through a precombusted (500°C, 4 h) 47 mm diameter GF/F filter. Filtration was carried out using a Whatman glass filtering system and a hand vacuum pump. These sub-samples were stored frozen for later analysis of urea (only in 2001) or TDN (only in 2002). The brown-glass bottles were stoppered using plastic caps with teflon seals in order to avoid contamination with plastic-derived organics.

C) From the carboys only, a 100 mL subsample was collected in brown-glass bottles containing 2 mL of Lugol solution for later phytoplankton identification.

D) Also from the carboys, a filtered subsample was placed in a 100 mL brown-glass bottle for later determination of alkalinity (only in 2001).

E) Description of sample processing from incubation experiments is presented in § 2.5.2 and 2.5.3.

2.4 Analytical methods

2.4.1 Nutrient analysis

Most dissolved nutrients were measured using colorimetric techniques, which involve a chemical reaction with the nutrient of interest in order to produce a coloured compound. The intensity of the colour produced is proportional to the concentration of the nutrient present, and can be measured by spectrophotometry within a range as predicted by the Beer-Lambert's law (Hydes, 1984; Hydes & Wright, 1999; Hansen & Koroleff, 1999).

2.4.1.1 Note: Limit of detection

The limit of detection can be defined as the smallest amount or concentration that can reliably be measured above a background signal (*e.g.* Christian, 1994; Currie, 1997; Fifield, 2000) and its concept and calculation are still a topic under discussion (Currie, 1997). During this work the limit of detection for the different chemical methods used, was calculated as twice the standard deviation of the mean background (blank) error (Fifield, 2000); *i.e.* expressed in terms of concentration.

2.4.1.2 Nitrate, Phosphate and Silicate

During this research **nitrate**, **phosphate**, and **silicate** were measured by segmented-continuous-flow using a Burkard Scientific SFA-2 Auto-analyser as described by Hydes (1984) and Hydes & Wright (1999). **Nitrate** measurement is based on its reduction to nitrite. The reduction is achieved by passing the sample through a copper-cadmium reduction column (Wood *et al.*, 1967). The nitrite produced then reacts with sulphanilamide to form a diazo compound, which is further coupled with N-(1-napthyl)-ethylendiamine to produce an azo dye that is measured at 540 nm (Hansen & Koroleff, 1999). Nitrate and nitrite were not measured separately, therefore values reported here as nitrate also include nitrite concentrations (*i.e.* NO_3^-=[NO_3^- + NO_2^-]). In the Southampton Water estuary however, nitrate accounts for 97-100% of the total oxidised nitrogen (Hydes & Wright, 1999). The determination of **phosphate** follows a modification of the method developed by Murphy & Riley (1962) as described by Hansen & Koroleff (1999). The method involves the reaction of phosphate ions with an acidified molybdate reagent to produce a phosphomolybdate heteropoly acid. This product is then reduced to a highly coloured blue compound with absorbance measured at 880 nm (Hansen & Koroleff, 1999; Hydes & Wright, 1999). Finally, the analysis of dissolved **silicate** is based on the reaction of a sample with acidic molybdate to form a yellow silicomolybdic acid. The silicomolybdic acid is then reduced with ascorbic acid to produce an intense blue-coloured complex with the absorbance measured at a wavelength of 660 nm (Hansen & Koroleff, 1999; Hydes & Wright, 1999). Thus, calibrations were carried out daily by preparing a series of standards containing nitrate, phosphate and silicate as shown in **Table 2.3**. Examples of calibration curves are presented in Appendix A.0.1. Standards and blanks were prepared with saline water; 40 g of NaCl L^{-1} of Milli-Q water (Hydes, 1984; Hydes & Wright, 1999). Samples for nitrate and phosphate were defrosted under running tap water just before starting the analysis. Blanks, single standards or full calibration curves were run between batches of samples in order to correct for any possible drift of the base line and/or carry over effects. The base line was also checked for any possible contamination of reagents by running low nutrient seawater (Ocean Scientific International; batch LNS10, salinity 35, nutrients <1.0 μmol L^{-1}) between batches of samples. Whenever a measured concentration was higher than the top standard of the calibration range, the sample was diluted proportionally with artificial seawater. All standards, blanks and samples were analysed in triplicate. Calculated mean limits of detection were 0.93±0.46, 0.10±0.04 and 0.58±0.37 μmol L^{-1} for nitrate, phosphate and silicate respectively.

2.4.1.3 Ammonium

Ammonium in estuarine samples was measured using the **indophenol-blue** method as described by Parsons *et al.* (1984). Recommendations given by Aminot *et al.* (1997) and

Table 2.3: Concentration range of standards prepared for nutrient analysis by segmented-continuous-flow (μmol L^{-1}).

	Nitrate	**Phosphate**	**Silicate**
Std 1	10.0	0.5	10.0
Std 2	40.0	1.0	20.0
Std 3	60.0	2.0	30.0
Std 4	80.0	3.0	40.0

Analytical grade Potassium nitrate (KNO_3^-), Potassium dihydrogen phosphate (KH_2PO_4), and Disodium hexafluorosilicate (Na_2SiF_6) were used to prepare standards.

by Hansen & Koroleff (1999) were adopted. The indophenol-blue method, first reported by Berthelot in 1859 (Solorzano, 1969; Aminot, 1983), consists of a complex reaction. Although the exact mechanism is not fully understood (Aminot *et al.*, 1997; Hansen & Koroleff, 1999), the reaction is believed to proceed as follows; ammonium reacts with hypochlorite to produce monochloramine under alkaline conditions, then in the presence of sodium nitroprusside as a catalyst, the monochloramine reacts with two molecules of phenol. The product of this reaction is the indophenol-blue (Aminot, 1983; Aminot *et al.*, 1997; Hansen & Koroleff, 1999) and absorbance can be measured at a wavelength of 640 nm (Parsons *et al.*, 1984). Ammonium-free water (**AFW**) was produced daily by passing Milli-Q water (18.2 MΩ cm^{-1}) through an ion exchange column (see Appendix A.0.2). The AFW was then and used to prepare reagents, stock solutions, standards and blanks. The concentration range of standards prepared to calibrate the method is presented in **Table 2.4**. Reagents and stock solutions were stored in dark-glass bottles (kept in a fridge when not in use), and were renewed at least every two weeks. In order to avoid contamination, a well acknowledged problem in the determination of ammonium, AFW was used to prepare standards and blanks instead of artificial seawater. Nonetheless, internal standards were used in replicates of selected estuarine samples to verify that ammonium concentrations were reproducible as in AFW. Whenever a measured concentration was higher than the top standard of the calibration range, the corresponding sample was diluted proportionally with Milli-Q water. Dilution in this way minimizes contamination since the blue colour develops after 1 h in dark conditions. All analyses were carried out in 4 replicates. 10 mL aliquots were pipetted into glass vials directly from the brown-glass bottles containing the sample (see § 2.3 for reference). A set of automatic pipettes and glass vials were used exclusively for this purpose. Following the addition of reagents, samples were left to react for about 2 h inside a dark plastic box. The colour absorbance was then measured in a 1 cm cuvette using a U-2000 Hitachi spectrophotometer. This instrument facilitates working with hazardous chemicals since it is equipped with a sipper that can extract the sample straight from the glass vials, reducing

in this way direct contact with the analyst. The mean limit of detection of this method was 0.22±0.18 μmol L^{-1}. Additional information is presented in Appendix A.0.2.

Table 2.4: Concentration range of standards prepared for ammonium analysis by colorimetric and fluorometric techniques (μmol L^{-1}).

	Ammonium
Std 1	1.0
Std 2	2.5
Std 3	5.0
Std 4	7.5
Std 5	10.0

Analytical grade Ammonium sulphate ($(NH_4)_2SO_4$) was used to prepare standards.

Ammonium measurements were made to test the MgO-DeVarda's alloy and steam distillation techniques using the **fluorometric method** developed by Kérouel & Aminot (1997) as adapted by Holmes *et al.* (1999). This method is based on the reaction of ammonium with orthophthaldialdehyde (**OPA**), which produces a highly fluorescent compound. A water sample is allowed to react for 3-8 h in the dark after the addition of a mixed reagent containing sodium sulphite (1 g Na_2SO_3/125 mL water), sodium tetraborate (80 g $B_4Na_2O_7$/2 L water) and OPA (4 g/100 mL C_2H_5OH ultra-pure). The fluorescence of the sample is then measured at 360 nm excitation and 420 nm emission (Holmes *et al.*, 1999). For this work, the method was calibrated at the concentration range shown in Table 2.4. An example of a calibration curve is presented in appendix Appendix A.0.2. Daily produced ammonium-free water was used to prepare standards and blanks. Analyses were carried out (in 4 replicates) by pouring 1 mL of sample (reagent or blank) into a 50 mL plastic centrifuge tube containing 5 mL of mixed reagent. The tube was then capped and placed in a rack inside a dark-plastic box. The fluorescence was subsequently measured in a 1 cm fluorometer-cuvette using a Perkin-Elmer LS-5 Luminescence spectrometer. Samples (testing-standards) with a concentration higher that the top standard of the calibration were proportionally diluted with ammonium-free water. Between analysis the tubes were kept capped with 5 mL of mixed reagent, which was removed just before a new analysis. In this way, ammonium contamination is minimized and any ammonium present in the tube reacts and is thus removed. The sample:reagent volume ratio used here (0.2) was slightly modified from that used by Holmes *et al.* (1999) of 0.25, however no effect was observed and analysis results were always satisfactory. The mean limit of detection of this method with the equipment used was 0.2±0.2 μmol L^{-1}.

Table 2.5: Concentration range of standards prepared for determination of urea in estuarine water samples (μmol L^{-1}).

	Urea
Std 1	0.1
Std 2	0.5
Std 3	1.0
Std 4	2.0
Std 5	4.0
Std 6	6.0
Std 7	8.0
Std 8	10.0

Analytical grade Urea ($CO(NH_2)_2$) was used to prepare standards.

2.4.1.4 Urea

Urea was measured manually according to the technique developed by Mulvenna & Savidge (1992) as adapted by Goeyens *et al.* (1998). This method is in itself an adapted and improved version (DeManche *et al.*, 1973; Aminot & Kérouel, 1982; Mulvenna & Savidge, 1992; Goeyens *et al.*, 1998) of the first method for urea determination in seawater (Newell *et al.*, 1967), which in turn is an adaptation of a clinical analysis (Beale & Croft, 1961, cited by Newell *et al.*, 1967). This colorimetric technique is based on the reaction of urea with diacetylmonoxime, which produces a red compound with absorbance measured at a wavelength of 520 nm. Analyses during this work were carried out using a set of 40 mL glass vials used exclusively for this purpose. Vials were washed following the cleaning protocol mentioned in § 2.3. The calibration of the method was done at the concentration range shown in table 2.5. Standards, blanks and reagents were prepared with fresh Milli-Q water. Reagents and the stock standard solution were kept stored in a fridge and were renewed every 2 weeks. Stored samples were defrosted just after the analysis, and clean automatic pipettes were used to transfer the sample to the analysis vials. Thus, after the addition of reagents, 10 mL of sample (3 replicates) were left to react for 72 h at 22±1°C inside a grey thick-plastic box. The absorbance of the sample was then measured using a U-2000 Hitachi spectrophotometer with a sipper sampler. Special care was taken when measuring the absorbance since the colour of the sample degrades relatively rapidly at ambient temperatures of 27°C and/or if exposed to direct light (Goeyens *et al.*, 1998). Despite the time that sample preparation and the reaction itself require, this technique proved to be highly reliable. The mean limit of detection of the method during this work was 0.03±0.02 μmol L^{-1}. Additional information is presented in Appendix A.0.3.

2.4.1.5 Total dissolved nitrogen and dissolved organic nitrogen

As yet, there is no direct method for measuring dissolved organic nitrogen (**DON**) in natural waters. DON is therefore estimated by independently measuring the total dissolved nitrogen (**TDN**) and the dissolved inorganic component (*i.e.* nitrate, nitrite and ammonium) of a given sample. The sum of the inorganic nitrogen species is then subtracted from the TDN measured in a particular sample (Walsh, 1989; Benner *et al.*, 1993; Hopkinson *et al.*, 1993; Bronk *et al.*, 2000; Bronk, 2002; Sharp, 2002). This can be expressed in a simple way was as follows,

$$[DON] = [TDN] - [DIN] \tag{2.1}$$

Where the dissolved inorganic nitrogen concentration is given by,

$$[DIN] = [NO_3^- + NO_2^- + NH_4^+] \tag{2.2}$$

Since each of the measurements has an associated analytical error and uncertainty, the standard deviation of the DON concentration was calculated by conducting a simple error propagation analysis given by,

$$S_{DON} = \sqrt{(S_{TDN}^2 + S_{NO_3^-+NO_2^-}^2 + S_{NH_4^+}^2)} \tag{2.3}$$

Where S^2 is the variance of replicate measurements for independent analyses (Christian, 1994; Bevington, 1969, cited by Bronk *et al.*, 2000).

When compared with the UV and persulphate oxidation methods, the **high temperature catalytic oxidation** (**HTCO**) approach is less prone to sample contamination when measuring TDN since it involves less handling and less chemical manipulations (Sharp *et al.*, 2002). During this research, TDN concentration was measured by HTCO using a total organic carbon analyser (Shimadzu TOC-5000A) coupled to a pyrochemiluminescent nitrogen specific GC detector (Antek 705E). The instrument includes a Shimadzu Class-VP chromatography laboratory automated software system for peak-area integration. The HTCO analysis consists of the injection of a decarbonated sample[1] into a platinum-coated catalyst[2] at high temperature[3] under an ultra-pure oxygen environment. The combustion of the sample converts all nitrogen forms to nitrogen oxides (NO_x). These gases are further dehumidified and dried while passing through a series of devices within the instrument. Eventually, chemiluminescent NO_2 species are produced during the last stage of the analysis by mixing the NO_x with O_3 (Álvarez Salgado &

[1] Particularly important for DOC determinations.
[2] Al_2O_3 is used as a catalyst.
[3] At a temperature of 950°C with the instrument used.

Table 2.6: Concentration range of standards prepared for TDN (μmol L^{-1}).

	Caffeine
Std 1	20.0
Std 2	50.0
Std 3	100.0
Std 4[a]	200.0
Std 5	500.0
Std 6	700.0
Std 7	1000.0

Analytical grade caffeine ($C_8H_{10}N_4O_2$) and potassium nitrate (KNO_3)were used to prepare standards.

[a]Mid range standards, see text for reference.

Miller, 1998; Sharp *et al.*, 2002). The method was calibrated within the concentration range shown in **Table 2.6**. A calibration curve example is presented in Appendix A.0.4. The main calibration standard was prepared with analytical grade caffeine ($C_8H_{10}N_4O_2$). However, in order to verify in a simple way the oxidation efficiency of the analysis, a second 'mid range concentration' standard (200 μmol L^{-1}N) was prepared with analytical grade potassium nitrate (KNO_3). Both mid range standards produced similar results when re-calculating their concentration; 201±7 μmol L^{-1} N-caffeine (n=15) and 203±5 μmol L^{-1} N-potassium nitrate (n=11). Milli-Q water is recommended for calibration purposes in TDN/TOC analysis due to its low organic nitrogen content (Álvarez Salgado & Miller, 1998), however a further step was considered here and UV-radiated (4 h) Milli-Q water was used to prepare standards and blanks. Stored samples were defrosted at room temperature prior to analysis. Prior to injection, 10 mL of sample (including standards and blanks) were placed in a precombusted (4 h at 550°C) glass vial and decarbonated by bubbling nitrogen through after the addition of 50 μL of 10% HCl. Every sample was injected 4 times or more if data peaks were inconsistent. Blank variability is a well acknowledged problem in TDN/TOC determinations, therefore possible drifts of the calibration were verified by running blanks and mid range standards every 5 samples and at the end of a day of analysis. The mean limit of detection estimated for this analysis was on average 7.0±7 μmol L^{-1}.

2.4.2 Mass spectrometric analysis: Particulate nitrogen, Particulate Carbon, ^{15}N and ^{13}C

Particulate carbon and nitrogen, and ^{15}N and ^{13}C samples were analysed by elemental analysis continuous flow isotope ratio mass spectrometry (EA-IRMS), using either an

ANCA-SL EA linked to a PDZ Europa mass spectrometer[4] or an Eurovector EA 3028-HT linked to a GV Isoprime mass spectrometer[5] with the Mass Lynx^{TM} v.3.6i software installed.

Analysis fundamentals; in nature nitrogen is present as a mixture of its two stable isotopes, ^{14}N and ^{15}N. With the former constituting ~99.63% and the later ~0.366% (Fiedler & Proksch, 1975; Sigman & Casciotti, 2001). The principle of the analysis is therefore based on the determination of the ^{15}N to ^{14}N ratio of a given sample, *i.e.* the ^{15}N atom percent[6]. That is (see eq., 2.4),

$$at\% = \frac{^{30}N + \frac{1}{2}{}^{29}N}{(^{28}N + ^{29}N + ^{30}N)} \times 100 \tag{2.4}$$

where *at%* represents the ratio of the ^{15}N atoms to the total number of nitrogen atoms present in the sample (Fiedler & Proksch, 1975). The same principle applies for the analysis of ^{13}C, which is measured as CO_2 and whose masses are 44, 45 and 46. The analyser of an IRMS instrument is thus composed of *i)* an analyser tube (with its centre flattened laterally and curved through an angle of 60° (commonly), *ii)* an inlet system for the admission of nitrogen gas into the analyser tube; *iii)* an ion source where nitrogen molecules are bombarded with electrons, become charged and accelerated; *iv)* a magnetic field where the charged molecules are separated into different paths according to their mass to charge ratio, and momentum; *v)* a collector, placed at the end of the analyser tube where the molecules discharge and whose discharged currents are further amplified; and *vi)* a recorder which registers the amplified currents (Fiedler & Proksch, 1975; Mulvaney, 1993).

The analysis was carried out by loading the samples (packed into tin capsules)[7] into the EA auto-sampler. Each sample is dropped into a furnace-reactor set at 1030°C[8] where the samples are combusted to their gas species, *i.e.* CO_2, H_2O and N_2O (Owens & Rees, 1989; Mulvaney, 1993). Just after the sample is dropped, oxygen is injected to help the combustion, increasing the temperature of the reactor to ~1600°C[9]. The gases are further carried within a helium stream through the reactor, which is filled with chromium oxide (a catalyst) and silvered cobalt (a halides trap). The gases then pass through a second reactor filled with reduced copper wires and set to 650°C[8], where N_2O is reduced to N_2. The mixture of gases then flows through a H_2O trap and a gas

[4]At the ACMA-Isotope Unit, Dental School, University of Newcastle.

[5]At the IRMS Lab, School of Ocean and Earth Scince, Southampton Oceanography Centre, University of Southampton.

[6]The ^{15}N atom percent is also referred to as ^{15}N percent abundance or ^{15}N percent enrichment.

[7]Preparation of samples is described later in subsections 2.5.2 and 2.5.3.

[8]Michael Bolshaw *pers., comm.,* 2004, IRMS Lab, School of Ocean and Earth Scince, Southampton Oceanography Centre, University of Southampton.

[9]Gillian Taylor *pers., comm.,* 2004, ACMA-Isotope Unit, Dental School, University of Newcastle.

chromatography column (held at a constant temperature of ~48°C[9]) where the N_2 and CO_2 are separated. The purified N_2 and CO_2 are thus admitted into the IRMS. Integration of the ion beams of standards and samples allow the determination of total N and C, as well as the isotopic ratios (Preston & Owens, 1983; Owens & Rees, 1989). Analyses were carried out using two different sensitivity methods; a low sensitivity method for ^{13}C and ^{15}N (sensitivity = 1 nA 3 μg-C^{-1} and 1 nA 8 μg-N^{-1}) and a high sensitivity only for ^{15}N samples (sensitivity = 1 nA 2.7 μg-N^{-1}). When only ^{15}N was determined, a CO_2 trap was also used, connected after the H_2O trap. Standards were prepared by *i)* weighing solid standards into tin capsules containing 13 or 18 mm precombusted (500°C, 4 h) GF/F filters, and by *ii)* absorbing standard solutions onto GF/F filters (prepared as above) which were subsequently dried (4 h, <60°C) and then packed into tin capsules. Analytical grade leucine ($C_6H_{13}NO_2$), caffeine ($C_8H_{10}N_4O_2$), tyrosine ($C_9O_3H_{11}N$), urea ($CO(NH_2)_2$) and ^{15}N-labelled ammonium sulphate ($(^{15}NH_4)_2SO_4$) were used for this purpose. Calibration standards were prepared from 9-60 μg-N and 4-40 μg-C for the low sensitivity method, and from 1.8-28 μg-N for the high sensitivity method. Blanks were prepared by packing GF/F filters into tin capsules. All raw data was blank-corrected. Additional information is presented in Appendix A.0.5.

2.4.3 Chlorophyll *a* determination

Stored frozen filters for chlorophyll *a* (**Chl-*a***) determination were placed in 15 mL centrifuge tubes and 8 mL of 90% acetone were then added. Chl-*a* was subsequently extracted by sonicating the samples for 30 sec followed by centrifuging the tubes for 10 min at 3000 rpm. A sonicator probe (Vibra Cell, Sonics and Materials) set at 5 output control and 50% pulser duty-cycle was used. The Chl-*a* concentration of the extract was eventually obtained by measuring the fluorescence of the sample in a Turner 10-AU fluorometer (with digital readout and automatic sensitivity adjustments). The performance of the analysis is based on the method described by Welschmeyer (1994), which consist of optimising the lamp/filter combination of the fluorometer making the readings specific for Chl-*a* (and chlorophyllide *a*). The fluorometer was calibrated daily by measuring the fluorescence of a diluted Chl-*a* standard in triplicate (Sigma). The concentration of the standard was determined weekly following the spectrophotometric method described by Parsons *et al.* (1984). The calibration settings of the fluorometer were thus updated whenever the standard concentration changed. Finally, the actual concentration of the samples was calculated by taking into account the volume of estuarine water filtered and the volume of the extract as follows,

$$\textbf{Chl-}\boldsymbol{a}(\mu\text{g L}^{-1}) = [Chl - a]_{EXT} \times \frac{V_A}{V_S} \tag{2.5}$$

Where **Chl-*a*** is the actual concentration of the sample in μg L^{-1}, $[\textbf{Chl-}a]_{EXT}$ is the chlorophyll concentration of the extract in μg L^{-1}, V_A is the volume of acetone (8 mL in this case) and V_S is the volume of water sample filtered (50 mL during this work).

2.4.4 Alkalinity determination

The alkalinity of estuarine samples was determined in the lab using a potentiometric titration technique with single acid addition. Briefly, the pH (to 3 decimal places) and temperature of a 20 mL sample was measured in triplicate using a Mettler Δ-3500 pH meter equipped with an InLab 418 pH probe. The pH of the sample was determined both before and after the gradual addition of 0.01 N HCl. Acid additions of on average 5.6$\pm$0.3 mL were made using a 665 Dosimat Ω-Metrohm with keypad, and were stopped when the pH was in the range 3-4 (overall 3.8). The pH meter was calibrated daily using Sigma buffer solutions of pH 4, 7 and 10. In this way, the volume of sample, acid concentration and volume of acid added were used to calculate alkalinity with the following formula,

$$A_T = \left(\frac{1000}{V_S} \times V_A \times N - \frac{1000}{V_S} \times (V_S + V_A) \times \frac{a_H}{f_H} \right) \times \frac{1000}{\sigma} \times 1000 \qquad (2.6)$$

where $\boldsymbol{A_T}$ is the total alkalinity (μmol kg^{-1}), $\boldsymbol{V_S}$ is the sample volume (mL), $\boldsymbol{V_A}$ is the volume of acid added (mL), $\boldsymbol{N}$ is the normality of the acid, $\boldsymbol{a_H}$ is the proton activity (10^{-pH}) and $\boldsymbol{f_H}$ is an empirical coefficient which is a function of the chlorinity or salinity, and σ is the estuarine water density. The information summarised above was taken from Parsons *et al.* (1984), Boss (1996), Anderson *et al.* (1999) and D. A. Crawford (*pers., comm.*).

2.5 ^{15}N and ^{13}C tracer incubation experiments

2.5.1 The technique

Incubations were carried out according to the ^{15}N-tracer method described by Dugdale & Goering (1967). The ^{15}N-tracer method, which has been widely used (*e.g.* Glibert, 1982; Bronk & Glibert, 1991, 1993a,b; Slawyk & Raimbault, 1995; Bronk *et al.*, 1998; Slawyk *et al.*, 1998; Tremblay *et al.*, 2000; Raimbault *et al.*, 2000) consists of the enrichment of a natural seawater sample with a known quantity of a ^{15}N isotopically labelled compound (*e.g.* $K^{15}NO_3$, $^{15}NH_4Cl$, $CO(^{15}NH_2)_2$). The addition of the tracer should be ideally $\leq$10% of that of the ambient N-nutrient concentration, since a greater enrichment could stimulate the phytoplankton activity (Dugdale & Goering, 1967) and the result could be overestimated (Glibert & Capone, 1993). This is particularly true for oligotrophic systems, where the nutrient levels are close to the limit of detection (Glibert & Capone,

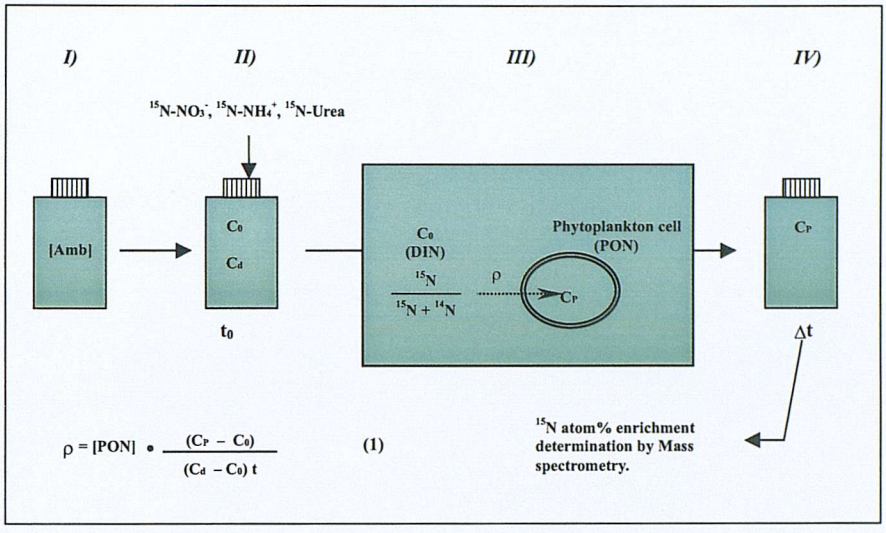

Figure 2.2: **Schematic representation of the nitrogen labelled (^{15}N) uptake technique.** *I)* Sample collected for incubation with ambient nutrient concentrations ([Amb]). *II)* Addition of ^{15}N-tracer (*e.g.* ^{15}N-nitrate, ^{15}N-ammonium, ^{15}N-urea). *III)* Nitrogen uptake. *IV)* End of incubation; sample is filtered and particulate nitrogen collected for determination of ^{15}N atom % enrichment by mass spectrometry. Net uptake rate is calculated with equation **(1)**, which is defined as follows. ρ, uptake rate. **[PON]**, particulate nitrogen concentration. $\mathbf{C}_p$, concentration of the N label (atom % ^{15}N) in the particulate phase after incubation. $\mathbf{C_0}$, concentration of the N label (atom % ^{15}N) in the particulate phase (nominator) or in the dissolved phase (denominator) at time 0. $\mathbf{C}_d$-$\mathbf{C_0}$, concentration of the N label (atom % ^{15}N) in the dissolved phase at time 0 and **t**, incubation time.

1993). Thus, the transport of the tracer into different particulate or dissolved pools is then monitored with time. This is achieved by measuring the change in isotopic enrichment (^{15}N:^{14}N ratio) in the substrate and particulate fractions (Glibert & Capone, 1993). A schematic representation showing the fundamentals of this technique is presented in **Fig. 2.2**. However, since a proportion of the nitrogen taken up can either be regenerated as ammonium or released as dissolved organic nitrogen during the incubation, it must be noted that figure Fig. 2.2 represents a **net uptake** rather than a **total** (*i.e.* **gross**) **uptake** of nitrogen (Bronk *et al.*, 1994). The equations presented in the following subsection are used to clarify the method.

2.5.1.1 Calculation of nitrogen and carbon uptake rates.

The equations used to calculate nutrient uptake rates have been presented (*e.g.* Dugdale & Goering, 1967; Fiedler & Proksch, 1975; Harrison, 1978; Caperon *et al.*, 1979; Glibert *et al.*, 1982; Bronk & Glibert, 1991, 1993a,b; Glibert & Capone, 1993; Slawyk & Raimbault, 1995; Bronk *et al.*, 1998; Slawyk *et al.*, 1998), reviewed and discussed (*e.g.* Fisher & Haines, 1979; Slawyk *et al.*, 1979; Dugdale & Wilkerson, 1986; Kanda *et al.*, 1987; Glibert & Garside, 1989; Legendre & Gosselin, 1996; Bronk & Ward, 2000; Slawyk *et al.*, 2000) in several publications. For consistency with most recent works, the notation used or recommended by Glibert & Capone (1993), Bronk *et al.* (1994, 1998) and Bronk &

Ward (2000) was adopted in this work.

Net uptake rate

The transport rate $\boldsymbol{V}$ of an inorganic ^{15}N-nitrogen species from a dissolved inorganic nitrogen pool $\boldsymbol{DINat\%_{XS}}$ (*i.e.* C_d–C_0 in Fig. 2.2) into the particulate nitrogen fraction $\boldsymbol{PNat\%_{XS}}$ (*i.e.* C_p–C_0 in Fig. 2.2) after a given time $\boldsymbol{t}$, can be expressed as

$$V = \frac{PN\text{at}\%_{XS}}{DIN\text{at}\%_{XS} \times t} \tag{2.7}$$

where the subscript at$\%_{XS}$ denotes the ^{15}N atom percent excess (*i.e.* ^{15}N enrichment) in the respective nitrogen pool, and the transport rate has therefore units of $\mathbf{t}^{-1}$ (*e.g.* h^{-1} or d^{-1}). Thus, this transport rate multiplied by the concentration of particulate organic nitrogen [PON] defines the net nitrogen uptake rate ρ, and equation (1) in figure 2.2 can be re-written as,

$$\rho = [\text{PON}] \times \frac{PN\text{at}\%_{XS}}{DIN\text{at}\%_{XS} \times t} \tag{2.8}$$

with units of mass per volume per time (*e.g.* μmol L^{-1} h^{-1}). In this way, in order to satisfy the terms in Eq. 2.8 the following are required; the concentration of DIN and PON, the percentage enrichment of the PN as determined by mass spectrometry, the ^{15}N percentage enrichment and concentration in the sample of the ^{15}N-tracer added, and the natural abundance (atom percent) of ^{15}N (*e.g.* 0.3663%, Bury *et al.* 1995, 2001). The calculation can be illustrated with the following example. During a 4 h incubation experiment a given volume of estuarine water sample has been enriched to a concentration of 0.1 μmol L^{-1} with ^{15}N enriched (99.1%) $K^{15}NO_3$. The measured NO_3^- concentration of the sample was 6.9 μmol L^{-1}. The concentration of PON collected by filtration at the end of the incubation was 25.6 μmol L^{-1} and was 0.5735% enriched with ^{15}N as determined by mass spectrometry. Assuming a natural ^{15}N abundance of 0.3663%, the calculation proceeds as follows,

$$\rho = 25.6 \times \left(\frac{0.5735 - 0.3663}{\left(\frac{(6.9 \times 0.3663) + (0.1 \times 99.1)}{6.9 + 0.1} - 0.3663 \right) \times 4} \right) = 0.94 \tag{2.9}$$

The net nitrate uptake rate in this example is thus 0.94 μmol L^{-1} h^{-1}.

Gross uptake rate

In order to calculate the gross uptake rate of nitrate, the ^{15}N atom % enrichment of the particulate nitrogen (*i.e.* gross atom % enrichment of the PN) must be first corrected for any loss of the label to the dissolved organic fraction. This correction is given by,

$$PN_G\text{at}\%_{XS} = \frac{([\text{PN}] \times PN\text{at}\%_{XS}) + ([\text{DON}] \times DON\text{at}\%_{XS})}{[\text{PN}]} \tag{2.10}$$

where $PN_G at\%_{XS}$ denotes gross atom % enrichment of the PN, [PN] and [DON] are the concentrations of the particulate and dissolved organic nitrogen at the end of the incubation time, and $PNat\%_{XS}$ and $DONat\%_{XS}$ are the ^{15}N excess in the particulate and dissolved organic fractions. A small amount of standard was used as a carrier (explained later in subsection 2.5.3), and its addition needs to be considered in the calculations. For instance, the DON at% enrichment is calculated and corrected for the carrier as follows.

$$DONat\% = \frac{(at\% \times ([\text{DON}] + [Std_{Carr}])) - ([Std_{Carr}] \times \text{Nat at\%})}{[\text{DON}]} \tag{2.11}$$

Where at% is the atom percent enrichment of ^{15}N of the sample as measured by mass spectrometry, $[\text{Std}_{Carr}]$ is the concentration of the standard used as a carrier, Nat at% is the natural ^{15}N abundance (*i.e.* 0.3663%), and the other terms are as above. In this way, $PN_G at\%_{XS}$ (Eq. 2.10) can be substituted for $PNat\%_{XS}$ in Eq. 2.8, and in turn, the gross uptake rate (ρ_G) can now be defined as,

$$\rho_G = \frac{([\text{PN}] \times PNat\%_{XS}) + ([\text{DON}] \times DONat\%_{XS})}{DINat\%_{XS} \times t} \tag{2.12}$$

where the gross uptake rate is expressed in units of mass per volume per time (*e.g.* μmol L^{-1} h^{-1}).

Dissolved organic nitrogen release

The dissolved organic nitrogen release rate can thus simply be calculated as the difference between the gross uptake rate and the net uptake rate (Bronk *et al.*, 1994),

$$DON_{REL} = \rho_G - \rho \tag{2.13}$$

where DON_{REL} is the release rate of dissolved organic nitrogen in units of mass per volume per time (*e.g.* μmol L^{-1} h^{-1}), and the other terms are defined as above. As can be seen from the equations above, the measurement of dissolved organic nitrogen and the ^{15}N enrichment of this pool are required in order to satisfy the terms of the equations.

Ammonium uptake and regeneration

One of the basic assumptions of the uptake model (Eq. 2.8) is that the ^{15}N atom % enrichment (*i.e.* $DINat\%_{XS}$ in Eq. 2.8) remains constant through the incubation time (Glibert *et al.*, 1982). Nonetheless, when a natural sample is enriched with a ^{15}N-labelled compound such as ammonium (or urea, for example), the regeneration of unlabelled substrate (*e.g.* due to bacterial remineralization of organic matter, excretion by grazers or zooplankton sloppy feeding) gradually reduces (*i.e.* dilutes) the atom % enrichment (Glibert *et al.*, 1982; Glibert & Garside, 1989). It is possible however, to account for the dilution effect and therefore estimate the ammonium regeneration rate. In this work, the

dilution model described by Glibert *et al.* (1982) and Glibert & Capone (1993), which is based on the models of Caperon *et al.* (1979) and Blackburn (1979) has been used. Also, the terminology used by Glibert *et al.* (1982) is adopted. Reviews, formulae derivation and modification of the dilution model can be found in several works (*e.g.* Garside & Glibert, 1984; Laws, 1984, 1985; Kanda *et al.*, 1987; Glibert, 1988; Glibert & Garside, 1989).

Regeneration

If it is assumed that the regeneration (*i.e.* dilution) and uptake rates are constant with time and that the label is not regenerated during the incubation, the ambient concentration of NH_4^+ as a function of time can be expressed as,

$$P_{(t)} = P_0 + (d - i)t \tag{2.14}$$

where $P_{(t)}$ and P_0 are the ambient NH_4^+ concentrations at time t and time zero, d is the dilution rate and i is the net uptake rate. By further assuming that the uptake is similar for both ^{14}N and ^{15}N (*i.e.* isotopic fractionation is negligible), then the change in the ^{15}N atom % enrichment of the ammonium pool as a function of time *R(t)*, is given by,

$$\frac{dR(t)}{dt} = -d \times \frac{R(t)}{P(t)} \tag{2.15}$$

where *P(t)* is the ammonium pool size (*i.e.* $^{14}N + {}^{15}N$) as a function of time and the other terms are defined as above. In this way, d and i can be calculated by simultaneously solving Eqs., 2.14 and 2.15 to yield,

$$ln(R_{(t)} - \text{Nat at\%}) = ln(R_0 - \text{Nat at\%}) - \left[\frac{d}{d-i}\right]\left[ln\frac{P_{(t)}}{P_0}\right] \tag{2.16}$$

where all the terms are as previously defined. Also, the calculation has been improved by correcting $R_{(t)}$ and R_0 for the ^{15}N natural abundance (Nat at%), *i.e.* to obtain the $at\%_{XS}$. With some simple algebraic manipulations d and i can be solved for. The dilution of the isotope with time is therefore an exponential function which depends on the initial ^{15}N atom % enrichment, the uptake and remineralization rates and the concentration of NH_4^+ at the beginning and at the end of the incubation (Glibert *et al.*, 1982).

Uptake

Knowing the change in the ^{15}N atom% of the ammonium substrate during the incubation, the calculation of the ammonium uptake can also be improved. Given that,

$$R_{(t)} = R_0[e^{(-kt)}] \tag{2.17}$$

where

$$k = -\frac{ln[\frac{R_{(t)}}{R_0}]}{t} \tag{2.18}$$

an exponential average $\bar{R}$ between R_0 and $R_{(t)}$, which takes into account the dilution of the isotope, can be calculated by integrating $R_{(t)}$ from time zero to time t,

$$\overline{R} = \frac{R_0}{t}\int_0^t [e^{(-kt)}]dt \tag{2.19}$$

to give,

$$\overline{R} = \frac{R_0}{kt}[1 - e^{(-kt)}] \tag{2.20}$$

this average can thus be substituted by $DIN\text{at}\%_{XS}$ in Eq. 2.8, and using a capital 'ρ' to denote the corrected net uptake rate $P_{NH_4^+}$, a new equation can be written as follows,

$$P_{NH_4^+} = [\text{PN}] \times \frac{PN\text{at}\%_{XS}}{\overline{R} \times t} \tag{2.21}$$

where $P_{NH_4^+}$ has units of mass per volume per time (*e.g.* μmol L^{-1} h^{-1}).

Carbon net uptake rate.

The net carbon uptake rate is calculated with the same model used to calculate the net nitrogen uptake rate (*e.g.* Slawyk *et al.*, 1977, 1979; Fisher & Haines, 1979; Hama *et al.*, 1983; Bury *et al.*, 1995). In this way the particulate organic carbon concentration [POC] of a sample collected by filtration at the end of an incubation is substituted for [PON] in Eq. 2.8 and the ^{13}C atom % enrichment, as determined by mass spectrometry, is substituted for $PNat\%_{XS}$. The ^{13}C atom % enrichment of the dissolved fraction is in turn substituted for $DINat\%_{XS}$. In this research the concentration of total dissolved inorganic carbon (C_t) was estimated from pH measurements and alkalinity determinations (§ 2.4.4), and calculated using thermodynamic equations and constants, plus salinity and temperature (expressed as absolute temperature, *i.e.* °K) measurements *in situ* and in the water samples. Thus, using *i)* the following stability constants,

$$K_1 = \frac{HCO_3^-\{H^+\}}{H_2CO_3^*} \tag{2.22}$$

$$K_2 = \frac{CO_3^{2-}\{H^+\}}{HCO_3^-} \tag{2.23}$$

$$K_B = \frac{B(OH)_4^-\{H^+\}}{B(OH)_3} \tag{2.24}$$

$$K_W = \frac{\{\mathrm{H^+}\}}{[\mathrm{OH^-}]} \tag{2.25}$$

ii) the following mass balance equations,

$$A_T = \mathrm{HCO_3^-} + 2\mathrm{CO_3^{2-}} + \mathrm{B(OH)_4^-} - \{\mathrm{H^+}\} + [\mathrm{OH^-}] \tag{2.26}$$

$$C_T = \mathrm{H_2CO_3^*} + 2\mathrm{HCO_3^-} + \mathrm{CO_3^{2-}} \tag{2.27}$$

$$Ca = [H_2CO_3] + [CO_2(aq)] \tag{2.28}$$

$$B_T = \mathrm{B(OH)_3} + \mathrm{B(OH)_4^-} \tag{2.29}$$

and *iii)* the definition of carbonate alkalinity (A_C),

$$A_C = \mathrm{HCO_3^-} + 2\mathrm{CO_3^{2-}} \tag{2.30}$$

it is possible to solve for A_C and total carbon (C_T), given the measurements of pH and alkalinity of a water sample. Hence, the following equations emerge

$$A_C = A_T + \{\mathrm{H^+}\} - \frac{K_W}{\{\mathrm{H^+}\}} - \frac{B_T}{\left(1 + \frac{\{\mathrm{H^+}\}}{K_B}\right)} \tag{2.31}$$

$$C_t = \frac{A_C\left(\frac{\{H^+\}^2}{K_1} + \{H^+\} + K_2\right)}{\{H^+\} + 2K_2} \tag{2.32}$$

The calculation of the different constants were taken from the works of Roy *et al.* (1993, 1994), Dickson (1990), Hansson (1973) cited by Anderson *et al.* (1999), and Dickson & Riley (1979). Complementary information, revision of constants, and derivation of equations were taken from several works (*e.g.* Culberson & Pytkowicz, 1973; Weiss, 1974; Millero, 1979; Anderson & Wedborg, 1985; Millero *et al.*, 1993). The equations presented here are based on the descriptions given by Morel (1983), Copin-Montégut (1996) and Anderson *et al.* (1999). The calculation of C_T was facilitated by using a spreadsheet written by D. A. Crawford[10] which is based on the equations described above.

[10]David. A. Crawford *pers., comm.*, 2001, Southampton Oceanography Centre.

2.5.2 Experiments carried out in 2001.

On returning to the lab from the sampling surveys water samples collected from 2 m depth were sub-sampled from the carboys, and divided into five sets of three separate 500 mL polycarbonate bottles per station. Additions were then made of ^{13}C-HCO_3 ($NaH^{13}CO_3$ 98.8 atom % ^{13}C) and ^{15}N-NO_3 ($K^{15}NO_3$ 99.1 atom % ^{15}N) both in the same bottle, ^{15}N-NH_4 ($Cl^{15}NH_4$ 99.2 atom % ^{15}N), and ^{15}N-urea ($CO(^{15}NH_2)_2$ 99.0 atom % ^{15}N), to a concentration of 0.1 μmol L^{-1} for nitrogen tracers and to 0.1 mmol L^{-1} for the carbon tracer. The incubation bottles were gently shaken after the tracer additions. In order to make tracer additions of 0.1 mL, thus having minimal impact on the salinity of the sample, stock solutions were prepared at a concentration of 500 μmol L^{-1} for ^{15}N-tracers, and 500 mmol L^{-1} for the ^{13}C-tracer. A PAR profile was measured from the pontoon[11], and the depth of the 100%, 50%, 10% and 1% of the subsurface PAR was estimated. Incubations were thus set up by deploying the bottles *in situ* at 4 photic depths plus a set of bottles in the dark (**Fig. 2.3**). Dark conditions were achieved by covering the bottles with thick black plastic bags. All incubations were initiated at about 13:00 h GMT and were terminated after 4 h by filtration of the sample (20 mL in duplicate) through precombusted (500°C, 4 h) GF/F filters (13 mm diameter). In order to avoid cell rupture and thus release of tracer from the particulate fraction, filtrations were done at low vacuum (<150 mm Hg) using three 60 mL filtration units simultaneously. Individual filtration times were ~5 min. Filters were rinsed with pre-filtered seawater (from the respective station) to remove the excess of tracer, and then stored frozen in duplicate in Petri slides. Before determination of the tracer present in the particulate fraction, filters were dried (24 h at <60°C), and packed into tin capsules. Natural abundance values from plankton samples reported in the literature of 0.3663% and 1.092% for ^{15}N and ^{13}C respectively, were used to calculate uptake rates (Bury *et al.*, 1995, 2001). Neither the regeneration of ammonium, nor the release of dissolved organic nitrogen were accounted for during the experiments in 2001, therefore the values reported are net uptake rates (see § 2.5.1).

2.5.3 Experiments carried out in 2002.

Experiments in 2002 were designed to account for the ammonium isotope dilution and therefore to estimate ammonium regeneration, and to quantify the release of dissolved organic nitrogen from two nitrogen sources; ammonium and nitrate. Thus, on returning to the lab from the sampling surveys, water samples collected from 1 m depth were sub-sampled and divided as follows:

1) A set of two 500 mL polycarbonate bottles per station were filled with water sample

[11] Water front, Southampton Oceanography Centre.

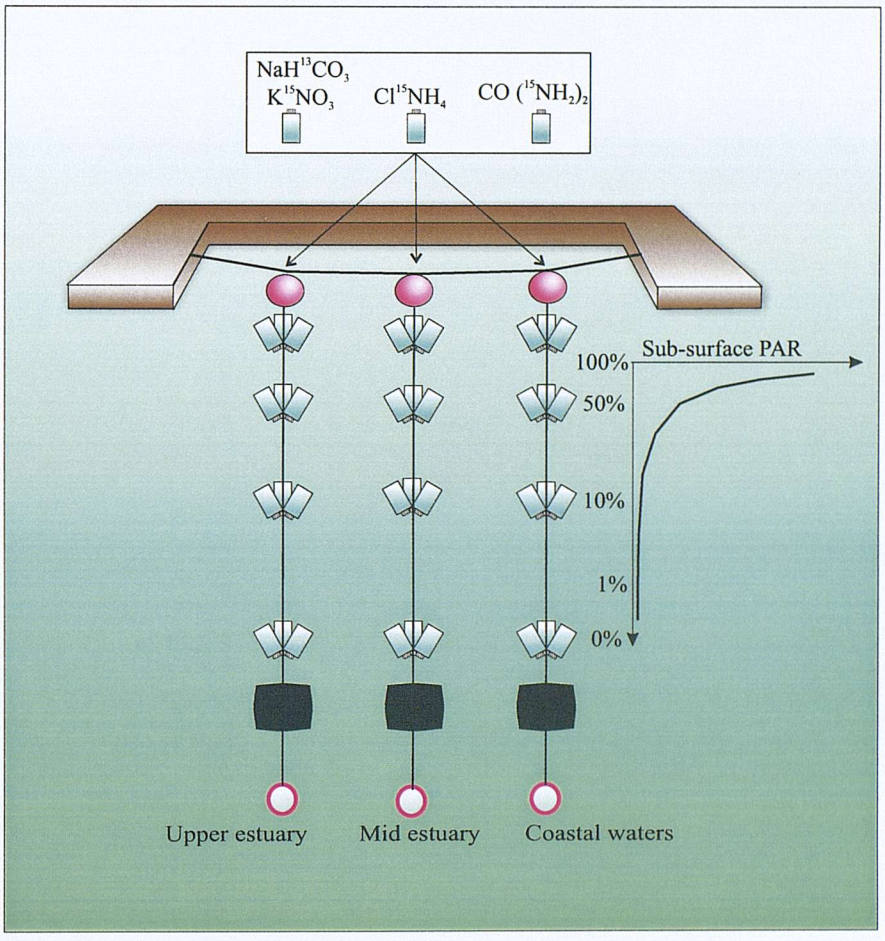

Figure 2.3: **Schematic representation of in situ incubation experiments in 2001**; suspended from the pontoon, waterfront Southampton Oceanography Centre.

and separate additions of ^{15}N-NO_3 and ^{15}N-NH_4 were then made to a concentration of 0.2 μmol L^{-1} for nitrate label and to a concentration of 0.15 μmol L^{-1} for the ammonium label. This set of bottles was designed as the initial conditions of the incubations (*i.e.* DON concentration at time 0, and particulate nitrogen (**PN**) atom percent enrichment at time 0). Therefore, just after the tracer additions the bottles were gently mixed and 300 mL of water immediately filtered through precombusted (500°C, 4 h) GF/F filters (47 mm diameter) using a glass filtration unit (35 or 32 mm diameter) and a hand vacuum pump. The filters were rinsed with pre-filtered seawater (from the respective station) to remove any excess of the ^{15}N-tracer and were kept frozen in Petri slides until processing for ^{15}N determination by mass spectrometry. 100 mL of the filtrate were collected in pre-combusted (550°C, 4 h) brown-glass bottles and then stored frozen for later determination of total dissolved nitrogen (**TDN**). In order to avoid a large period of time filtering initial condition ^{15}N-labelled bottles and an enormous amount of new generated samples and filters, all bottles labelled with $^{15}NO_3$ designed as the initial conditions of the incubations were processed as above. However, incubation bottles labelled with $^{15}NH_4$ were processed on a random basis, and were assumed to be representative of the initial conditions of the ^{15}N-ammonium incubations. Filtration of all samples designated as initial conditions on a given date lasted for ~30 min.

2) At the same time step '1' (above) was being carried out, four (500 mL) polycarbonate bottles per station were filled with water sample, and tracer additions were made (as above). Only on the first date of tracer experiments, two bottles per station were deployed at 0.5 m (~65% of subsurface PAR) and two bottles per station were deployed at the same depth but covered with dark-plastic bags (*i.e.* dark conditions). On all the following dates a PAR profile was measured from the pontoon just after the ^{15}N-tracer additions, and the depth of the 100% and 50% of the subsurface PAR was determined. Thus, incubations were set up by deploying the bottles in situ at 2 photic depths (**Fig. 2.4**). These two photic depths were aimed to target the highest nutrient uptake and release rates. Incubations were initiated at about 13:00 h GMT and were terminated by filtration after 4 h. 300 mL of sample were filtered through precombusted 47 mm diameter GF/F filters (as above). The filters were rinsed with pre-filtered seawater (from the respective station) and were kept frozen in Petri slides until preparation for ^{15}N enrichment determination. From the filtrate, an aliquote of 100 mL of water was collected and stored frozen in precombusted brown-glass bottles. This water was later used to measure TDN, and to determine the ^{15}N atom percent enrichment of the ammonium and dissolved organic nitrogen (DON) pools. Special care was taken at this step to retain the filtrate before the filters were rinsed with pre-filtered seawater. No further filtration was done through a smaller pore-size filter, therefore during this research the DON is operationally considered as the sample recovered from the GF/F (0.7 μm nominal pore- size) filtrates. From the

sample remaining in the incubation bottles, 50 mL of water were filtered through a 25 mm diameter GF/F filter (as in § **2.3**) and samples directly collected into brown-glass bottles containing 2 mL of phenol solution. These samples were stored in a fridge for later ammonium analysis. The concentration of ammonium at the end of the incubation is required to calculate the isotope dilution, and therefore to estimate the regeneration rate of ammonium (Glibert *et al.*, 1982). A further volume of water (50 mL) was filtered and collected into 2 plastic vials. These samples were stored frozen for later determination of nitrate and phosphate. The filters used were also kept frozen (as in § **2.3**) for later determination of chlorophyll *a*. These measurements were done in order to investigate possible changes in the concentration of a given variable during the incubation period. **3)** Filtrates from the **incubations with ^{15}N-ammonium** were defrosted and homogenised by gently mixing the bottle. 20 mL of the sample were used to measure TDN. The remaining 80 mL were equally split in two and thus, duplicate 40 mL aliquots were processed using **steam distillation** to remove and collect the ammonium, and to isolate the DON. A detailed description of the steam distillation procedure is presented below. The ammonium and DON once separated, were **concentrated by evaporation** (for ~7 h at 80°C) down to ~4 mL. At this volume the salt in the water started to precipitate, however this process did not seem to have a major effect on the sample[12]. The concentrate was absorbed (200-500 μL) on a precombusted GF/F filter (13 mm) which was subsequently dried (24 h at <60°C) and packed into tin capsules for ^{15}N determination. Just before drying the filters, a 1 μmol spike of either N-urea or N-ammonium -for organic and inorganic nitrogen species respectively- was added as carrier (50 μL of a 20 mmol L^{-1} N-urea or N-ammonium solution) to provide enough nitrogen for mass spectrometric analysis. The carrier addition was accounted for in the calculations of the uptake rates according to the equations presented in subsection **2.5.1.1**. The concentrate containing DON also contained unlabelled nitrate, which was not physically removed. However, as the concentration of nitrate was measured at the end of the incubation, the atom percent enrichment of DON was mathematically corrected.

4) Filtrates from the **incubations with ^{15}N-nitrate** were defrosted and homogenised as above. 20 mL of the sample were also used to measure TDN and the remaining 80 mL equally split in two. Thus, duplicate 40 mL aliquots were processed with **magnesium oxide (MgO)** and **DeVarda's alloy (DV)** to remove the ammonium and nitrate, and to isolate the DON. Once the reaction was completed, the sample was filtered through a precombusted GF/F filter to remove the excess MgO and DV. A detailed description of this procedure is presented below. The sample containing the isolated DON was then concentrated by evaporation and filters prepared to measure ^{15}N atom percent enrichment (as above).

[12]Glibert PM, *pers., comm.*, September 2003.

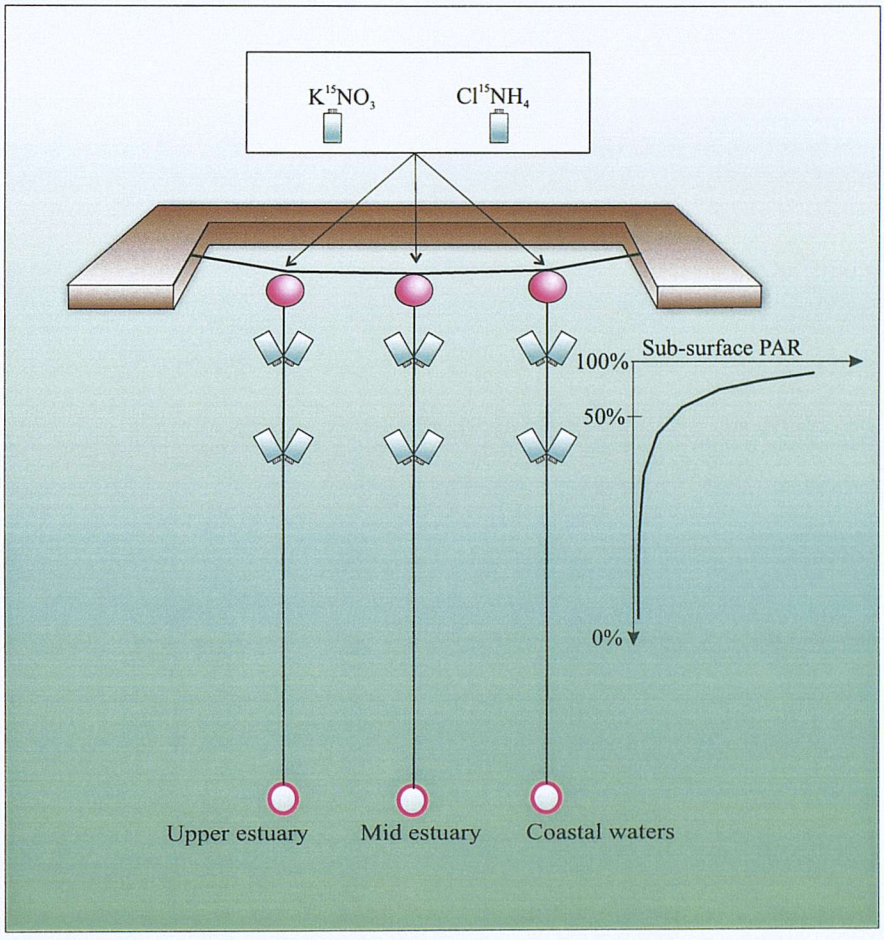

Figure 2.4: **Schematic representation of in situ incubation experiments in 2002**; suspended from the pontoon, waterfront Southampton Oceanography Centre.

5) GF/F filters (47 mm diameter) stored frozen in the Petri slides were dried for 24 h at ~60°C, and then a filter punch used to produce duplicate cut filters (17.5 mm diameter). Special care was taken at this step to avoid loss of the particulate material collected. The duplicate cut filters were then packed into separate tin capsules for determination of the ^{15}N atom % enrichment.

2.5.3.1 Isolation of the Dissolved Organic Nitrogen pool

A combination of chemical and physical techniques were applied in order to remove the ^{15}N-ammonium and ^{15}N-nitrate present in the filtrates at the end of the incubations, and therefore to isolate the dissolved organic nitrogen pool. The isolated nitrogen pools can then be prepared for determination of the ^{15}Natom percent enrichment, which is required to calculate nutrient uptake, regeneration and release rates. ^{15}N-ammonium incubations were conducted to calculate the regeneration of ammonium, to correct the ammonium uptake rates for isotopic dilution and to quantify the release of DON. The steam distillation technique allows isolation of DON by removing the ammonium from a sample, and at the same time allows the collection of the ammonium evolved. Incubations with ^{15}N-nitrate were conducted to calculate the nitrate uptake rates and to quantify the release of DON. In this case, chemical reactions are carried out to remove the ammonium and nitrate present in the filtrate. The techniques applied on each type of incubation are described in detail below.

- **Isolation of DON by Steam Distillation**

Fundamentals: the pK_a value of the acid-base pair NH_4^+-NH_3 is 9.3 (Stumm & Morgan, 1996), consequently, at the mean pH of seawater (~8.2) the ammonium ion is the dominant species (see **Fig. 2.5**). The steam distillation technique begins therefore with the addition of a base to a water sample in order to increase the pH. The increase in pH favours the presence of ammonia (*i.e.* ammonium is transformed into NH_3). Degassing of ammonia is helped by heating the sample using a hot plate. Eventually, a stream of vapour that further passes through a condenser is used as a carrier for the ammonia evolved. The liquid condensed is then collected directly into an acid trap. The acid trap having the opposite effect to that of the base used at the beginning of the distillation.

Cleaning-protocol of material used: All glassware (Quick Fit) available for the distillation was either combusted (4 h at 550°C) or left soaking in 10% HCl for 3 days. In the latter case, the material was subsequently *i)* washed with phosphate and ammonia-free liquid detergent and tap water, *ii)* rinsed with 10% HCl, *iii)* rinsed with distilled water and finally, *iv)* rinsed with Milli-Q water.

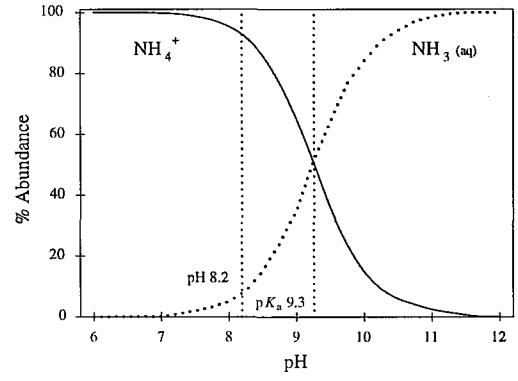

Figure 2.5: **NH_x percentage abundance in seawater as a function of the pH.** Adapted from Morel (1983).

System testing: Prior to the processing of estuarine samples the steam distillation, system and technique, were extensively tested with a series of blanks and standards containing ammonium, nitrate and urea (*i.e.* as representative of the DON pool). Nitrate was added in order to simulate the presence of all 3 N species in an estuarine sample. Standards were prepared within a concentration range (**Table 2.7**) similar to the nutrient levels measured in the estuary during this and other works (*e.g.* Hydes & Wright, 1999; Homewood, 2003). Fresh Milli-Q water was used to prepare blanks, standards and reagents.

Table 2.7: Concentration range (μmol L^{-1}) of standards prepared to test the steam distillation technique.

	Urea	Ammonium	Nitrate
Std 1	0.5	0.5	2.0
Std 2	1.0	1.0	20.0
Std 3	5.0	5.0	20.0
Std 4	10.0	10.0	40.0
Std 5	10.0	15.0	30.0
Std 6	10.0	20.0	10.0
Std 7	2.0	30.0	60.0
Std 8	50.0	30.0	80.0

Procedure (1): Distillations were carried out by pouring 40 mL of blank or standard into a 500 mL vacuum-flask. This flask was placed on a hot plate, and immediately connected to the condenser just after the addition of 1 mL of a 0.125 M sodium borate buffer-solution (Bronk & Ward, 1999). It was observed, by previous testing with estuarine water samples, that this addition increases the pH to >9. At the same time, ammonium-free water was kept boiling in an opened 500 mL flask. This flask was connected to

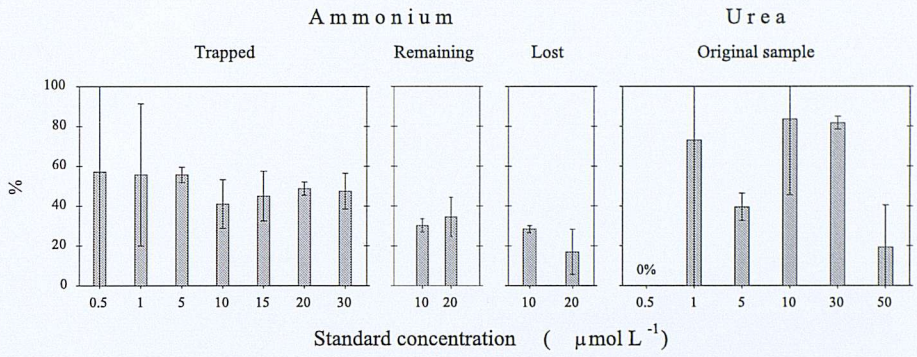

Figure 2.6: **Percentage of ammonium trapped, ammonium remaining in the original sample, ammonium lost and urea present in the original sample after steam distillations;** *procedure 1.* Error bars show either the standard difference of duplicates or the standard deviation of replicate distillations (n>2). Error bars larger than 50% are not shown complete for graph-size consistency.

the sample flask with a silicon rubber tube attached to the vacuum outlet. A plastic tube was passed through the vacuum outlet and was curved downwards to deliver the steam. The rubber tube was kept closed with a tube clamp. After 5 min, the flask containing boiling water was closed with a glass tap and the tube clamp released. The distillation was terminated after collecting 10 mL of the condensed liquid directly into a 50 mL conical flask containing 10 mL of a 0.0024 N HCl solution (Glibert & Capone, 1993). An adapted Pasteur pipette was used to deliver the condensed liquid into the acid trap. In order to avoid cross contamination, the system was carefully rinsed with ammonium free water and 'dummy' distillations (*i.e.* NH_4^+ free water and buffer) were carried out between sample distillations (either blanks or standards). The acid trap and the original sample were collected in precombusted 50 mL brown-glass bottles after each distillation, and ammonium and urea were later analysed. Ammonium was measured using the indophenol-blue method, and urea was measured using the diacetylmonoxime method (both described in § **2.4**). Data from the chemical analysis was corrected for the analytical blanks and distillation blanks. **Results** were variable and showed that only 49±19% of the **ammonium** contained in the original sample was trapped (n=27), 33±8% remained in the original sample (n=6) and 21±11% was lost (n=6); this was likely due to extreme bubbling induced in the trap before the vapour condensed. Values from the lower concentration standards were particularly variable; *i.e.* 0.5 and 1.0 μmol L^{-1} NH_4^+ (see **Fig. 2.6**). Results from the **urea** analysis were also variable and showed a recovery of 53±46% (n=21). This value was however affected by accidental contamination of the top standard, and 0% recovery of at least one of the lower standards. Recovery of urea in the range 5-30 μmol L^{-1} was 73±30% (see **Fig. 2.6** for individual standards). It was also observed that the volume in the sample flask increased about 30 mL due to condensation of the vapour and although recovery data was corrected for dilution, results were far from satisfactory. Therefore, in order to improve the method modifications were made as

follows.

Procedure (2): 40 mL of blank or standard were poured into a 100 mL vacuum-flask. This flask was then placed on a hot plate-magnetic stirrer, and connected to the condenser just after the addition of 1 mL of sodium borate buffer. The buffer solution was prepared with 25.5 g sodium borate ($NaBO_2 \cdot {}_4H_2O$) in a 500 mL solution of 0.2 N NaOH (Harrison, 1978). It was observed that 1 mL of buffer increased the sample pH to slightly higher than 10. Thus, after 5 minutes the flask with boiling water was closed and the tube clamp was released. This time the silicon tube was connected to the sample flask through a glass Quick-Fit inlet-tube. In this way the steam flux through the sample was improved and the use of a smaller flask to contain the sample helped to reduce the amount of steam condensed within it. Degassing of ammonium was improved by using 4 or 5 small Teflon-coated magnetic-stirrers (*i.e.* acting as boiling chips, but much easier to clean). Distillations were terminated after collecting 10 mL of the condensed liquid directly into a 70 mL test tube (Quick-fit) containing 10 mL of a 0.005 M sulphuric acid solution (Hasegawa *et al.*, 2000a,c,b). A glass diffuser was used to improve the delivery of the condensed liquid into the acid trap[13]. Since the ammonium trapped was to be concentrated through evaporation, sulphuric acid was preferred over hydrochloric acid; nitrogen is lost when NH_4Cl is heated at temperatures higher than 90°C, whereas $(NH_4)_2SO_4$ is stable up to 235°C (Mulvaney, 1993). In order to avoid cross contamination the system was carefully rinsed with ammonium-free water and 'dummy' distillations were also carried out. The exact volumes of the acid trap and the original sample were taken into account to calculate the mass of ammonium transferred and the mass of the urea remaining. In this way, a new series of distillations were carried out with standards prepared at the concentrations shown in **Table 2.8**. Ammonium was measured using a fluorometric method and urea was measured using the diacetylmonoxime method (both described in § **2.4**).

Table 2.8: Concentration (μmol L^{-1}) of standards prepared for testing the steam distillation technique; *procedure 2.*

	Urea	Ammonium	Nitrate
Std 1	10.0	25.0	80.0
Std 2	10.0	10.0	80.0

Results showed a relatively good improvement, with 70±3% of the **ammonium** trapped (n=10) and a 107±3% recovery of **urea** (n=5). The percentage of ammonium lost and ammonium remaining in the original sample were reduced (see **Fig. 2.7**). Isolation of the DON pool by steam distillation (as well as with DeVarda's alloy, described next)

[13]Statham P. J., *pers., comm.*, September 2003.

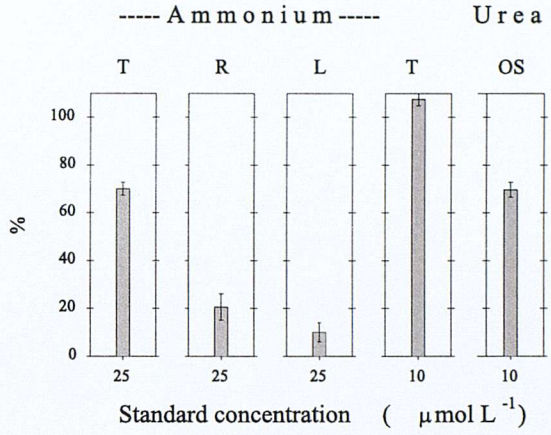

Figure 2.7: **Percentage** of ammonium **T**rapped, ammonium **R**emaining in the original sample and ammonium **L**ost after steam distillations using a 25 μmol L^{-1} ammonium standard (first three bars). Percentage of ammonium **T**rapped and urea present in the **O**riginal **S**ample after steam distillations using a 10 μmol L^{-1} ammonium and urea standard (last two bars). Results following the *procedure 2*. Error bars show standard deviations of replicate distillations (n=5 or 10).

proved to be a very time consuming and labour intensive (each distillation lasts 15 min). More than three months were fully dedicated to the setting up of this technique and no further attempt was made to improve the results. It was therefore decided to process the estuarine samples designated to measure ammonium regeneration and release of DON from $^{15}N\text{-}NH_4^+$ uptake following the ***procedure 2***. A schematic representation of the distillation system used with this procedure is shown in **Fig. 2.8**.

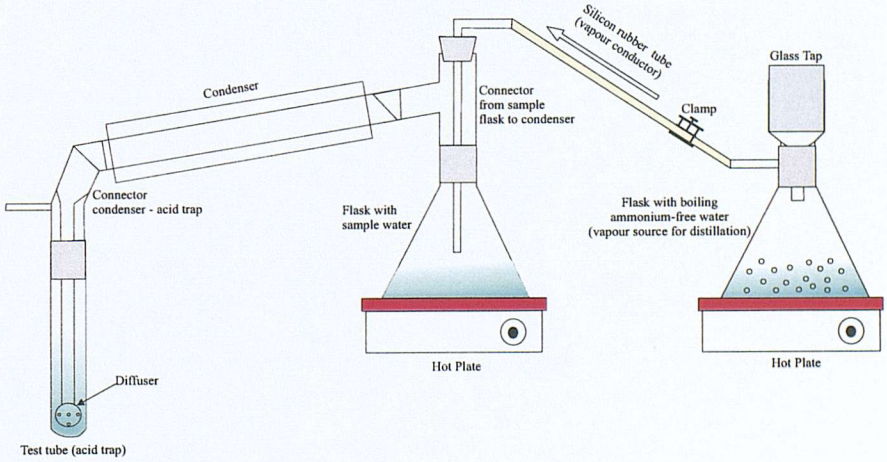

Figure 2.8: **Schematic representation of the steam distillation system** (figures not scaled).

- **Isolation of DON with magnesium oxide (MgO) and DeVarda's alloy (DV)**

Isolation of DON using this method is achieved by bringing a sample close to boiling point after the addition of a base (MgO) and a strong reducing agent (DV). In this way nitrate is reduced to nitrite, and nitrite is further reduced to ammonia. The increase in pH helps to remove the ammonium as ammonia, which is lost during the heating process. Thus, in order to test the method a series of blanks and standards were processed with MgO and DV. For this purpose, standards containing nitrate, urea and ammonium were prepared daily with fresh Milli-Q water at the concentrations shown in **Table 2.9**. As with the distillation system, a first test was carried out in order to establish reagent additions, adequate reaction time and removal/recovery of key nutrients. Urea was again used as representative of the DON pool and although ammonium was also included, complete removal was assumed and therefore was not chemically analysed. All materials required were previously washed following the cleaning protocol mentioned above (steam distillation technique). Prior to use, the MgO was combusted overnight at 500°C. The DV was manually grinded for a couple of hours with a ceramic mortar and pestle in order to increase its surface area, and therefore its reduction efficiency (Bronk & Ward, 1999). Also, in order to avoid contamination the DV was washed by stirring it on a hot plate at low temperature in a 0.01 N NaOH solution for ~1 h. After this step, the DV was rinsed with 10% HCl and then several times with Milli-Q water. Finally, the DV was dried overnight at 100°C (Bronk & Ward, 1999).

Table 2.9: Concentration range (μmol L^{-1}) of standards prepared to test the DeVarda's alloy method.

	Nitrate	Urea	Ammonium
Std 1	2.0	0.5	0.5
Std 2	5.0	0.5	0.5
Std 3	5.0	1.0	1.0
Std 4	20.0	5.0	5.0
Std 5	40.0	10.0	10.0
Std 6	60.0	2.0	30.0
Std 7	80.0	50.0	30.0

Procedure (1): A 50 mL Pyrex beaker containing 40 mL of blank or standard was placed on a hot plate-magnetic stirrer just after the addition of 1.5 mL of a saturated MgO solution and 0.5 g of DV (Bronk & Ward, 1999). A small Teflon-coated magnetic-stirrer was used to homogenise the sample at a moderate mixing rate. The pH of the sample increased to ~9.2 with the selected dose, as previously tested with 'dummy' estuarine water samples. In order to increase the temperature of the beaker contents to ~95°C,

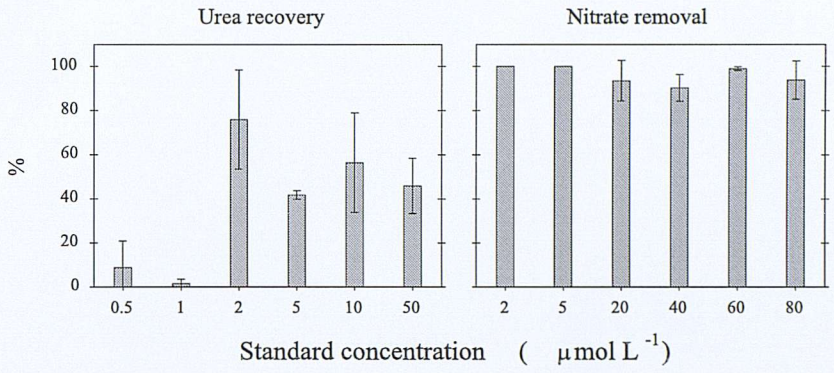

Figure 2.9: **Percentage recovery of urea and percentage removal of nitrate from samples processed with MgO and DeVarda's alloy;** *procedure 1.* Error bars show either standard differences of duplicate samples or standard deviation of replicate samples (n>3).

the temperature-settings of the hot plate available were previously tested. By keeping the temperature of sample lower than the boiling point, loss through bumping of water is avoided and decomposition of DON is reduced. Once the sample attained the target temperature (~9 min), the beaker contents were left reacting for another 30 min. After this period of time the reaction was terminated by removing the beaker from the hot plate. The contents were then allowed to cool down for about 5 min. Eventually the water was collected either in precombusted 50 mL brown-glass bottles for later analysis of urea, or in 25 mL plastic vials for later analysis of nitrate. Collection of sample was done carefully in order to avoid excess of MgO and DV. Urea was measured using the diacetylmonoxime method and nitrate was measured using a colorimetric technique (both described in § **2.4**). The interference of MgO and DV present in the samples was tested during the colorimetric analysis of nitrate. This was done by analysing several mixtures of equal amounts of a given standard or blank with a MgO/DV-processed sample. For example, a concentration of 40 μmol L^{-1} was measured by analysing a mixture of an 80 μmol L^{-1} standard with a 60 μmol L^{-1} MgO/DV-processed sample. This result suggested that the presence of MgO and DV had a negligible effect on the analysis, and that the nitrate was efficiently removed from the processed sample. No attempts were made to test the analysis of urea in a similar way. **Results** showed an average **removal of nitrate** of 96±4% (n=13), with reduced efficiency at high concentrations (see **Fig. 2.9**). **Urea** analysis however, showed an average **recovery** of only 41.4±24% (n=20), with lower recovery at low concentrations (see Fig. 2.9). Apparently low recovery of DON is due to the harsh conditions produced by the DV (Bronk & Ward, 1999). Nevertheless, as the recovery of urea was low, slight modifications were made in order to improve the technique.

Procedure (2): For the purpose of this further test a single standard containing urea, nitrate and ammonium at concentrations of 10.0, 80.0 and 25.0 μmol L^{-1} respectively, was prepared. Several simultaneous processing of blanks and standard were carried out,

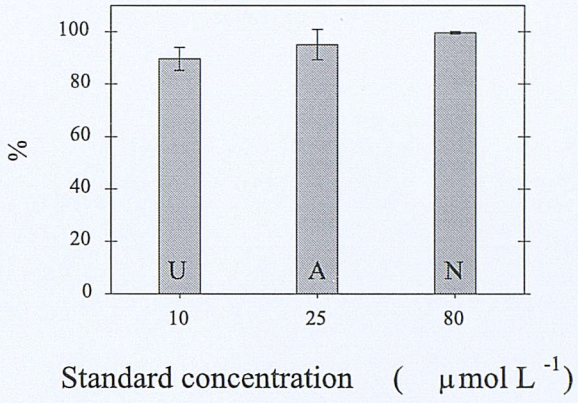

Figure 2.10: **Percentage recovery of urea, and percentage removal of nitrate and ammonium from samples processed with MgO and DeVarda's alloy;** *procedure 2.* **U** stands for urea, **A** for ammonium and **N** for nitrate. Error bars show standard deviation of replicate samples.

and removal of ammonium was this time verified. The same volume of sample (standard or blank) and the same beaker size described above were used. A larger hot plate (non-magnetic stirrer function) with a more homogeneous surface temperature was used this time. A new magnesium oxide solution was prepared with 10 g MgO in 250 mL Milli-Q water so that if well mixed, the addition of 1 mL to a 40 mL sample provided a similar MgO:Sample-volume ratio as that of the method described by Slawyk & Raimbault (1995), and Slawyk *et al.* (1998) of 300 mg/300 mL. It was observed that this addition increased the pH of the sample to ~9.5. The beaker containing the sample was again placed on the hot plate after the addition of MgO and DV. The reaction however, was left for 1 h once the beaker contents attained the targeted temperature (~95°C). The beaker was then removed from the hot plate and was left to cool down for some minutes. At this stage the sample was filtered through a precombusted (25 mm diameter) GF/F filter using in line syringe filtering unit (Millipore Swinnex-25) in order to remove the excess MgO and DV. The sample was then collected in either precombusted 50 mL brown-glass bottles for later analysis of urea and ammonium, or in 25 mL plastic vials for later analysis of nitrate following the protocols described in § 2.3. Urea was measured using the diacetylmonoxime method, ammonium was measured with a fluorometric method and nitrate was measured using a colorimetric technique (methods described in § 2.4). Satisfactory **results** were obtained following this protocol, which showed a **recovery of urea** of 90±4% (n=10). Removal efficiency for nitrate (n=6) and ammonium (n=5) were 99.5±0.5% and 95±5% respectively (**Fig. 2.10**). It was thus decided to process the estuarine samples designated to measure the release of DON from $^{15}N\text{-}NO_3^-$ uptake following this protocol. In the case of estuarine samples however, after filtration to remove excess MgO and DV, the contents

were directly collected into clean 50 mL Pyrex beakers for evaporation.

Chapter 3

Nitrogen uptake in the Southampton Water estuary

3.1 Introduction

It has previously been observed that phytoplankton growth affects the temporal distribution of nutrients in the Southampton Water estuary, producing an annual cycle characterised by low concentrations during the productive spring-summer period (*e.g.* Kifle & Purdie, 1993; Hydes & Wright, 1999; Hydes, 2000). This however, coincides with a reduction in the riverine nutrient supply, which is strongly dependent on the river flux. In order to better understand the effect of phytoplankton growth on the nitrogen fluxes throughout the estuary, it is necessary to directly measure the uptake of N-nutrients. In the following chapter the results of the first stage of this study are presented.

3.2 Results

3.2.1 Salinity and Temperature

Throughout the estuary surface **salinity** increased from values of 21.9 in the brackish water, up to of 34.4 in the coastal waters of the system. The vertical distribution of salinity indicated that the water column was well mixed in the coastal waters, and tended to be more stratified towards the upper estuary (**Fig. 3.1**). Salinity data suggests that stratification in this part of the estuary is mainly driven by the input of fresh water, as indicated by the lower surface salinity values.

The water **temperature** increased predictably towards the summer months and decreased towards the autumn. Although the temperature varied similarly at the three selected stations, the range of variation was larger in the mid (8.8-20.3^{o}C) and upper

estuary (9.1-20.6°C) than in the coastal waters (11.6-20.1°C). The temperature remained >20°C from mid July and through August in the mid and upper estuary. During the same period the temperature was ⩽20°C in the coastal waters probably due to a well mixed condition of the water column. Strong thermal stratification however, was not apparent at any of the sampling stations (see Fig. B.1, Appendix B.0.6).

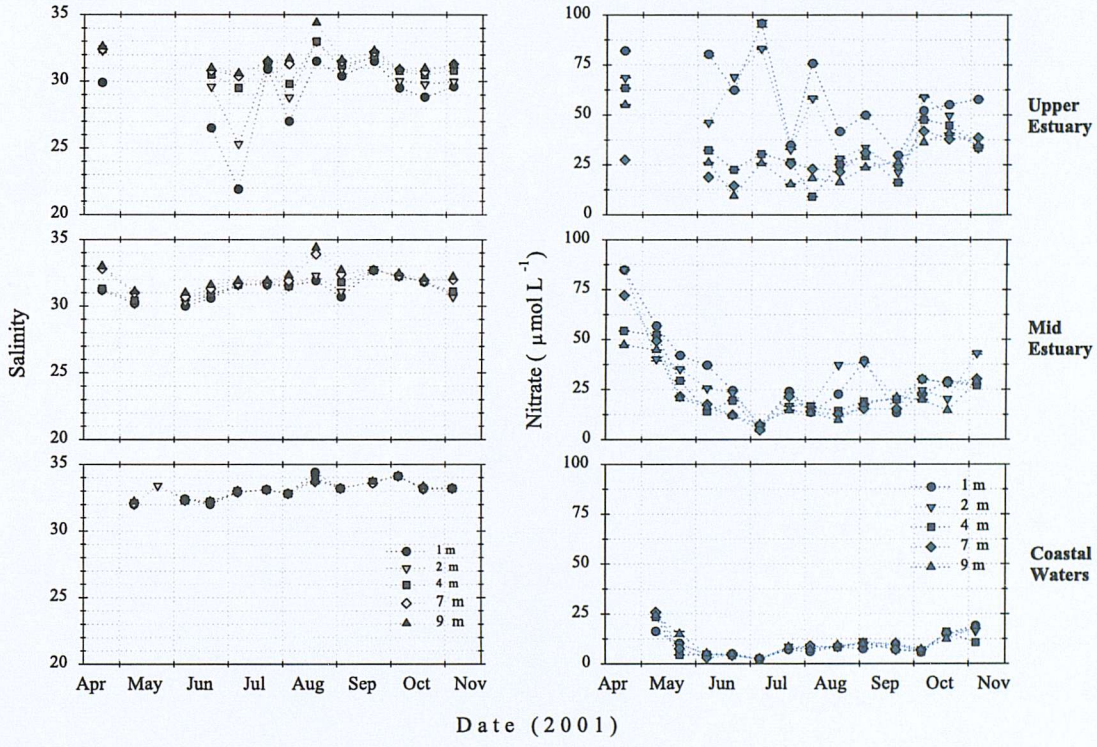

Figure 3.1: **Salinity and nitrate;** vertical, spatial and temporal distribution within Southampton Water estuary (2001). Error bars on right side panels show standard deviation of replicate (n=3) measurements. Symbols in the lower panels apply to all panels.

3.2.2 Nutrients

The range of nutrient concentrations at each of the 3 stations sampled within the Southampton Water estuary is presented in **Table 3.1** and the temporal distribution shown in **Figs. 3.1 and 3.3**. With the exception of urea, most nutrients presented similar temporal and spatial distributions; with coastal waters showing the lowest nutrient concentrations and relatively low vertical and temporal variability and, nutrient concentrations tending to increase towards the upper estuary. In general, the concentrations of **nitrate**, **silicate** and **phosphate** decreased with depth (Figs. 3.1 and 3.3). In the case of nitrate and silicate, a sharp decline in concentration was evident from April to July at all sites (Figs. 3.1 and 3.3). This decline was also apparent in the concentrations of phosphate in the mid estuary and coastal waters (Fig. 3.3). With the exception of urea, all nutrient levels

Table 3.1: Nutrient concentrations within Southampton Water estuary; range of variation during the productive spring–summer period in 2001 (concentrations are in μmol L^{-1}).

	Nitrate	**Ammonium**	**Urea**	**Silicate**	**Phosphate**
Upper estuary	<0.9 - 95.7	3.8 - 41.5	0.21 - 1.93	2.5 - 43.0	0.6 - 3.9
Mid estuary	4.6 - 85.0	0.3 - 12.5	0.19 - 2.56	<0.5 - 28.3	0.1 - 1.5
Coastal waters	2.3 - 25.9	<0.2 - 4.9	0.10 - 1.97	<0.5 - 11.8	<0.1 - 1.2

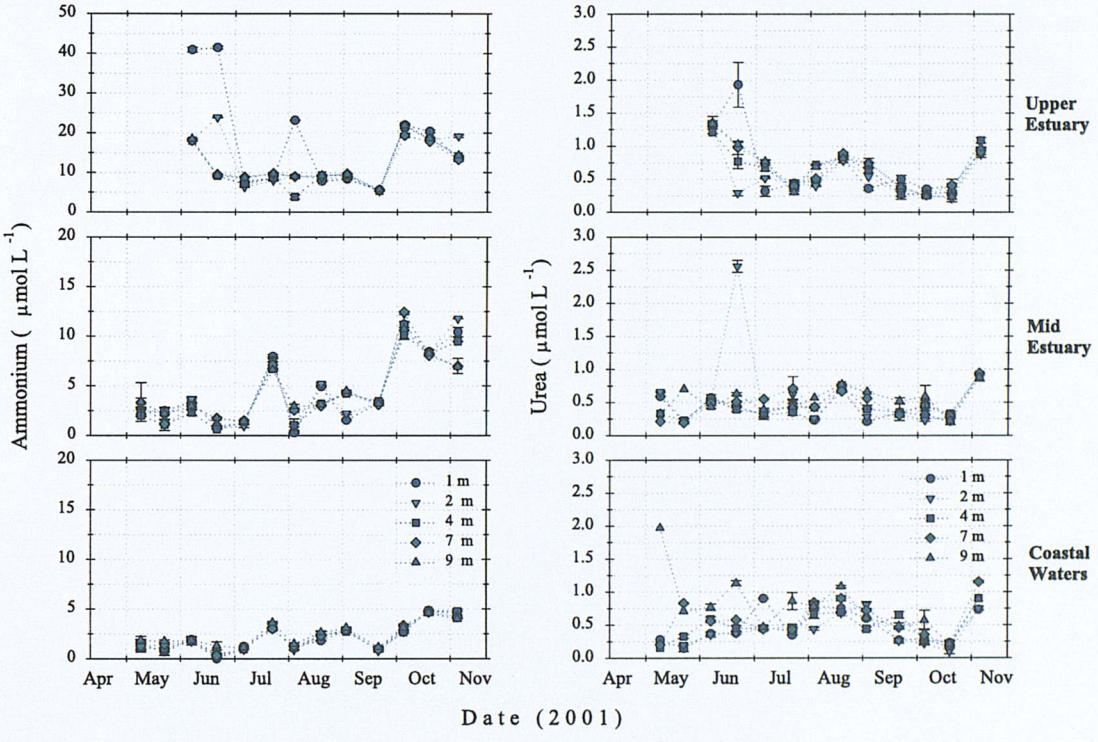

Figure 3.2: **Ammonium and urea;** vertical, spatial and temporal distribution within Southampton Water estuary (2001). Note different scale in left-upper panel. Error bars show the standard deviation of replicate (n=3) measurements. Symbols in the lower panels apply to all panels.

showed a gradual increase from July-August to November (see Figs. 3.1 to 3.3). The surface concentrations (*i.e.* at 1 and 2 m) of nitrate, silicate and phosphate were related to surface salinity in the mid and upper estuary, with higher concentrations at low salinities indicating nutrient-rich freshwater inputs. The vertical distribution of **ammonium** was nearly homogeneous throughout the sampling period, although higher surface values were measured on some dates in the upper estuary (Fig. 3.2). A decline in concentrations during summer was not observed, however ammonium concentrations increased towards November. Contrary to other nutrients, the temporal distribution of **urea** showed a slight increase during the summer months, decreased towards October and increased again towards November (Fig. 3.2). The temporal distribution of urea seemed to be relatively more variable in the upper estuary, the three stations however, exhibited similar ranges in

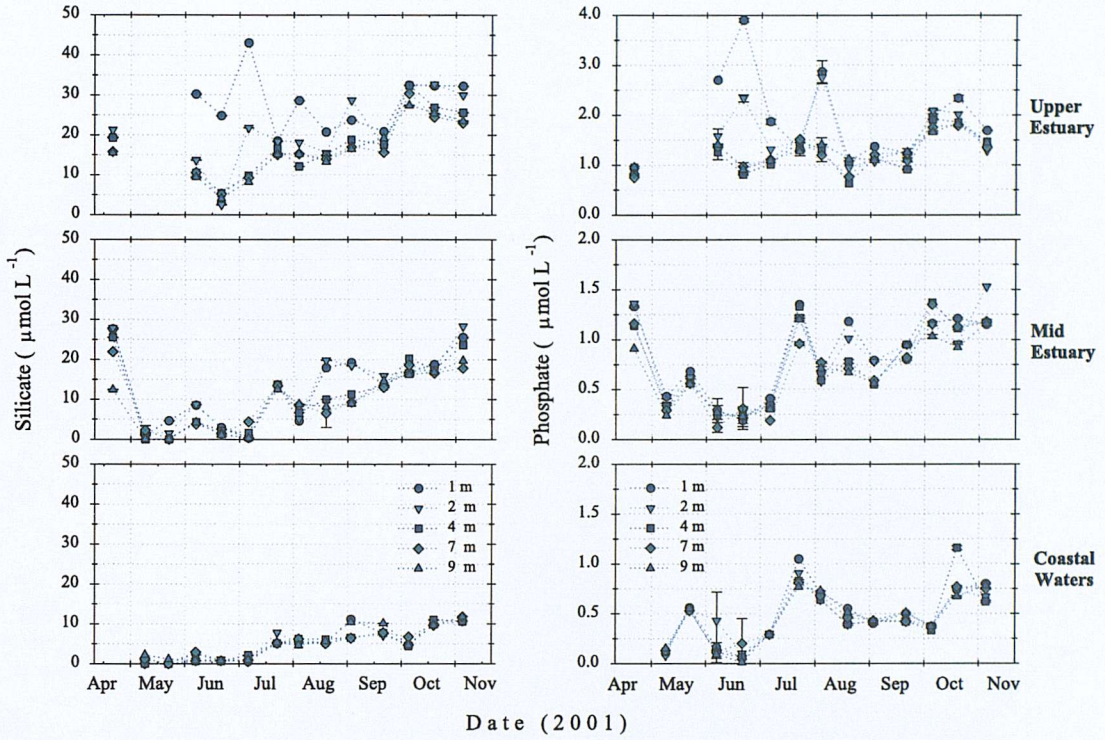

Figure 3.3: **Silicate and Phosphate;** vertical, spatial and temporal distribution within Southampton Water estuary (2001). Note different scales in upper panels. Error bars show the standard deviation of replicate (n=3) measurements. Symbols in the lower panels apply to all panels.

concentration (see Table 3.1). In addition, unlike other nutrients, the vertical distribution of urea generally showed higher concentrations with depth.

3.2.3 Irradiance

The irradiance attenuation coefficient (k) was calculated for the three sampling stations and the pontoon using logged downwelling photosynthetically active radiation (**PAR**) data from *in situ* measurements. Hourly incident irradiance data obtained from the SOC Met-Station for 2001 was transformed to dimensions of PAR and averaged over the ^{15}N-tracer incubation period (4 h). Both of the above sets of data were used to calculate the mean water column PAR down to the depth of the 1% of subsurface PAR (see Appendix B.0.7). k exhibited high temporal variation at all sites and although did not show a particular trend, in the mid and upper estuary it seemed to increase from May to October (see **Fig. 3.4**). The attenuation coefficient ranged from 0.5 to 1.2, 0.4 to 1.0, 0.4 to 1.0 and 0.5 to 1.2 m^{-1} at the pontoon, coastal waters, mid and upper estuary respectively. The 4 h averaged surface incident irradiance (E_0) varied between 204.4 and 1291.0 μmol m^{-2} s^{-1} during the period when incubation experiments were carried out. E_0 was >531.8 μmol m^{-2} s^{-1} before September and decreased after to values <306.3

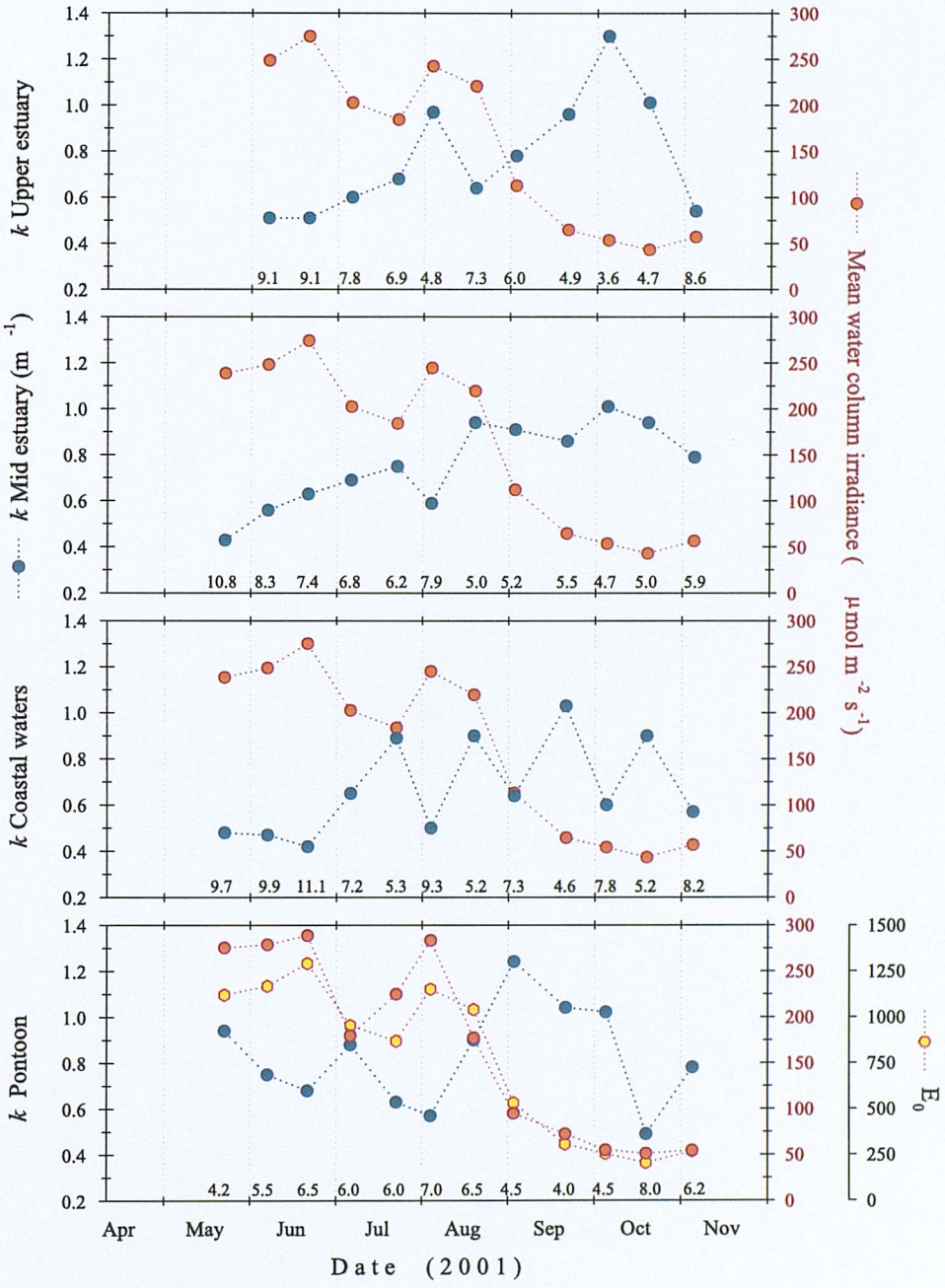

Figure 3.4: **Attenuation coefficient (k) and mean water column irradiance at the three sampling stations and at the pontoon.** The incident irradiance (E_o) is shown in the lower panel. Numbers at the bottom of each panel are the depth (m) of the 1% of subsurface PAR.

μmol m^{-2} s^{-1} (see Fig. 3.4). The mean water column irradiance varied between 51.1 and 288.6 μmol m^{-2} s^{-1} at the pontoon, and varied similarly at the three sampling stations within a range of 43.0 to 275.1 μmol m^{-2} s^{-1} (see Fig. 3.4). The euphotic water column seemed to be deeper at the three sampling stations between May and June, and became shallower towards October as suggested by the depth of the 1% subsurface PAR (see Fig. 3.4). At the pontoon, the euphotic water column was rather shallow throughout the sampling period.

3.2.4 Chlorophyll *a*

The spatial and temporal distribution of chlorophyll *a* (Chl-*a*) is presented in **Fig. 3.5**. Concentrations varied between 0.3 and ~64 μg L^{-1}. The spatial distribution of Chl-*a* reflected that of the nutrient concentrations, with lower values in the coastal waters increasing towards the inner estuary. Highest concentrations were mainly found in the upper layers of the water column (*i.e.* decreasing with depth). Four Chl-*a* peaks ranging from 21 to 64 μg L^{-1} were observed during the sampling period on the 21-May, 4-Jul, 1-Aug and 30-Aug, although a second small peak occurred in the coastal waters on the 19-June (see Fig. 3.5). An early peak was recorded in the coastal waters and mid estuary in mid May (data not available for the upper estuary). High Chl-*a* concentrations found at depth on this particular date suggest the sinking of phytoplankton cells. Later microscopic analysis reveled it was mainly *Phaeocystis* spp[1]. The other three Chl-*a* peaks decreased in intensity with time in the upper estuary and coastal waters. In the mid estuary, the three peaks were of similar concentration (see Fig. 3.5). After September, Chl-*a* concentrations were <2.3 μg L^{-1} at all sites.

3.2.5 Particulate organic nitrogen (PON) and particulate organic carbon (POC)

The spatial and temporal distribution of PON and POC is presented in **Fig. 3.6**. Data correspond to samples collected at a depth of 2 m (*i.e.* from water collected for the incubation experiments). Values ranged between 3.0 and 30.4 μmol-N L^{-1} and 48.2 to 272.7 μmol-C L^{-1}. Concentrations closely followed the temporal distribution of the 2 m depth Chl-*a* . Highest values were measured during the productive spring-summer period and decreased in magnitud from the upper estuary down to the coastal waters. The POC to PON ratios varied between 7.6 and 23.2, 7.5 and 20.2, and 7.8 and 18.4 in the coastal waters, mid and upper estuary respectively. Nonetheless, the average POC to PON ratios were similar between sampling stations; 14.7±3.9, 12.2±4.4 and 12.9±4.3 (same order as

[1]Arantza Iriarte *pers., comm.*, 2002. Postdoctoral fellow, School of Ocean and Earth Science, Southampton Ocenography Centre, University of Southampton.

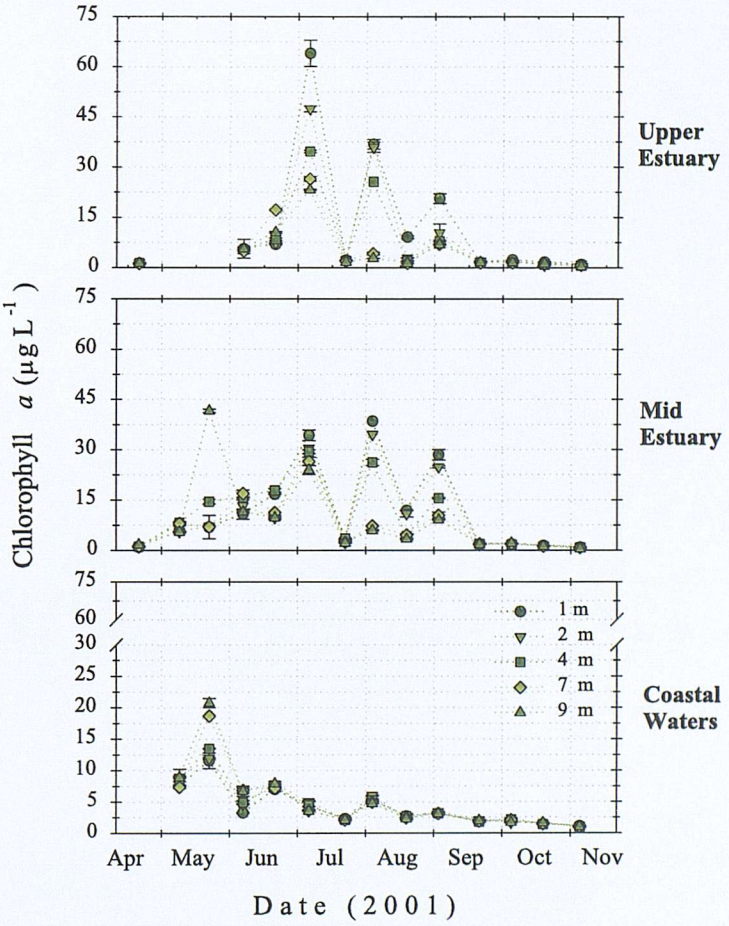

Figure 3.5: **Chlorophyll** *a*; vertical, spatial and temporal distribution within Southampton Water estuary (2001). Error bars show the standard difference of duplicate measurements. Symbols in the lower panel apply to all panels. Note different scale in lower panel (break on y axis).

above).

3.2.6 Nitrogen and carbon uptake

Ideally, nutrient enrichment with tracer additions in the incubation bottles is recommended to be $\leqslant$10% of the ambient nutrient concentration. This is because a higher level may enhance phytoplankton nutrient uptake, therefore overestimating natural uptake rates (see § 2.5.1, Ch. 2). In this study it was not possible to determine the ambient nutrient concentrations immediatly before the inubations. However, the ^{13}C and ^{15}N-standard additions made, generally produced enrichments within the recommended range (see **Table 3.2**). Although in some cases ^{15}N-tracer additions resulted in high enrichments, stimulation of phytoplankton activity was unlikely, since overall other N-nutrients were relatively abundant at all times during the incubation experiments. For example, on one ocassion when the enrichment with ^{15}N-urea was 100% of the ambient concentration (0.1 μmol L^{-1}, coastal waters, 15-Aug-2001), the nitrate and ammonium ambient concentrations were 15.0 and 4.8 μmol L^{-1} respectively.

Table 3.2: Nutrient enrichment in incubation bottles with either ^{15}N-tracer or ^{13}C-tracer additions; mean value (bold characters) and range (in parentheses).

	Enrichment % of ambient concentration
Nitrate	**0.7** (0.1 - 4.2)
Ammonium	**4.2** (0.4 - 12.8[a])
Urea	**25.2** (3.1 - 50.0[b])
Bicarbonate	**4.3** (3.9 - 4.9)

[a]200% on one ocassion (value not considered in the mean).
[b]100% on one ocassion (value not considered in the mean).

A total of 1049 samples (including replicates) were generated in 2001, although not all of these were analysed. Samples for duplicate analysis were chosen randomly. A total of 757 samples were analysed, which included all dates and all depths. Reproducibility was satisfactory, with standard differences of duplicate samples being <10% in most cases. For example, on the 01-Aug the standard difference was 6.4, 8.9 and 0.9% of the net carbon, nitrate and urea uptake respectively at 136.5 μmol m^{-2} s^{-1} (100% subsurface PAR) in the upper estuary (see Fig. 3.7). On the same date and at the same station, the standard difference of ammonium uptake was 4.8% at 68.2 μmol m^{-2} s^{-1} (50% subsurface PAR; see Fig. 3.7).

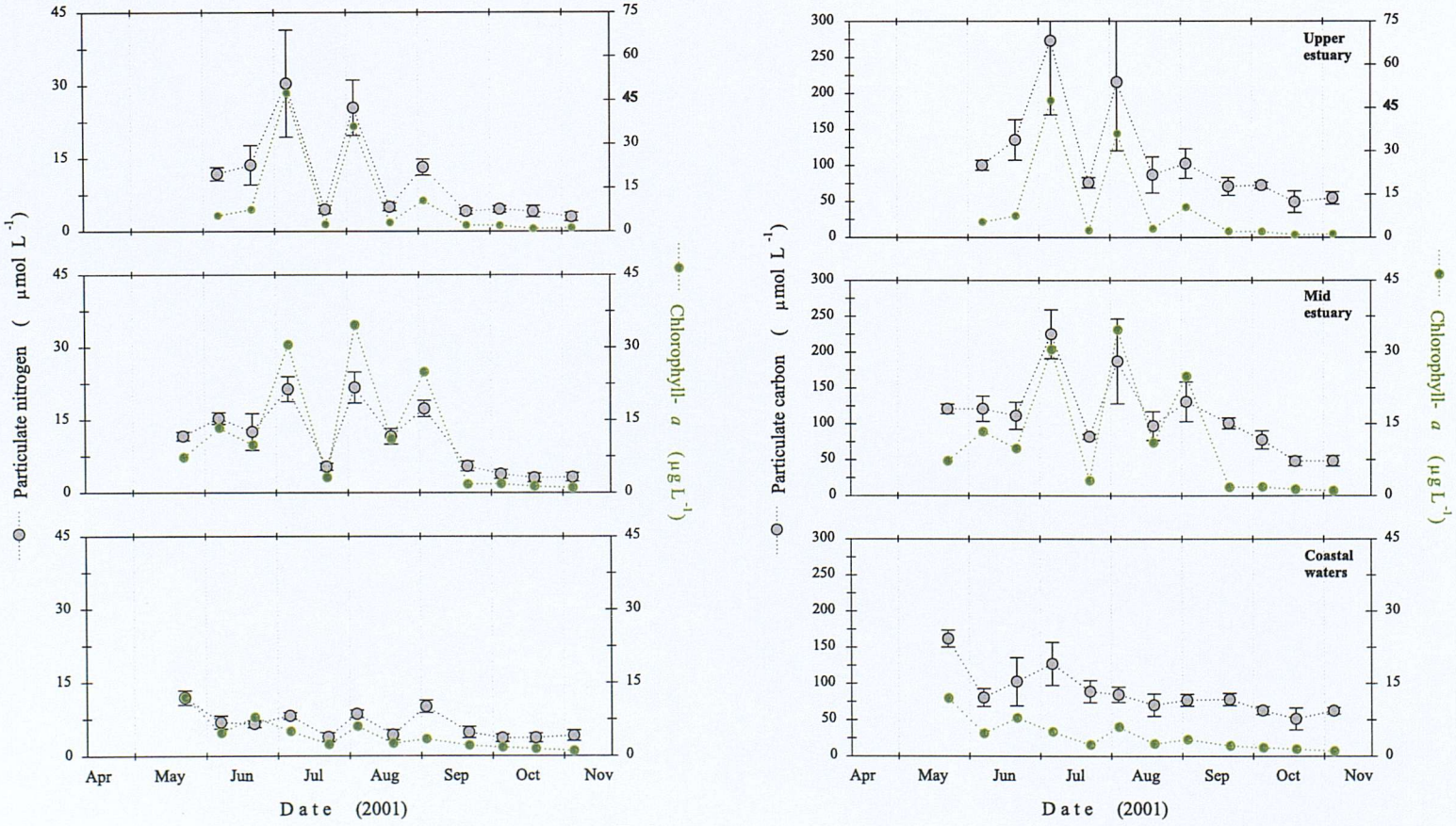

Figure 3.6: **Particulate organic carbon (PC) and particulate organic nitrogen (PN);** productive spring-summer period in 2001. Upper estuary (upper panels), mid estuary (mid panels) and coastal waters (lower panels). Error bars represent standard deviations of replicate measurements (n=5). Chl-*a* values from 2 m depth are shown as reference.

3.2.6.1 Nitrogen and carbon net uptake rates (ρ)

Net uptake rates of nitrogen and carbon presented a Michaelis-Menten-like response to irradiance during the productive spring-summer period. Highest rates were measured at 100% and 50% of subsurface PAR (see **Fig. 3.7**), and in some cases there was an indication of photoinhibition (*i.e.* $\rho_{100\%} < \rho_{50\%}$). After September however, when the productive period ended, not all nutrients showed the same response to irradiance and in some cases the uptake seemed constant with increasing PAR (see Fig. 3.7). The range of net uptake rates in the euphotic water column and in dark incubations is summarised in **Table 3.3**. Overall, nitrogen and carbon net uptake rates from light and dark conditions were higher in the mid and upper estuary. In the euphotic water column the uptake of ammonium and carbon tended to increase towards the upper estuary, whereas in the case of nitrate and urea, higher uptake rates were measured in the mid estuary (see Table 3.3). In dark incubations, the uptake rates of nitrate and ammonium tended to increase towards the upper estuary and in the case of urea and carbon uptake, higher rates were measured in the mid estuary (see Table 3.3). Some of the highest dark uptake rates of N-nutrients (specially from the mid and upper estuary) were comparable with uptake values from light bottles, and in the case of ammonium and nitrate dark uptake from the mid and upper estuary, values were on average higher or similar to light uptake rates measured in the coastal waters (see Table 3.3).

Table 3.3: Nitrogen and carbon net uptake rates in Southampton Water estuary; mean (bold) and range of variation (parentheses) during the productive spring–summer period in 2001. Upper part of the table includes values from the euphotic water column (*i.e.* from 1 to 100% subsurface PAR). Lower part are values from dark incubations.

	Nitrate	**Ammonium**	**Urea**	**Carbon**
		μmol-N L^{-1} h^{-1}		μmol-C L^{-1} h^{-1}
Light uptake				
Upper estuary	**0.231**	**0.550**	**0.030**	**8.084**
	(0.001 - 2.600)	(0.003 - 5.158)	(0.000 - 0.332)	(0.000 - 107.934)
Mid estuary	**0.279**	**0.179**	**0.077**	**5.914**
	(0.004 - 3.974)	(0.012 - 0.650)	(0.000 - 0.667)	(0.000 - 71.467)
Coastal waters	**0.023**	**0.064**	**0.016**	**1.607**
	(0.001 - 0.173)	(0.004 - 0.299)	(0.000 - 0.107)	(0.000 - 11.192)
Dark uptake				
Upper estuary	**0.043**	**0.142**	**0.003**	**0.033**
	(0.004 - 0.143)	(0.019 - 0.421)	(0.000 - 0.013)	(0.000 - 0.183)
Mid estuary	**0.028**	**0.070**	**0.013**	**0.040**
	(0.000 - 0.058)	(0.001 - 0.172)	(0.000 - 0.073)	(0.000 - 0.204)
Coastal waters	**0.006**	**0.028**	**0.003**	**0.12**
	(0.002 - 0.011)	(0.003 - 0.090)	(0.000 - 0.008)	(0.000 - 0.060)

3.2.6.2 Integrated total nitrogen and carbon uptake rates

The nitrogen and carbon net uptake rates were integrated for each station from the depth of 100% subsurface PAR down to the depth of 1% of subsurface PAR (see Appendix B.0.8). Integrated rates are summarised in **Table 3.4** and presented in **Fig. 3.8**. Overall, integrated uptake rates were higher in the inner estuary with the average uptake rate increasing towards the upper estuary (see Table 3.4 and Fig. 3.8). Integrated total nitrogen and carbon uptake rates increased as the productive spring-summer period evolved, showing a maximun at the three sampling sites in mid summer (01-Aug). Both, nitrogen and carbon integrated rates closely followed the temporal distribution of the 2 m depth Chl-*a* concentration (see Fig. 3.8). Integrated rates were relatively high all through the productive period and decreased sharply towards the autumn months. Similarly to Chl-*a* concentrations, integrated nitrogen and carbon uptake rates were markedly lower after September, suggesting the end of the spring-summer productive period in the Southampton Water estuary. In general, the C to N integrated uptake ratios decreased from the coastal waters to the upper estuary (see Table 3.4).

Dark incubations

Overall, total nitrogen and carbon uptake from dark incubations were also higher in the inner estuary, although undetectable carbon uptake rates were recorded at all sites on some dates (see Fig. 3.8). The dark uptake of carbon presented a similar temporal pattern at all sites, showing a maximum in early August. Nitrogen dark uptake rates exhibited a similar temporal trend in the coastal waters and mid estuary. However, while high dark nitrogen uptake rates were measured mainly in May-June and early August in the coastal waters, dark rates were relatively high from May to end of August in the mid estuary (see Fig. 3.8). In the upper estuary the nitrogen dark uptake seemed to decrease with time (see Fig. 3.8). The C to N dark uptake ratios whenever the carbon uptake was >0, ranged between 0.03 and 1.82, 0.05 and 1.84 and 0.02 and 0.62 in coastal waters, mid and upper estuary respectively.

3.2.6.3 Integrated N-uptake rates; nitrate, ammonium and urea

Integrated N-uptake rates of each of the nitrogen sources investigated are summarised in **Table 3.4** and shown in **Fig. 3.9**. Overall, highest integrated nitrate and ammonium uptake rates were measured in the inner estuary. Integrated urea uptake however, was highest in the mid estuary and of similar magnitude in the coastal waters and upper estuary (see Table 3.4). In the case of **nitrate**, integrated rates ranging from 0.580 to 7.393 mmol-N m^{-2} h^{-1} were recorded on 05-Jun, 19-Jun, 04-Jul and 01-Aug in the upper estuary. On other dates, uptake rates were <0.317 mmol-N m^{-2} h^{-1} at this site. Apart from two dates, nitrate uptake rates in the mid estuary were relatively high, with val-

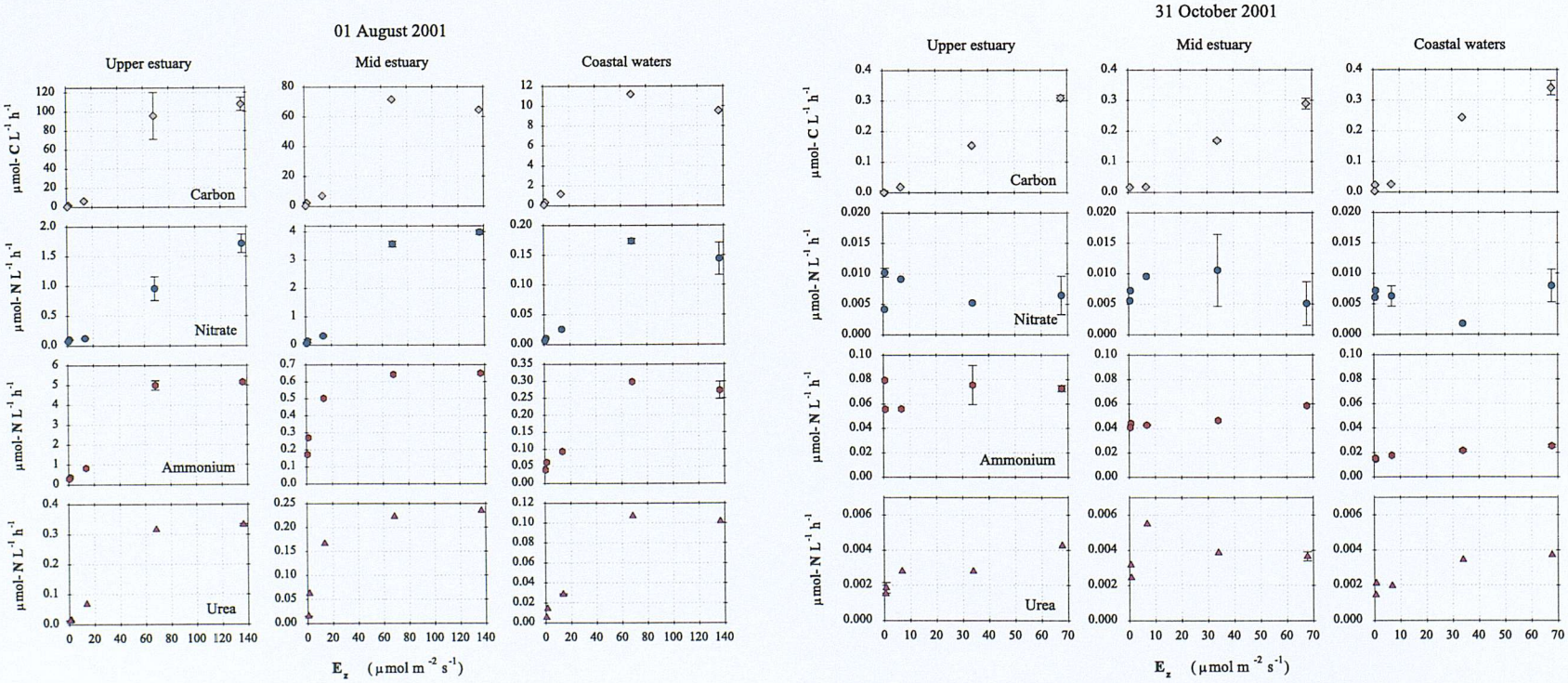

Figure 3.7: **Nitrogen and carbon net uptake rates plotted against downwelling PAR (E_z);** examples from two representative dates. Rates measured on the 01-Aug were selected as representative of the productive spring-summer period in 2001 (overall, on this date the highest rates in 2001 were recorded). Rates measured on the 31-Oct were selected as representative of non-productive months and was the last tracer experiment carriedout in 2001. Note different scales. Error bars show the standard difference of random duplicate measurements.

Table 3.4: Depth integrated nitrogen and carbon uptake rates (mmol m^{-2} h^{-1}) in the Southampton Water estuary; mean (bold) and range of variation (parentheses) during the productive spring–summer period in 2001. Total nitrogen uptake (TN) is the sum of integrated nitrate, ammonium and urea uptake rates. The C to N integrated uptake ratios are also presented.

	Nitrate	Ammonium	Urea	TN	Carbon	C:N
Upper estuary	**1.15**	**2.40**	**0.15**	**3.70**	**34.13**	**6.3**
	(0.03 - 7.39)	(0.03 - 9.87)	(<0.01 - 0.65)	(0.07 - 13.05)	(0.20 - 166.52)	(0.3 - 14.2)
Mid estuary	**1.49**	**1.12**	**0.52**	**3.13**	**31.22**	**8.1**
	(0.03 - 10.60)	(0.12 - 3.83)	(<0.01 - 3.58)	(0.18 - 15.67)	(0.44 - 204.87)	(1.3 - 17.6)
Coastal waters	**0.17**	**0.45**	**0.14**	**0.76**	**11.23**	**12.4**
	(0.02 - 0.62)	(0.03 - 1.38)	(<0.01 - 0.67)	(0.06 - 2.47)	(0.60 - 37.73)	(3.9 - 28.3)

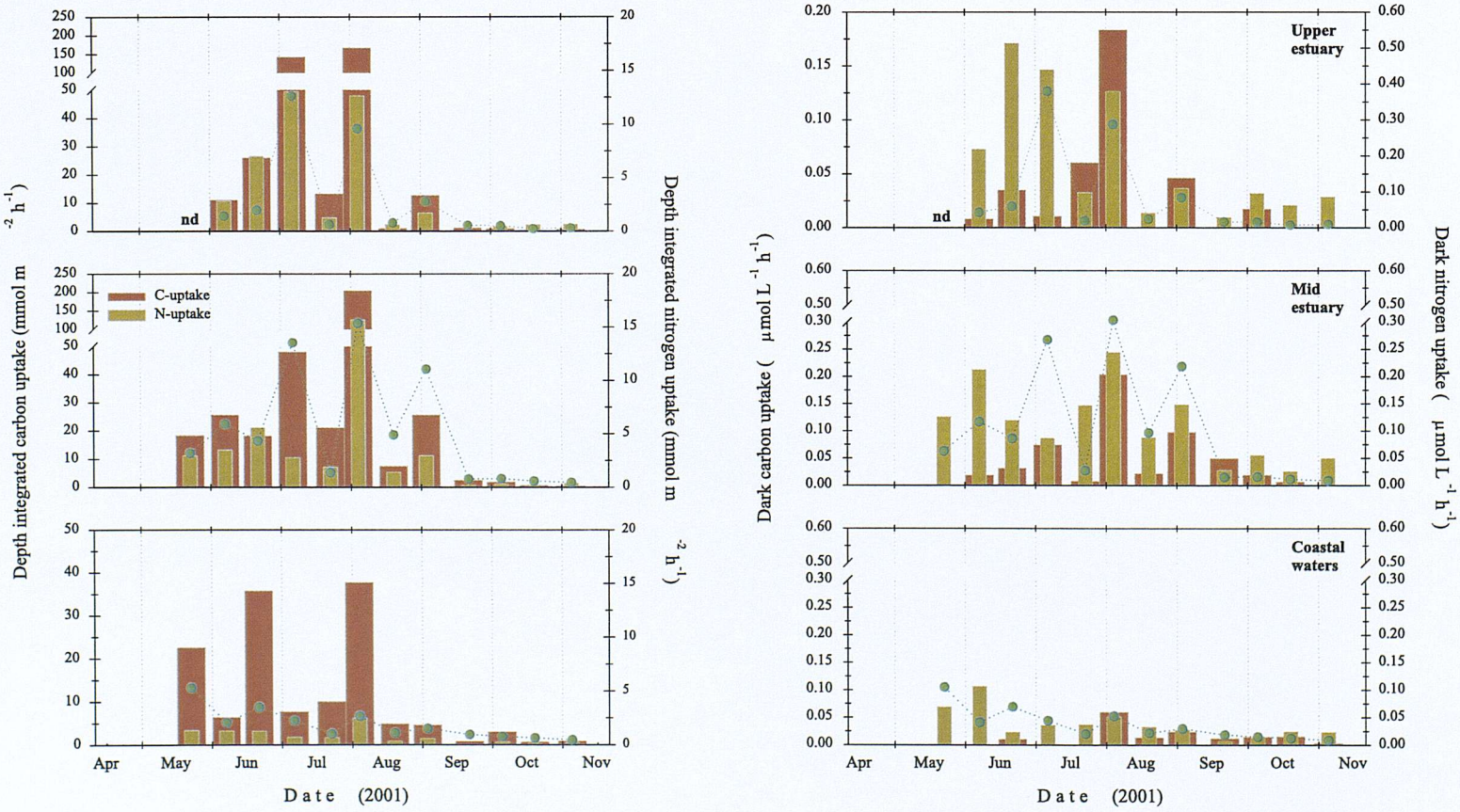

Figure 3.8: **Depth integrated and dark carbon and nitrogen uptake rates;** productive spring-summer period in 2001. Total nitrogen uptake is the sum of nitrate, ammonium and urea integrated rates. Chl-*a* (•) measured at 2 m from respective sampling sites is shown as reference (although scale is not shown, symbols are plotted at the same scale as in Fig. 3.5). Note different scales; breaks on y axis (nd = no data available).

ues generally >1.0 mmol-N m^{-2} h^{-1} between May and August and showing a maximum on 01-Aug. In the coastal waters, nitrate integrated values ranged between 0.036 and 0.621 mmol-N m^{-2} h^{-1} from May to August, and were <0.045 on the remaining dates. In general, the temporal variability of the integrated nitrate uptake coincided with the temporal variation of the 2 m depth Chl-*a* concentrations at all sites, *i.e.* integrated rates increased when the Chl-*a* values also increased (see Fig. 3.9). Integrated **ammonium** uptake rates exhibited high temporal variability and were relatively high at all sites from May to August, with values generally >0.043, >0.573 and >0.415 mmol-N m^{-2} h^{-1} in the coastal waters, mid and upper estuary respectively. After September integrated values were < 0.213, <0.263 and <0.529 mmol-N m^{-2} h^{-1} (same order as above). A maximum integrated ammonium uptake rate was recorded on 01-Aug at all sites. Integrated uptake rates of **urea** followed the temporal distribution of the 2 m depth Chl-*a* concentrations in the coastal waters and upper estuary and exhibited high temporal variability in the mid estuary. In general, integrated values of urea uptake were also higher from May to August at all sampling sites, ranging between 0.043 and 0.674, 0.125 and 3.575, and 0.035 and 0.647 mmol-N m^{-2} h^{-1} in the coastal waters, mid and upper estuary respectively. A maximum integrated rate was recorded on 01-Aug in the upper estuary, and on 19-Jun in the coastal waters and mid estuary. Integrated values of urea were <0.024 mmol-N m^{-2} h^{-1} after September at all sites.

Dark uptake of nitrate, ammonium and urea

The dark uptake values of nitrate, ammonium and urea are summarised in Table 3.3 and data plotted in Fig. 3.9 (right side panels). In general, highest dark uptake rates of the three nitrogen sources investigated were measured in the inner estuary. The dark uptake of nitrate in the mid and upper estuary seemed to follow the temporal distribution of the 2 m Chl-*a*, that is, higher dark uptake rates coincided with higher Chl-*a* values (see Fig. 3.9). In the coastal waters no temporal trend was apparent in the dark uptake of nitrate and values were <0.011 μmol-N L^{-1} h^{-1} throughout the sampling period. The dark uptake of ammonium exhibited high temporal variability and although highest values were recorded from May to August, relatively high rates were measured throughout the sampling period at all sites (see Fig. 3.9). Dark uptake rates of urea were comparatively low all through the sampling period in the coastal waters and upper estuary, with an average of 0.003 μmol-N L^{-1} h^{-1} at both sites and values generally <0.013 μmol-N L^{-1} h^{-1} (see Table 3.3 and Fig. 3.9). In the mid estuary, dark uptake rates of urea varied between 0.003 and 0.073 μmol-N L^{-1} h^{-1} from May to August, showing a maximum on the 19-Jun. Dark uptake rates of urea were close to 0 (*e.g.* <0.5 nmol L^{-1} h^{-1}) on the 01 and 15-Oct at the three samplings stations.

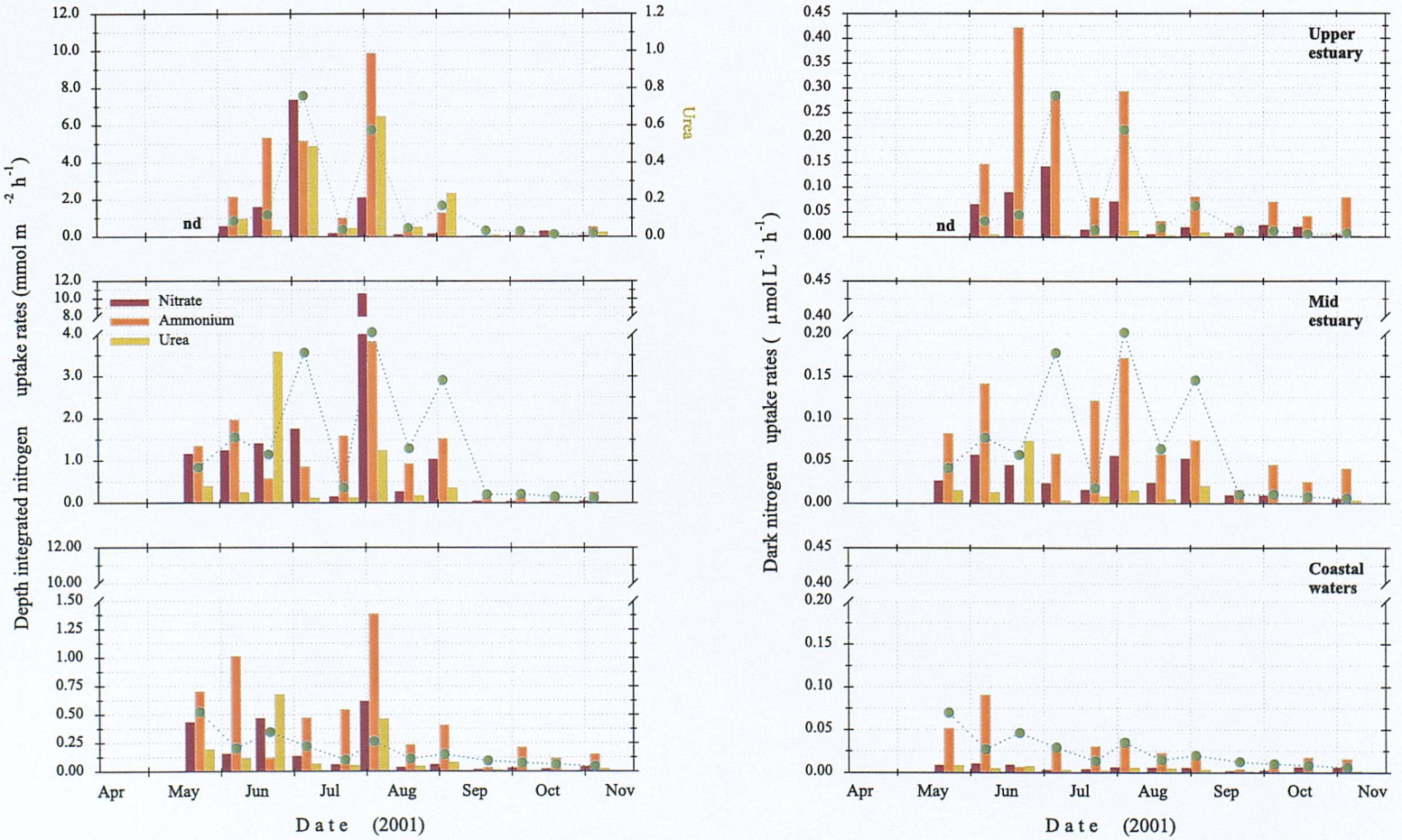

Figure 3.9: **Depth integrated nitrogen uptake rates and dark net uptake rates;** productive spring-summer period in 2001. 2 m Chl-a (•) from respective sampling sites are shown as reference (although scale is not shown, symbols are plotted at the same scale as in Fig. 3.5). Note different scales (breaks on y axis) and additional axis for urea in upper left panel (nd = no data available).

3.2.6.4 Relative contribution of different N-sources to total N-uptake

The contribution of each nitrogen source to total nitrogen uptake was calculated from depth integrated and dark uptake rates as follows,

$$\%Contribution = \left(\frac{\rho_x}{\rho_N + \rho_A + \rho_U}\right) \times 100 \tag{3.1}$$

where ρ_N is the nitrate uptake, ρ_A is the ammonium uptake, ρ_U is the urea uptake and ρ_x is either ρ_N, ρ_A or ρ_U. The mean percent contribution of each nitrogen source to total nitrogen uptake is summarised in **Table 3.5** and the temporal variation in the percent contributions presented in **Fig. 3.10**. Overall, the total nitrogen uptake from integrated uptake and dark uptake rates was dominated by the uptake of ammonium at all sites during the productive spring-summer period in 2001 (see Table 3.5 and Fig. 3.10). In

Table 3.5: Relative contribution (%) of the different nitrogen sources studied to total nitrogen uptake in the Southampton Water estuary, calculated from integrated uptake and dark uptake rates. Mean (bold) and range (parentheses) percent contribution during the productive spring–summer period in 2001.

	Nitrate %	**Ammonium** %	**Urea** %
Light uptake			
Upper estuary	**26.2**	**68.6**	**5.1**
	(9.7 - 56.7)	(39.6 - 85.1)	(0.4 - 13.9)
Mid estuary	**31.1**	**56.8**	**12.2**
	(8.3 - 67.6)	(10.3 - 85.0)	(0.6 - 62.2)
Coastal waters	**20.2**	**65.6**	**14.2**
	(9.4 - 37.2)	(9.5 - 86.3)	(1.1 - 53.3)
Dark uptake			
Upper estuary	**21.8**	**75.6**	**2.6**
	(4.9 - 32.7)	(66.8 - 93.3)	(0.2 - 7.2)
Mid estuary	**23.3**	**66.2**	**10.6**
	(0.0 - 37.8)	(0.7 - 98.2)	(0.3 - 61.4)
Coastal waters	**19.9**	**70.0**	**10.0**
	(8.3 - 41.2)	(26.9 - 85.5)	(1.2 - 31.9)

the upper estuary the contribution of nitrate from integrated uptake rates was dominant only on 04-Jul, 17-Sept and 15-Aug, and varied between 9.7 and 23.2% on other dates (see Fig. 3.10). In the mid estuary the contribution of nitrate was generally higher from May to September, and was the dominant source on the 07-Jul and 01-Aug (see Fig. 3.10). In the coastal waters the temporal contribution of nitrate varied within a relatively small range (see Table 3.5) and did not dominate over the other nitrogen sources (see Fig. 3.10). The contribution of urea seemed to increase gradually in the upper estuary from 3.4% in

May to 13.9% in August, with the percent contribution decreasing after the maximum. In the mid estuary and coastal waters the contribution of urea was dominant on 19-Jun, varying within a small range at both sites on other dates (0.6-13.8% and 1.1-18.7% respectively). The percent contribution of nitrate from dark incubations did not seem to exhibit a temporal trend and although on one occasion its contribution was 0% in the mid estuary (15-Oct), it generally contributed $\geqslant$4.9% at all sites (see Table 3.5 and Fig. 3.10). Dark nitrate uptake was dominant only on 19-Jun in the coastal waters (Fig. 3.10). The contribution of dark uptake of urea approximately reflected the temporal variation exhibited by the contribution of urea from integrated uptake at all sites, and showed a dominant contribution on 19-Jun in the mid estuary only (see Fig. 3.10).

3.3 Discussion

3.3.1 Nutrients and Chl-*a* in the Southampton Water estuary

Seasonal changes in nutrient and chlorophyll *a* concentrations measured during the present study are in good agreement with previous observations within the Southampton Water estuarine system. The annual cycle of phytoplankton growth, produced with lower nutrient concentrations during the productive period (*i.e.* March to September) evident from the temporal distribution of nitrate and silicate, and seemed to affect also the phosphate concentrations in the mid estuary and coastal waters (Figs. 3.1 and 3.3). In the case of nitrate, surface (*i.e.* 1 m depth) concentrations in the coastal waters and mid estuary for example, decreased from 16.2 to 2.6 and 84.8 to 6.8 μmol L^{-1} respectively from the 20-Apr to the 04-Jul, and then increased gradually to 19.0 and 27.7 μmol L^{-1} (see Fig. 3.1). On the same dates, surface silicate values decreased from 27.6 μmol L^{-1} to values close to the limit of detection (see Table 3.1) in the mid estuary, and seemed to remain $<$2.5 μmol L^{-1} before the 04-Jul in the coastal waters (Fig. 3.3). After this period, silicate surface concentrations recovered to 25.5 and 10.6 μmol L^{-1} in the mid estuary and coastal waters respectively on the 31-Oct (Fig. 3.3). In the mid estuary phosphate concentrations decreased from 1.33 to 0.41 μmol L^{-1}, and in the coastal waters values seemed to decrease to 0.29 μmol L^{-1} during the same period (Fig. 3.3). Phosphate levels then increased gradually to 1.15 and 0.8 μmol L^{-1} in the mid estuary and coastal waters respectively on the 31-Oct (Fig. 3.3). The annual cycle in nutrient concentrations measured at 1 and 2 m depth in the upper estuary seemed to be 'shadowed' by the influx of nutrient-rich fresh water as suggested by the high nutrient levels coinciding with low salinity values; *e.g.* 04-Jul, 01-Aug and 16-Aug (Figs. 3.1 to 3.3). Nonetheless, the annual cycle can be appreciated at other depths (Figs. 3.1 to 3.3). In the case of ammonium, urea and phosphate, it has been documented that concentrations of these nutrients are mainly supplied by point-sources such as sewage effluent discharges and therefore do not

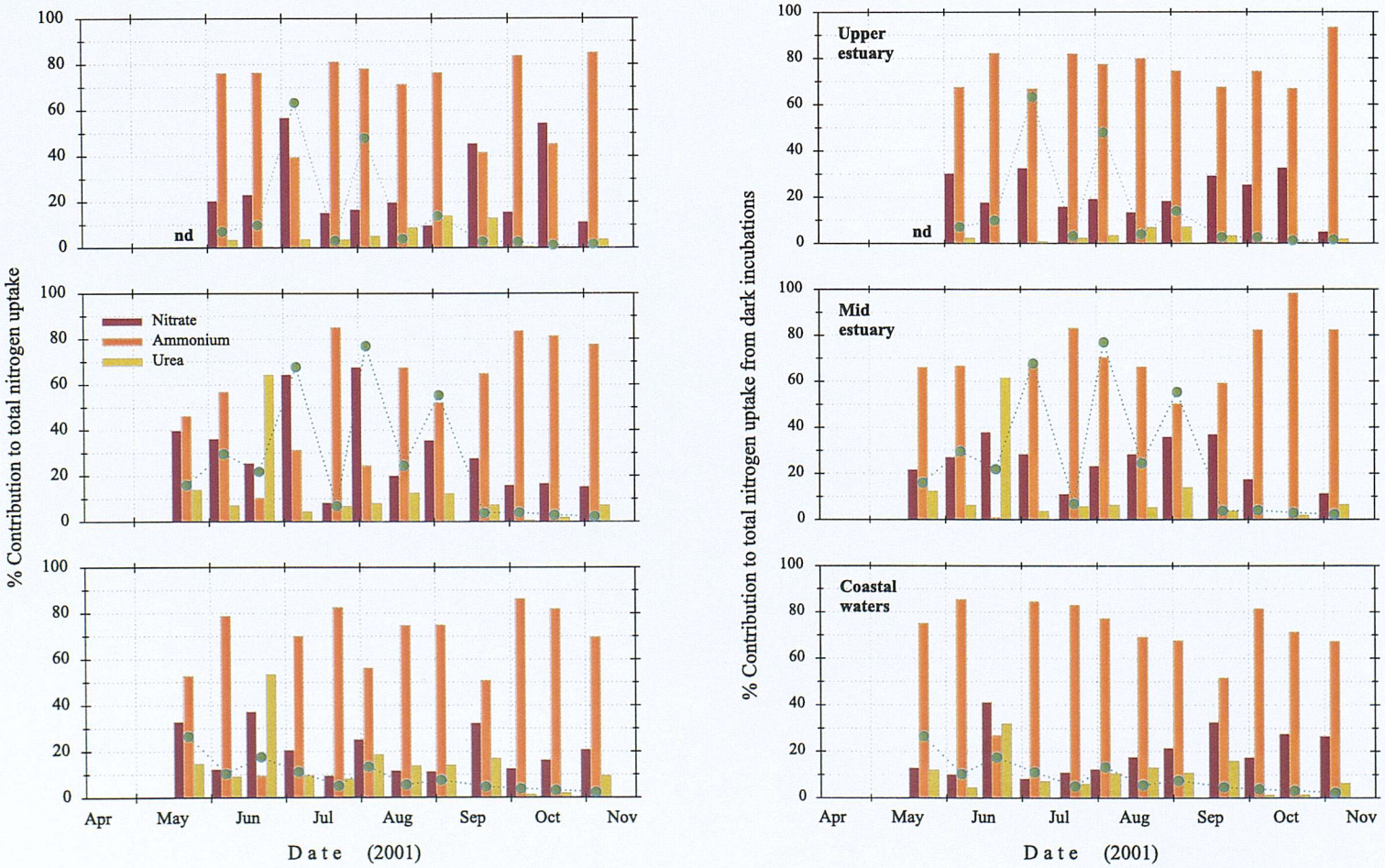

Figure 3.10: **Contribution of each nitrogen source to total nitrogen uptake from integrated uptake and dark uptake rates;** productive spring-summer period in 2001 (nd = no data available). The temporal distribution of the 2 m Chl-*a* (•) from respective sampling sites is shown as reference (although the scale is not shown, symbols are plotted at the same scale as in Fig. 3.5).

exhibit the annual cycle trend (Hydes & Wright, 1999). In the present study the temporal distributions of ammonium and phosphate showed peaks in concentration that did not seem to be related to fresh water inputs. For example, a marked concentration peak was observed on the 20-Jul, with surface concentrations of 7.95 and 3.0 μmol L^{-1} of ammonium and 1.35 and 1.0 μmol L^{-1} of phosphate in the mid estuary and coastal waters respectively (Figs. 3.2 and 3.3). This peak however, can also be appreciated in the silicate concentrations, although not in nitrate. It is likely that water of similar salinity and nitrate concentration was being supplied by the Itchen estuary. This may explain why the peak was not detected in the upper estuary. Concentrations of ammonium and phosphate in the Itchen estuary have been reported to be higher than concentrations in the Test estuary, although concentrations of nitrate have been reported to be higher in the latter (Hydes & Wright, 1999). The temporal distribution of urea did not seem to be related to ammonium or phosphate and although some peaks in urea concentrations were recorded (*e.g.* 19-June mid and upper estuary, Fig. 3.2), generally relatively high levels were observed throughout the productive period, particularly from June to mid September (see Fig. 3.2). Besides, the concentrations of urea were generally higher at depth (see Fig. 3.2). Urea is a low molecular weight compound that can be rapidly recycled in the water column (Glibert *et al.*, 1991; Berman *et al.*, 1999; Bronk, 2002; Lomas *et al.*, 2002; Berman & Bronk, 2003), and can be supplied by regeneration from the sediments (Herbert, 1999; Berman & Bronk, 2003) and by excretion from organisms (Bronk, 2002; Berman & Bronk, 2003). The fact that in the present study the concentrations of urea were highest during the productive period and were generally higher at depth, may represent an indication of a combination of recycling in the water column and regeneration from sediments. Both processes would be expected to be enhanced during the productive period, since phytoplankton growth would stimulate the activity of grazers and thus the supply of organic matter to the sediments (*e.g.* Grenz *et al.*, 2000). However, with the nutrient data available it is difficult to further interpret these observations.

Nutrient levels and their spatial distribution during this research are also in good agreement with the range of concentrations and spatial distributions previously reported for the Southampton Water estuary. For example, it has been observed that nitrate concentrations are lowest at the mouth of the estuary, and values >60 μmol L^{-1} have been recorded in the mid estuary (*e.g.* Iriarte & Purdie, 1994). In the present study lower nitrate concentrations were measured in the coastal waters, and levels of up to 95.7 μmol L^{-1} were recorded in the upper estuary (Fig. 3.1). In the case of ammonium, concentrations >40 μmol L^{-1} have been measured at salinities below 25, while concentrations <20 μmol L^{-1} have been recorded at higher salinities (*e.g.* Kifle & Purdie, 1993; Hydes & Wright, 1999). Ammonium concentrations measured in 2001 in the system reached values of up to 41.5 μmol L^{-1} at salinities <30 (*e.g.* mid and upper estuary) and concentrations

<5.0 μmol L^{-1} were measured at salinities >30 (*e.g.* coastal waters) (see Figs. 3.1 and 3.2). In fact, with the exception of urea, all nutrient levels tended to be low at high salinities and high at low salinities. In this research, urea as a proportion of the total dissolved nitrogen species measured (*i.e.* urea, nitrate+nitrite and ammonium), constituted from 0.3-2.0%, 0.6-9.6% and 0.5-11.6% in the uppper estuary, mid estuary and coastal waters respectively. This is in good agreement with a previous study in the Southampton Water estuary in which urea as a proportion of the total dissolved nitrogen species (urea, nitrite, nitrate, and ammonium) has been determined within the range 0.8-16.4% in the mid estuary and 0.1-9.9% in the coastal waters (Ashe, 1996). Apparently there have not been reports for the upper estuary. Ashe (1996) reported that levels of urea within the system are generally <2 μmol L^{-1}, which also agrees well with the concentrations measured during this research, with values $\leqslant$2.56 μmol L^{-1} at all sampling sites (see Table 3.1 and Fig. 3.2). Measured concentrations of urea in the Southampton Water estuary are also similar to concentrations measured in estuaries such as Chesapeake Bay (1972-1998) for example, with values within the range 0.49 to 0.91 μmol L^{-1} (Lomas *et al.*, 2002), but are lower than those measured in coastal environments such as the Gulf of St. Lawrence of up to $\sim$10 μmol L^{-1} (Tremblay *et al.*, 2000).

Concentrations of particulate organic carbon (POC) and nitrogen (PON) have been reported to vary from 7.4 to 71.1 μmol-C L^{-1} and <0.1 to 9.0 μmol-N L^{-1} in the coastal waters and between 11.1 to 160.9 μmol-C L^{-1} and 0.4 to 26.4 μmol-N L^{-1} in the mid estuary from winter to summer, that is, showing the highest values during the productive period (Leakey *et al.*, 1992). During the present study, POC and PON varied from 51.4 to 161.8 μmol-C L^{-1} and 3.6 to 11.9 μmol-N L^{-1} in the coastal waters and from 48.2 to 224.9 μmol-C L^{-1} and 3.1 to 21.7 μmol-N L^{-1} in the mid estuary from May to October (see Fig. 3.6). POC and PON in the upper estuary ranged between 49.5 and 272.7 μmol-C L^{-1} and 2.9 and 30.4 μmol-N L^{-1} during this period (apparently there are no previous reports of POC and PON in the literature for this part of the estuary). In general, highest values of POC and PON in the present study were measured during the productive period (*i.e.* from May to September) and closely followed the temporal distribution of the 2 m depth Chl-*a* (see Fig. 3.6). However, the concomitant increase in Chl-*a* and PON and POC concentrations was not proportional; results suggest higher chlorophyll production relative to PON and POC during the productive period, indicating phytoplankton growth (see **Fig. 3.11**).

Chl-*a* concentrations measured in 2001 were highest between May and mid September, and during this period four peaks were recorded (see Fig. 3.5). The magnitude of these peaks are within the range of Chl-*a* concentrations reported in the literature for the Southampton Water estuary. For example, surface chlorophyll peaks of >20 μg L^{-1} and >40 μg L^{-1} have been measured in the coastal waters and the mid estuary respectively,

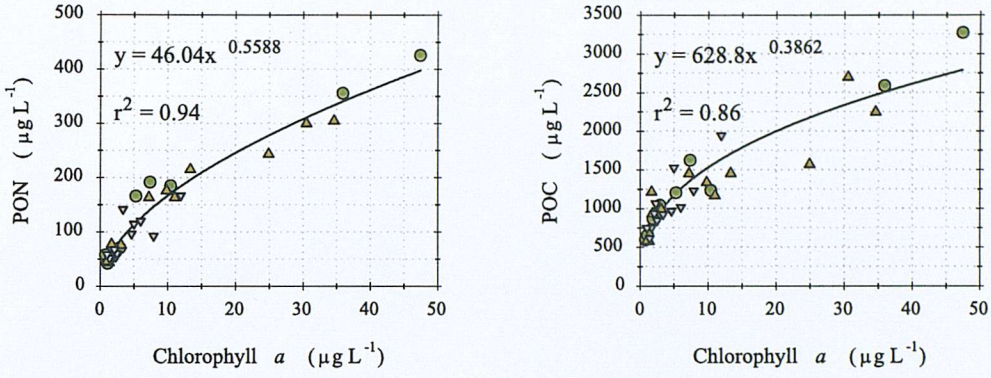

Figure 3.11: **PON and POC plotted against Chl-*a*.** The power relation includes data from the three sampling sites. Symbols indicate upper estuary (circles), mid estuary (triangles up) and coastal waters (triangles down).

between April and July (*e.g.* Iriarte, 1991; Leakey *et al.*, 1992; Kifle & Purdie, 1993; Iriarte & Purdie, 1994; Proença, 1994). This is consistent with the concentrations of up to 20.7 and up to 41.6 μg L^{-1} measured during this work also in the coastal waters and mid estuary (see Fig. 3.5). However, during this research maximum Chl-*a* peaks at this sites were measured at 9 m depth (see Fig. 3.5), which was due to the to the accumulation of *Phaeocystis* spp. cells, as shown by microscopic analysis. In fact, *Phaeocystis* sphere-like colonies were visible to the naked eye in the water samples collected at these sites on the 21-May. In the upper estuary, two Chl-*a* peaks of up to 64.0 and 36.8 μg L^{-1} coincided with relatively strong stratification, as suggested by the vertical distribution of salinity on the 04-Jul and 01-Aug (see Figs. 3.1 and 3.5). On these two dates, highest differences between surface (1 m) and depth (9 m) salinity of 8.7 and 4.7 respectively, were recorded. Stratification has also been observed to be stronger in the upper estuary, and has been associated with red tide occurrence (*e.g.* Crawford *et al.*, 1997), although no red tide was observed in the period May-September 2001.

3.3.2 Nitrogen uptake in the Southampton Water estuary

3.3.2.1 N uptake in the Southampton Water estuary and other systems

The experiments carried out during this investigation have shown that the uptake of the three nitrogen sources studied respond to downwelling PAR in a Michaelis-Menten like fashion (Fig. 3.7), with highest uptake rates occurring at the 100 and 50% subsurface PAR levels. Although in some cases the uptake of nitrogen and carbon seemed to exhibit photoinhibition (*i.e.* ρ at 100% subsurface PAR $< \rho$ at 50% subsurface PAR), these results indicate that the uptake of dissolved nitrogen strongly depends on light availability in the

Southampton Water estuary. Nitrogen and carbon uptake rates integrated throughout the euphotic water column showed that higher uptake rates occurred during the productive period and that highest values coincided with the Chl-*a* peaks (*i.e.* phytoplankton blooms) observed (Figs. 3.8 and 3.9), suggesting phytoplankton activity played a major role in controlling the fate of dissolved nitrogen species. The seasonal change of the integrated uptake rates of nitrogen and carbon, together with the seasonal change of Chl-*a* marked the end of the productive spring-summer period in 2001, with uptake rates and chlorophyll concentrations dropping drastically from August to September as the averaged light availability declined (Figs. 3.4, 3.8 and 3.9). The dark nitrogen uptake rates were in some cases comparable with uptake under light conditions (see Table 3.3), and particularly when comparing dark uptake rates from an estuarine environment (*e.g.* inner estuary) with coastal waters (see Table 3.3).

Net nitrogen uptake rates measured in the present work are comparable with reports in the literature, although some rates are at the high end of ranges found in other systems. For instance, the high nitrate and ammonium uptake rates of up to 3.974 and 5.158 μmol L^{-1} h^{-1} respectively measured in the inner estuary (see Table 3.3) are close to those measured by Carpenter & Dunham (1985) in a relatively small estuary (~4 km long), of up to 7.24 and 7.59 μmol L^{-1} h^{-1} of nitrate and ammonium respectively. On average however, values from the inner part of Southampton Water estuary (SW) are similar to uptake rates observed in large estuaries such as Chesapeake Bay (*e.g.* Bronk & Glibert, 1993a; Bronk *et al.*, 1994, 1998)(see Tables 3.3, 3.6 and 3.7). Uptake rates from coastal waters of the SW estuary are also consistent with values reported for coastal systems such as the English Channel (L'Helguen *et al.*, 1996), Monterey Bay (Kudela & Dugdale, 2000), California Bight (Ward & Bronk, 2001) or the Southern North Sea (Weston *et al.*, 2004) for example (see Tables 3.6 and 3.7). Overall, nitrogen uptake rates measured in Southampton Water are relatively high compared with other estuaries within the UK and continental Europe, and other marine systems (see Tables 3.6 and 3.7).

Although high nitrate and ammonium uptake rates have been measured in turbid DIN-rich estuaries such as the Thames (Middelburg & Nieuwenhuize, 2000b), The Ems, Scheldt, Loire, Gironde, Douro and Rhine (Middelburg & Nieuwenhuize, 2000a), it has been observed that heterotrophic bacteria accounts for most of the nitrogen assimilated in these estuaries (Middelburg & Nieuwenhuize, 2000a,b). The high nitrogen uptake rates measured in the Southampton Water estuary are most likely the result of the elevated primary production rates reached during the phytoplankton blooms typical of this system. Southampton Water is a non-turbid estuary that has been shown to exhibit some of the highest Chl-*a* peaks compared with other system (*e.g.* see Table 1 in Cebrián & Valiela, 1999) and where high seasonal-integrated primary production rates of 43.2 and 67.6 g C m^{-2} in spring (Apr-Jun) and 126.3 and 54.2 g C m^{-2} in summer (Jul-Sep) have

Table 3.6: Nitrogen uptake rates in the Southampton Water estuary and other estuarine systems. Dimensions are in nmol L^{-1} h^{-1} for comparison with low uptake rates reported in the literature.

Study area	**Nitrogen uptake rates**					**Authors**
Estuarine systems	**Nitrate**	**Ammonium**	**Urea**	**FAA**	**DON**	
Inner Southampton Water	⩽1.0 - 3,974	1.0 - 5,158	⩽1.0 - 667.0			Present study (2001)
Inner Southampton Water	1.0 - 533	5.0 - 1,165				Present study (2002)
Thames estuary	1.0 - 1,440	3.0 - 420.0	0.1 - 7.0	6.0 - 150.0		Middelburg & Nieuwenhuize (2000a)
The Ems, Scheldt, Loire, Gironde, Douro & Rhine	0.25 - 250.0	5.0 - 1,560				Middelburg & Nieuwenhuize (2000b)
Chesapeake Bay	0 - ∼300	∼5 - 1,200	∼50 - ∼600			Bronk *et al.* (1998)
The Tweed	<0.2	<0.3	<0.1			Shaw *et al.* (1998a)
The Humber	<4.0 - <12.0	∼4.0 - 15.5	<4.0			Shaw *et al.* (1998b)
Lower Chesapeake Bay		30.4 - 237.6				Bronk *et al.* (1994)
Upper Chesapeake Bay	478.4	100.0				Bronk *et al.* (1994)
Chesapeake Bay	90.0 - 360	80.0 - 500.0			140 - 530	Bronk & Glibert (1993a)
Choptank River		∼100.0 - 1,100				Bronk & Glibert (1993b)
Chesapeake Bay Plume	2.0 - 560.0	1.0 - 850.0	8.0 - 670.0			Glibert & Garside (1992)*
Chesapeake Bay	∼50.0 - 490.0	∼ 100.0				Bronk & Glibert (1991)
Choptank River		367.0 - 605.0				Bronk & Glibert (1991)
Chesapeake Bay	1.0 - 166.0	4.0 - 743.0				Horrigan *et al.* (1990)*
Delaware estuary	0.0 - 100.0	13.0 - 280.0				Pennock (1987)*
Carmans River estuary	0.0 - 7,240	0.0 - 7,590	0.0 - 600.0			Carpenter & Dunham (1985)
Chesapeake Bay		32.0 - 517.0				Wheeler *et al.* (1982)

* Taken from L'Helguen *et al.* (1996).

Table 3.7: Nitrogen uptake rates (nmol L^{-1} h^{-1}) in some coastal and open ocean systems.

Study area	Nitrogen uptake rates					Authors
Coastal systems	**Nitrate**	**Ammonium**	**Urea**	**FAA**	**DON**	
Coastal Southampton Water	1.0 - 173.0	3.0 - 299.0	⩽1.0 - 107.0			Present study (2001)
Coastal Southampton Water	1.0 - 87.0	1.0 - 1,242				Present study (2002)
Southern North Sea	0.0 - 56.0	0.0 - 45.0				Weston *et al.* (2004)
Monterey Bay	<5.0 - 175.0	<10.0 - 550.0				Ward & Bronk (2001)
California Bight	<10.0 - 45.0	<10.0 - 80.0				Ward & Bronk (2001)
Armorican Shelf, France	2.1 - 26.3	3.2 - 38.1				Maguer *et al.* (2000)
Monterey Bay	~50.0 - 600.0	<50.0 - 700.0				Kudela & Dugdale (2000)
Western English Channel	1.0 - 48.0	1.0 - 41.0	1.0 -15.0			L'Helguen *et al.* (1996)
Bellinghausen Sea	0.09 - 47.2	0.03 - 31.2	nd - 59.0			Bury *et al.* (1995)
Caribbean Sea		20.1 - 30.7				Bronk *et al.* (1994)
Southern California Bight	1.5 - 6.3	26.8 - 48.4				Bronk *et al.* (1994)
Auke Bay, Alaska	0.0 - 373.0	0.0 - 360.0				Kanda *et al.* (1990)*
Scotian Shelf		0.0 - 63.0	0.0 - 53.0			Cochlan (1986)*
Bedford Basin	0.0 - 285.0	30.0 - 413.0				Roche (1983)*
Narragansett Bay	0.0 - 307.0	7.0 - 744.0	0.0 - 266.0			Furnas (1983)*
Oslofjord	0.0 - 265.0	1.0 - 402.0				Paasche & Kristiansen (1982)*
Vineyard Sound	0.0 - 22.0	0.0 - 100.0				Glibert (1982)*
Apex of the NY Bight	0.0 - 480.0	10.0 - 850.0				Garside (1981)*
Open Ocean systems						
North Atlantic	<2.0 - 53.0	<2.0 - 8.0				Bury *et al.* (2001)
Equatorial Pacific	<0.4 - <2.0					Raimbault *et al.* (2000)

* Taken from L'Helguen *et al.* (1996).

been estimated respectively for the mid estuary and coastal waters (Iriarte & Purdie, 1994). During the present study integrated carbon uptake rates of up to 37.7, 204.8 and 166.5 mmol-C m^{-2} h^{-1} were determined respectively in the coastal waters, mid and upper estuary during the productive period (May to September), and imply a concomitant high uptake of nitrogen in order to meet the N requirements of the phytoplankton population growth. The fact that overall nitrogen and carbon uptake rates responded to downwelling PAR (Fig. 3.7) and that high integrated carbon and total nitrogen uptake rates were in general highest when highest Chl-*a* values were observed (Fig. 3.8), strongly suggests that phytoplankton activity accounted for most of the nitrogen uptake. Furthermore, the uptake of the three nitrogen sources studied showed a marked decrease when the Chl-*a* levels dropped after September (Fig. 3.9). In addition, it must be also noted that the uptake experiments were carried out with water samples collected from 2 m depth and that these samples were subjected to different *in situ* light conditions, and therefore the results represent the response of the phytoplankton populations from the selected sites to the chosen light levels (*i.e.* 100, 50, 10, 1 and 0% of subsurface PAR). In the case of heterotrophic bacteria, it has been observed that these microorganisms obtain most of their N requirements (even >100%) from dissolved free and dissolved combined amino acids in estuaries and coastal waters (*e.g.* Fuhrman, 1990; Jorgensen *et al.*, 1999b,a), and can be out-competed by autotrophs at elevated substrate concentrations (Suttle *et al.*, 1990). Bacterial production is usually higher with increasing turbidity (Goosen *et al.*, 1999).

3.3.3 Contribution of different nitrogen sources to total nitrogen uptake

Results from the present study have demonstrated that overall the total nitrogen uptake was dominated by the uptake of ammonium at the three selected sites within the estuary (see Table 3.5 and Fig. 3.10), contributing with a global average (*i.e.* including all sampling sites) of 63.7% from integrated uptake and 70.6% from dark uptake rates. The results also showed that the global average contribution from the other nitrogen sources was 25.8 and 21.7% from nitrate and 10.5 and 7.7% from urea, from integrated and dark uptake rates respectively.

The contribution of ammonium uptake from integrated and dark uptake rates did not exhibit a temporal trend at any of the sampling sites and the contribution of nitrate and urea uptake exhibited temporal and spatial variability (Fig. 3.10). In the case of nitrate uptake, highest and/or dominant contributions coincided with Chl-*a* peaks during the productive period (May to September) in the mid estuary and coastal waters (Fig. 3.10), but only coincided with one Chl-*a* peak (19-Jun) in the upper estuary (Fig. 3.10). The

same trend was also observed for the contribution of urea, but only in the coastal waters (Fig. 3.10). On average, the contribution of urea from integrated and dark uptake rates seemed to be more important from the upper estuary down to the coastal waters (Table 3.5), while the contribution of nitrate seemed to be more important in the order mid estuary>upper estuary>costal waters (Table 3.5). Although the contribution of ammonium was in general dominant over the other N sources, its average contribution seemed to be lower in the mid estuary and similar in the coastal waters and upper estuary (Table 3.5). These findings are in general consistent with observations in the Carmans River estuary for example, where Carpenter & Dunham (1985) observed that the importance of urea uptake to the total nitrogen uptake increase from the top of the estuary down to the Bellport Bay waters, reaching a contribution of 25%. Carpenter & Dunham (1985) also found that the highest contribution of ammonium uptake (55.7%) occurred in the upper estuary and together with urea contributed 72.5% of the total uptake at the mouth of the estuary, whereas the highest averaged contribution of nitrate uptake (77.6%) was recorded in the mid estuary.

The high contribution of ammonium to total nitrogen uptake is well aknowledged in many field studies and laboratory experiments (*e.g.* L'Helguen *et al.*, 1996; Dortch, 1990; Bronk & Ward, 1999; Maguer *et al.*, 2000; Ward & Bronk, 2001; Weston *et al.*, 2004) and in some works it has been suggested that nitrate uptake is inhibited by ammonium, at concentrations $\gtrsim$1 μmol L^{-1} (reviewed by Dortch, 1990). However, the interaction of ammonium and nitrate is complex and several works suggest that although ammonium can promote the inhibition of nitrate uptake, the effect rarely suppress the uptake of nitrate (Dortch, 1990). Moreover, overall dominance of nitrate uptake has been also recorded (*e.g.* Carpenter & Dunham, 1985). The utilization of specific nitrogen sources may be related to the dominant phytoplankton groups, which in turn may be affected by the prevalent physical environment (*i.e.* light availability, temperature and salinity) in a given ecosystem. In some studies for example, the seasonal changes in total nitrogen uptake have been observed to be positively related to water temperature (Carpenter & Dunham, 1985; L'Helguen *et al.*, 1996). Laboratory and field experiments carried out by Lomas & Glibert (1999a) with estuarine diatoms and dinoflagellates (grown at 180 μmol m^{-2} s^{-1}), showed that diatoms presented higher half inhibition concentration values (K_i=0.24 - 4.64 μmol L^{-1}) than dinoflagellates. That is, nitrate uptake by diatoms can be inhibited by higher concentrations of ammonium relative to the inhibiting ammonium concentration affecting nitrate uptake by dinoflagellates. These authors pointed out that even at ammonium concentrations of 200 μmol L^{-1}, nitrate was not completly inhibited (*e.g.* average 80%). Lomas & Glibert (1999a) also observed that, with the exception of one dinoflagellate spp., the inhibition of nitrate uptake decreased as the growth-temperature decreased and suggested that this fact was probably due to the different optimal temperatures of

the enzymes related to nitrate reduction or assimilation of ammonium. In addition, dinoflagellates have been shown to exhibit high nitrate reductase activity during blooms, even when ammonium is abundant relative to nitrate concentrations (Harrison, 1973). In the Carmans River estuary for instance, Carpenter & Dunham (1985) found that the highest contribution of nitrate to the total nitrogen uptake in the mid estuary was probably linked to the dominance of dinoflagellates. The dominance of specific nitrogen sources may also be related to the availability of N-nutrients. For example, some works have shown shifts from dominance of nitrate uptake to dominance of ammonium uptake as the nitrate levels declined after a phytoplankton bloom (*e.g.* Bronk *et al.*, 1998; Kudela & Dugdale, 2000; Bury *et al.*, 2001), or as the nitrate levels declined as upwelled water travels along the shelf break (Joint *et al.*, 2001). In summary, the interaction between the uptake of different nitrogen sources is affected by physical forcings acting contemporaneously on phytoplankton populations, and recent research suggests that the extent of the effect may be related to the conditions regulating the physiological machinery of specific phytoplankton groups (*e.g.* Dortch, 1990; Lomas & Glibert, 1999a; Lomas *et al.*, 2000).

In order to assess the interaction between nitrate and ammonium uptake, some researchers (*e.g.* Carpenter & Dunham, 1985; Dortch, 1990; Weston *et al.*, 2004) have used the relative preference index (RPI) Eq. 3.2, put forward by McCarthy *et al.* (1977);

$$RPI_{NO_3^-} = \frac{\frac{\rho NO_3^-}{\sum \rho_N}}{\frac{[NO_3^-]}{[\sum N]}} \tag{3.2}$$

where the ratio of nitrate uptake (ρNO_3^-) to the sum of nitrogen sources taken up ($\sum \rho_N$) is compared with the relative abundance of nitrate ($[NO_3^-]$) with respect to the total dissolved N-nutrients ($[\sum N]$). Values <1 indicate preference for ammonium. However there are several difficulties with the interpretation of this index, and which have been discussed in detail by Dortch (1990). The RPI applied to the results of this investigation for example, produced values ranging from 0.1 to 0.7, 0.1 to 0.9 and 0.1 to 1.1 for the coastal waters, mid and upper estuary respectively. These index values however, are affected by the strong dependence of the uptake rates on the availability of light through the euphotic water column and thus decrease with depth overall. Therefore the apparent preference would be different for the same phytoplankton population under the same N-nutrient ambient levels.

In the present study, the seasonal changes of integrated nitrogen uptake rates did not seem to be related to the seasonal changes in temperature or to N-nutrient levels at any of the selected sites. In general, results indicate that the uptake of ammonium and nitrate from integrated and dark uptake rates increased concomitantly, although not necessarily in a linear fashion (**Fig. 3.12** left side panels). However, the contribution

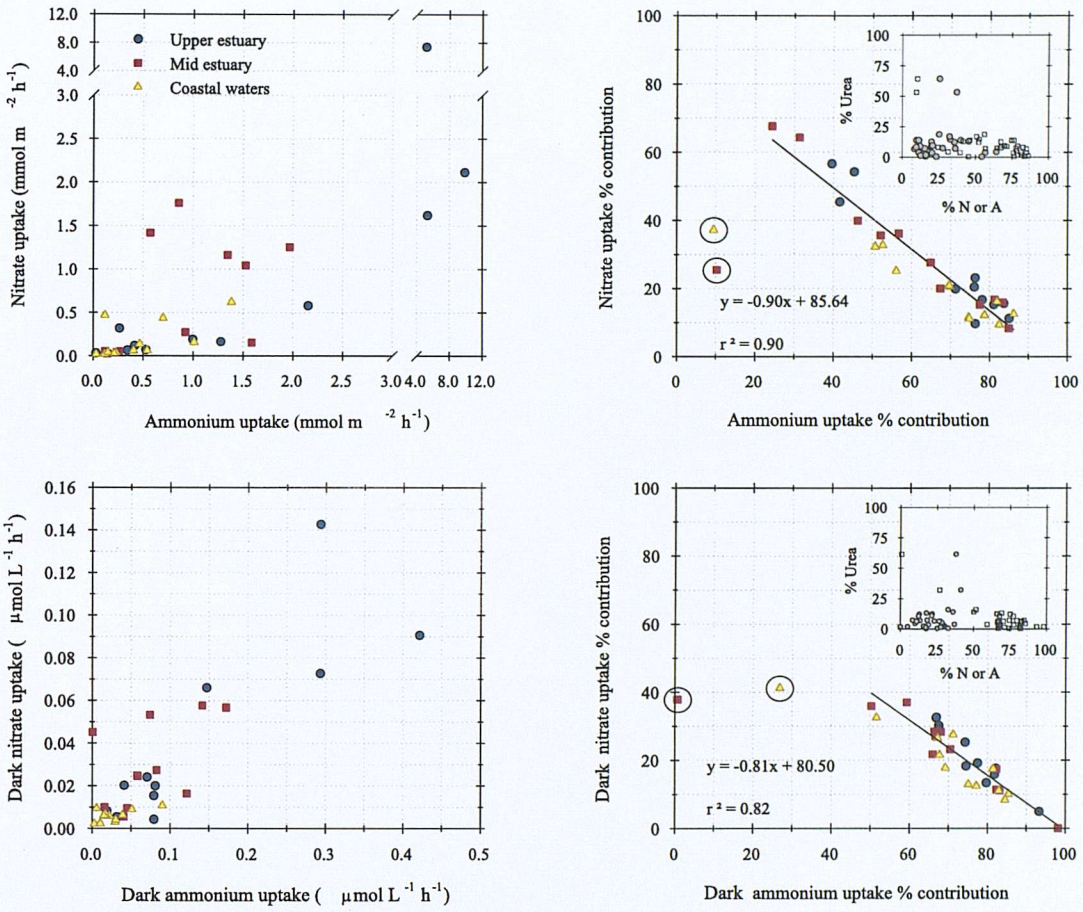

Figure 3.12: **Relation between nitrogen sources from integrated and dark uptake rates;** uptake rates and relative percent contribution to total nitrogen uptake. Symbols represent the upper estuary (blue circles), mid estuary (red squares) and coastal waters (yellow triangles). Encircled symbols in right side panels were not considered in the regression and represent the date (19-Jun) when the uptake of urea was dominant. The inserted smaller plots on the right side panels show the relation between the relative contribution of urea with respect to the contributions of nitrate (grey circles) and ammonium (open squares).

of both nitrogen sources exhibited a negative linear relation, with the contribution of nitrate decreasing as the contribution of of ammonium uptake increased (Fig. 3.12 right side panels). When plotting either the uptake or contribution of urea against the uptake or contribution of nitrate or ammonium no relationship was apparent (Fig. 3.12 inserted plots left side panels). These results suggests that ammonium and nitrate were the main sources supplying the N required by phytoplankton growth, and that urea was likely taken up as complement nitrogen source.

The interaction between nitrate and ammonium uptake may be also related to the dominant phytoplankton species in the Southampton Water estuary. Preliminary results[2]

[2]Due to time constrictions, it has been possible to count cells only from the coastal waters. Cell counts were carried out by Ben Green at the Southampton Oceanography Centre, using the method described by Utermöhl (1958).

of phytoplankton cell counts from the coastal waters showed high numbers of diatoms from May to July (Figs. 3.13 and 3.14). During this period, diatom concentrations reached >120 000 cells L^{-1}, whereas highest numbers of dinoflagellates and flagellates were ~1 400 cells L^{-1} and ~2 000 cells L^{-1} respectively. A single Haptophyte species (*e.g. Phaeosystis* spp.) peak was observed, with a concentration of ~1 200 cells L^{-1}. These results are in good agreement with previous observations in the Southampton Water estuary that have shown that the spring bloom in the system is commonly dominated by diatoms, while dinoflagellates and flagellate dominate the summer bloom (Leakey *et al.*, 1992; Kifle & Purdie, 1993; Howard *et al.*, 1995; Ali, 2003). Recent research has shown that the spatial distribution of phytoplankton species is dominated by diatoms and flagellates in the coastal waters, diatoms and mainly dinoflagellates in the mid estuary during summer, and diatoms, flagellates, and ciliates varying with time in the upper estuary (Ali, 2003). Reports in the literature suggest that the uptake of nitrate by diatoms may be more affected by temperature than dinoflagellates (*e.g.* Harrison, 1973; Carpenter & Dunham, 1985; Lomas & Glibert, 1999a). Although a relation between the uptake rates and temperature was not apparent during this study, seasonal changes in the water temperature of ~12^{o}C can be observed between April and August (see Appendix B.0.6, Fig. B.1) and may influence the uptake of nitrogen by the dominant phytoplankton groups within the system. Relative contributions of nitrate uptake in the mid estuary for example, were generally highest during the warmest months (July-August) (see Fig. 3.10 and Fig. B.1, Appendix B.0.6), the period when dinoflagellates have been shown to be dominant (*e.g.* Ali, 2003). In the upper estuary, highest contributions of nitrate were observed in June and September (see Fig. 3.10) for instance, and diatoms have been observed to dominate in June at this site and diatoms, dinoflagellaes and ciliates in September (Ali, 2003). The scenario is however complicated, and the availability of light may also play an important role in controlling the uptake of nitrogen within the system. The complexity is nonetheless interesting and prompts more research in this field.

3.3.4 Nitrogen removal by phytoplankton

Depletion rates

The removal of nitrate by phytoplankton growth has been previously assesed in the Southampton Water estuary (Hydes & Wright, 1999; Hydes, 2000) with the use of mixing diagrams. This has been done by drawing regression lines (*e.g.* NO_3^- *vs* salinity) from the most seaward sample to the next most saline and calculating the Pearson's moment correlation coefficient until it becomes insignificant and an estimation of a zero salinity (the intercept) can be obtained (Hydes & Wright, 1999; Hydes, 2000). The deficit of nitrate has been thus calculated relative to the theoretical conservative mixing. This method however, has been found difficult to apply to ammonium for example, due

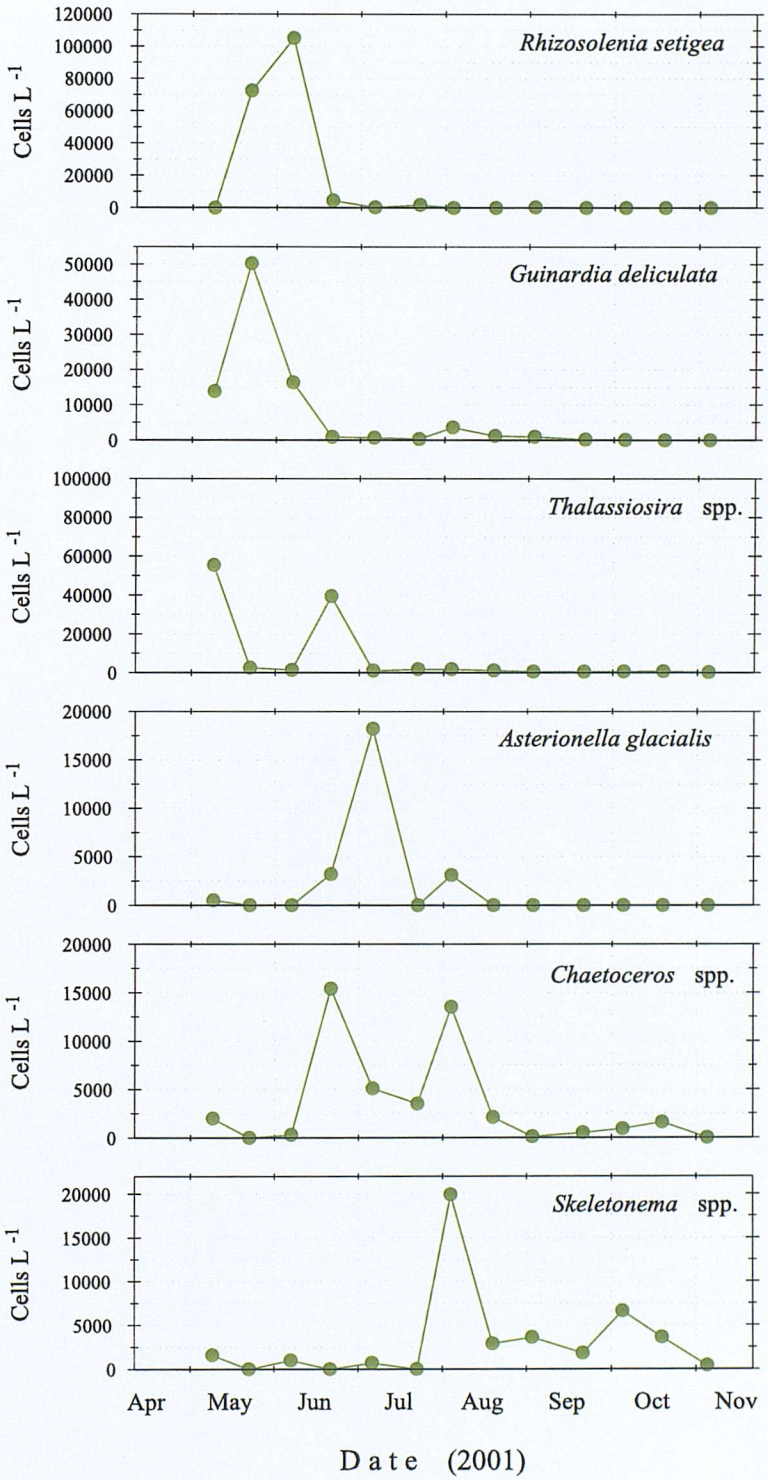

Figure 3.13: **Temporal distribution of dominant diatoms in the coastal waters of the Southampton Water estuary during 2001.** Note different scales on y axis.

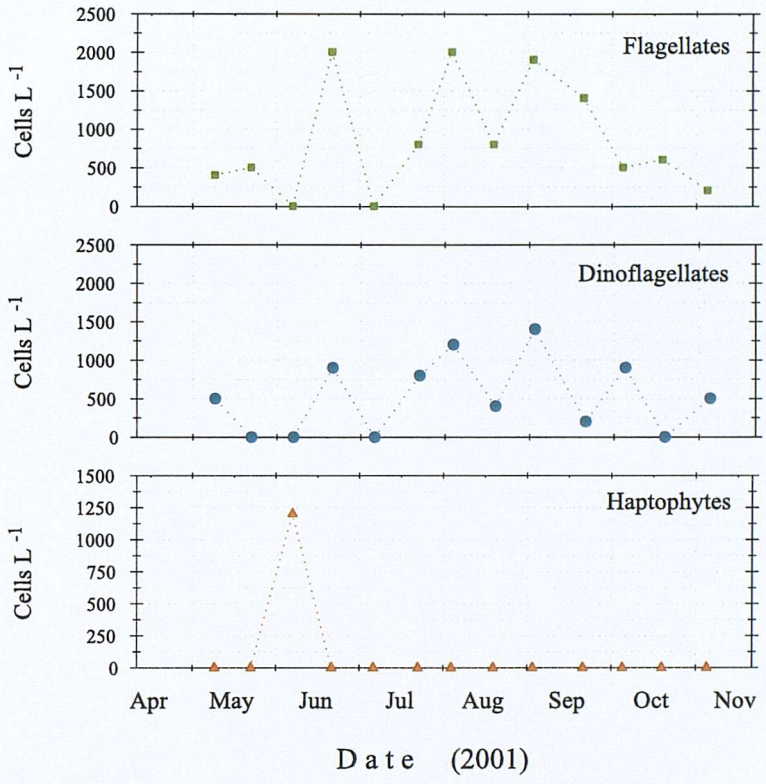

Figure 3.14: **Temporal distribution of flagellates, dinoflagellates and haptophytes (*e.g.* *Phaeosystis* spp.) in the coastal waters of the Southampton Water estuary during 2001.** Note different scales on y axis.

to its non-conservative behaviour (Hydes & Wright, 1999; Hydes, 2000). In the present study, even at high chlorophyll *a* levels nitrate appeared to exhibit conservative behaviour (**Fig. 3.15**), whereas in the case of ammonium and urea, no conservative behaviour is apparent (Fig. 3.15). If in Fig. 3.15, a line is drawn from the most brackish data point (salinity 21.9, nitrate 95.7 μmol L^{-1}) to the most saline data point (salinity 33, nitrate 2.7 μmol L^{-1}), nitrate seemed to exhibit overall conservative behaviour (see Fig. 3.15) and the second data point (nitrate 83.2 μmol L^{-1}, salinity 25.3) would suggest a nitrate source (see Fig. 3.15). However, this second data point corresponds to a depth of 2 m, thus suggesting nitrate removal at 1 m depth (*i.e.* the first and most brackish data point). Furthermore, assuming that the most brackish data point is representative of the upper estuary end member and assuming conservative behaviour, a simple calculation can be done to determine the concentration of nitrate at the estuary mouth end member; *i.e.* given that salinity changed in a ratio 21.9/33, then the concentration of nitrate at the most saline data point should be approximately equal to $\frac{21.9}{33} \times 95.7 = 63.5$ μmol L^{-1} (dotted line and black circle inside a square in Fig. 3.15), instead of the 2.7 μmol L^{-1} measured. This simple exercise shows that mixing diagrams can be somewhat misleading, and suggests that a large removal of nitrate is likely taking place within the estuary.

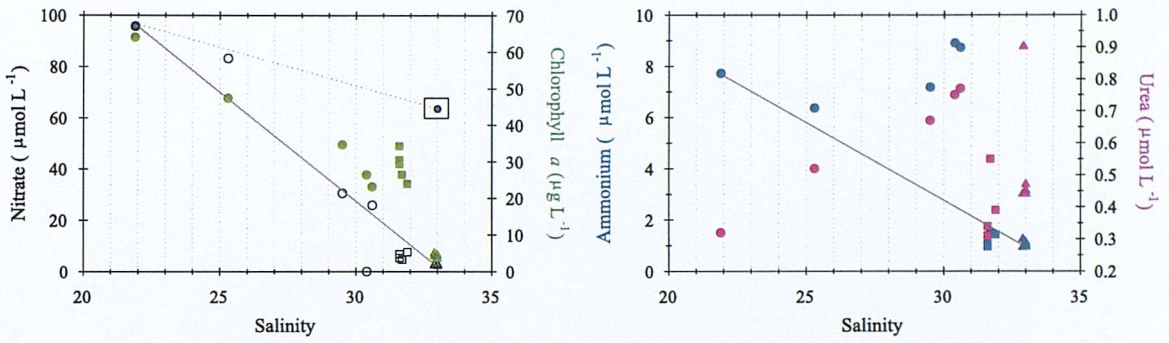

Figure 3.15: **Nitrate, chlorophyll *a*, ammonium and urea plotted against salinity.** The data shown correspond to measurements carried out on the 04-July, one of the dates when Chl-*a* peaks were observed and some of the highest nitrogen uptake rates measured. Symbols represent the upper estuary (circles), the mid estuary (squares) and the coastal waters (triangles). Data include values from the five depths sampled (*i.e.* 1, 2, 4, 7 and 9 m). For solid line, dotted line and data point inside a square see text below. Two examples more are presented in Appendix B.0.9, Fig. B.2.

By directly measuring the uptake rates of different N-sources, it is possible to estimate their removal by phytoplankton growth by calculating the depletion rates of the ambient N-nutrient concentrations (Shaw *et al.*, 1998a). The calculation is simply done by obtaining the ratio of the uptake rate of each nitrogen source to its respective N-nutrient ambient concentration. That is,

$$Depletion\ rate = \left(\frac{\rho}{[N]}\right) \times 100 \tag{3.3}$$

where the ρ represents the uptake of nitrate, ammonium or urea (*e.g.* μmol L^{-1} h^{-1}), $[N]$ represents the ambient levels of the respective nitrogen source (*e.g.* μmol L^{-1}) and where the *Depletion rate* is expressed in % h^{-1}. The impact of nitrogen uptake on the ambient levels was evaluated in two ways. First, by using the uptake rates from the different light levels and the ambient N-nutrient concentration of water collected for the incubation. Second by calculating the depletion rate using the integrated uptake rates and the integrated (from 1 m depth down to 9 m) ambient nutrient concentrations, assuming it was representative of the N-nutrients content within the euphotic water column. The depletion rates from net uptake rates and integrated values showed a broad range of variation (**Table 3.8**), particularly when considering depletion at different light levels. On average the results were fairly similar when comparing the depletion of the different nitrogen sources with the respective site (Table 3.8). In general, highest depletion rates were reached from May to August (data not shown), and were more significant at the 100 and 50% of subsurface PAR (data not shown). From Table 3.8 can be noted that phytoplankton growth produced a relative higher impact on the three nitrogen sources

investigated in the mid estuary.

Table 3.8: Nitrate, ammonium and urea depletion rates (% h^{-1}) calculated from net uptake rates and from uptake rates and N-nutrient concentrations integrated throughout the euphotic water column. Mean (bold) and range of variation (parentheses) during the productive spring–summer period in 2001.

	Nitrate	**Ammonium**	**Urea**
From net uptake			
Upper estuary	**0.6**	**4.6**	**5.5**
	(<0.1 - 18.4)	(<0.1 - 58.0)	(0.1 - 83.0)
Mid estuary	**1.4**	**8.0**	**10.9**
	(<0.1 - 23.2)	(0.1 - 59.6)	(0.1 - 90.4)
Coastal waters	**0.3**	**5.9**	**3.6**
	(<0.1 - 2.2)	(0.3 - 37.3)	(0.1 - 24.3)
From integrated uptake			
Upper estuary	**0.4**	**2.7**	**2.5**
	(<0.1 - 1.8)	(0.1 - 15.0)	(0.1 - 14.1)
Mid estuary	**1.2**	**5.9**	**11.0**
	(<0.1 - 8.8)	(0.2 - 28.0)	(<0.1 - 51.5)
Coastal waters	**0.4**	**3.7**	**3.0**
	(<0.1 - 1.3)	(0.3 - 14.9)	(0.1 - 15.1)

The depletion rates calculated from integrated values suggests that the impact of nitrogen uptake by phytoplankton populations can be significant during the productive period in the Southampton Water estuary, accounting for up to ~9, 28 and 50% of the removal of nitrate, ammonium and urea from the euphotic water column in one hour. In turn, the depletion rates calculated from uptake at different light levels suggest that the magnitude of the effect depends on the availability of light in the water column and therefore the major impact takes place in the upper layers; in the Southampton Water estuary the depth of the 50% subsurface PAR was found at an average depth of 1.1±0.3 m in 2001. Furthermore, these results also suggest that nitrogen removal can be even more significant during the high water stand, that in the system can last up to 3 h. Water column depletion rates of up to 13, 15 and 12% d^{-1} for nitrate, ammonium and urea respectively have been estimated for the turbid Humber plume (Shaw *et al.*, 1998b). Mean depletion rates of nitrate, ammonium and urea of respectively <0.5, <6.0 and <4% h^{-1} have been reported for the non-turbid Tweed estuary (Shaw *et al.*, 1998a) and of 15 to 23 % h^{-1} for ammonium estimated for the Carmans River estuary by Shaw *et al.* (1998a), using data from Carpenter & Dunham (1985). As compared with these results, depletion rates estimated for the Southampton Water estuary are relatively high, suggesting that phytoplankton growth can have an important impact on the nitrogen levels in non-turbid estuaries such as the Southampton Water estuary during productive periods.

Table 3.9: Nitrate, ammonium and urea turnover times (d) calculated from net uptake rates and from uptake rates and N-nutrient concentrations integrated throughout the euphotic water column. Mean (bold) and range of variation (parentheses) during the productive spring–summer period in 2001.

	Nitrate	Ammonium	Urea
From net uptake			
Upper estuary	**102.8**	**9.4**	**7.7**
	(0.2 - 1590)	(0.1 - 85.7)	(0.1 - 34)
Mid estuary	**59.5**	**4.5**	**6.8**
	(0.2 - 352)	(0.07 - 37.2)	(0.05 - 68.2)
Coastal waters	**63.6**	**3.4**	**7.2**
	(1.9 - 383)	(0.1 - 12.5)	(0.2 - 58.1)
From integrated uptake			
Upper estuary	**86.4**	**12.3**	**12.2**
	(2.3 - 242)	(0.3 - 62.1)	(0.3 - 46.7)
Mid estuary	**74.3**	**5.1**	**11.7**
	(0.5 - 280.9)	(0.1 - 19)	(0.1 - 83.7)
Coastal waters	**62**	**4.1**	**9.2**
	(3.1 - 217.6)	(0.3 - 13.5)	(0.3 - 38.8)

Turnover times

The magnitude of the depletion rates of the nitrogen sources studied are reflected in their turn over times (**Table 3.9**). Values suggest that ammonium and urea are rapidly recycled in the Southampton Water estuary, and that even when phytoplankton growth can have significant impacts on the ambient levels of nitrate, this nutrient appears to be supplied at a much higher rate than its removal. However, as can be expected, the turnover times are lower during the productive period (data not shown) and are lower in the upper layers of the water column (data not shown). The turnover times of the nitrogen sources studied therefore depend on the input rate to the system and on the intensity of phytoplankton activity. In general, the turnover times of N-nutrients estimated for the Southampton Water estuary are consistent with values reported in the literature. For example, turnover times of 1.4 - 20, 22 -232, and 4.2 - 69 d have been reported for ammonium, nitrate and urea in Thames estuary (Middelburg & Nieuwenhuize, 2000a), of up to 168, >1000 and up to 548 d (same order as above) in the Humber plume (Shaw *et al.*, 1998b) and of up to 40 and >100 d for ammonium and nitrate respectively, in the southern North Sea (Weston *et al.*, 2004). These turnover times thus indicate that in general, as expected, reduced forms of nitrogen are recycled at a faster rate than oxidised species.

Concluding remarks

This research has produced the first direct measurements of nitrogen uptake in the

Southampton Water estuary, and demonstrates that high nitrogen uptake rates can be reached during the productive spring-summer period. Results obtained during the first stage of this investigation have also shown that nitrogen uptake rates in this system can be higher than those observed in other UK and European estuaries. It must be noted that neither the transfer of the nitrate uptake to the dissolved organic nitrogen pool, nor the regeneration of urea and ammonium were accounted for during the first stage of this investigation and therefore the uptake rates presented may underestimate the total uptake (*i.e.* gross uptake).

Coastal marine ecosystems have been subjected for decades to alterations due to human activities (Herbert, 1999). The production of energy and fertilisers, and cultivation of crops fix nitrogen at a higher rate than natural systems. This has greatly altered the global nitrogen biogeochemical cycle (Galloway *et al.*, 1995). In coastal systems such as estuaries a consequence of this problem is the eutrophication (nutrient enrichment mainly with nitrogen and phosphorus) of the seaward flowing waters (Smith et al., 1999). Nitrogen eutrophication is of great concern to scientist and coastal managers since it may produce deleterious effects such as toxic algal blooms, shifts in ecosystem species composition, degradation of water quality, or losses of commercial fisheries for example (Smith et al., 1999). However, the whole system consists of a complex chain of processes that require the understanding of each of its components if we aim to prevent irreversible impacts to aquatic natural resources (Seitzinger & Sanders, 1997; Herbert, 1999; Smith *et al.*, 1999). Available data shows that nitrate concentrations in the Southampton Water (SW) estuarine system have increased during the last few decades, and also indicate that the main sources of ammonium and urea are sewage effluents (Ashe, 1996; Hydes & Wright, 1999). However, results from the present work have shown that phytoplankton activity can significantly affect the ambient levels of N-nutrients during the spring-summer productive period Table 3.8, and potentially reduce them by up to threefold during diurnal slack water periods.

Chapter 4

Nitrogen cycling in Southampton Water estuary

4.1 Introduction

In order to further investigate the effect of phytoplankton growth on the nitrogen fluxes in the Southampton Water estuary, in 2002 it was aimed to quantify the release of dissolved organic nitrogen (**DON**) from ^{15}N-nitrate uptake, and the release of DON and regeneration of ammonium from ^{15}N-ammonium uptake experiments. Results from 2001 showed that net uptake rates were maximum at the 100% and 50% of subsurface PAR. Therefore in 2002, ^{15}N-tracer experiments were carried out at these PAR levels; *i.e.* assuming that DON release and ammonium regeneration rates would be also maximum. The experimental procedure and chemical analyses involved in quantifying DON release and ammonium regeneration rates proved to be very time consuming and labour intensive. Approximately half a year was dedicated exclusively to the setting up of the techniques used. Because of this it was not possible to processes all samples. Thus, *in situ* incubations carried out at 100% PAR with water collected from the mid estuary were selected as representative. During the experiments carried out in 2002 measurements of nutrients (except silicate) and chlorophyll concentrations were made before starting the incubations and also when the incubations were terminated, thus allowing detectable changes in these variables during the incubation period. In this chapter, results of the second stage of this research are presented and discussed in terms of the factors affecting the cycling of nitrogen by phytoplankton populations within Southampton Water estuary.

4.2 Results

Rough weather conditions made sampling more difficult in 2002. Due to either heavy rain, strong swell or both, only water from 1 m depth was collected from the coastal waters on the 23-May. On the 10-June and 09-July the coastal waters were inaccessible, and on the latter date only water from 1 m depth was collected from the mid and upper estuary. Gaps in the data presented were thus inevitable.

4.2.1 Salinity and Temperature

The vertical, spatial and temporal distribution of salinity is presented in **Fig. 4.1**. Surface **salinity** measured in 2002 increased from the upper estuary down to the coastal waters, with a variation range of 26.3 - 33.2 in the former and 33.2 - 34.5 in the latter. Measurements carried out at 1, 2 and 9 m depth indicated that the influx of freshwater induced stratification of the water column in the mid and upper estuary. Stratification appeared to be stronger in the upper estuary. The vertical distribution of salinity also showed that the water column in the coastal waters was well mixed (see Fig. 4.1).

Due to problems with the underwater cable of the YSI multi probe, the water **temperature** data set was not complete in 2002. Malfunctioning of the instrument and rough weather conditions made temperature measurements only possible on 7 occasions (25-Apr to 07-Aug). During this period the data available showed an increase in the water temperature from values of 11.7, 12.2 and 12.1^{o}C to values of 19.5, 20.0 and 19.9^{o}C in the costal waters, mid and upper estuary respectively. Thermal stratification was not apparent; *i.e.* the vertical distribution of temperature was nearly homogeneous at all sampling sites (see Fig. B.1, Appendix B.0.6).

4.2.2 Nutrients

Overall, nutrient concentrations decreased from the upper estuary towards the coastal waters, where comparatively low vertical and temporal variability was observed. The range of variation in the concentration of nutrients measured in 2002 is presented in **Table 4.1**. The vertical, spatial and temporal distribution of nutrients within the system are shown in **Figures 4.2 and 4.3**. **Nitrate**, **silicate** and **phosphate** showed a seasonal cycle (although was less evident in the distribution of phosphate), with concentrations decreasing towards the summer months and then increasing towards fall. A seasonal trend in the distribution of **ammonium** was not apparent (Fig. 4.2). Peaks in the concentration of nutrients observed throughout the sampling period in the mid and upper estuary coincided with low salinity values, indicating the infiux of nutrient-rich fresh water. Thus, concentrations were generally lower at depth. With the exception of one sampling date

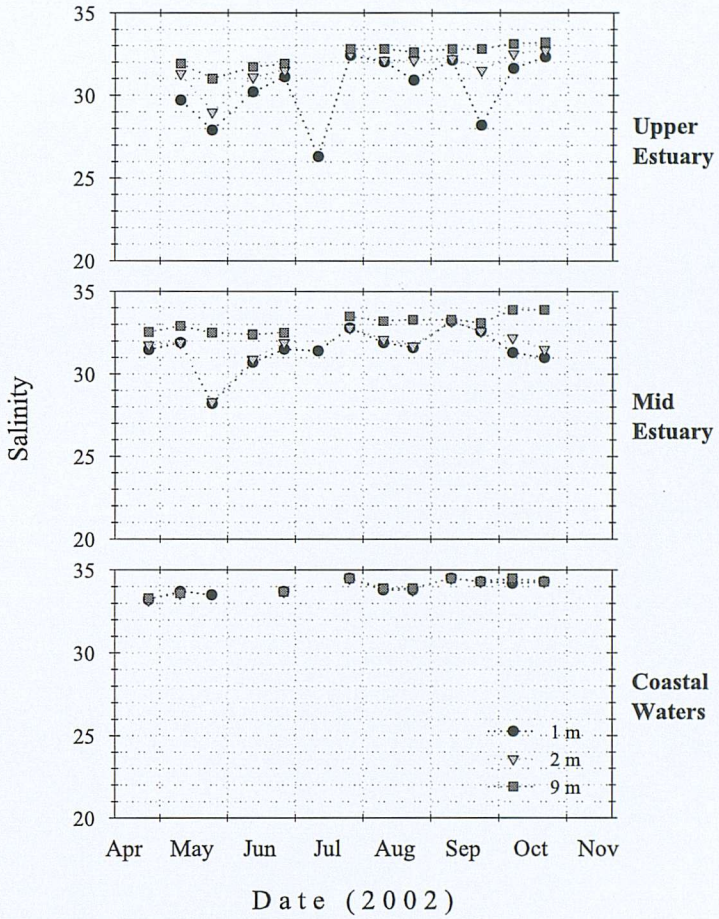

Figure 4.1: **Salinity;** vertical, spatial and temporal distribution within Southampton Water estuary (2002). Symbols in the lower panel apply to all panels.

(19-Sept) when higher nutrient concentrations were measured at 9 m depth, vertical distributions showed higher nutrient levels in surface samples. On the 09-Jul a peak in nutrient concentration was measured in the upper estuary. This peak was particularly high for ammonium and phosphate and reached concentrations of 216.9 and 4.9 μmol L^{-1} respectively. Results from total dissolved nitrogen and dissolved organic nitrogen measurements are presented in § 2.4.1.5.

4.2.3 Irradiance

The seasonal changes of the irradiance attenuation coefficient (k), the incident irradiance (E_0) averaged over the incubation period (4 h) and the mean irradiance available within the upper layer of the water column, *i.e.* from the 100 to the 50% of subsurface PAR (Mean $E_{Z(50\%)}$) recorded at the pontoon during 2002 are shown in **Fig. 4.4**[1]. k values

[1]Data including the attenuation coefficient, depth of the euphotic water column and the mean water column irradiance calculated for the three sampling sites is presented in Fig. B.3, Appendix B.0.10.

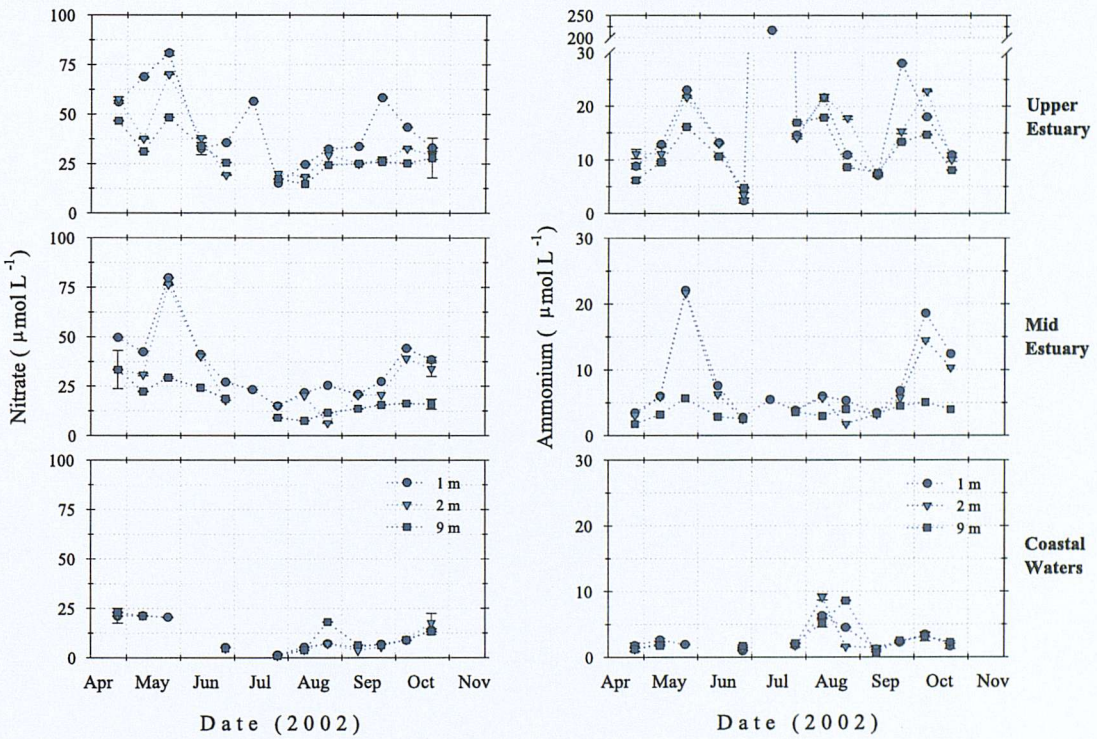

Figure 4.2: **Nitrate and ammonium;** vertical, spatial and temporal distribution within Southampton Water estuary (2002). Note different scale in right-upper panel. Error bars show the standard deviation of replicate (n=3) measurements. Symbols in the lower panels apply to all panels.

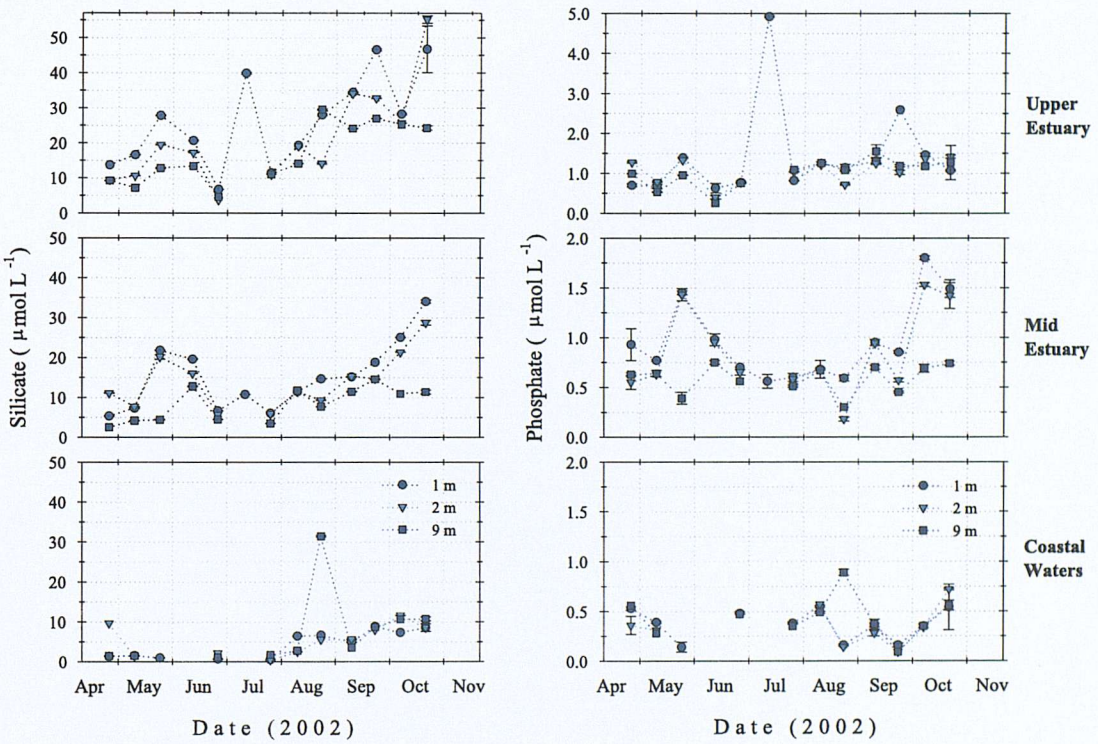

Figure 4.3: **Silicate and Phosphate;** vertical, spatial and temporal distribution within Southampton Water estuary (2002). Note different scale right-upper panels. Error bars show the standard deviation of replicate (n=3) measurements. Symbols in the lower panels apply to all panels.

Table 4.1: Nutrient concentrations within Southampton Water estuary; range of variation during the productive spring–summer period in 2002 (concentrations are in μmol L^{-1}).

	Nitrate	Ammonium	Silicate	Phosphate
Upper estuary	14.7 - 80.8	2.4 - 216.9[a]	3.6 - 55.1	0.3 - 4.9
Mid estuary	6.4 - 79.8	1.7 - 22.0	2.5 - 34.0	0.2 - 1.8
Coastal waters	1.0 - 22.9	0.6 - 9.1	<0.5 - 31.4	<0.1 - 1.2

[a]Apart from this extremely high value, concentrations at this site were <30 μmol L^{-1}.

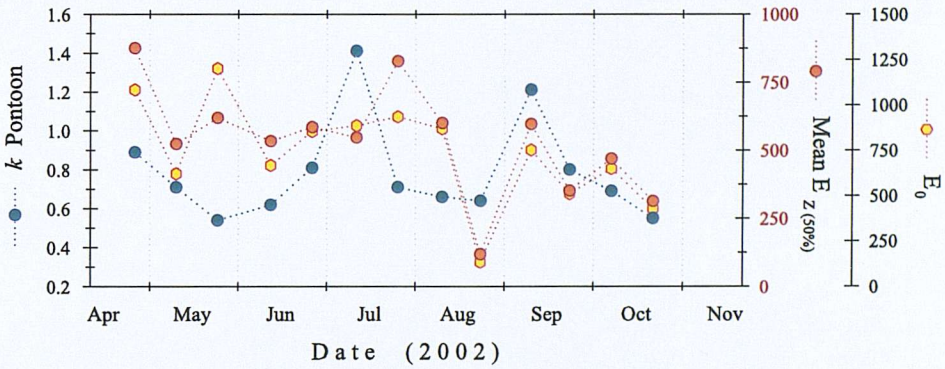

Figure 4.4: **Irradiance attenuation coefficient (k), 4 h averaged incident irradiance (E_0) and mean surface layer irradiance ($E_{Z(50\%)}$) during 2002.**

varied between 0.54 and 1.44 m^{-1}, showing two high values on the 09-Jul and 06-Sept (Fig. 4.4) and varying between the minimum value recorded and 0.89 m^{-1} on other dates. The incident irradiance averaged over the incubation period ranged from 134.3 to 1201.3 μmol m^{-2} s^{-1}, showing a marked decrease on the 20-Aug to the minimum value recorded during the sampling period (see Fig. 4.4). The mean irradiance calculated for the upper layer of the water column varied between 118.5 and 875.1 μmol m^{-2} s^{-1}, and closely followed the seasonal changes of the incident irradiance (see Fig. 4.4). On average values estimated for the upper layer of the water column represented 74±11% of the incident irradiance.

4.2.4 Chlorophyll *a*

The spatial and temporal distribution of chlorophyll *a* (Chl-*a*) measured in 2002 is presented in **figure Fig. 4.5**. Concentrations ranged from 0.5 up to 18.2 μg L^{-1}. With the exception of two dates (25-Apr and 24-Jun) where high levels were measured at depth in the coastal waters and mid estuary, concentrations were higher near the surface. Highest Chl-*a* concentrations were measured in the mid and upper estuary. Several peaks were observed through the estuary from June to September. An early peak seemed to have occurred on the 25-Apr in the coastal waters and mid estuary, with values of 4.4 and

5.6 μg L^{-1} respectively; both of them measured at 9 m depth. Four further peaks were recorded at the three sampling sites and were characterised by a sharp increase on the 24-Jun to maximum values of 18.3, 12.7 and 9.9 μg L^{-1} in the upper estuary, mid estuary and coastal waters respectively. In the mid estuary this peak was measured at 9 m depth. Although the chlorophyll levels in the mid estuary remained high ($\sim$12.7 μg L^{-1}) on the 23-Jul and 07-Aug, the magnitude of the peaks observed decreased steadily to values of 5.4, 6.7 and 2.4 μg L^{-1}in the upper estuary, mid estuary and coastal waters respectively. While the stratification of the water column in the mid and upper was well reflected in the vertical distribution of Chl-*a* at these sites, the well-mixed condition was also reflected in the vertical distribution in the coastal waters (see Figs. 4.1 and 4.5).

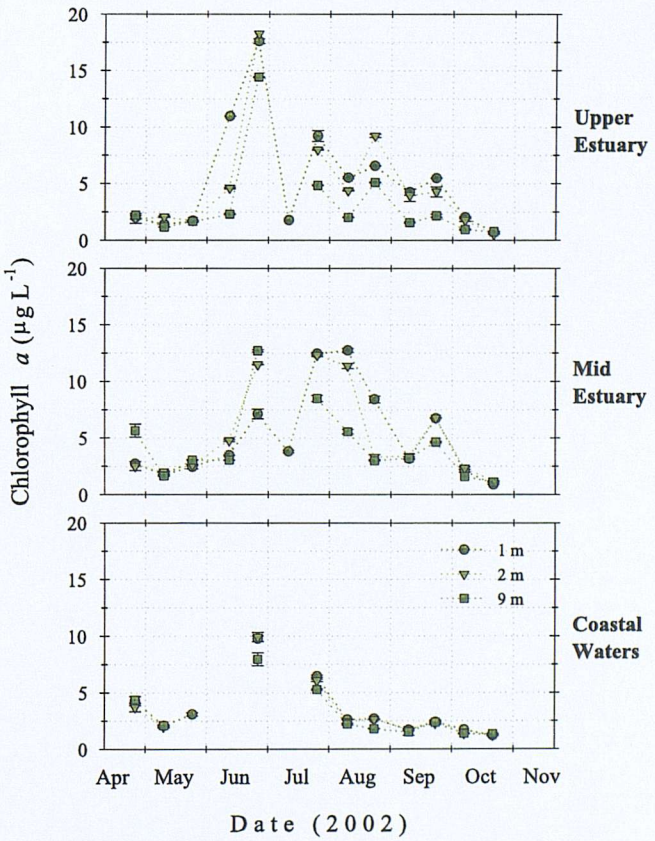

Figure 4.5: **Chlorophyll** *a*; vertical, spatial and temporal distribution within Southampton Water estuary (2002). Error bars show the standard difference of duplicate measurements. Symbols in the lower panel apply to all panels.

4.2.5 Particulate organic nitrogen (PON)

The spatial and temporal distribution of PON in 2002 are shown in **Fig. 4.6** . The values shown correspond to measurements of samples collected from 1 m depth (*i.e.* samples collected for the incubation experiments). PON concentrations increased as the productive

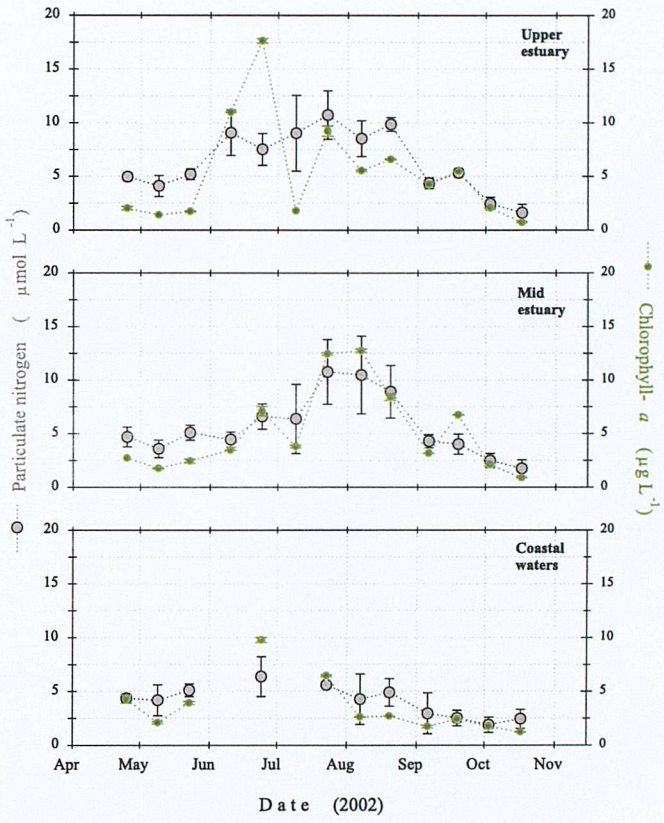

Figure 4.6: **Particulate organic nitrogen (PON);** productive spring-summer period in 2002. Error bars represent standard deviations of replicate measurements (n=6). Chl-*a* values from 1 m depth are shown as reference.

spring-summer period developed. A maximum value of 6.4 μmol L^{-1} was reached in the coastal waters on the 24-Jun and maximum values of 12.0 and 10.7 μmol L^{-1} were later measured in the mid and upper estuary respectively, on the 23-Jul (Fig. 4.6). Concentrations in the mid and upper estuary were of a similar magnitude, and were generally higher than concentrations measured in the coastal waters. Relatively high PON concentrations (*e.g.* >7.5 μmol L^{-1}) were measured in the upper estuary during June, July and August and similar concentrations were measured in the mid estuary from mid July to august (Fig. 4.6). With few exceptions (*e.g.* 24-Jun and 09-Jul, upper estuary), the seasonal changes in PON concentrations closely followed the seasonal trend of chlorophyll *a* (Fig. 4.6). Overall, the PON concentrations decreased gradually towards the end of the sampling period to values of 2.45, 1.76 and 1.62 μmol L^{-1} in the coastal waters, mid and upper estuary respectively.

4.2.6 Incubation experiments

4.2.6.1 Chlorophyll *a* and nutrient concentration changes during incubations

Measurements of Chl-*a* and nutrients made on subsamples collected at the beginning and at the end of the ^{15}N-tracer experiments showed changes in concentrations during the 4 h incubation period. Increases in Chl-*a* concentrations of up to 5.9, 12.6 and 2.0 μg L^{-1} were observed throughout the sampling period in the upper estuary, mid estuary and coastal waters respectively (**Fig. 4.7**). Changes however, were larger between July and September (see Fig. 4.7). On some dates Chl-*a* concentrations seemed to decrease relative to the original concentration in the upper estuary and coastal waters, but appeared to be only significant on the 24-Jun (see Fig. 4.7). In general, Chl-*a* measurements from both incubation treatments (*i.e.* ^{15}N-NO_3^- and ^{15}N-NH_4^+) and both PAR levels (*i.e.* 100 and 50% of subsurface PAR) were consistent (see Fig. 4.7). Decreases in the concentrations of nitrate of up to 32.0, 26.0 and 7.4 μmol L^{-1} and ammonium of up to 13.9, 4.1 and 3.7 μmol L^{-1} were measured in samples from the upper estuary, mid estuary and coastal waters, respectively (see **Figs. 4.8 and 4.9**). These measurements showed the overall temporal trend of the concentration changes during the incubation period, although results from the two ^{15}N treatments were not consistent in some cases. The concentrations of phosphate either seemed to increase or decrease, with values ranging between +0.5 and -4.1 μmol L^{-1} of the original concentration and showing no apparent trend (data is presented in Fig. B.4, Appendix B.0.11). In the case of phosphate, results from the two different ^{15}N-treatments seemed to be more consistent (see Fig. B.4, Appendix B.0.11).

4.2.6.2 Dissolved organic nitrogen (DON).

Although care was taken when storing the glass bottles containing water samples -both in terms of handling and volume capacity- for TDN analysis, a few of them were broken presumably during freezing. Three bottles were found cracked at the time of analysis and produced relatively anomalous results. For example, the TDN concentration measured from a cracked-bottle containing water subsampled before the incubation experiments (03-Oct) was 58.9 μmol L^{-1}, while the concentration measured in water subsampled from both, $^{15}NO_3^-$ and $^{15}NH_4^+$ incubation treatments (non cracked-bottles), were 73.8 and 74.3 μmol L^{-1}, respectively. When calculating the DON concentration (*i.e.* [DON]=[TDN]-[NO_3^-+NH_4^+]) a negative value resulted from the original sample, whereas the DON measured from the other bottles were 12.8 and 11.7 μmol L^{-1}. The consistency between the measurements from non cracked-bottles suggested that the concentration measured in the original sample was likely erroneous. In the other case (23-May), TDN measurements of cracked-bottles containing water subsampled at the end of the incubation experiments showed concentrations of 93.1 and 91.0 μmol L^{-1} from $^{15}NO_3^-$ and $^{15}NH_4^+$ treatments re-

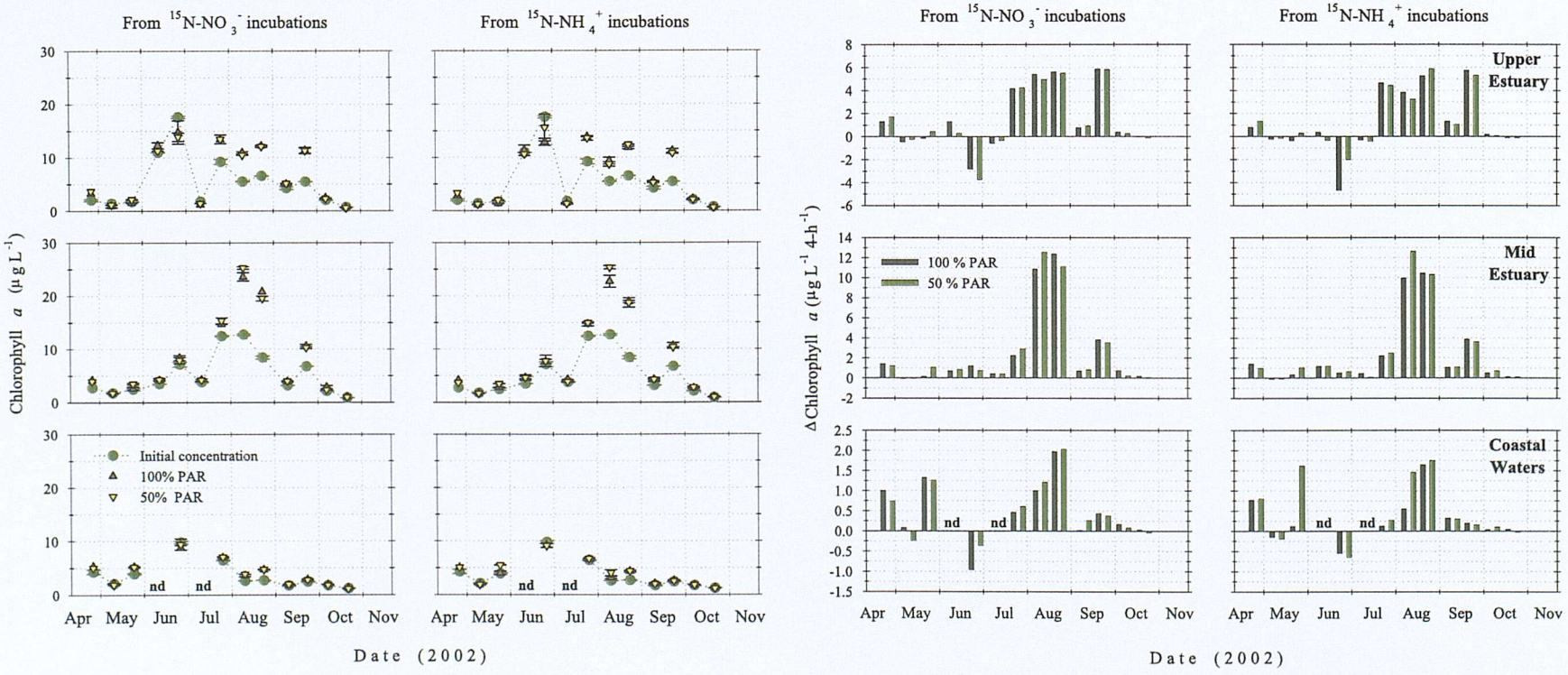

Figure 4.7: **Chlorophyll a changes during the incubation period.** Left set of panels show Chl-a concentrations measured from incubations deployed at 100 and 50% of subsurface PAR relative to the Chl-a measured before the incubation (original), both from incubations with ^{15}N-NO_3^- and with ^{15}N-NH_4^+. Error bars represent the standard difference of duplicate measurements. Right set of panels show Δ-Chl-a (*i.e.* concentrations measured at the end of incubation minus original concentration), from incubations deployed at both PAR levels and from both ^{15}N-treatments. Note different y axis scales (nd = no data available).

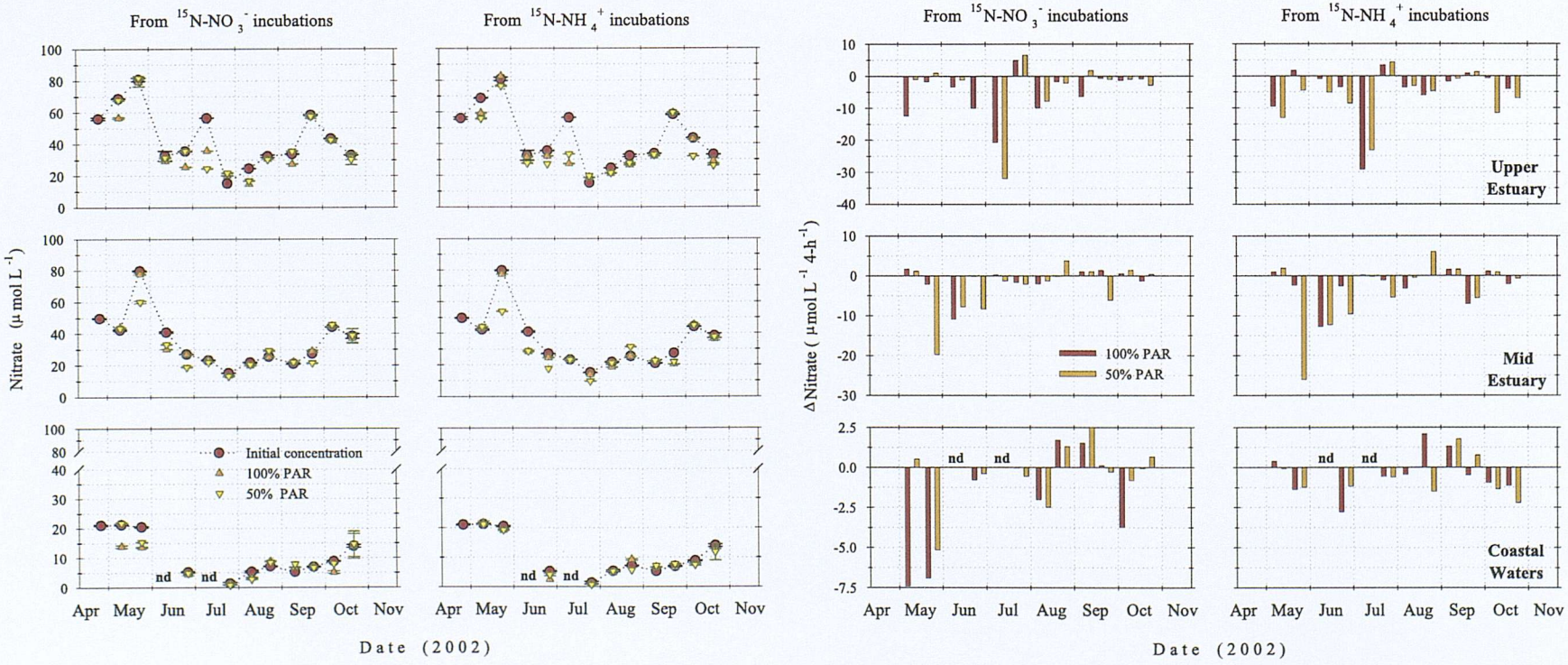

Figure 4.8: **Nitrate concentration changes during the incubation period.** Left set of panels show nitrate concentrations measured from incubations deployed at 100 and 50% of subsurface PAR relative to the nitrate measured before the incubation (original), both from incubations with ^{15}N-NO_3^- and with ^{15}N-NH_4^+. Error bars represent the standard deviation of replicate (n=3) measurements. Right set of panels show Δ-nitrate (*i.e.* concentrations measured at the end of incubation minus original concentration), from incubations deployed at both PAR levels and from both ^{15}N-treatments. Note different y axis scales (nd = no data available).

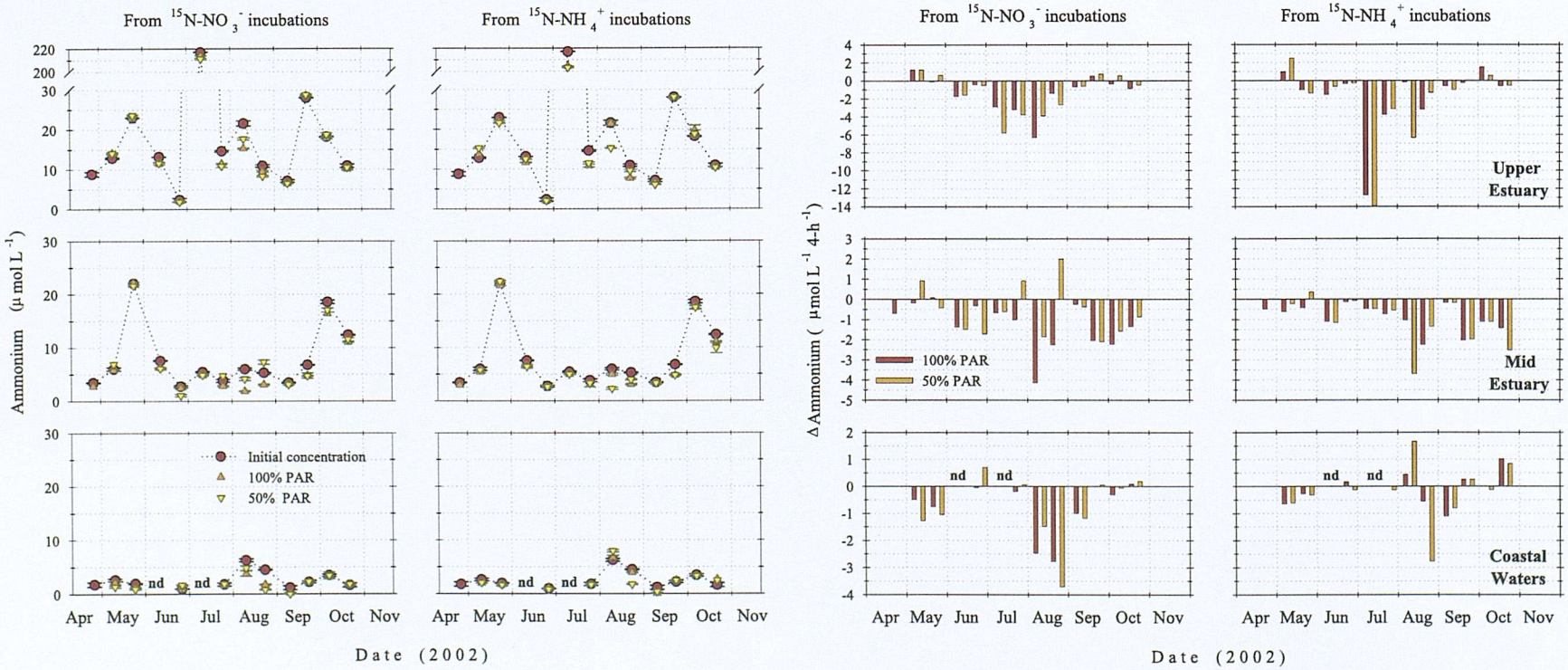

Figure 4.9: **Ammonium concentration changes during the incubation period.** Left set of panels show ammonium concentrations measured from incubations deployed at 100 and 50% of subsurface PAR relative to the ammonium measured before the incubation (original), both from incubations with ^{15}N-NO_3^- and with ^{15}N-NH_4^+. Error bars represent the standard deviation of replicate (n=3) measurements. Right set of panels show Δ-ammonium (*i.e.* concentrations measured at the end of incubation minus original concentration), from incubations deployed at both PAR levels and from both ^{15}N-treatments. Note different y axis scales (nd = no data available).

spectively, while the original subsampled water showed a concentration of 106.1 μmol L^{-1}. The DON concentration from the cracked-bottles resulted thus in negative values. Nitrate and ammonium from the same date showed concentrations of 79.7 and 22.1 μmol L^{-1} respectively in the original sample, 77.6 and 22.1 μmol L^{-1} from the $^{15}NO_3^-$ treatment and 77.4 and 21.6 μmol L^{-1} from the $^{15}NH_4^+$ treatment, suggesting also that TDN results from the cracked-bottles were likely erroneous. Overall TDN measured in the subsamples collected at the end of the experiments showed a decrease of up to 4% relative to the original concentration. Thus, for data representation and explanation purposes, the likely-erroneous values were corrected taking into account these small changes. It must be therefore kept in mind that the TDN and DON values in the original sample on the 03-Oct, and that the TDN, DON, and the DON release rate from the 23-May are only approximations.

The temporal distribution of **TDN** was similar to that of surface nitrate concentrations, and ranged between 28.74 and 106.1 μmol L^{-1} (data not shown). **DON** concentrations appeared to increase gradually from the 25-Apr towards the end of the sampling period, varying between 1.9 and 22.5 μmol L^{-1}. Taking into account both the measurements in the original samples and in the subsamples collected at the end of the incubations, the contributions of nitrate, ammonium and DON to the TDN were 64±12, 12±5 and 24±12% respectively. Although changes in the DON concentrations at the end of the incubations of up to +6.3 μmol L^{-1} (*i.e.* increase) and up to -2.2 μmol L^{-1} (*i.e.* decrease) were also observed, it is difficult to distinguish whether there was a real change. This is because variations in the concentrations of nitrate and ammonium affect directly the estimation of DON (since DON=[TDN]-[NO_3^-+NH_4^+]). Nonetheless, DON concentrations estimated for subsamples collected from ^{15}N-NO_3^- and ^{15}N-NH_4^+ treatments are approximately similar (see Fig. 4.10), and varied within a similar range (0.3 - 22.6 and 4.0 - 27.2 μmol L^{-1} from nitrate and ammonium tracer incubations respectively).

4.2.7 Nitrogen net uptake rates in 2002

The nutrient enrichment with tracer additions previously shown (Ch. 3, § 3.2.6, table 3.2) also applies to uptake experiments in 2002. Enrichments with ^{15}N-nitrate and ^{15}N-ammonium were on average <5% of the ambient nutrient concentrations. 520 samples (*i.e.* filters for isotope determination) were generated in 2002. Of these, 316 samples were analysed, which included duplicate analysis of all samples prepared to quantify DON release and ammonium regeneration. Samples for duplicate determinations of net uptake rates were chosen randomly. Standard differences of duplicate analyses were generally <10%.

The range of nitrate and ammonium uptake rates measured in 2002 is summarised in

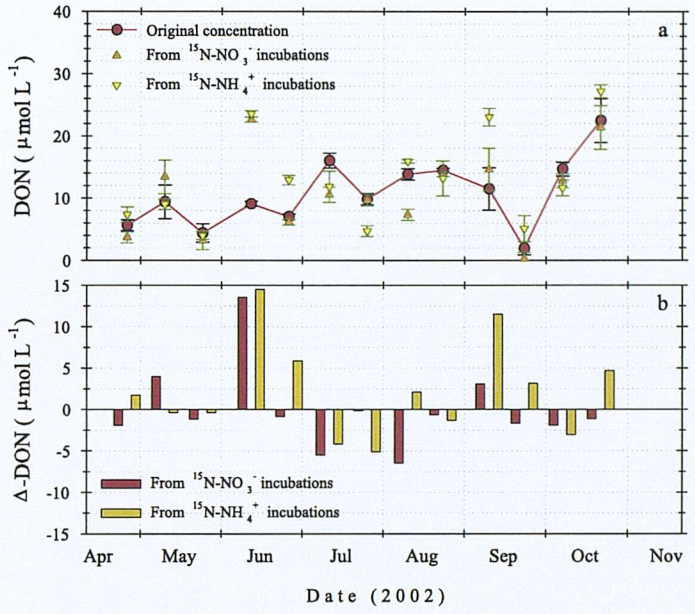

Figure 4.10: **Temporal distribution of dissolved organic nitrogen (DON) and DON concentration changes during the incubation period measured at the mid estuary (NW Netley navigation buoy).** Temporal distribution and concentration changes relative to original concentration (a) and Δ-DON (b) measured from incubations with ^{15}N-NO_3^- and with ^{15}N-NH_4^+. Error bars in panel (a) represent the standard deviation of replicate (n=3) measurements.

Table 4.2 and the spatial and temporal variations are shown in **Fig. 4.11**. In general, highest rates were measured in the mid estuary and lowest in the coastal waters, although a comparatively high rate was also measured at the latter site (ammonium, 23-Jul). Generally, higher **nitrate** net uptake rates were measured at the level of 50% of subsurface PAR in the inner estuary. It must be noted however, that on the first date of experiments a set of bottles was deployed at 0.5 m depth and other set of bottles was incubated in dark conditions (see Ch. 2, § 2.5, subsection 2.5.3). In the upper estuary a maximum rate corresponding to the 65% subsurface PAR was recorded at the beginning of the sampling period. Two peaks of 0.091 and 0.103 μmol L^{-1} h^{-1} (23-May and 24-Jun respectively) were later observed at this PAR level, after which values were < 0.027 μmol L^{-1} h^{-1} and appeared to decrease gradually. In contrast, peaks observed at the 50% of subsurface PAR seemed to increase progressively until a maximum of 0.233 μmol L^{-1} h^{-1} was reached on the 06-Sept. No relation was apparent between nitrate uptake rates and Chl-*a* concentration in the upper estuary. On some occasions however, either low or high uptake rates coincided with decreases or increases respectively, in the mean irradiance estimated down to the depth of the 50% of subsurface PAR (mean $E_{Z(50\%)}$) (see Fig. 4.11). Nitrate uptake rates in the mid estuary showed values generally >0.020 μmol L^{-1} h^{-1} between 23-May and 06-Sept, increasing to a maximum value on the 23-Jul and then decreasing

Table 4.2: Net nitrate and ammonium uptake rates in Southampton Water estuary; mean (bold) and range of variation (parentheses) during the productive spring–summer period in 2002.

	Nitrate μmol-N L^{-1} h^{-1}	**Ammonium** μmol-N L^{-1} h^{-1}
Upper estuary	**0.051**	**0.177**
	(0.001 - 0.293)	(0.008 - 0.897)
Mid estuary	**0.075**	**0.198**
	(0.002 - 0.533)	(0.005 - 1.165)
Coastal waters	**0.015**	**0.143**
	(0.001 - 0.087)	(0.001 - 1.242)

(see Fig. 4.11). Uptake rates at the 100% PAR level seemed to follow the temporal trend of Chl-*a* and ΔChl-*a* until the 07-Aug, when a maximum rate of 0.303 μmol L^{-1} h^{-1} was reached at this PAR level. Uptake rates measured at the 50% of subsurface PAR seemed to be related the mean $E_{Z(50\%)}$ in some cases. For instance, the maximum uptake rate at this PAR level coincided with the second highest mean $E_{Z(50\%)}$ during the sampling period (23-Jul). In the coastal waters a maximum uptake rate corresponding to the 65% subsurface PAR level was measured on the 25-Apr, and apart from a low value recorded on the 24-Jun, rates from both PAR levels were of similar magnitude at this site. On this same date, the highest peak corresponding to the lower PAR level was measured (see Fig. 4.11). Nitrate uptake rates in the coastal waters seemed to follow the temporal distribution of Chl-*a* (see Fig. 4.7). As compared with nitrate, **ammonium** net uptake rates presented a well defined temporal pattern. Ammonium uptake rates were generally higher at the 100% subsurface PAR level. This was particularly true during the period (mid June to August) where the highest rates were attained. On other dates, uptake rates were of similar magnitudes at the two PAR levels. In the mid and upper estuary rates followed approximately the same temporal trend, increasing gradually until a maximum was reached on the 07-Aug and then decreasing (see Fig. 4.11). In the coastal waters the highest peak was observed on the 23-Jul and corresponded to the 100% subsurface PAR (Fig. 4.11). Apart from this peak, ammonium net uptake rates were <0.300 μmol L^{-1} h^{-1} at this site. Ammonium net uptake rates presented a similar behaviour to that of the changes in chlorophyll (*i.e.* Chl-*a* measured at the end of the incubations), although the trend is not that clear in the coastal waters (see fig. 4.7). The contribution of each nitrogen source to the total measured uptake, *e.g.* $\%Contribution = \left(\frac{\rho_{NO_3^-}}{\rho_{NO_3^-}+\rho_{NH_4^+}}\right) \times 100$, was dominated by the uptake of ammonium at the three sampling sites and at both PAR levels. The mean percent contribution of ammonium uptake was 84±18, 77±19 and 74±25% in the coastal waters, mid and upper estuary respectively. Comparatively higher percent contributions were observed at 100% subsurface PAR in the case of ammonium uptake and at 50% subsurface PAR in the case of nitrate uptake.

4.2.7.1 Dissolved organic nitrogen release and ammonium regeneration rates

Gross nitrate uptake and DON release from nitrate uptake

The temporal variation of gross nitrate uptake and DON release rates are shown in **Fig. 4.12**. Gross nitrate uptake rates ranged between 0.010 and 1.295 μmol L^{-1} h^{-1} over the sampling period, with a mean value of 0.436±0.416 μmol L^{-1} h^{-1}. A sharp increase was observed during spring, reaching a maximum value on the 23-May. Gross uptake rates decreased during the summer months down to a minimum value, until another sharp increase occurred up to a rate of 1.292 μmol L^{-1} h^{-1}. DON release rates presented a similar temporal pattern to that of the gross nitrate uptake, with values ranging from 0.001 to 1.290 μmol L^{-1} h^{-1} and a mean of 0.383±435 μmol L^{-1} h^{-1}. On average, the net uptake rates of nitrate represented 25±32% of the gross uptake rates, with a range of between <1 to 88%. In other words, 74±32% of the nitrogen taken up as nitrate was released as DON. Only on three occasions (23-Jul, 07-Aug and 19-Sept) did the net uptake rates represented more than 50% of the gross uptake rate. Overall, moderate or low DON release and gross uptake rates occurred when Chl-*a* values measured at the end of the incubations were relatively high (24-Jun to 19-Sept).

Ammonium regeneration and DON release rates from ammonium uptake

Net ammonium uptake rates corrected for isotopic dilution followed the temporal trend of net uptake rates, although in a more pronounced fashion (*i.e.* in general showing higher values). Values varied between 0.030 and 5.825 μmol L^{-1} h^{-1}. Highest rates were measured on three consecutive dates (23-Jul, 07 and 20-Aug), with values >1.260 μmol L^{-1} h^{-1}. Two smaller peaks of 0.798 and 0.540 μmol L^{-1} h^{-1} were observed on the 10-Jun and 19-Sept respectively. Overall, net uptake rates represented 31±9% of the uptake rates corrected for isotope dilution, although varying within a range of 20 to 54%. Differences between net and corrected uptake rates were larger at high net uptake rates (see Fig. 4.13, upper panel). In other words, uptake rates calculated without taking into account the effect of isotope dilution during the incubation period, were underestimated by a factor ranging from 1.8 to 5. The gross ammonium uptake presented values ranging from 0.045 up to 5.841 μmol L^{-1} h^{-1}, and were only slightly higher (~3% in general) than the corrected uptake rates (difference smaller than symbols in Fig. 4.13). Ammonium regeneration rates varied between 0.360 and 5.603 μmol L^{-1} h^{-1}, and showed exactly the same temporal trend as the gross and corrected uptake rates (*i.e.* highest regeneration rates coincided with highest uptake rates). The corrected uptake and the ammonium regeneration rates appeared to closely followed the pattern of Chl-*a* changes in the incubation bottles (see Fig. 4.13). DON release rates from ammonium uptake were $\leqslant$0.019 μmol L^{-1} h^{-1}, and represented on average 3.1% of the gross ammonium uptake within a range of 0 to 16%. As a proportion of the total DON release (*i.e.* the sum of release rates

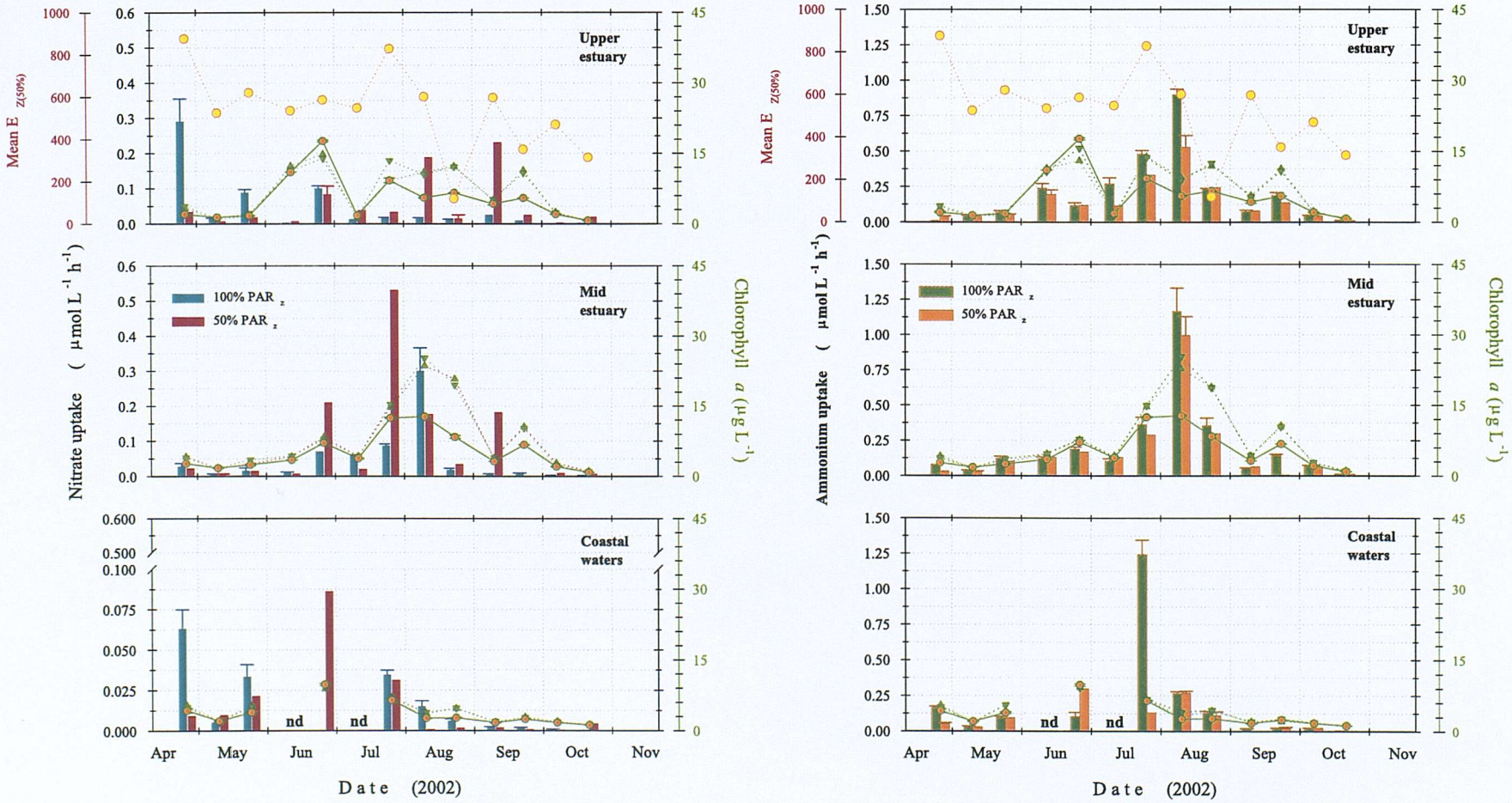

Figure 4.11: **Nitrate and ammonium net uptake rates;** productive spring-summer period in 2002 (nd = no data available). Error bars represent the standard difference of duplicate analysis. Note different scale in left lower panel ('y' axis break). Mean $PAR_{Z(50\%)}$ in the upper panels and Chl-a are shown as a reference. Symbols for chlorophyll are ΔChl-a measured at the 100% (triangles up) and 50% (triangles down) of subsurface PAR and original concentration (circles).

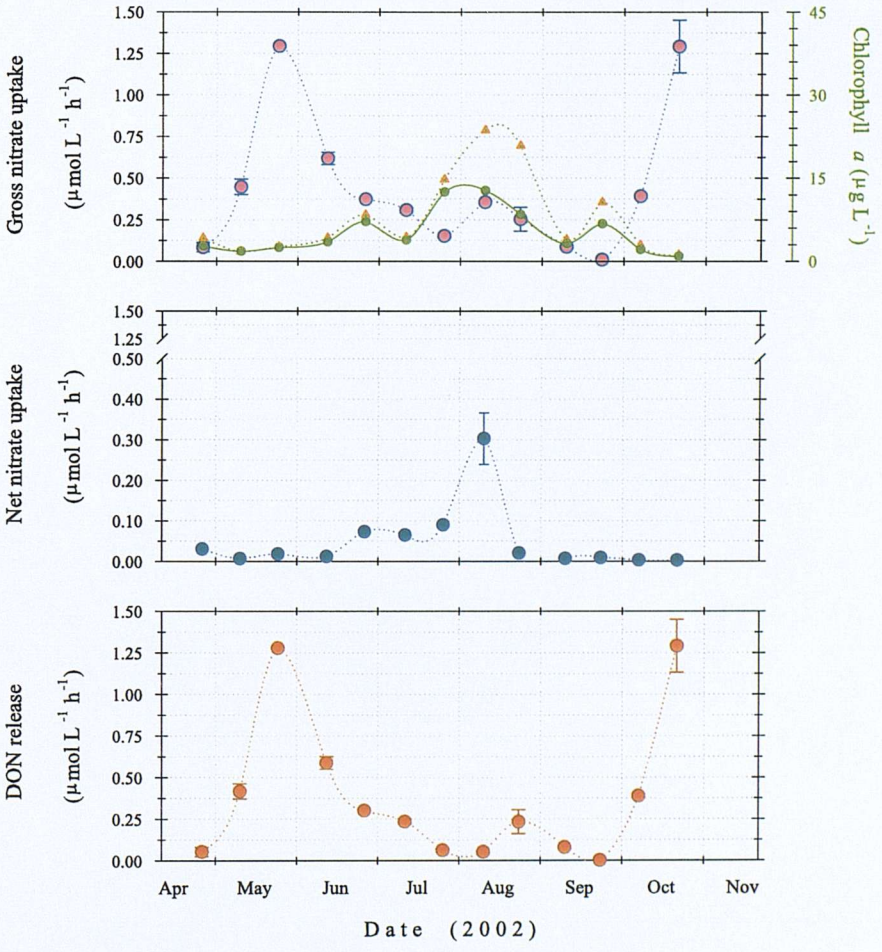

Figure 4.12: **Gross nitrate uptake and DON release rates in the mid estuary measured at the 100% of subsurface PAR;** productive spring-summer period in 2002. Chlorophyll symbols in upper panel represent the original concentration (circles) and the Chl-*a* measured at the end of the incubation (triangles). Net nitrate uptake rates are also shown (same as in Fig. 4.11, left-mid panel). Error bars represent the standard difference of duplicate measurements.

from ammonium and nitrate uptake), DON release from ammonium uptake represented an average of 6.1%, varying from 0 to 25%.

4.3 Discussion

4.3.1 Nutrients and Chlorophyll

Seasonal changes in the concentration of nutrients and Chl-*a* measured in 2002 are in good agreement with previous reports for the system (*e.g.* Leakey *et al.*, 1992; Kifle & Purdie, 1993; Iriarte & Purdie, 1994; Proença, 1994; Hydes & Wright, 1999; Ali, 2003; Homewood, 2003). The annual productive cycle appeared to affect mainly the concentrations of nitrate and silicate, which showed lower values during the period June to September (see Figs. 4.2 and 4.3). This trend was not clear in the concentrations of phosphate and ammonium (see Figs. 4.2 and 4.3), which have been reported to be supplied to the estuary mostly by sewage effluents (Hydes & Wright, 1999). Signs of nutrient decline however, seemed to be 'hidden' in some cases by inputs of fresh water, as suggested by the temporal distribution of salinity (see Fig. 4.1). That is, concentration peaks recorded for all nutrients throughout the sampling period in 2002 coincided with low salinity values in the inner estuary, and were more evident on the 23-May, 09-Jul, 20-Aug and 19-Sept (see Figs. 4.1 to 4.3). Ambient levels of silicate appeared to recover sooner in the year than nitrate; low concentrations (with the exception of the peaks related to low salinity) of silicate were measured from the 25-Apr to the 23-Jul, with levels then increasing gradually to concentrations higher than those measured at the beginning of the sampling period (see Fig. 4.3). Nitrate concentrations in contrast, decreased steadily until overall lowest levels were measured on the 23-Jul and 07-Aug (see Fig. 4.2). After these dates nitrate levels seemed to increase slowly towards the end of the sampling period, although the concentrations measured at this point were not higher than those measured on the 25-Apr (see Fig. 4.2). The fact that silicate concentrations are lower during the period mentioned above and that levels recovered sooner relative to nitrate, agrees well with the seasonal succession of phytoplankton species observed within the Southampton Water estuary, since the blooming of diatoms during the spring months (*e.g.* Howard *et al.*, 1995; Ali, 2003) would imply removal of silicate from the water column. In addition, the contemporaneous and slightly displaced decline in the levels of nitrate indicates that the productive spring-summer period was still progressing, likely undergoing phytoplankton population changes probably with different nutrient requirements.

Seasonal changes in Chl-*a* concentrations during 2002 showed peaks <18 μg L^{-1}, which are relatively low as compared with the high values that have sometimes been measured within the system (*e.g.* 64 μg L^{-1}, this study 2001). These values however, are in good

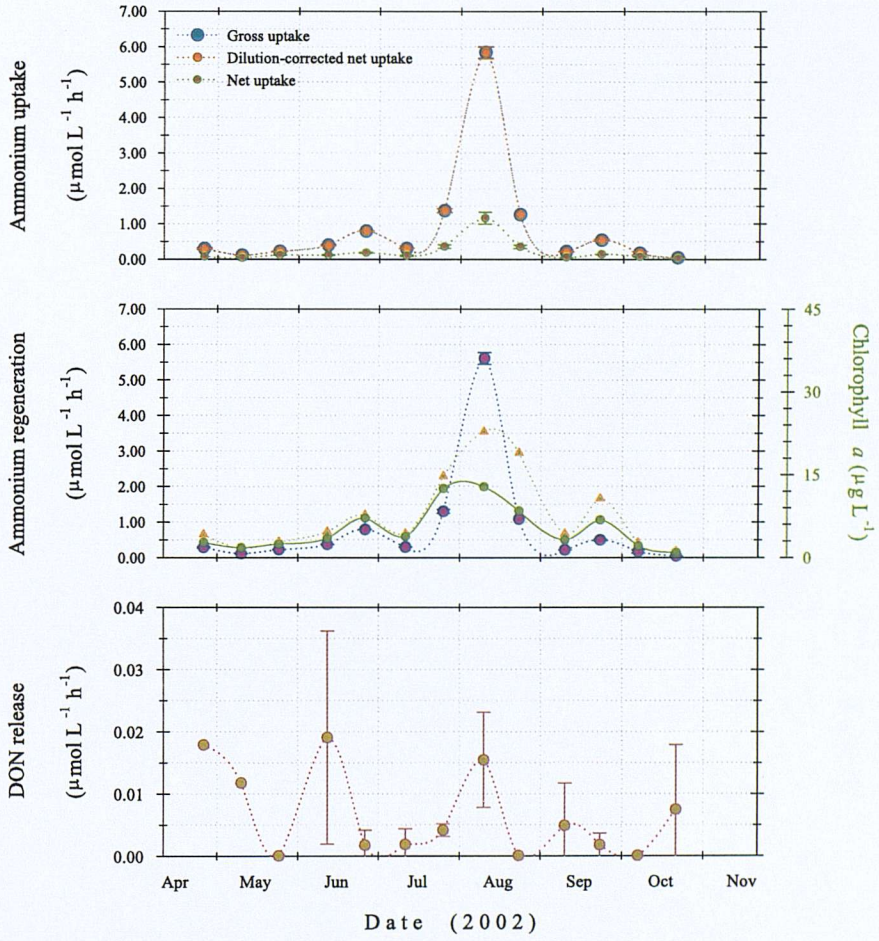

Figure 4.13: **Ammonium net uptake corrected for isotope dilution, gross ammonium uptake and DON release rates in the mid estuary measured at the 100% of subsurface PAR;** productive spring-summer period in 2002. Chlorophyll symbols in mid panel represent the original concentration (circles) and the Chl-*a* measured at the end of the incubation (triangles). Net ammonium uptake rates are also shown (same as in Fig. 4.11, right-mid panel). Error bars represent the standard difference of duplicate measurements.

agreement with the range of concentrations measured during previous studies (*e.g.* Iriarte, 1991; Leakey *et al.*, 1992; Kifle & Purdie, 1993; Iriarte & Purdie, 1994; Ali, 2003). In general, highest Chl-*a* values were recorded during the period June to September, and were relatively higher in the inner estuary (see Fig. 4.5). Although blooms of the phototrophic ciliate *Mesodinium rubrum* have been observed to be recurrent (*e.g.* Crawford *et al.*, 1997) and a regular component of the Southampton Water estuary phytoplankton populations (*e.g.* Ali, 2003), no red tide was observed during the productive spring-summer period in 2002.

The levels of dissolved organic nitrogen (DON) measured in the present study (see subsection 4.2.6.2 and Fig. 4.10) also agree well with the values previously reported for the system of up to ~50 μmol L^{-1} (Hydes & Wright, 1999; Homewood, 2003) and are comparable with values reported for other estuarine systems, which range from 0.6 to 65.0 μmol L^{-1} (Bronk, 2002; Berman & Bronk, 2003), and with values reported for the surface ocean, deep ocean, coastal and continental shelf, estuaries and rivers which range from 0.51 to 90.0 μmol L^{-1} (Bronk, 2002; Berman & Bronk, 2003). In the Southampton Water estuary, DON has been found to be more significant in the coastal waters relative to the inner estuary, with contributions to the total dissolved nitrogen (TDN) of up to 80% in the coastal waters (Calshot navigation buoy) and of up to 40% and 19% in the mid (Dockhead) and upper estuary (Redbridge) respectively (Hydes & Wright, 1999). The few measurements previously made in samples collected from the Southampton Water estuary have shown that DON as a proportion of TDN overall appeared to decrease from 65% in autumn (Nov-1995), to 31% in winter (Jan-1996) and to non detectable levels in spring in the coastal waters (Hydes & Wright, 1999), with a similar temporal trend in the mid estuary but with proportions of 40%, 8% and non detectable levels (Hydes & Wright, 1999). DON levels at these two sites have then shown contributions to the TDN of 82 and 40% respectively, in summer (Jun-1996) (Hydes & Wright, 1999). In the upper estuary, DON concentrations have been estimated to vary between 6 and 24 % as a proportion of the TDN (Hydes & Wright, 1999; Homewood, 2003). In the present study, although DON concentrations in the mid estuary (NW Netley navigation buoy) seemed to increase from the 25-Apr to the 17-Oct 2002 (see Fig. 4.10), its contribution to the TDN did not appeared to exhibit a seasonal trend (data not shown). Generally, higher contributions were estimated during the period 09-Jul to 09-Sept, with values varying between 32 and 36%.

Measurements of nitrate, ammonium, phosphate and DON at the beginning and at the end of incubation experiments showed changes in the ambient concentrations over a period of 4 hours (see § 4.2.6). In general, results from the two ^{15}N-treatments and from the two selected PAR level conditions showed similar general trends in concentration changes during the incubation period (see Figs. 4.8 and 4.9 in § 4.2.6, and Fig. B.4

in Appendix B.0.11). On some occasions however, results from either ^{15}N treatments or PAR levels did not seemed to be consistent. It was therefore difficult to evaluate the extent of changes in concentration because each of the analytical techniques used have associated errors and particular limits of detection and sensitivity. Measurements of DON changes during the incubation were particularly difficult to estimate, since DON precision is affected by the measurements of TDN, nitrate and ammonium. When measured changes are compared with net uptake rates, values do not seem to match in most cases (see Table 4.3), although when gross uptake rates are compared, some of the measured changes appear to be fairly close to the uptake value (see Table 4.3). In the case of nitrate for instance, ΔNO_3^- values on the 09-May and 24-Jun are approximately similar (see Table 4.3). The same can be observed for ΔNH_4^+ on the 09-May, 10-Jun and 19-Sept (see Table 4.3), although in the case of the DON, measured changes in concentration did not appear to reflect the release of DON from incubations with ^{15}N-nitrate for example (data not shown). Changes in the concentration of chlorophyll however, showed good agreement between measurements from the two ^{15}N-treatments (see Table 4.3) and from the two PAR levels selected (see Fig. 4.7). This fact, suggests that the inconsistency found in measurements of nutrient concentration changes was likely related to the analytical errors associated with each of the techniques used and indicates that if accurate measurements of nitrogen removal are to be achieved, direct measurements of N-uptake using ^{15}N-tracer techniques represents a powerful tool. With the measured changes in the Chl-*a* concentration, it was possible to estimate a rate of Chl-*a* production (Eq. 4.1). The temporal variation of chlorophyll *a* production rates (Chl-a_{PR}) showed highest values in the period July to September, with values at the 100% of subsurface PAR of up to 0.5, 2.9 and 1.5 $\mu g\ L^{-1}\ h^{-1}$ in the coastal waters, mid and upper estuary respectively (Fig. 4.14). At the 50% of subsurface PAR Chl-a_{PR} were similar, with values of up to 0.5, 3.1 and 1.4 $\mu g\ L^{-1}\ h^{-1}$ (same order as above). In general, production rates of chlorophyll in the mid estuary appeared to be positively correlated to the net uptake rates of nitrate and ammonium, and to the gross uptake of ammonium (see Fig. 4.15). A relation between Chl-a_{PR} and the gross uptake of nitrate was not observed (see Fig. 4.15).

$$Chl_{PR} = \frac{Chl_t - Chl_0}{t} \qquad (4.1)$$

Where Chl_{PR} is chlorophyll production rate, Chl_t is the chlorophyll measured at time t, Chl_0 is the chlorophyll measured at time 0, and t is the incubation period (h).

4.3.2 Nitrogen uptake and release rates

Net nitrogen uptake rates measured in 2002 are in good agreement with values reported in the literature for other coastal systems (*e.g.* Bronk *et al.*, 1994; L'Helguen *et al.*, 1996; Berg *et al.*, 1997; Shaw *et al.*, 1998a,b; Kudela & Dugdale, 2000; Tremblay *et al.*,

Table 4.3: Comparison between ΔChl-a (μg L^{-1} h^{-1}), ΔNO_3^- (μmol L^{-1} h^{-1}), ΔNH_4^+ (μmol L^{-1} h^{-1}), nitrate and ammonium net uptake (μmol L^{-1} h^{-1}) and gross nitrogen and ammonium uptake rates (μmol L^{-1} h^{-1}). ΔChl-a values measured from ^{15}N-nitrate incubations (left table) and ^{15}N-ammonium incubations (right table) are shown. ΔNO_3^- and ΔNH_4^+ are the mean value measurements from both ^{15}N-treatments at the 100% of subsurface PAR (±standard difference); nd = no data available.

J day	Date	ΔChl-a	ΔNO_3^-	ρNO_3^-	$\rho_G NO_3^-$
115	*25-Apr*	**0.36**	**nd**	**0.030**	**0.084**
129	*09-May*	**0.00**	**0.33**±0.12	**0.006**	**0.447**
143	*23-May*	**0.04**	**-0.56**±0.06	**0.018**	**1.295**
161	*10-Jun*	**0.18**	**-2.95**±0.33	**0.011**	**0.619**
175	*24-Jun*	**0.31**	**-0.34**±0.43	**0.073**	**0.373**
190	*09-Jul*	**0.11**	**0.04**±0.01	**0.065**	**0.307**
204	*23-Jul*	**0.57**	**-0.35**±0.08	**0.089**	**0.152**
219	*07-Aug*	**2.72**	**-0.65**±0.21	**0.303**	**0.355**
232	*20-Aug*	**3.10**	**-0.02**±0.02	**0.020**	**0.253**
249	*06-Sept*	**0.18**	**0.33**±0.08	**0.006**	**0.086**
262	*19-Sept*	**0.96**	**-0.71**±1.49	**0.008**	**0.010**
276	*03-Oct*	**0.19**	**0.20**±0.10	**0.002**	**0.391**
290	*17-Oct*	**0.05**	**-0.42**±0.14	**0.002**	**1.292**

ΔChl-a	ΔNH_4^+	ρNH_4^+	$\rho_G NH_4^+$
0.35	**-0.15**±0.04	**0.078**	**0.303**
-0.03	**-0.10**±0.08	**0.038**	**0.117**
0.09	**-0.04**±0.09	**0.123**	**0.226**
0.30	**-0.31**±0.05	**0.122**	**0.405**
0.13	**-0.06**±0.03	**0.189**	**0.799**
0.12	**-0.14**±0.03	**0.104**	**0.306**
0.56	**-0.22**±0.05	**0.362**	**1.375**
2.50	**-0.65**±0.55	**1.165**	**5.841**
2.62	**-0.57**±0.00	**0.356**	**1.260**
0.27	**-0.05**±0.01	**0.055**	**0.221**
0.97	**-0.51**±0.00	**0.145**	**0.542**
0.13	**-0.42**±0.20	**0.069**	**0.171**
0.04	**-0.35**±0.01	**0.012**	**0.045**

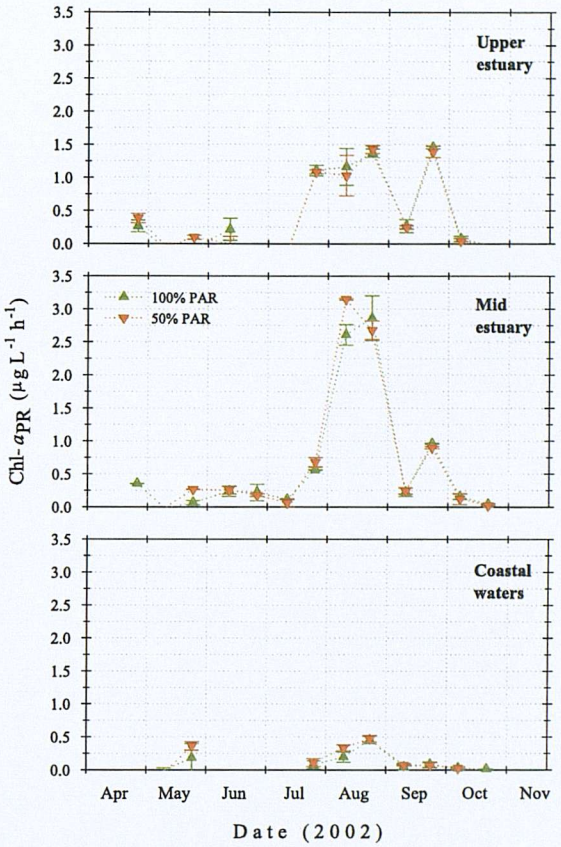

Figure 4.14: **Temporal variation of chlorophyll *a* production rates within the Southampton Water estuary;** productive spring-sumer period in 2002.

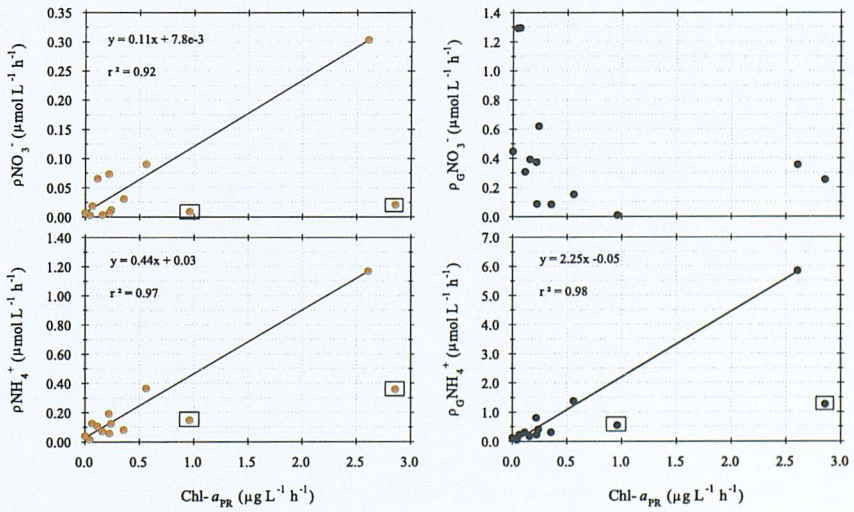

Figure 4.15: **Net and gross nitrate and ammonium uptake rates as a function of chlorophyll *a* production rates**; mid estuary, productive spring-summer period in 2002. Data inside square were not considered in the regression lines.

2000; Ward & Bronk, 2001; Weston *et al.*, 2004) (see Tables 3.6 and 3.7, Ch. 3, § 3.3, subsection 3.3.2,). Nitrate uptake rates were generally higher at the level of 50% of subsurface PAR than at the 100% level in the inner estuary (see Fig. 4.11). In contrast, ammonium uptake rates were usually higher at the 100% of subsurface PAR at all sites (see Fig. 4.11). Uptake rates from both nutrients were higher in the mid and upper estuary, although highest rates were reached at the former site. Nitrate uptake rates did not exhibit a clear temporal trend in the upper estuary, where the magnitude of the uptake rates measured at 100% of subsurface PAR seemed to decrease with time, while rates measured at 50% of subsurface PAR seemed to increase (Fig. 4.11). In the mid estuary and coastal waters, nitrate uptake rates appeared to be related to the temporal changes in Chl-*a* and the increase in chlorophyll levels over the incubation period (ΔChl-*a*). In the case of ammonium, uptake rates presented a more defined temporal pattern which was characterised by highest values during the summer months (see Fig. 4.11). Ammonium uptake rates also seemed to follow the temporal trend of Chl-*a* and ΔChl-*a* (see Fig. 4.11), indicating a close link to phytoplankton production. The gross uptake of nitrate (ρ_G NO_3^-) showed two maximum rates, one in early summer and another in early autumn (see Fig. 4.12). Contrary to net nitrate uptake rates (ρ NO_3^-), lower ρ_G NO_3^- rates were measured during the most productive months (mid June to mid September).

Rates of dissolved organic nitrogen release (DON_{REL}) exhibited a similar temporal pattern to that of ρ_G NO_3^- (see Fig. 4.12). On average, 74±32% of the ρ_G NO_3^- was released as DON within a range of between 12.2 and 99.8%. These values are in good agreement with observations in other systems. Ward & Bronk (2001) for example, reported that in the Southern California Bight and Monterey Bay, 3 to 100% of the nitrate taken up was released as DON. Also, Hu & Smith (1998) found that 8 to 19% of the nitrate taken up was released as DON in the Ross Sea. The ammonium uptake corrected for isotope dilution (P NH_4^+) increased to a maximum during summer (August), following the temporal changes in Chl-*a* and ΔChl-*a*. Ammonium regeneration (NH_{4REG}^+) rates showed a similar temporal trend, although with slightly lower values. The release of DON from ammonium uptake presented several peaks through out the sampling period which decreased in magnitude with time (see Fig. 4.13). Overall, DON_{REL} rates from ammonium uptake (on average 3% of ρ_G NH_4^+) were much lower that DON_{REL} from nitrate uptake. This proportion seem to be low relative to observations in other systems, but the range is similar to values reported in the literature. In the Monterey Bay for instance, Bronk & Ward (1999) observed that more DON was released from ammonium uptake in March (1993), but DON_{REL} from ammonium and nitrate uptake were similar in September (1993). These authors also observed that the release of DON from both, ammonium and nitrate increased with depth (for reference see Fig. 9 in Bronk & Ward, 1999). In another study involving only DON_{REL} from ammonium uptake, Bronk *et al.*

(1998) found that DON_{REL} rates changed between months, accounting for 32, 10 and 36% of the ρ_G NH_4^+ in May, August and October respectively.

During the present research, water from the ^{15}N-tracer experiments was filtered using GF/F filters, and therefore it is likely that an important proportion of heterotrophic bacteria was also retained together with phytoplankton cells. Although with the information available it is difficult to distinguish the effect of heterotrophic bacteria on the uptake of nitrogen, the general patterns observed (*e.g.* the increase of nitrogen uptake rates when Chl-*a* concentrations also increased) indicate that phytoplankton growth was probably dominating the uptake of nitrogen within the Southampton Water estuary, particularly of nitrate. Ammonium is known to be taken up by marine heterotrophic bacteria at levels accounting for 3 to 78% of the total nitrogen uptake measured in different marine systems (Kirchman, 2000). Uptake of ammonium by heterotrophic bacteria however, has been shown to decrease from oceanic waters to estuarine waters. In the Delaware estuary for example, Hoch & Kirchman (1995) found that bacterial uptake accounted for 10 to 25% of the total nitrogen uptake in the coastal waters of the system, but accounted for <5% in the inner estuary (for reference see Figs. 5 and 6 in Hoch & Kirchman, 1995). These authors observed that phytoplankton dominated the uptake of ammonium throughout the estuary in summer 1990 and that bacterial uptake increased towards the mouth of the bay. Hoch & Kirchman (1995) found that in the inner estuary, 50 to 200% of the bacterial nitrogen demand was accounted for by the uptake of dissolved free amino acids. In a recent publication, Kirchman & Borch (2003) suggested that the uptake of dissolved inorganic nitrogen in the Delaware estuary was limited by the availability of organic carbon. In fact, the uptake of ammonium by heterotrophic bacteria and bacterial growth rates have been observed to be limited by the availability of organic carbon in oceanic waters (Kirchman & Wheeler, 1990; Kirchman & Rich, 1997; Rivkin & Anderson, 1997). Thus, assuming that phytoplankton activity accounts for most of the nitrogen uptake measured within the Southampton Water estuary, in the following sections, the factors which are likely to control the cycling of nitrogen in this system are discussed.

The variability in the uptake of individual nitrogen sources may be influenced by the dominant species in the phytoplankton population or a mixture of phytoplankton species at a given time. Different phytoplankton species are likely to respond in a particular way to the various physical and biological forcings they experience within the system. As shown in the previous chapter, N-uptake profiles showed a Michaelis-Menten-like response to PAR, indicating uptake rates strongly depend on light. It was also noted that in some cases there were indications of photoinhibition, as suggested by the lower uptake rates measured at the 100% subsurface PAR relative to rates measured at the 50% subsurface PAR level. Photoinhibition of nitrate uptake at relatively high PAR values has been also observed in systems such as the Humber estuary (Shaw *et al.*, 1998b), the Strait

of Georgia (Cochlan *et al.*, 1991) and the Ross Sea (Hu & Smith, 1998). It is possible that the uptake of nitrate presented some degree of photoinhibition in the inner estuary. Photoinhibition would be expected during the period when highest incident irradiance (and mean $E_{Z(50\%)}$) were measured. However, higher nitrate uptake rates in the upper estuary occurred during this period. In the mid estuary signs of photoinhibition appeared to be clearer. For example, on the date of the second highest calculated mean $E_{Z(50\%)}$ (23-Jul, Fig. 4.4), the maximum nitrate uptake rate was measured and corresponded to the 50% of subsurface PAR. On average, nitrate uptake rates at the 50% of subsurface PAR represented 60.8 and 61.2% of the total nitrate uptake, *i.e.* $\frac{1}{n}\sum \frac{\rho NO_3^- 50\%}{\rho NO_3^- 100\% + \rho NO_3^- 50\%}$, in the upper and mid estuary respectively. Indications of photoinhibition however, were also observed for ammonium and urea in 2001 and has been reported for other coastal systems too (*e.g.* Shaw *et al.*, 1998b), although uptake rates of ammonium in 2002 did not seem to be photoinhibited. Photoinhibition thus seems to be only one of many factors influencing the temporal trends observed in the uptake of N-nutrients.

Results presented here and reports in recent related literature provide helpful information in identifying the processes which are likely to affect the growth of phytoplankton and therefore have an impact on the cycling of nitrogen in the Southampton Water estuary. As a summary, in the mid panels of figure Fig. 4.7 it can be noted that during the first six sampling dates (25-Apr to 09Jul), the concentration of Chl-*a* remained relatively constant through out the incubation period, although a tendency for chlorophyll concentrations to increase with time is also observed. During the same dates, DON_{REL} rates from NO_3^- uptake increased to a maximum value. Some of the highest DON_{REL} rates from NH_4^+ uptake also occurred at this time (see Figs. 4.12 and 4.13). Towards the highest productive period however (apart from one date), ΔChl-*a* concentrations started to increase (Fig. 4.7, mid panels). During this period, ρ NO_3^- reached a maximum and the respective DON_{REL} rates a minimum (see Fig. 4.12). Contemporaneously, P NH_4^+ and NH_{4REG}^+ increased to the highest values recorded during the sampling period, closely following the values of ΔChl-*a* (see Fig. 4.13). After September, while DON_{REL} from nitrate uptake increased again, ρ NO_3^-, NH_{4REG}^+, P NH_4^+ and ΔChl-*a* decreased.

Lomas & Glibert (1999b) carried out experimental work with diatom-dominated populations from Chesapeake and Delaware Bays (1 h incubations). These authors observed that the uptake of nitrate decreased an average of 46% with increasing experimental temperature in the range of 7 to 25°C. On the contrary, the uptake of ammonium and urea increased by 179 and 86% respectively, within this range. They also found that diatoms exhibited non-saturating NO_3^- kinetics in a concentration range of up to 180 μmol L^{-1}. Lomas & Glibert (1999b) hypothesized that diatoms take up and store NO_3^- at low temperatures and high nitrate concentrations, and use this high intracellular NO_3^- as an oxidant to dissipate periodic overflow of electron energy through nitrate reductase (NR)

activity. They suggested that the release of DON or nitrite for example, are the means by which the excess energy is dissipated. From several cited works, these authors observed that the range of DON_{REL} rates has been found to be 6 to 79% of the nitrate taken up during the incubations. In a later work, Lomas *et al.* (2000), found that nitrogen-replete diatoms (*Skeletonema costatum*, *Thalassiosira weissflogii* and *Chaetoceros* sp.) released NH_4^+ when exposed to a rapid increase in irradiance (300 - 750 μmol m^{-2} s^{-1}) relative to experimental growth irradiance (40 - 120 μmol m^{-2} s^{-1}), with a release of NH_4^+ accounting for 84% of the NO_3^- taken up. Flagellate species (*Dunaliella tertiolecta*, *Pavluva lutheri* and *Prorocentrum minimum*) on the contrary, exhibited net NH_4^+ uptake under both irradiance regimes. Release of NO_2^- increased <1% in diatoms and decreased 4% in flagellates. Using only one representative species from the two groups, *S. costatum* and *P. minimum*, these authors found that net uptake rates of NH_4^+ at 15 and 20°C changed to net NH_4^+ release rates at 10°C. In the case of the flagellate species, no significant changes were observed. In experiments carried out in Southern California Bight and Monterey Bay, Ward & Bronk (2001) found that the DON_{REL} accounted for 3 to 100% of the ρ_G NO_3^-. They observed that DON_{REL} was positively correlated with NH_{4REG}^+, implying that grazing (by zooplankton and protozoan) was a major mechanism inducing DON_{REL}. High rates of DON_{REL} as a proportion of ρ_G NH_4^+ has been recorded in experiments with *Synechococcus* clones (isolated from oceanic and costal systems) under N-sufficient growth (Bronk, 1999). Release rates decreased by a factor of 4-7 when NH_4^+ was depleted. Increases in the rates on DON_{REL} with increasing levels in irradiance have been also observed in systems where nitrate uptake is strongly dependent on light such as the Ross Sea (*e.g.* Hu & Smith, 1998).

In the Southampton Water estuary in 2002, the water column temperature in the mid estuary was <17.2°C before July. During the same period, the E_0 and the mean $E_{Z(50\%)}$ were relatively high, ranging between ~700-1200 and 530-875 μmol m^{-2} s^{-1} respectively. Also, at this time of the year the surface concentration of nutrients was relatively high, with levels up to 79.8, 22.0, 21.8, and 1.45 μmol L^{-1} of NO_3^-, NH_4^+, PO_4^{3-} and $Si(OH)_4$ respectively. According to the information above, these physical conditions appear to be favourable for the growth of diatoms. Ali (2003) noted that a temperature of ~14 °C and a mean water column irradiance[2] of 100 W h m^{-2} d^{-1} appeared to be required for the onset of the spring diatom bloom in 1999. This author also found that diatoms outcompete flagellates and dinoflagellates under optimum light conditions. In the present research, rates of DON_{REL} accounted for up to 95% of the ρ_G NO_3^- between the 25-Apr and the 24-Jun. Assuming that diatoms were the dominant group during this period in

[2]Ali (2003) irradiance data is not fully comparable however, with the irradiance data presented here. Ali calculated the mean water column PAR by summing up hourly global irradiance with dimensions of W h m^{-2} d^{-1} to suit the requirements of her research. In the present study, data was selected and averaged for the ^{15}N-incubation period only, and PAR dimensions of μmol m^{-2} s^{-1} were used for consistency with related works.

2002, it is likely that the high rates of DON_{REL} were due to the dominance of diatoms and, by comparison to Lomas *et al.* (2000) findings, also due to the effect of the high levels of E_0 and mean $E_{Z(50\%)}$. That is, diatoms were probably releasing DON in order to dissipate the excess of energy absorbed. Lomas *et al.* (2000) calculated that the DON_{REL} rates they measured, accounted for up to 60% of the total electrons harvested. Although DON_{REL} has been also reported as a result of sloppy feeding by grazers, these release rates are expected to be related to high NH^+_{4REG} rates (Ward & Bronk, 2001). Besides, an increase in the population of heterotrophs is more likely to occur after an increase in phytoplankton biomass; *i.e.* during or after a bloom event (*e.g.* Cloern, 1996).

From the 25-Apr to the 24-Jun, the surface Chl-*a* reached the first peak (7.1 μg L^{-1}) measured during the sampling period, at the time when the DON_{REL} decreased sharply. Towards the summer months, the water column seemed to reach temperatures >19.5°C. The fresh water flux into the system is usually low relative to winter, but it can be enough to induce a vertical density gradient in the inner estuary. Ali (2003), pointed out that flagellates in Southampton Water estuary tended to dominate in stratified regions. As a result of the low river influx and and relatively high biological activity, surface concentrations of nutrients were low during that period (15.0, 3.5, 6.0 and 0.6 μmol L^{-1} of NO_3^-, NH_4^+, PO_4^{3-} and $Si(OH)_4$ respectively), whereas E_0 and the mean $E_{Z(50\%)}$ levels were still relatively high; ~850 and ~600 μmol m^{-2} s^{-1}. According to information in the literature, the above conditions are likely appropriate for the growth of flagellates and dinoflagellates. In the period from the 23/July to the 19/September 2002, ρ_G NO_3^- reached the highest values, while DON_{REL} from NO_3^- uptake showed the lowest; ~14% of the ρ_G NO_3^-. Maximum peaks in surface Chl-*a* occurred at this time as well, and ΔChl-*a* attained values of nearly 12 μg L^{-1} over 4 h (*i.e.* incubation period). Simultaneously the ρ_G NH_4^+ and NH^+_{4REG} rates reached maximum values (5.841 and 5.603 μmol L^{-1} h^{-1} respectively) and DON_{REL} from NH_4^+ uptake was low, representing <2% of the ρ_G NH_4^+. The increase of NH^+_{4REG} rates in summer has also been reported in other systems. For example, in the plume of Chesapeake Bay estuary it has been observed that NH^+_{4REG} rates increase from winter to summer and are highly positively correlated with the temperature (Glibert *et al.*, 1991, 1992). Results from the present research are consistent with this observation. Thus, assuming that flagellates and dinoflagellates were the dominant groups, it is likely that the uptake and release rates were representative of their presence at this time of the year. Although in this study a relation between DON_{REL} and NH^+_{4REG} rate was not observed, it is likely that the uptake of NO_3^- was being used for particle production as suggested by the low DON_{REL} from NO_3^- uptake. The surplus demand of nitrogen was probably supplied by NH_4^+, implied by the high uptake of this nutrient. Both, high rates of nitrogen uptake and NH^+_{4REG} suggest a balance between autotrophic and heterotrophic processes.

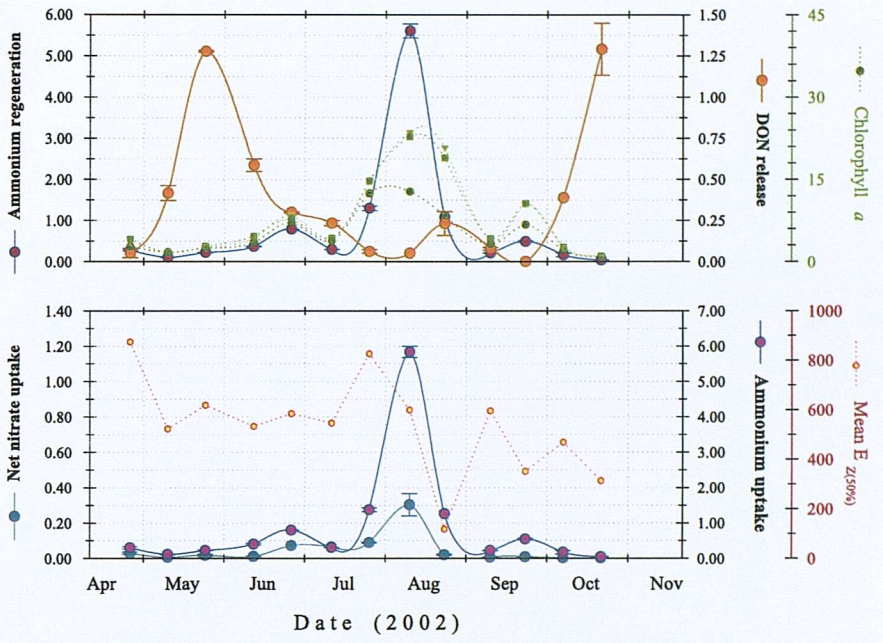

Figure 4.16: **Summary of uptake, release and regeneration rates from the mid estuary (NW Netley navigation buoy);** productive spring-summer period in 2002. Also shown in upper panel; Chl-*a* at *t*0 (dark-green circles), dark-green and clear-green lines are ΔChl-*a* from NH_4^+ (green squares) and NO_3^- uptake (green triangles-down) respectively. Also shown in lower panel; mean $E_{z(50\%)}$ (*i.e.* mean PAR available down to the depth of 50% of subsurface PAR). Uptake, regeneration and release rates have dimensions of μmol-N L^{-1} h^{-1}, Chl-*a* has dimensions of μg L^{-1} and mean $E_{z(50\%)}$ has dimensions of μmol m^{-2} s^{-1}.

After September the levels of E_0, the mean $E_{Z(50\%)}$ and the water column temperature started to decrease and the river flux and therefore nutrient supply increased, probably giving the appropriate conditions for a stressed phytoplankton population to recover. The rates of ρ_G NO_3^-, ρ_G NH_4^+ and NH_{4REG}^+ also diminished. However, the rates of DON_{REL} from NO_3^- uptake increased to a second maximum, probably due to grazing by a now increased heterothophic population. The results discussed above are summarised in Fig. 4.16.

Uptake rates of ammonium in the upper estuary and coastal water showed similar temporal variations to those observed in the mid estuary. It is possible that ammonium regeneration and dissolved organic nitrogen release also share some similarities. This is difficult to evaluate however, since apparently in the upper estuary the patterns observed in the uptake rates did not matched those observed for chlorophyll. The case also applies for nitrate uptake and particularly in this part of the estuary, where the temporal variation of the uptake measured at 100% and 50% subsurface PAR was opposite. It is clear that more studies are needed in order to understand the effect of particular phytoplankton

species on the uptake of N-nutrients, which is beyond the objectives of this research. The information available however, represents an insight to the understanding of the impact of phytoplankton on the principal nitrogen sources. This is a relevant issue in the context of eutrophication and its possible effects on the ecosystem.

As remarked by Cloern (1996) and discussed in detail by Levin (1992), an important issue in ecology is the problem of pattern and scale; pattern is a description of variability in time and space, where the mechanisms of pattern formation depend on the scale. During the present work and in most of the related and cited studies, experiments were carried out at scales of time from minutes to a few days. In particular, the experiments carried out during this research reflect processes that occur in a few hours. The results of the experiments were directly affected or controlled by the *in situ* conditions prevailing at the time. These experiments were done at mid day, when uptake rates were likely maximum.

Nitrogen depletion rates and turnover times

Depletion rates (% h^{-1}) of N-nutrients were calculated in order to evaluate the impact of phytoplankton growth on the ambient levels of nitrate and ammonium in 2002 (**Table 4.4**). In general, the uptake of nitrate appeared to have a major impact on the nitrate ambient levels at the 50% of subsurface PAR, whereas the uptake of ammonium appeared to have a major impact at the 100% of subsurface PAR (Table 4.4). As compared with the inner estuary, a higher proportion of nitrate appeared to be removed in the coastal waters, where uptake rates accounted for up to 9% of the hourly nitrate removal (see Table 4.4). In the case of ammonium, higher proportions seemed to be removed from the coastal waters and mid estuary, with ammonium uptake rates accounting for up to ~20% of the hourly ammonium removal (see Table 4.4). It appeared thus, that although higher uptake rates of nitrate and ammonium were generally measured in the inner estuary relative to the coastal waters (see § 4.2.7), major impacts on the ambient levels of the two N-sources investigated were reached in the mid estuary (in the case of ammonium) and coastal waters (in the case of nitrate and ammonium) during the period 21-Apr to 17-Oct in 2002. However, it must be noted that the concentrations of nitrate and ammonium are overall lower in the coastal waters than in the inner estuary (*e.g.* Iriarte, 1993; Kifle & Purdie, 1993; Iriarte & Purdie, 1994; Hydes & Wright, 1999; Ali, 2003), and in general the ambient levels of these N-sources increase towards the upper estuary (*i.e.* this study). On average, the concentrations of nitrate and ammonium during the study period in 2002, were 10.3±6.6, 27.8±16.3 and 35.7±16.3 μmol NO_3^- L^{-1} and 2.7±2.1, 6.3±5.1 and 13.2±6.0[3] μmol NH_4^+ L^{-1} for the coastal waters, mid and upper estuary respectively. The impact of the N-uptake on the ambient levels thus seemed to be higher in the coastal waters or mid estuary because concentrations were lower at this site

[3]The extremely high value of ~217 μmol L^{-1} of ammonium measured in the upper estuary on the 09-Jul was not considered for this average value.

Table 4.4: Nitrate and ammonium depletion rates and turnover times calculated from net uptake rates measured at the 100% and 50% of subsurface PAR. Mean (bold) and range (parentheses) during the productive spring–summer period in 2002.

	Depletion rate (% h^{-1})		Turnover time (d)	
	Nitrate	**Ammonium**	**Nitrate**	**Ammonium**
From 100% PAR				
Upper estuary	**0.1**	**1.5**	**311**	**14.5**
	(<0.1 - 0.5)	(0.1 - 4.8)	(8 - 2141)	(1 - 48)
Mid estuary	**0.2**	**4.0**	**199**	**6**
	(<0.1 - 1.4)	(0.1 - 19.5)	(3 - 780)	(0.2 - 45)
Coastal waters	**0.3**	**3.5**	**186**	**3.5**
	(<0.1 - 2.5)	(0.4 - 18.1)	(1.6 - 747)	(0.4 - 18)
From 50% PAR				
Upper estuary	**0.2**	**1.3**	**113**	**15.5**
	(<0.1 - 0.8)	(<0.1 - 5.0)	(5 - 419)	(0.8 - 80)
Mid estuary	**0.5**	**3.4**	**99**	**11.4**
	(<0.1 - 3.5)	(<0.1 - 16.7)	(1 - 256)	(0.3 - 59)
Coastal waters	**1.0**	**2.8**	**143**	**24**
	(<0.1 - 9.0)	(<0.1 - 7.4)	(0.5 - 505)	(0.6 - 219)

relative to the generally high concentrations measured in the inner estuary (particularly in the upper estuary).

The relative low uptake rates of nitrate and ammonium measured in 2002, can be appreciated in the turnover times of these two N-nutrients. In the case of nitrate, turnover times appeared to be lower if uptake rates measure at the 50% of subsurface PAR are considered (see Table 4.4), although seemed to be fairly similar in the mid estuary and coastal waters at the both PAR levels selected for the ^{15}N-tracer experiments. As expected, ammonium seemed to be recycled much faster that nitrate, even though extremely high concentrations can be measured on some occasions (*e.g.* see Table 4.1). From Table 4.4 it can be noted that the mid estuary appears to be a place where in general the nitrate and particularly ammonium are recycled at a faster rate, as suggested by the larger proportion of removal and therefore to the shorter turnover times.

Care must be taken however, when evaluating the impact of biological processes on the levels of the different nitrogen species. If the gross uptake of nitrate measured in the mid estuary at the 100% of subsurface PAR is used for the calculation of the depletion rates, the average proportion of nitrate removed at this site increased to 1.2% h^{-1} within a range of <0.1 to 3.4% h^{-1}. This hourly proportion of removal would appeared to be still low, nonetheless is 6 times larger that the averaged obtained from considering the net uptake rates of nitrate (see Table 4.4). The effect of this larger proportion of removal on the turnover times of nitrate is rather significant, leading to an average turnover time of 14.4

days within a range of 1.2 to 120 days. The implication of this, is that a large proportion of the nitrate that has been taken up has been released as dissolved organic nitrogen, and represents another nitrogen substrate for microorganisms to use. A similar situation emerged for the removal of ammonium, and when calculating the depletion rates using the gross uptake rate obtained from the net uptake rates corrected for isotope dilution, the average depletion rate of ammonium was 17.3% h^{-1} and within a range of 0.4 to 97.7% h^{-1}. That is, an average hourly removal 4.3 times larger than that calculated from net uptake rates without correction for isotope dilution. In consequence, this larger impact on the ambient levels of ammonium are reflected in an average turnover time of 2 days within a range of <0.5 to 11.4 days. Apparently there are no reports in the literature commenting on the effects of DON_{REL} and ρ_G NH_4^+ (*i.e.* calculated from P NH_4^+) on the calculation of turnover times and depletion rates of N-nutrients. As a final comment, it must be noted that the depletion rates and turnover times during this research were calculated from the uptake of nitrogen by phytoplankton (and probably bacteria) in the water column. That is, the turnover times and depletions rates are assumed to be due to phytoplankton activity during the spring-summer productive period. A more significant estimate of the total nitrogen removal from the system and a better estimate of the nitrogen turnover times may be obtained through a mass balance approach, where the net sinks and inputs of the various nitrogen sources can be evaluated over appropriate time scales.

Chapter 5

A comparison between the productive spring-summer period in 2001 and 2002

5.1 Introduction

Phytoplankton blooms within the Southampton Water estuary (SW) generally develop between the months of March and September each year (Leakey *et al.*, 1992; Kifle & Purdie, 1993; Iriarte & Purdie, 1994; Howard *et al.*, 1995; Crawford *et al.*, 1997; Hydes & Wright, 1999; Holley & Hydes, 2002; Ali, 2003). The timing and magnitude of these blooms however, have been shown to exhibit high interannual variability (*e.g.* Fig. 5.1), and recent research (*e.g.* Hydes & Wright, 1999; Holley & Hydes, 2002; Ali, 2003; Iriarte & Purdie, in press) has been focused on understanding the factors that control their development and magnitude. Recent work has shown that light availability plays an important role in triggering phytoplankton blooms within the estuary (Ali, 2003), and depletion of silicate and phosphate have been suggested to limit phytoplankton populations after bloom events (Ali, 2003). The interaction of physical factors acting upon phytoplankton physiology is complex because they may have effects on different time scales within a given system (Levin, 1992; Cloern, 1996). In addition, different forcings are likely to act contemporaneously and phytoplankton species may exhibit diverse responses (*e.g.* Dortch, 1990; Lomas & Glibert, 1999a,b; Lomas *et al.*, 2000). In the Southampton Water estuary for example, Ali (2003) found that a mean water column irradiance of 100 W h m^{-2} d^{-1}, together with a water temperature of $\sim$14°C and slight water column stratification appeared to be required for the blooming of diatoms in the spring 1999. In addition, the seasonal variation of physical factors (*e.g.* light and temperature) is combined with the availability of essential nutrients, thus generating changes within the phytoplankton

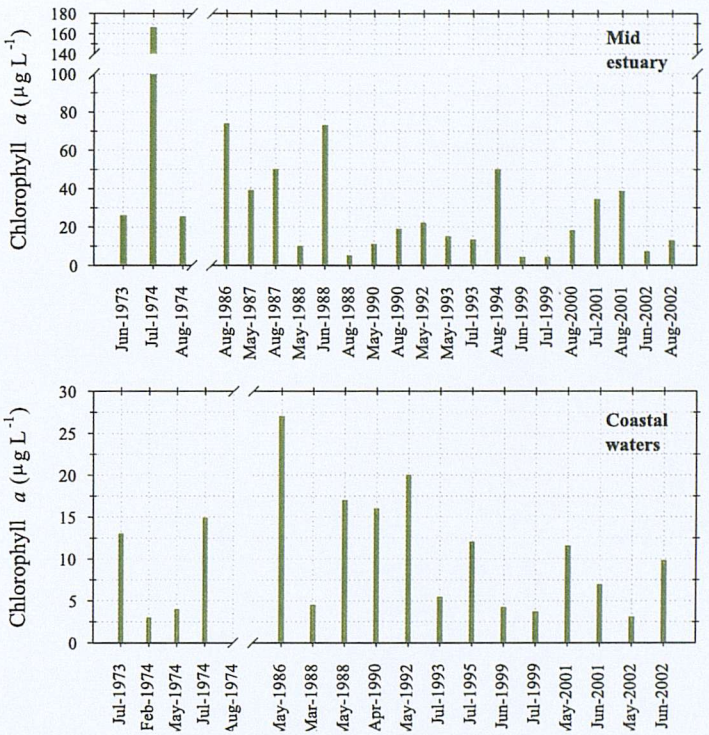

Figure 5.1: **Chlorophyll concentration; interannual variability in the mid estuary and coastal waters.** Adapted from Table 1.3 in Ali (2003), and from data presented in Howard *et al.* (1995), Hydes & Wright (1999), Ali (2003) and the present study. Note different scales and breaks in axes.

community structure. The temporal variability in the uptake rates of nitrogen as well as the 'preferential' uptake of a particular N-source (*e.g.* NO_3^-, NH_4^+ and $CO(NH_2)_2$) would therefore be expected to be related to the factors controlling the growth of phytoplankton. In the present work, ^{15}N-tracer incubation experiments were applied to study, for the first time in the Southampton Water estuary, the uptake of different nitrogen sources, and measurements were made to determine the seasonal changes in levels of nutrients and chlorophyll *a* during the productive spring-summer period in 2001 and 2002. Overall, results from the various measurements showed lower levels of Chl-*a* and lower nitrogen uptake rates during the productive period in 2002, although the levels of nutrients were approximately similar during both years. In the present chapter, uptake rates measured at the 100 and 50% of subsurface PAR, surface Chl-*a* and nutrient concentrations, and irradiance data from 2001 and 2002, are used to discuss the differences found between the two years studied.

5.2 Chlorophyll *a* levels

In 2001, surface (1 m) Chl-*a* concentrations of up to 64 (04-Jul), 38.5 (01-Aug) and 11.5 (21-May) μg L^{-1} were respectively measured in the upper estuary, mid estuary and

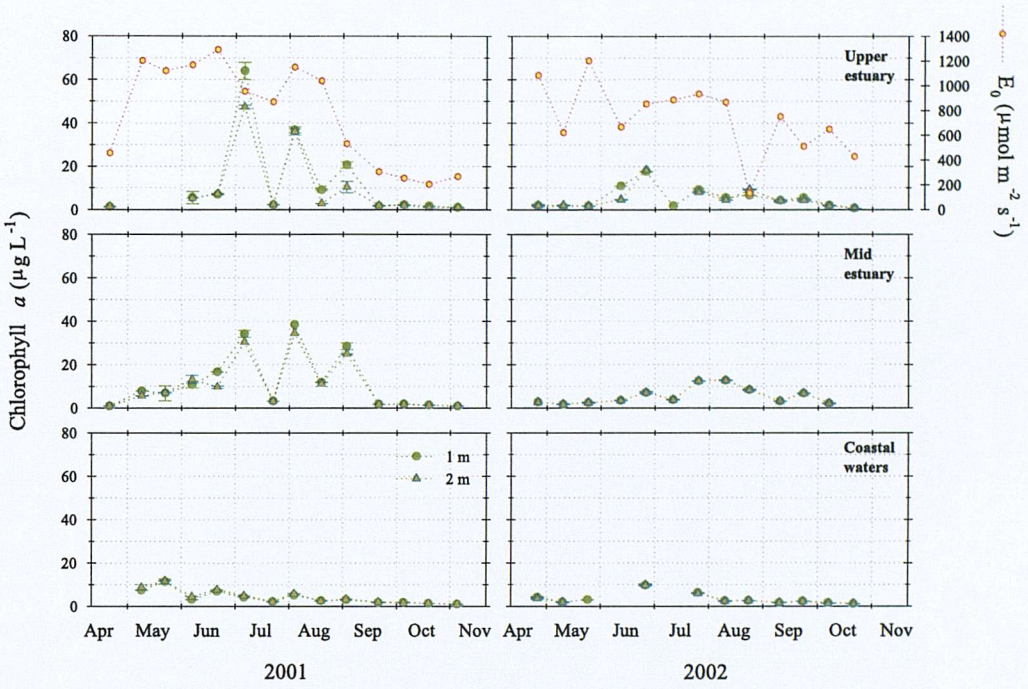

Figure 5.2: **Surface (1 and 2 m) chlorophyll *a* concentration during the productive spring-summer period in 2001 and 2002 in the Southampton Water estuary.** Error bars represent the standard difference of duplicate measurements. Incident irradiance (E_0) averaged over the incubation period is also shown.

coastal waters, whereas in 2002 highest values were 17.6 (10-Jun), 12.7 (07-Aug) and 9.8 (24-Jun) μg L^{-1} (same order as above). Highest Chl-*a* concentrations measured in 2002, thus represented 27.5, 33.0 and 84.6% (same order as above) of those measured in 2001. The difference between 2002 and 2001 in the mid estuary and coastal waters would further increase if highest chlorophyll concentrations are considered instead of surface values. In 2001 the highest Chl-*a* concentrations at these two sites were measured at a depth of 9 m, with respective values of 41.6 and 20.7 μg L^{-1} on the 21-May (see Fig. 3.5, § 3.2.4, Ch. 3). In 2001, the first surface chlorophyll peak was measured in the coastal waters on the 21-May (see Fig. 5.2), and levels then decreased gradually towards November (see Fig. 5.2). In the mid and upper estuary, the first peak was measured about 6 weeks later on the 04-Jul (see Fig. 5.2). In the upper estuary the following Chl-*a* peaks decreased in magnitude, whereas in the mid estuary the highest peak was recorded on the 01-Aug (see Fig. 5.2). In 2002 the first Chl-*a* peak in the coastal waters was recorded about a month later relative to the previous year, but on the same date (24-Jun) the first peak in the mid and upper estuary was also measured (see Fig. 5.2). In fact, in the coastal waters and upper estuary this first peak represented the highest chlorophyll level recorded for these two sites in 2002. In the case of the mid estuary highest Chl-*a* concentrations were measured on the 23-Jul and 07-Aug (see Fig. 5.2). The timing of chlorophyll peaks seemed to be consistent between the two years in the mid and upper estuary, and appeared to

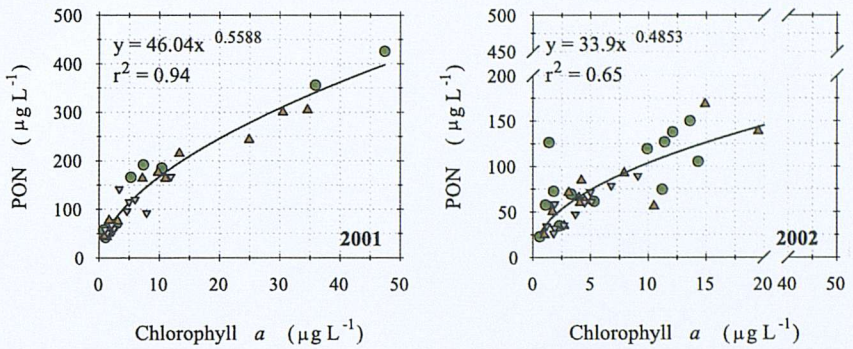

Figure 5.3: **PON plotted against Chl-*a*, 2001 and 2002.** The power relation includes data from the three sampling sites. Symbols indicate upper estuary (circles), mid estuary (triangles up) and coastal waters (triangles down).

be about a month delayed in the coastal waters in 2002 relative to 2001. Chlorophyll levels in the latter site, were approximately similar between the two years and appeared to be in good agreement with the historical record of Chl-*a* levels measured at this site, with peaks in the range of 3.0 to 27.0 μg L^{-1} (see Fig. 5.1). Chlorophyll levels in the mid estuary are also in good agreement with the historical record, although levels between the two years studied here were much lower in 2002. Although beyond the objectives of this comparison chapter, it is worth noting that from Fig. 5.1 it would appear that the magnitude of the Chl-*a* peaks have decreased with time. Particulate organic nitrogen (PON) concentrations measured in 2002 were also lower that in 2001 (see Fig. 5.3). In general, PON increased with increasing Chl-*a* levels, although in 2002 there was probably more detrital nitrogen than in 2001 as indicated by the poorer power-fit (see Fig. 5.3). Moreover, Chl-*a* levels may have been influenced by a higher degree of light attenuation in 2002 (*i.e.* phytoplankton growth as indicated by the levels of Chl-*a* may have been comparatively more light limited).

5.3 Nitrogen net uptake rates

The seasonal changes in the levels of chlorophyll during 2001 and 2002 were reflected in the magnitude of nitrogen uptake rates at the three selected stations. That is, with the exception of the upper estuary in 2002, seasonal changes in the net uptake rates of nitrate and ammonium appeared to follow the seasonal trend of chlorophyll levels (see Figs. 5.4 and 5.5). High nitrate and ammonium uptake rates measured at the 100 and 50% of subsurface PAR coincided with high Chl-*a* concentrations in most cases (see Figs. 5.4 and 5.5). This characteristic is particularly clear in the seasonal changes of nitrate uptake (see Fig. 5.4). Highest chlorophyll levels however, did not seem to imply highest uptake rates (*e.g.* 20-Jul coastal waters, Figs. 5.4 and 5.5), although higher uptake rates were

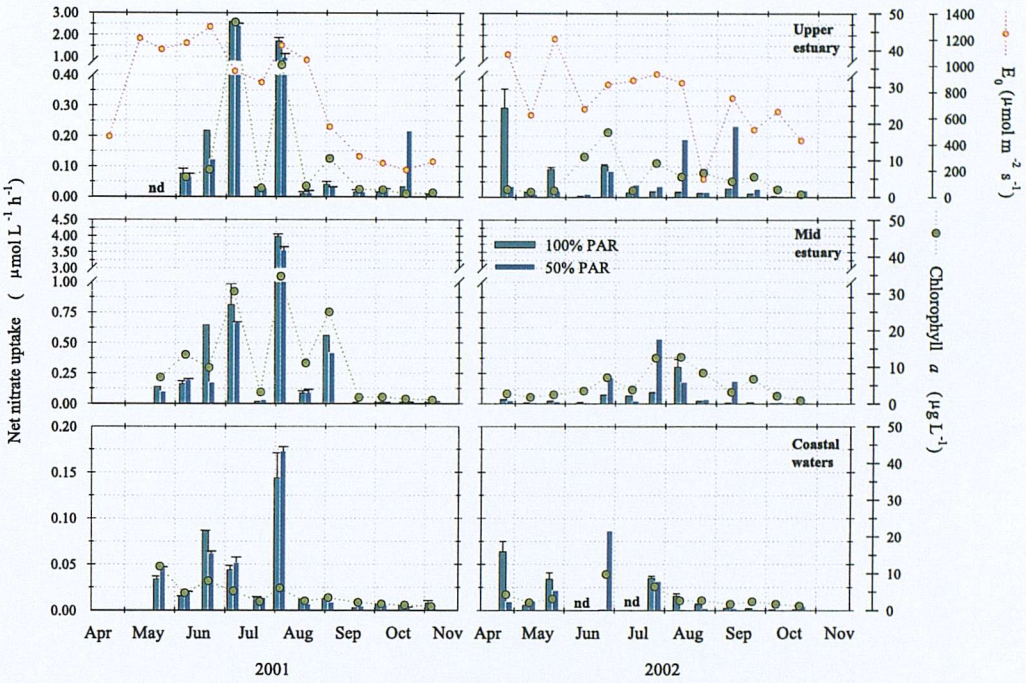

Figure 5.4: **Nitrate uptake measured at 100 and 50% of subsurface PAR, during the productive spring-summer period in 2001 and 2002.** Chlorophyll *a* from 2 m (2001) and 1 m (2002) depth, and 4-h averaged incident irradiance (E_0) are also shown. Error bars represent the standard difference of duplicate measurements. Note different scales (nd = no data available).

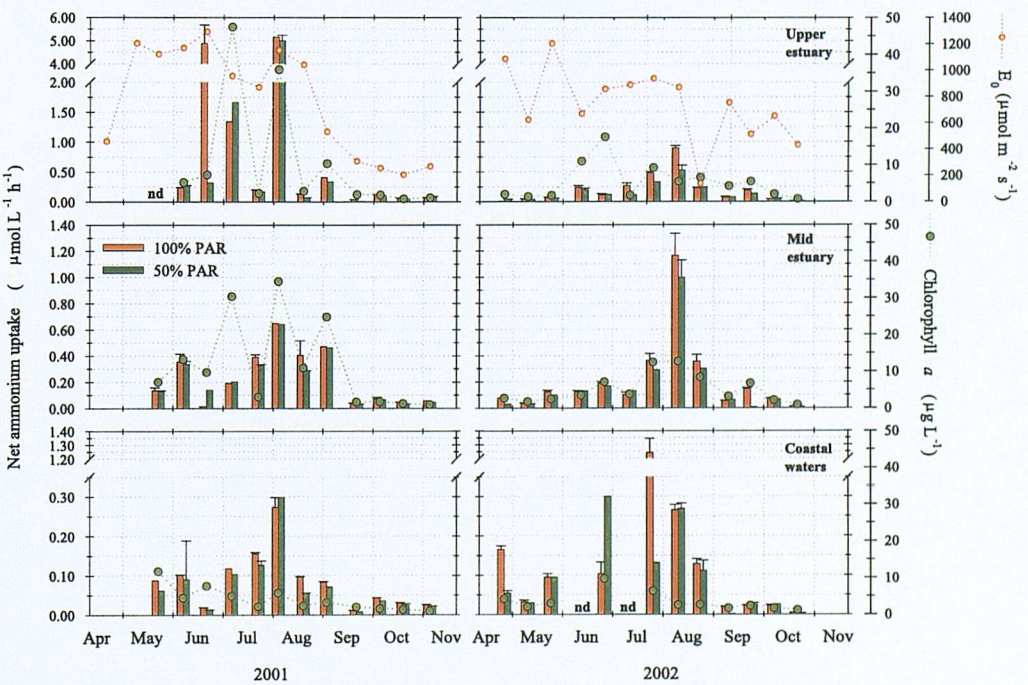

Figure 5.5: **Ammonium uptake measured at 100 and 50% of subsurface PAR, during the productive spring-summer period in 2001 and 2002.** Chlorophyll and E_0 data as in Fig. 5.4. Note different scales (nd = no data available).

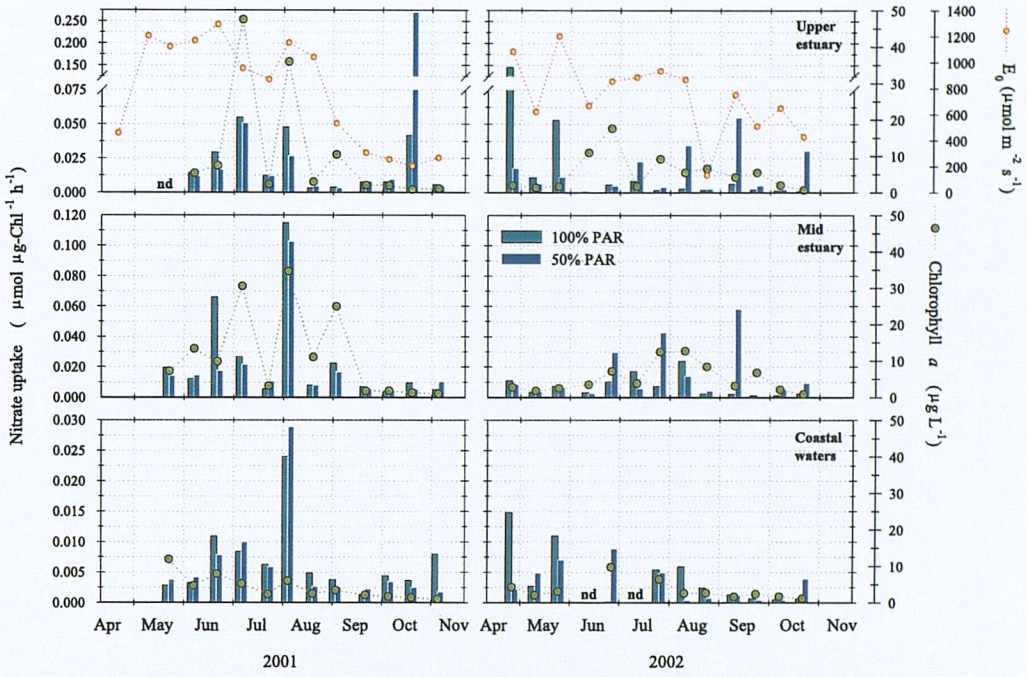

Figure 5.6: **Chlorophyll normalised nitrate uptake measured at 100 and 50% of subsurface PAR, during the productive spring-summer period in 2001 and 2002.** Chlorophyll and E_0 data as in Fig. 5.4. Note different scales (nd = no data available).

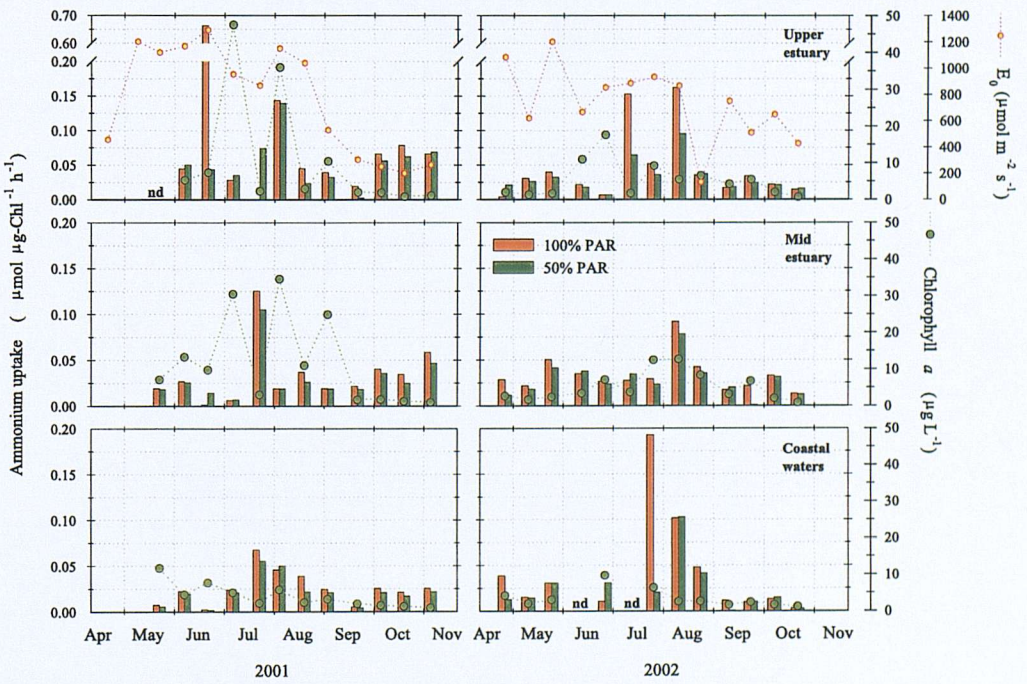

Figure 5.7: **Chlorophyll ammonium nitrate uptake measured at 100 and 50% of subsurface PAR, during the productive spring-summer period in 2001 and 2002.** Chlorophyll and E_0 data as in Fig. 5.4. Note different scales (nd = no data available).

overall reached within the period April/May to August of both years (see Figs. 5.4 and 5.5). In the case of nitrate, uptake rates measured during 2001 were higher than those measured in 2002, particularly in the mid and upper estuary (Fig. 5.4). In 2001 nitrate net uptake rates reached values of 2.600, 3.974 and 0.173 μmol-N L^{-1} h^{-1} in the upper estuary, mid estuary and coastal waters respectively, whereas maximum values in 2002 were 0.293, 0.533 and 0.087 μmol-N L^{-1} h^{-1} (same order as above). That is, maximum values in 2002 represented about 11, 13, and 50% respectively, of those measured in 2001. In the case of ammonium, higher uptake rates were measured in the upper estuary in 2001, but appeared to be fairly similar between the two years in the mid estuary and coastal waters (Fig. 5.5). The highest ammonium uptake rates measured in 2002 in the upper estuary represented 17% of the highest rate measured in 2001. However, in the mid estuary and coastal waters, highest uptake rates in 2002 represented an increase of 79% and 316% respectively, relative to highest uptake rates measured in 2001. When net uptake rates were normalised to chlorophyll (*i.e.* μmol-N (μg-Chl-*a*)$^{-1}$ h^{-1}), values seemed to be more comparable between the two years studied (see Figs. 5.6 and 5.7). In some cases, elevated normalised uptake rates appeared to be the result of high nitrogen uptake rates, low chlorophyll values or a combination of both (*e.g.* nitrate uptake 01-Aug-2001 coastal waters Fig. 5.6). In 2002, nitrate and ammonium net uptake rates measured in the upper estuary appeared to vary from the general trends observed at the other sites and during the previous year. Nitrate uptake did not seem to exhibit a clear relation with chlorophyll, and while at other stations higher rates were reached within the period April/May to August, in the upper estuary higher uptake rates were measured from May to July at the 100% of subsurface PAR and from July to September at the 50% of subsurface PAR (see Fig. 5.4). In the case of ammonium, uptake rates did not present a clear relation with chlorophyll either, although they did show higher uptake rates within the period June to August (see Fig. 5.5).

It is interesting to note that during 2001, a year when higher Chl-*a* concentrations were measured relative to 2002, higher uptake rates of nitrate were also reached at all sites (see Fig. 5.4). This situation also applies for ammonium uptake in the upper estuary (see Fig. 5.5). In the mid estuary and coastal waters however, ammonium uptake rates appeared to be of similar magnitude between the two years, even though Chl-*a* levels were lower in 2002. Highest ammonium uptake rates were actually reached in 2002 at these two sites, but were comparatively lower in the upper estuary (see Fig. 5.5). It thus appear that there was a factor (or factors) having a major effect on the uptake of nitrate throughout the estuary in 2002, and also on the uptake of ammonium in the upper estuary.

5.4 Availability of light and nutrients

Although Chl-*a* concentrations measured in 2002 were lower than those measured in 2001, the availability of nutrients did not seem to be limiting to phytoplankton growth. That is, ambient nutrient concentrations were rather similar in both years, and with the exception of silicate and phosphate in the coastal waters, surface levels were never found below the limit of detection. Nitrate and ammonium surface concentrations for example appeared to be fairly similar between 2001 and 2002 (see Fig. 5.8). Moreover, highest surface ammonium concentrations were measured in 2002 (see Fig. 5.8). Although in some published works it has been argued that ammonium at concentrations $\gtrsim 1$ μmol L^{-1} inhibit the uptake of nitrate (*e.g.* see Dortch, 1990), in the Southampton Water estuary nitrate and ammonium concentrations are usually present at saturating levels. Besides, the fact some of the highest uptake rates of nitrate and ammonium measured, were reached contemporaneously (*e.g.* 01-Aug-2001, Figs. 5.4 and 5.5), does not seem to suggest nitrate uptake inhibition by ammonium. With data available in the literature, Dortch (1990) hypothesised that preference for ammonium would be maximal with low light and nitrogen deficiency, whereas inhibition would be maximal with nitrogen sufficiency and low light. This did not seem to be the case during the productive period in the Southampton Water estuary however, since N-nutrients were still relatively abundant and some of the highest light levels recorded during the period were being measured.

Incident irradiance (E_0) averaged over the incubation period also appeared to be fairly similar between the productive spring-summer period (May to September) in 2001 and 2002 (*e.g.* see Fig. 5.2). However, when a mean value is obtained, it would seem that E_0 was higher or was sustained for longer during the period May to August in 2001 than in 2002 (see Fig. 5.2). Mean E_0 values for the above period were 1036$\pm$228 and 771$\pm$311 μmol m^{-2} s^{-1} for 2001 and 2002 respectively. Data from this research presented in Fig. 3.7, § 3.2.6, Ch. 3, indicated that the uptake rates of nitrate, ammonium and urea were strongly dependent on the availability of light throughout the water column. The light available within the water column in turn depends on the attenuation coefficient (k) and E_0. From a simple point of view, it would be thus expected that higher uptake rates would occur when higher E_0 prevail. Nevertheless, on some occasions when light levels were relatively high, the uptake rates of nitrate, ammonium and urea were low. It should be noted however, that among the three nitrogen sources studied in 2001, ammonium exhibited highest dark uptake rates, indicating that the uptake of ammonium is less affected at low or zero light levels. It also must be noted that light data presented here, is an average of irradiance obtained over the incubation period. On times scales of few weeks to months, the availability of light throughout water column is thought to be a major factor controlling phytoplankton populations in the Southampton Water estuary

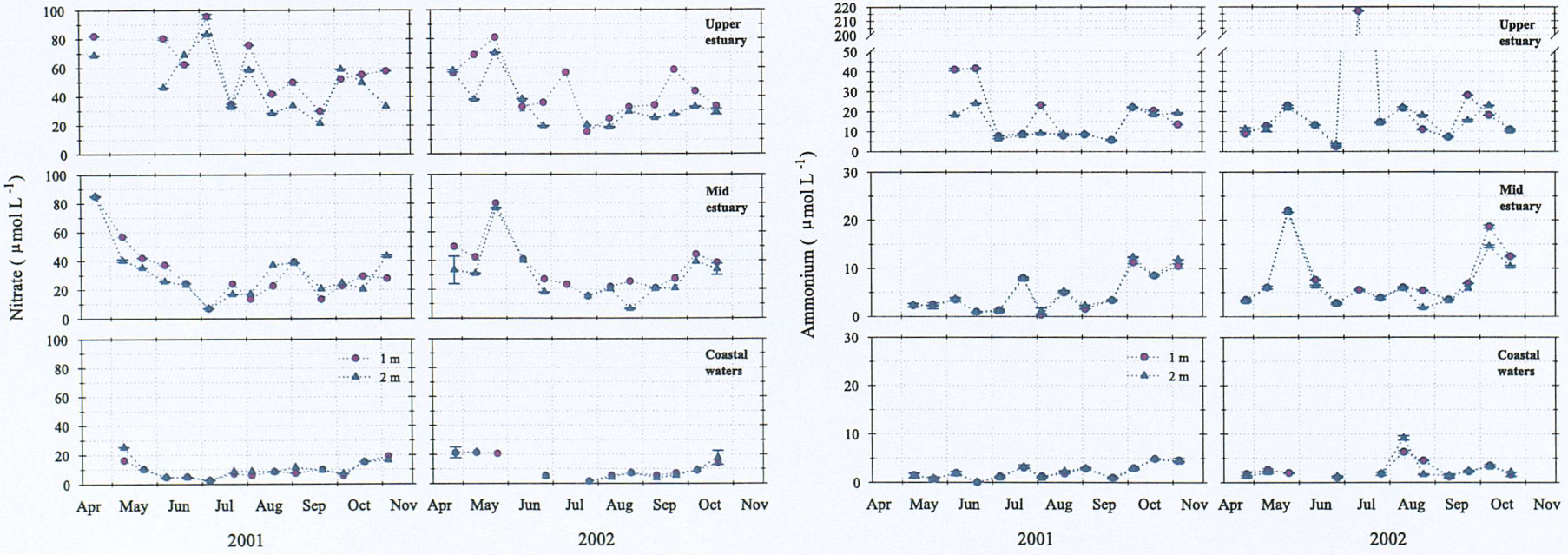

Figure 5.8: **Nitrate and ammonium surface concentrations (1 and 2 m depth) during the productive spring-summer period in 2001 and 2002.** Error bars represent the standard deviation of replicate measurements.

(*e.g.* Holley & Hydes, 2002; Ali, 2003). In a 5 year comparative study, Iriarte & Purdie (in press) found that at Calshot (*i.e.* coastal waters of the Southampton water estuarine system), Chl-*a* levels >10 μg L^{-1} occurred only when the mean water column irradiance (*i.e.* PAR) averaged over the previous 7 days was >380 W h m^{-2} d^{-1} and the irradiance attenuation coefficient (k) was $\leqslant$0.5 m^{-1}. When comparing the timing of the spring bloom at Calshot (commonly occurring in May), Iriarte & Purdie (in press) found that k and the precipitation rate were higher during May 2002 relative to other years, and suggested that the delay of the spring bloom in 2002 (which occurred in June) was due to the less irradiance available throughout the water column (*i.e.* the water column was more turbid and the cloud cover more significant).

Despite the water temperature data set for 2002 being incomplete, from the information available it seems that temperature values between the two years were also similar (see Fig. B.1, Appendix B.0.6). The only apparent difference being perhaps, that variability between measurements (*i.e.* in time scales of about two weeks) was higher during 2001 (see Fig. B.1, Appendix B.0.6). That is, the gradual increase in water temperature towards the summer months seemed to be 'smoother' in 2002, with temperature values in 2001 showing variations of about -2 or +2 °C between sampling dates (see Fig. B.1, Appendix B.0.6). In the previous chapter it has been discussed that the water temperature may play a major role particularly in regulating the activity of nitrate reductase, which has been demonstrated to be temperature dependent and more active at low temperatures (*e.g.* Lomas & Glibert, 1999a,b; Lomas *et al.*, 2000). It is therefore possible that the water column temperature controls the availability of phytoplankton organisms to take up a given nitrogen source. From information in the literature, the uptake of nitrate would be expected to be more influenced by temperature than the uptake of ammonium or urea, which have been found to be taken up at faster rates with increasing temperature (*e.g.* Lomas & Glibert, 1999b).

The ability to predict the magnitude and timing of phytoplankton blooms in estuaries relies on understanding of the factors that control the physiology of phytoplankton populations. The task is however complicated since the combined effects of light, temperature and nutrient levels appears to vary among phytoplankton groups or even phytoplankton species (Dortch, 1990; Cochlan *et al.*, 1991; Peperzak, 1993; Peperzak *et al.*, 1998; Lomas & Glibert, 1999a,b; Lomas *et al.*, 2000). In addition, the physical environment (*i.e.* stratification and mixing) also plays an important role by keeping cells where light and nutrients are available, or mixing them throughout the water column. Furthermore, the interactions between autotrophs and heterotrophs (*e.g.* species competition and grazing) are also likely to influence the availability of phytoplankton populations to bloom.

5.5 The impact of phytoplankton growth on the levels of nitrogen

The differences in nitrogen uptake rates between 2001 and 2002 implied larger impacts on the nitrogen levels in 2001. While in 2001 surface (100 and 50% of subsurface PAR) nitrate depletion rates of up to 3.1 and 23.2% h^{-1} were respectively calculated only for the upper and mid estuary, in 2002 maximal depletion rates at these two sites were 0.8 and 3.5% h^{-1}, respectively. Nitrate removal in the coastal waters was similar between the two years on some occasions, although higher depletion rates were reached in 2002. At this site, depletion rates varied from 0.1 to 2.2% h^{-1} during the period 21-May to 01-Oct-2001, and from 0.1 and 9.0% h^{-1} during the period 25-Apr to 20-Aug-2002[1]. That is, although similar depletion rates were reached in the coastal waters in 2001 and 2002, the impact on the nitrate appeared to be maintained for longer in 2001. The period during which the uptake of nitrate had major impact was also longer in 2001 at the other two stations. In the case of ammonium, the difference in removal was also marked. While maximum depletion rates in 2001 of up to 58, 59.6 and 37.3% h^{-1} were reached in the upper estuary, mid estuary and coastal waters respectively, maximum depletion rates in 2002 were 5.0, 10.5 and 10.8% h^{-1} (same order as above). Although the impact on the levels of ammonium was greater in 2001, removal was observed through out the sampling period in both years. The uptake of urea was measured only in 2001, and from the available data, depletion rates of up to 90.4, 78.9 and 85.7% h^{-1} were estimated for the upper estuary, mid estuary and coastal waters.

As expected, the difference in the uptake rates between the two years studied, resulted in longer turnover times in 2002. Considering the uptake rates measured at the 100 and 50% of subsurface PAR, the longest turnover times estimated for nitrate during 2001 were 265, 353 and 383 days in the upper estuary, mid estuary and coastal waters, respectively. In 2002 longest turnover times were 2141, 780 and 747 days (same order as above). In the case of ammonium the situation was less extreme, with longer turnover times of 49.8, 11, and 8.5 days in 2001, and 79.6, 59.2, and 219 days in 2002 estimated for the upper estuary, mid estuary and coastal waters respectively. However, in most cases during the productive period in both years (*i.e.* between April/May and September), turnover times were on average 2.2 days in 2001 and 6.8 days in 2002. Longer turnover times for urea for the upper estuary, mid estuary and coastal waters were 13.4, 17.3 and 21.6 days, with a global average of 1.3 days during the period May to September 2001. The water residence time in the Southampton Water estuary has been estimated to be approximately 5 to 10 days (Sharples, 2000), which suggests that $\gtrsim$100% of the ammonium and urea measured

[1]Apart from the depletion rate of 9.0% h^{-1}, which was calculated for the 50% of subsurface PAR, depletion rates during the period 25-Apr to 20-Aug-2002 were <2.6% h^{-1} at this site.

at any time (at least during the productive spring-summer period) can be recycled by phytoplankton activity within the estuary. In the case of nitrate however, with global turnover times of 26.7 and 97.4 days during the productive in 2001 and 2002 respectively, only a small proportion is likely to be removed by phytoplankton activity. The remaining nitrate would be expected to be flushed out of the estuary or denitrified.

It must be noted nevertheless, that during 2001 neither the gross uptake of any of the N-sources studied, nor the release of dissolved organic nitrogen or the regeneration of ammonium were measured. In addition, the net uptake rates of ammonium and urea were not corrected for isotope dilution. As presented in the previous chapter (Ch. 4, § 4.2.7.1), on average, net uptake rates of nitrate represented 25% of the gross uptake rates. That is, more than 70% of the nitrate taken up can be released as DON. In the case of ammonium, net uptake rates represented on average 31% of the uptake rates corrected for isotope dilution, indicating that the actual uptake rates of ammonium can be underestimated by up to ~70%. Since urea can also be regenerated in the water column by bacteria and zooplankton, dilution of the isotope enrichment is also likely to be affected. The removal of nitrate, ammonium and urea would thus be expected to be larger than estimated in 2001. This assumption in turn, would suggest that extensive phytoplankton blooms in the Southampton Water estuary represent a significant potential for nitrogen removal.

Chapter 6

Summary and conclusions

During the present research it was aimed to quantify the influence of phytoplankton activity on the removal of nitrogen through a non-turbid temperate estuary by directly measuring the uptake of N-nutrients. Results presented in Chapter 3 have shown that the seasonal variation in the uptake of nitrogen and carbon were consistent with the seasonal changes in the concentrations of Chl-*a*. That is, higher uptake rates of nitrogen and carbon were reached during the spring-summer productive period in 2001 and in general were maximum when highest Chl-*a* concentrations were measured. The ^{15}N and ^{13}C-tracer experiments carried out in 2001 have also shown that each of the three selected sites within the Southampton Water estuary exhibited spatial differences, with higher uptake rates being mainly reached in the mid and upper estuary. The spatial difference observed in the uptake rates, were also consistent with the spatial distribution of Chl-*a*. The information generated indicates that phytoplankton plays an important role on the cycling of nitrogen throughout the euphotic water column.

Nitrogen uptake rates measured in 2001 in the Southampton Water estuary were shown to be comparable with values reported in the literature for other estuaries and coastal marine systems. Some of the uptake rates measured were found to be at the high end of the range reported for other systems, suggesting that the impact on the N-nutrient levels can be significant during productive periods. Nitrogen uptake rates measured in the inner part of this non-turbid estuary were shown to be higher that those measured in turbid estuaries such as the Thames and Humber in the UK, or such as the Ems, Scheldt, Loire, Gironde, Douro and Rhine in continental Europe. In turn, nitrogen uptake rates measured in the coastal waters of the system were shown to be in good agreement with values reported for other coastal environments such as the English Channel, the Southern North Sea, Monterey Bay and California Bight.

Data presented in Chapter 3 showed that ammonium was the nitrogen source most taken up within the Southampton Water estuary. The average contribution of ammonium

to the total nitrogen uptake was >55% as determined from rates integrated throughout the euphotic water column, and >65% as determined from dark uptake rates at all sites. The contribution of nitrate was shown to be on average $\gtrsim$20% but <31%. Urea uptake was shown to account for between 2.6 and 14.2% of the total nitrogen uptake, with larger contributions under light conditions. Results showed that although ammonium appeared to be the dominant source of nitrogen, on a few occasions either nitrate or urea were also the dominant sources.

Direct measurements of nitrogen uptake allowed quantification of the removal of three different nitrogen species in 2001. It was demonstrated that removal of nitrate, ammonium and urea can be significant during the productive spring-summer period throughout the system, and particularly in the inner estuary. Depletion rates showed that up to ~9, 28 and 50% of nitrate, ammonium and urea can be respectively removed from the euphotic water column per hour. Depletion rates calculated from different light levels showed that the effect of nitrogen removal is maximal in the upper layers of the water column. At this level, the removal was shown to be up to 23, 60 and 90% h^{-1} of the ambient concentrations of nitrate, ammonium and urea, respectively. The results presented suggested that the removal of nitrogen removal from the euphotic water column and from the upper layer can potentially be up to threefold larger during diurnal slack water periods.

Turnover times showed as expected, that reduced forms of nitrogen are recycled at a faster rate than nitrate. On average, the turnover time of nitrate in the euphotic water column was 74 days, whereas the average turnover times of ammonium and urea were 7 and 11 days respectively.

Results presented in Chapter 4 showed that, with the exception of the upper estuary, the uptake rates of nitrate and ammonium in 2002 were also consistent with the seasonal changes in Chl-*a* levels. In 2002 highest uptake rates of nitrate and ammonium were also measured in the inner estuary, and ammonium was shown to be the dominant source of nitrogen, contributing on average with the 84, 77 and 74% of the total N-uptake in the coastal waters, mid and upper estuary respectively.

Results from incubation experiments in 2002 showed that on average 74±32% of the nitrate taken up during the productive spring-summer period was released as DON, which represents an additional nitrogen source for phytoplankton and other microbial communities. In the case of ammonium, the data generated during this investigation showed marked differences in the uptake rates when values were corrected for isotope dilution. Uptake rates without correction represented an average of 31±9% of those corrected. Results presented in Chapter 4 showed that both, the gross uptake of ammonium and the regeneration rates of ammonium exhibited a similar temporal trend, with a maximum on early August, suggesting that autotrophic and heterotrophic processes were probably in

balance. In Chapter 4 it was also shown that of the ammonium taken up, only an average of 3.1% was released as DON.

Nitrogen removal in 2002 showed depletion rates of up to 9, 3.5 and 0.8% h^{-1} of the ambient levels of nitrate and up to 5, 19.5 and 18.1% h^{-1} of the ambient levels of ammonium for the coastal waters, mid and upper estuary respectively. In the case of nitrate, depletion rates appeared to be higher at the 50% of subsurface PAR than at the 100% level, probably due to photoinhibition of nitrate uptake or to DON release.

Turnover times of nitrate in 2002 were shown to be on average >90 days at all sites. In contrast, average turnover times of ammonium were shown to be commonly <24 days. In Chapter 4 it was demonstrated that by taking into account the nitrate that has been taken up and released as DON, the depletion rates increased by a factor of 6. In turn, it was also shown that the turnover time of nitrate decreased from an average of 199 days, to an average of 14 days in the mid estuary. In the case of ammonium, it was demonstrated that by taking into account the effect of isotope dilution in the calculation of the gross uptake rate, depletion rates were on average 4.3 times grater than those calculated without considering isotope dilution. This it turn was shown to lead to an average ammonium turnover time of 2 days instead of the 6 days estimated without correction for isotope dilution.

Finally, in Ch. 5 the differences observed between the productive spring-summer period in 2001 and in 2002 were discussed. Chl-*a* concentrations were shown to be lower in 2002, and accordingly, nitrate uptake rates were also shown to be lower also in this year. The uptake of ammonium however, appeared to be fairly similar between the 2 years in the mid estuary and coastal waters. Results from both years showed that highest uptake rates were reached within the period April/May to August of both years. It was suggested, given the nitrogen turnover times due to phytoplankton activity and the water residence time of the Southampton Water estuary, that ammonium and urea are likely to be recycled within the estuary, but nitrate may be either exported or denitrified. When analysing the available nutrient, irradiance and temperature data, differences between the two years did not seem to be excessive, although temperature and irradiance changes on time scales of the sampling program, may have had an effect. Reports in recent literature suggest that the availability of light throughout the water column plays an important role in controlling the blooming of phytoplankton in the Southampton Water estuary, and it is thus likely that it also has a major effect on the cycling of nitrogen which is related to phytoplankton activity.

From this investigation the following conclusions can be drawn:

1. Phytoplankton growth represents an important sink of dissolved inorganic (partic-

ularly reduced species) and organic forms of nitrogen during productive periods in non-turbid estuaries.

2. Ammonium is likely to be the dominant source of nitrogen during productive periods in non-turbid estuaries, although nitrate and urea may also be significant sources depending on the environmental conditions affecting phytoplankton populations.

3. It is possible that in non-turbid estuaries a significant proportion of the nitrate taken up by phytoplankton is released as dissolved organic nitrogen, which represents an additional source of nitrogen for microbial communities.

4. In non-turbid estuaries such as the Southampton Water estuary, reduced forms of nitrogen (*i.e.* ammonium and urea) are likely to be recycled within the estuary, whereas oxidised forms (*i.e.* nitrate) are more likely to be exported or denitrified.

5. The effect of phytoplankton growth on the levels of nitrogen through estuaries can be underestimated if the gross uptake of the nitrogen forms of interest is not taken into account. In addition, in the case of reduced forms of nitrogen such as ammonium and urea (which can be rapidly regenerated in the water column), the effect of isotope dilution should also be taken into account when applying ^{15}N-tracer incubation techniques.

The aim of the present work was to evaluate the effect of phytoplankton on the cycling of nitrogen in non-turbid estuaries, however it is important to stress that heterotrophic bacteria and grazers also play an important role.

Further work

- The impact of phytoplankton growth on the nitrogen fluxes through estuaries could be improved by combining the direct measurements of nitrogen uptake with a mass balance approach and a coupled hydrodynamic/biogeochemical model. In this way, by analysing global inputs and sinks within a system over appropriate time scales, the effect of phytoplankton activity can be comparatively evaluated.

- In a system like the Southampton Water estuary, where the availability of light throughout the water column is known to play an important role in controlling the blooming of phytoplankton, it would be very useful to have a better understanding of the effects of irradiance on the uptake of nitrogen. Data generated during this research (*i.e.* uptake at different light levels) represents a source of information that can be used to evaluate the irradiance *vs* nitrogen uptake interactions.

APPENDICES

Appendix A

Analytical methods

Additional information regarding the analytical protocols described in the Methods chapter is presented in the following appendices. Detailed description of protocols commonly used within SOES/SOC labs and within the oceanographic scientific community can be found in several works (*e.g.* Hydes, 1984; Hydes & Wright, 1999). The information below is a brief description of the procedures (based on the cited works, Ch. 2) adopted to suit the requirements of this research. Examples of typical calibration results are also presented as reference material.

A.0.1 Nitrate, phosphate and silicate analysis

Calibration curves and sample data were obtained by measuring the peak heights from the chart recorder of the nutrient autoanalyser used (Ch. 2, subsection 2.4.1.2.). Examples of calibration curves obtained for nitrate, phosphate and silicate analysis are presented in Fig. A.1. Sample concentration data was calculated by relating the peak-heights produced

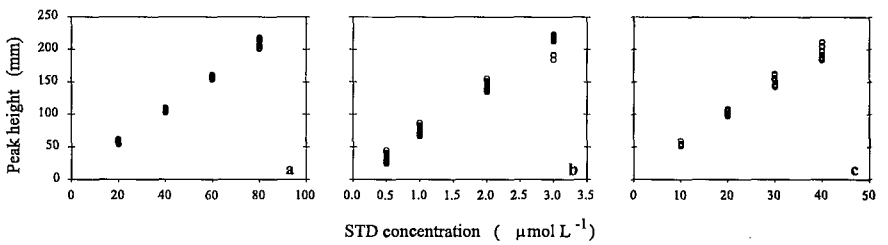

Figure A.1: Examples of calibration curves for nitrate (**a**), phosphate (**b**) and silicate (**c**) analysis. Each data point in the graph represents a different calibration curve; *i.e.* carried out on different dates.

by the standards to their respective concentration value. A linear regression was then obtained and the equation produced (Eq. A.1) modified (*i.e.* to obtain x) in order to calculate concentration values out of peak height values.

$$y = mx \pm b \tag{A.1}$$

Where y (the dependent variable) represents the height of the peaks, m (the slope) represents the height to concentration ratio, x (the indepentend variable) is the standard concentration (otherwise the sample concentration) and b (the intercept) is an 'estimation' of the blank.

NB: Sample concentrations of most variables (*i.e.* dissolved inorganic and organic nutrients, and particulate nitrogen and carbon) analysed during this research were calculated in a similar way; *i.e.* using the relation of the absorbance/fluorescence/peak-areas to the calibration standard-concentration. However, since all data was corrected for the analytical blank, the calculations were done using only the value of the slope (*i.e.* the value of the intercept was not considered).

A.0.2 Ammonium analysis in estuarine water samples

As described in chapter 2, subsection 2.4.1.3, ammonium free Milli-Q water was used for the preparation of reagents, standards and blanks. Measurements in samples, blanks and standards were done in four replicates. All glassware used was acid-washed with 10% HCl.

Calibration curve: a 1 mM stock standard solution was prepared by dissolving 0.066 g of analytical grade ammonium sulphate ($(NH_4)_2SO_4$) in 1 L of ammonium free water. From this solution a concentration range of 1.0, 2.5, 5.0, 7.5 and 10 μmol L^{-1} was prepared to produce the calibration curve. Ammonium free water was prepared daily by passing Milli-Q water through a glass column filled with 100 g of a cation exchange resin. The cation exchange resin was charged by running through 100 mL of 10% HCl. The water was collected once the pH was >5.5 and was kept in an airtight glass bottle. Typical calibration curves for the colorimetric and fluorescent method are shown in Fig. A.2.

Preparation of reagents:

- *Phenol Solution*; 10 g of phenol were dissolved in 100 mL of 95% v/v ethanol (under a fume cupboard).
- *Sodium nitroprusside* ($Na_2[Fe(CN)_5NO]\cdot 2H_2O$) *solution*; 1 g of sodium nitroprusside was dissolved in 200 mL of Milli-Q water and stored in a dark glass bottle. This solution is stable for at least 1 month.
- *Alkaline reagent*; 100 g of Sodium citrate and 5 g of Sodium hydroxide were dissolved in 500 mL of Milli-Q water. This solution is stable indefinitely.
- *Sodium hypochlorite solution* (NaClO); Sodium hypochlorite solution (Sigma) with

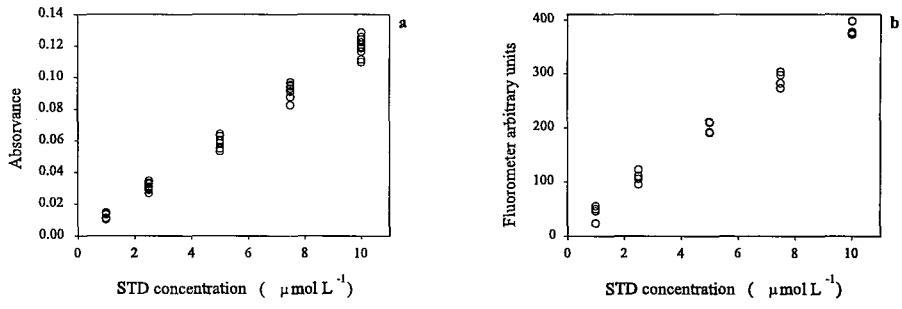

Figure A.2: Examples of calibration curves for ammonium analysis using a colorimetric method (**a**) and a fluorescence method (**b**). Each data point on the graph represents a different calibration curve; *i.e.* carried out on different dates.

10-13% available chlorine (*i.e.* 2.8-3.7 M) was used. The available chlorine of the solution was tested weekly as follows[1]:

1) 0.92 g of Sodium thiosulphate ($Na_2S_2O_3$) were dissolved in 50 mL of Milli-Q water (*i.e.* 0.1 M solution). *2)* 0.5 g of Potassium iodide (KI) were dissolved in 50 mL of a 0.5 M sulphuric acid solution (1.38 mL of concentrated, 98% H_2SO_4 in 50 mL of Milli-Q water). *3)* The later solution was then poured into a 100 mL Pyrex-glass beaker just after 1 mL of sodium hypochlorite solution was pipetted into it. *4)* The liberated iodine was thus titrated with the thiosulphate solution; 1 mL of thiosulphate solution $\simeq$ 0.1 mmol (1.77 mg) of positive monovalent chlorine (*i.e.* 3.54 mg of available chlorine). *5).* The hypochlorite solution was discarded whenever $\leqslant$10 mL of the thiosulphate solution were enough to titrate all the liberated iodine.

- *Oxidising solution*; the alkaline reagent and the sodium hypochlorite solution are mixed in a 4:1 proportion. This mixed reagent was kept stoppered while not in use and prepared fresh every day.

Experimental procedure:

- 2 mL of phenol solution was added to 50 mL of sample (once the phenol solution has been added, the samples can be stored in a refrigerator for up to 2 weeks).

- 10 mL of the sample were pipetted into a glass vial and *1)* 0.4 mL of phenol were added to 10 mL of standards and blanks, and mixed. *2)* 0.4 mL of Sodium nitroprusside solution were then added (to standards, blanks and samples) and mixed. *3)* 1 mL of the oxidising solution was added afterwards and mixed. *4)* The vials were allowed then to stand at room temperature (20-27 °C) for 2 hr in the dark. All vials were covered with parafilm. The coloured sample is stable for 24 hr after the reaction

[1]This method is based on the procedure described by Hansen & Koroleff (1999).

period. *5)* The absorbance was thus measured at 640 nm in a spectrophotometer using a 4 cm length cell and was finally blank corrected.

A.0.3 Determination of urea in estuarine water samples

The information below is additional to that presented in Ch. 2, subsection 2.4.1.4. Lab glassware and glass sample collection bottles were used, since plastic containers may produce interference. Reagents were prepared with UV irradiated Milli-Q water in order to minimise contamination with dissolved organics.

Calibration curve: 0.06 g of analytical grade Urea ($CO(NH_2)_2$) were dissolved in 500 mL UV irradiated Milli-Q water in order to produce a 2 mM stock solution. The calibration curve was prepared with a blank of UV irradiated Milli-Q water, and standard concentrations of 2, 4, 6, 8, and 10 μmol L^{-1}. The standards were prepared by pipetting 100, 200, 300, 400, 500 μL aliquots of the stock solution into 100 mL volumetric flasks, and making them up to 100 mL with UV irradiated Milli-Q water. Typical calibration curves of urea analysis are shown in Fig. A.3.

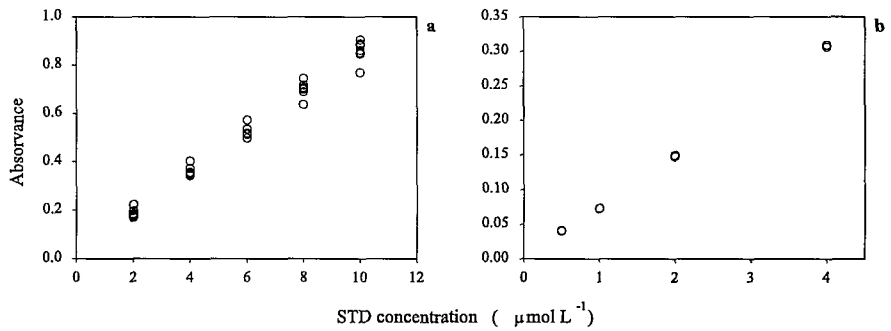

Figure A.3: Examples of calibration curves for urea analysis; large calibration range (**a**) and a short calibration range (**b**). Each data point on the graph represents a different calibration curve; *i.e.* carried out on different dates.

Preparation of reagents:

1. *Diacetylmonoxime* ($C_4H_7NO_2$) *solution*; 8.5 g were dissolved in 250 mL of UV irradiated Milli-Q water.

2. *Thiosemicarbazide* ($NH_2CSNHNH_2$) *solution*; 0.95 g were dissolved in 100 mL UV irradiated Milli-Q water.

3. *Sulphuric acid* (H_2SO_4) *solution*; 300 mL of concentrated sulphuric acid were diluted to 535 mL with UV irradiated Milli-Q water.

4. *Ferric chloride* ($FeCl_3$) *solution*; 0.15 g were dissolved in 10 mL UV irradiated Milli-Q water.

Working reagents:

- *Reagent A (mixture);* In a separate container (*e.g.* a Pyrex beaker), the diacetylmonoxime and thiosemicarbazide solutions were mixed in a 25 to 1 ratio.
- *Reagent B (mixture);* In a separate container (as above), the sulphuric acid and ferric chloride solutions were mixed in a 1070 to 1 ratio.

Experimental procedure:

- 10 mL of sample, standard or blank were pipetted (in three replicates) into glass vials.
- 0.7 mL of reagent A were added and mixed.
- 2.3 mL of Reagent B were added and mixed.
- Samples were left to react at ambient temperature in the dark (in racks inside a dark plastic box) for 72 hours. The absorbance was then measured in a spectrophotometer at 520 nm. While measuring the absorbance of one sample, the others were kept in the dark.

A.0.4 TDN analysis

The following information is additional to that presented in Ch. 2, subsection 2.4.1.5. An example of calibration data for total dissolved nitrogen (TDN) analysis is presented in Fig. A.4. Sample concentrations were calculated as described in Appendix A.0.1.

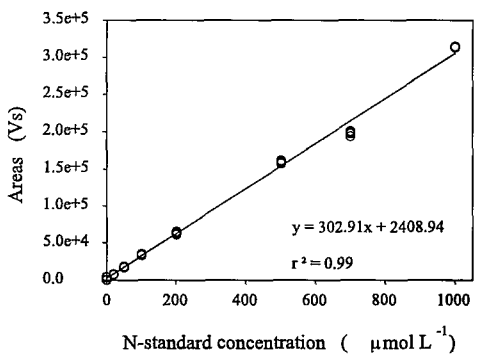

Figure A.4: Example of a calibration curve for TDN analysis. Data points are replicate N-standard masurements (4) of a given concentration.

A.0.5 Mass spectrometry

As described in subsection 2.4.2, Ch. 2, several compounds were used as standards during the mass spectrometric analyses. All different compounds produced similar results. Fig. A.5 and Fig. A.6 are a 'summary' of calibrations run on different dates, which include results produced by the different compounds. The graphics are intended as reference only. Calculation of particulate nitrogen and carbon of a given date were calculated with the calibration produced on that same date. Calculations were done as described in Appendix A.0.1. However, it is worth noting that these figures suggest that the mass spectrometric calibrations were reproducible throughout the analyses period (02 February-22 March, 2004). The reproducibility of atom% measurements was tested by analysing

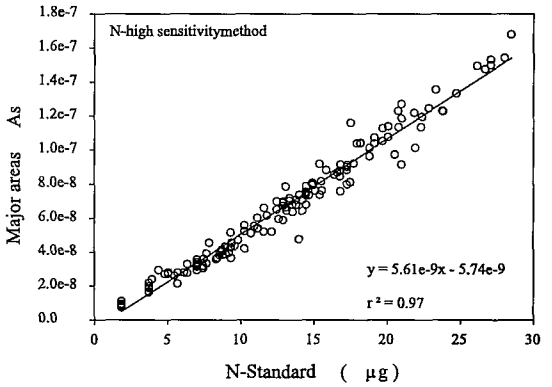

Figure A.5: Linear regression fit of all calibration data, N-high sensitivity method (n=153).

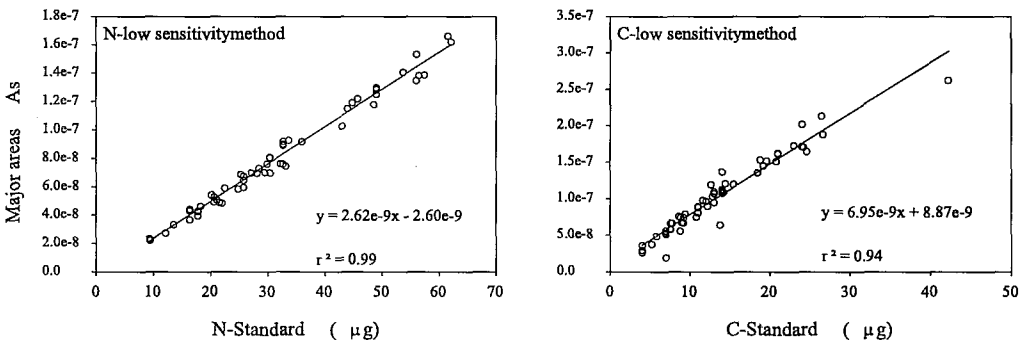

Figure A.6: Linear regression fits of all calibration data, N & C-low sensitivity method (n=61 and n=59 for nitrogen and carbon data respectively).

different amounts of ^{15}N-labelled and non-labelled N-standards. Results are shown in Fig. A.7. Linearity of ^{15}N-labelled ammonium sulphate at different atom% enrichments was also tested. Different amounts of standards labelled at a given atom% were analysed. Results are presented in Table A.1 and Fig. A.8.

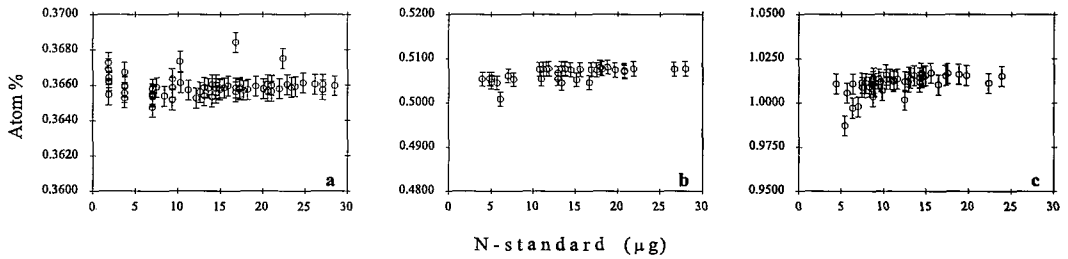

Figure A.7: Atom percent measurements of different amounts of ^{15}N-natural abundance (~0.3663%) and ^{15}N-labelled standards: **a**) non-labelled urea (mean = 0.3659±0.0006, n = 73); **b**) 0.5% labelled ammonium sulphate (mean = 0.5065±0.0016, n = 33); **c**) 1.0% labelled ammonium sulphate (mean = 1.0110±0.0057, n = 46).

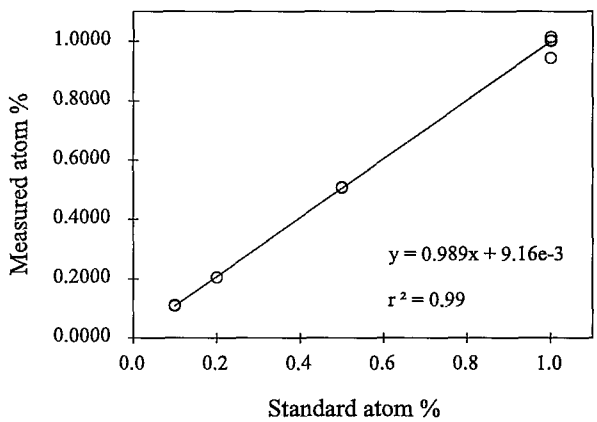

Figure A.8: Atom % linear regression fit of ^{15}N-labelled standards. Data is presented in table A.1.

Blank correction: subtraction of the analytical blank from the atom% measurements is important when the amount of nitrogen in the samples is relatively small. This is particularly true when calculating the ^{15}N-atom percent excess (at%$_{XS}$) of the samples. Fig. A.9 shows the effect of the blank relative to the size of the sample. % Difference in at%$_{XS}$ on the 'y' axis of the figure is given by,

$$\%Difference = \left(\frac{\text{at}\%_{XS(BLK)} - \text{at}\%_{XS}}{\text{at}\%_{XS}} \right) \times 100 \qquad \text{(A.2)}$$

where at%$_{XS(BLK)}$ is the blank corrected ^{15}N atom percent excess of the sample and at%$_{XS}$ is the measured atom percent excess of the sample (*i.e.* not blank corrected). The same applies for ^{13}C measurements (data not shown). All calibration standards prepared using GF/F filters were also blank corrected.

Table A.1: Atom% measurements of different amounts of ^{15}N-labelled standards.

N (μg)	Std atom%	Measured atom%
83.4	0.1	0.1078
73.4	0.1	0.1087
91.9	0.1	0.1083
103.7	0.2	0.2040
82.6	0.2	0.2041
74.7	0.2	0.2046
160.3	0.5	0.5048
99.3	0.5	0.5074
103.1	0.5	0.5078
78.3	1.0	1.0005
79.2	1.0	1.0023
131.1	1.0	0.9432
66.7	0.1	0.1107
85.9	0.1	0.1086
97.0	0.1	0.1089
141.2	0.2	0.2045
95.5	0.2	0.2042
103.3	0.2	0.2046
162.8	0.5	0.5078
118.3	0.5	0.5081
116.4	0.5	0.5080
67.5	1.0	1.0135
64.8	1.0	1.0139
62.4	1.0	1.0136

Analitical grade ^{15}N-labeled ammonium sulphate ($(^{15}NH_4)_2SO_4$) was used as standard.

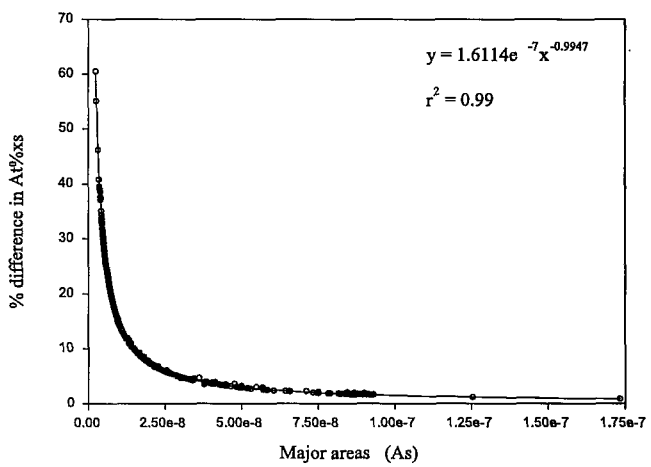

Figure A.9: Percent difference between blank corrected and not-blank corrected at%$_{XS}$ of samples from ^{15}N incubation experiments (results from the N-high sensitivity method are shown; n = 600). In this research most samples were <5.00e-8 As (5.00e-8 $\approx$ 0.713 μmol-N $\approx$ 9.98 μg-N).

Appendix B

Chapters 3 and 4.

B.0.6 Results: productive spring-summer period in 2001 and 2002

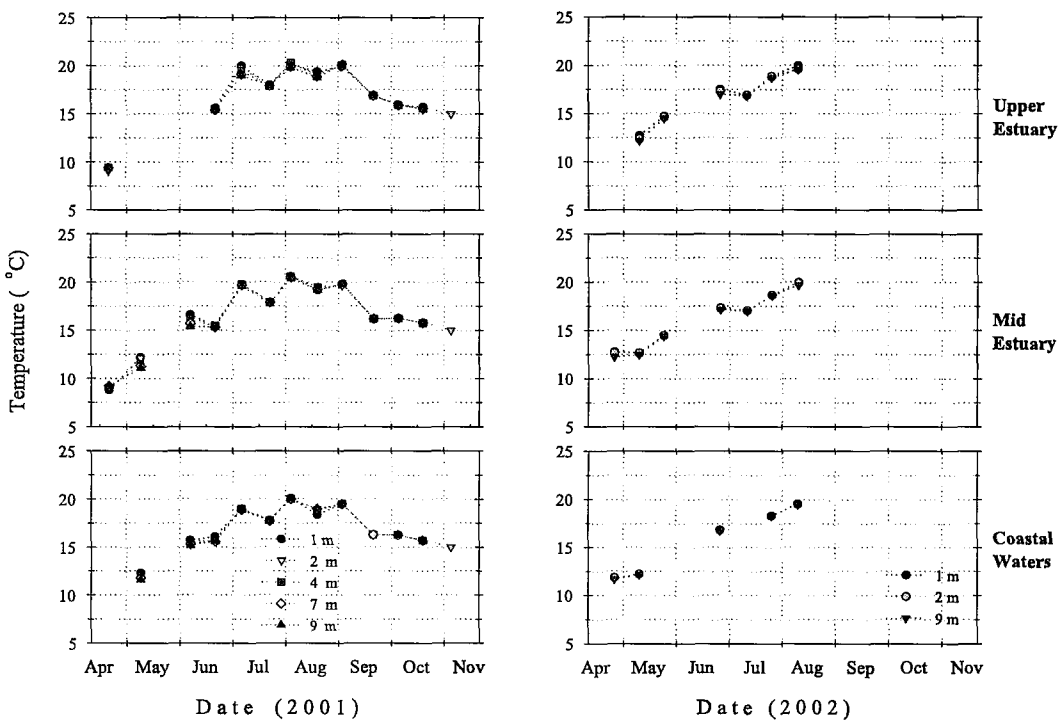

Figure B.1: **Temperature;** vertical, spatial and temporal distribution during 2001 and 2002 within Southampton Water estuary. Symbols in lower panels apply to all panels.

B.0.7 Irradiance data manipulation

Incident irradiance data was obtained from the SOC Met-Station on top of Node 3 in charge of Dr. Joanna Waniek. The station is ~100 m from the pontoon and within a

distance of ~10 km from furthest sampling sampling station (Calshot navigation buoy, coastal waters). The data is available within the SOES/SOC network as *total hourly solar energy* (kJ m^{-2} h^{-1}). For consistency with plant science and N-uptake related research (*e.g.* Cochlan *et al.*, 1991; Kirk, 1994; Falkowski & Raven, 1997; Lalli & Parsons, 1997; Bury *et al.*, 2001), solar energy was transformed to *photosynthetically active radiation* (PAR) with dimensions of μmol m^{-2} s^{-1}. The calculation was done using the following conversions,

- PAR $\approx$ 43% of the total solar energy[1]
- 1 J s^{-1} = 1 W
- 1 W = 4.16 μmol m^{-2} s^{-1}
- 1 mole $\equiv$ 1 quanta $\equiv$ 1 E $\equiv$ 6.022×10^{23}

where the symbols represent *joules* (J), *watts* (W) and *einsteins* (E); designating Avogadro's number of photons.

The irradiance *attenuation coefficient* was calculated using logged data from *in situ* PAR measurements and solving for k from the expression describing the downwelling irradiance (Eq. B.1); *i.e.* Beer-Lambert's law.

$$E_z = E_o e^{-kz} \tag{B.1}$$

to yield

$$k = \frac{1}{z} \cdot ln\left(\frac{E_o}{E_z}\right) \tag{B.2}$$

where E_z and E_o are respectively, the *downwelling* and *surface incident* irradiance (μmol m^{-2} s^{-1}), k is the *attenuation coefficient* (m^{-1}) and z is the *depth* (m) (*i.e.* Lalli & Parsons, 1997). In practice, k was calculated as the slope obtained from a linear regression fit between $ln(\frac{I_o}{I_z})$ and z, as the independent (*i.e.* x) and dependent (*i.e.* y) variables, respectively.

The *mean water column irradiance* was calculated as

$$\bar{E}_z = \frac{I_o}{kz}(1 - e^{-kz}) \tag{B.3}$$

where $\bar{E}_z$ represents the mean water column PAR (*e.g.* Riley, 1957; Peperzak, 1993; Lalli & Parsons, 1997) with dimensions of μmol m^{-2} s^{-1}, and the other terms are as previously defined.

[1] Joanna Waniek *pers., com.*, 2001, School of Ocean and Earth Science, Southampton Ocenography Centre, University of Southampton.

B.0.8 Water column integration of net N-uptake and PP rates

Nitrogen and carbon net uptake rates (ρ) were integrated throughout the euphotic water column from the depth (z) of 100% of subsurface PAR (just below the surface) down to the depth of 1% of subsurface PAR using the method of the *trapezoid sum*, Eq. B.4.

$$\frac{1}{2}\sum_{i=1}^{n}(\rho_i + \rho_{i+1}) \cdot (z_{i+1} - z_i) \tag{B.4}$$

The depths of the 50, 10 and 1% of subsurface PAR were estimated for each sampling station by solving for z from Eq. B.1 (previous subsection) using the respective k values and 4 h-averaged (*i.e.* the tracer incubation time) E_0 and E_z data.

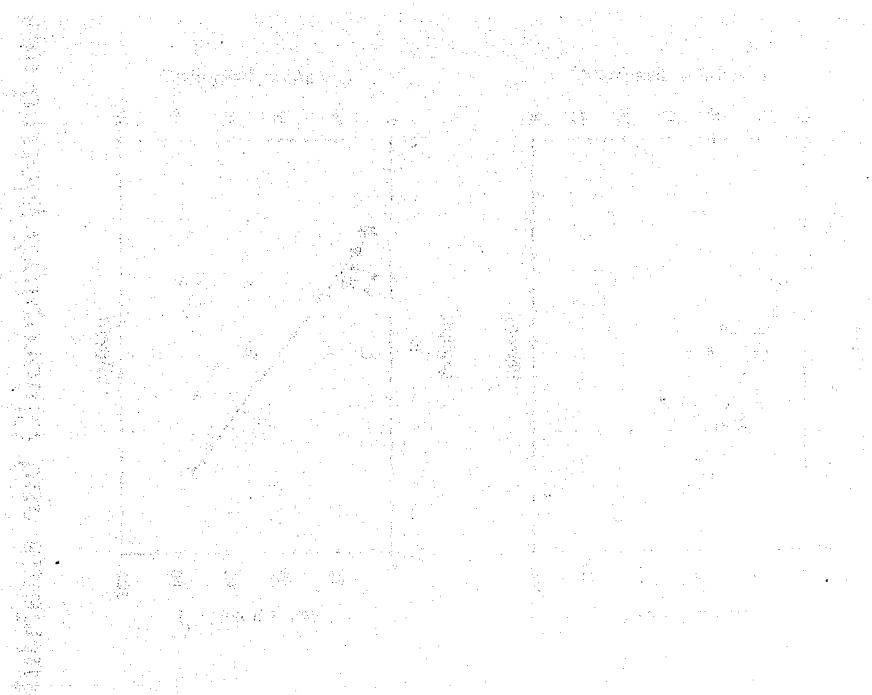

B.0.9 Nutrients and Chlorophyll plotted against salinity

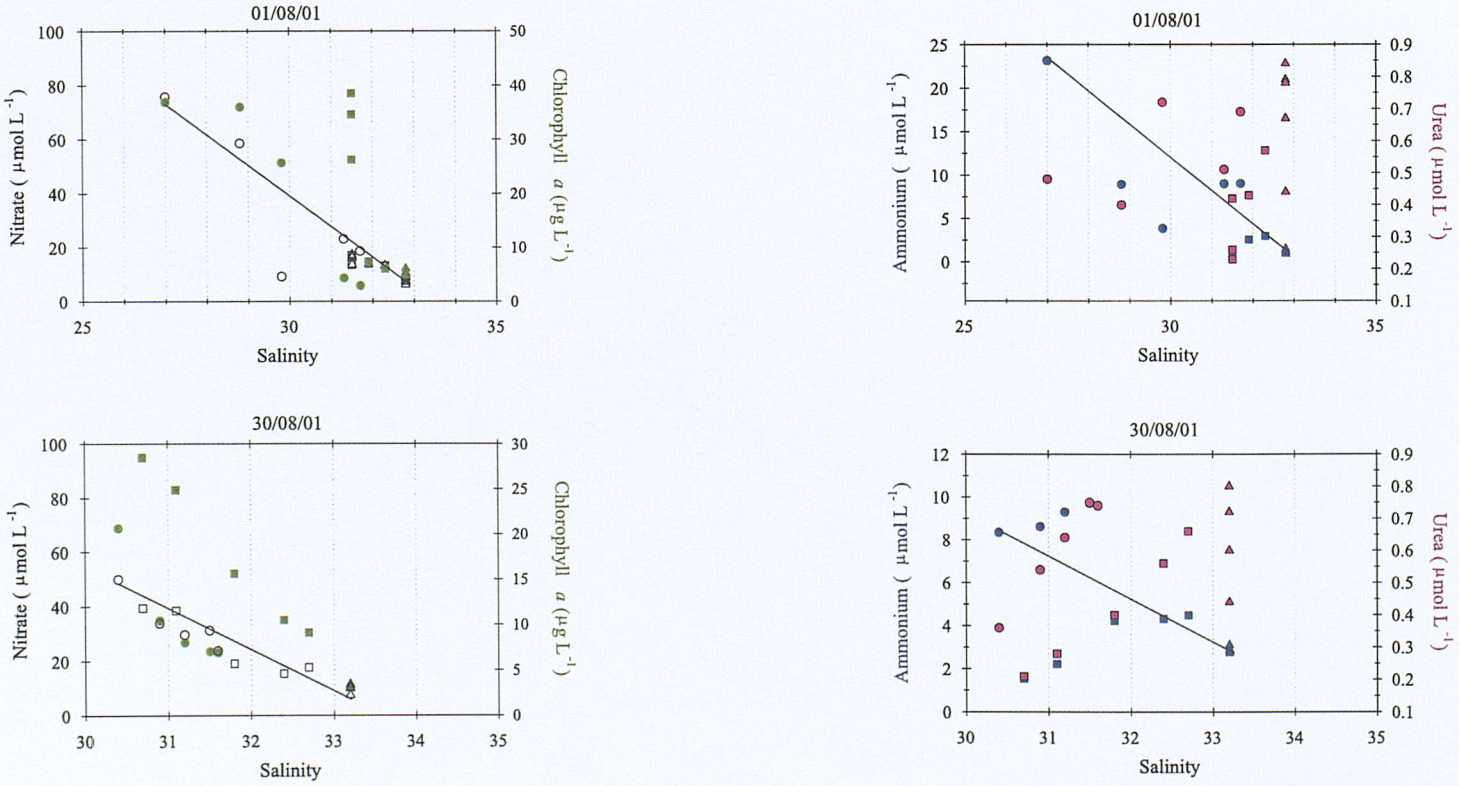

Figure B.2: **Nitrate, chlorophyll *a*, ammonium and urea plotted against salinity (examples).** The data shown correspond to measurements carried out on the 01 and 30-August 2001. Symbols represent the upper estuary (circles), the mid estuary (squares) and the coastal waters (triangles). Data include values from the five depths sampled (*i.e.* 1, 2, 4, 7 and 9 m). Note different salinity scales between upper and lower panels.

B.0.10 Irradiance in 2002

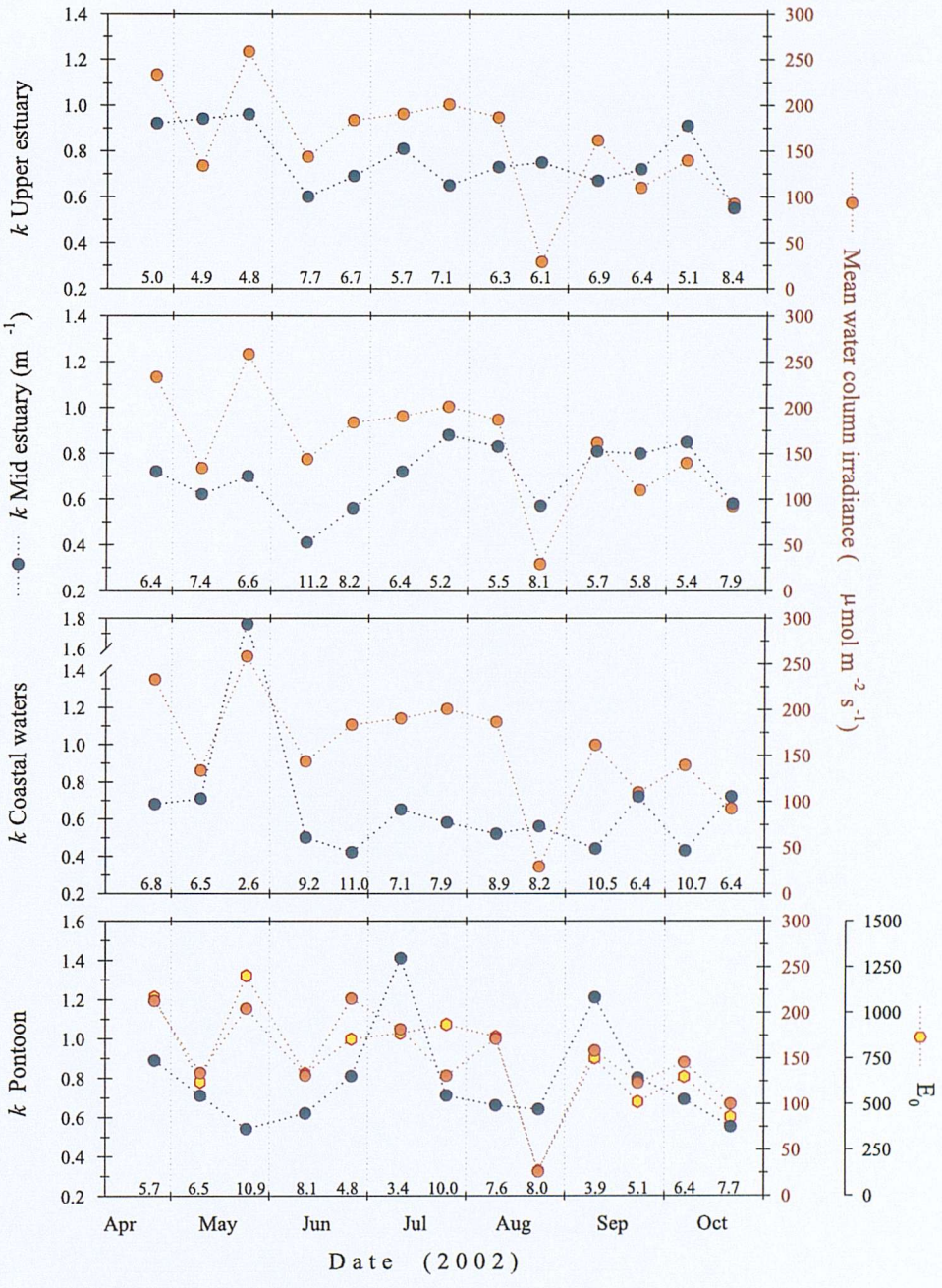

Figure B.3: **Attenuation coefficient (k) and mean water column irradiance at the three sampling stations and at the pontoon.** The incident irradiance (E_o) is shown in the lower panel. Numbers at the bottom of each panel are the depth (m) of the 1% of subsurface PAR.

B.0.11 Changes in nutrient concentration during the incubation period

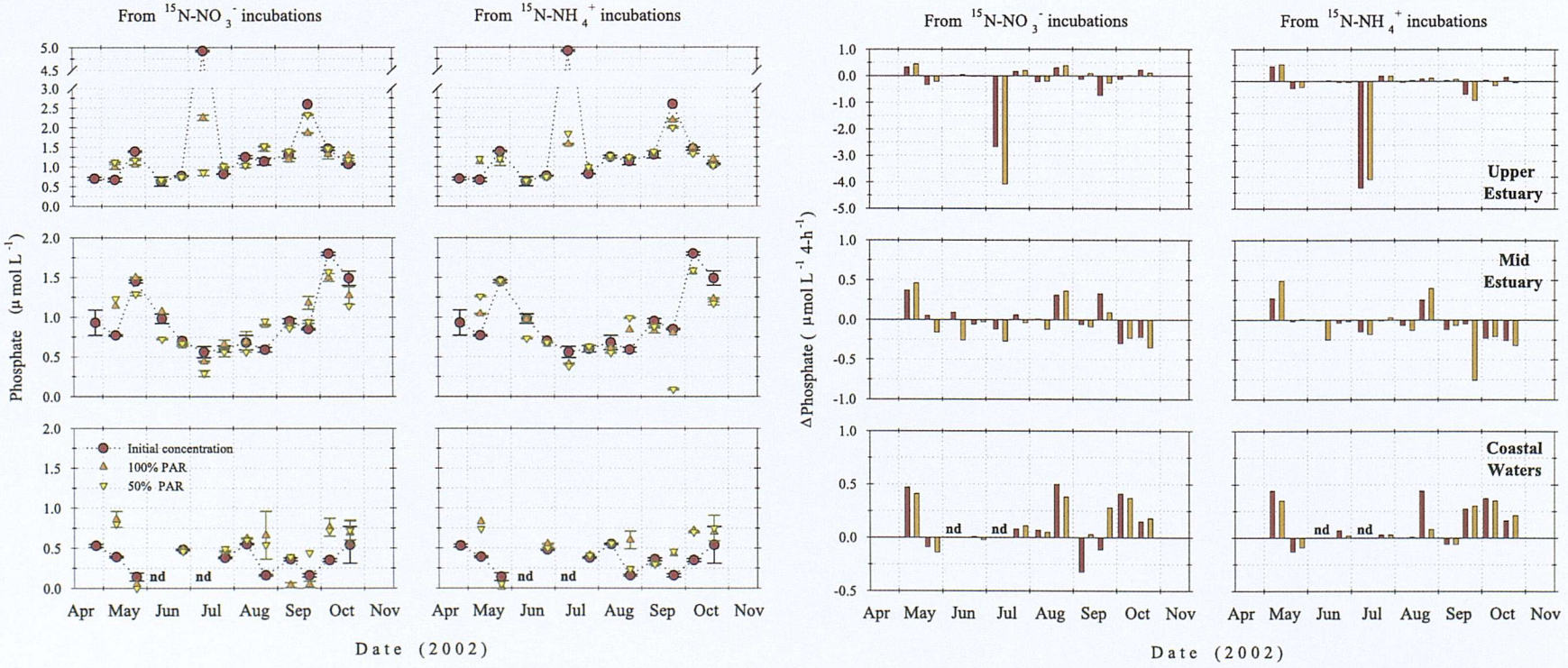

Figure B.4: **Phosphate concentration changes during the incubation period.** Left set of panels show phosphate concentrations measured from incubations deployed at 100 and 50% of subsurface PAR relative to the phosphate measured before the incubation (original), both from incubations with ^{15}N-NO_3^- and with ^{15}N-NH_4^+. Error bars represent the standard deviation of replicate (n=3) measurements. Right set of panels show Δ-phosphate (*i.e.* concentrations measured at the end of incubation minus original concentration), from incubations deployed at both PAR levels and from both ^{15}N-treatments. Note different y axis scales (nd = no data available).

References

Ali, E. M. (2003) Processes and Conditions Influencing Phytoplankton Growth and Bloom Initiation in a Macrotidal Estuary, Southampton Water. Ph.D. thesis, Graduate School of Ocean and Earth Science, Southampton Oceanography Centre, University of Southampton. 221 pp.

Álvarez Salgado, X. A. & A. E. J. Miller (1998) Simultaneous determination of dissolved organic carbon and total dissolved nitrogen in seawater by high temperature catalytic ixidation: conditions for precise shipboard measurements. *Marine Chemistry*, 62:325–333.

Aminot, A. (1983) Éléments nutritifs minéreaux dissous. In: Aminot, A. & M. Chaussepied (eds.), Manuel des analyses chimiques en milieu marin, chap. 6, pp. 93–150. Centre National pour l'Exploitation des Océans.

Aminot, A. & R. Kérouel (1982) Dosage automatique de l'urée dans l'eau de mer: une méthod très à la diacétylmonoxime. *Canadian Journal of Fisheries and Aquatic Science*, 39:174–183.

Aminot, A., D. S. Kirkwood & R. Kérouel (1997) Determination of ammonia in seawater by the indophenol-blue method: evaluation of the ICES NUTS I/C5 questionnaire. *Marine Chemistry*, 56:59–75.

Anderson, D. M. (2001) Phytoplankton Blooms. In: Steele, J. H., S. A. Thorpe & K. K. Turekian (eds.), Encyclopedia of Ocean Sciences, pp. 2179–2192. Academic Press, San Diego, CA.

Anderson, L. G., D. R. Turner, M. Wedborg & D. Dyrssen (1999) Determination of total alkalinity and total dissolved inorganic carbon. In: Grassgoff, K., K. Kremling & M. Ehrhardt (eds.), Methods of seawater analysis, chap. 8, pp. 127–148. WILEY-VCH, 3rd ed.

Anderson, L. G. & M. Wedborg (1985) Comparison of potentiometric and photometric titration methods for the determination of alkalinity and total carbonate in seawater. *Oceanologica Acta*, 8(4):479–483.

Ashe, C. (1996) Spatial and Temporal distribution of dissolved urea in the rivers Test, Itchen and Southampton Water between May 1995 and February 1996. B. Sc. Thesis, School of Ocean and Earth Science, Southampton Oceanography Centre, University of Southampton, 66 pp.

Balls, P. W. (1994) Nutrient inputs to estuaries from nine Scottish East Coast Rivers; influence of estuarine processes on inputs to the North Sea. *Estuarine, Coastal and Shelf Science*, 39(4):329–352.

Balls, W., N. Brockie, J. Dobson & W. Johnston (1996) Dissolved oxygen and nitrification in the upper Forth Estuary during summer (1982-92): patterns and trends. *Estuarine, Coastal and Shelf Science*, 42:117–134.

Beale, R. N. & D. Croft (1961) A sensitive method for the colorimetric determination of urea. *Journal of Clinical Pathology*, 14:418–424.

Benner, R., B. V. Bodungen, J. Farrington, J. Hedges, C. Lee, F. Mantoura, Y. Suzuki & P. M. Williams (1993) Measurement of dissolved organic carbon and nitrogen in natural waters: workshop report. *Marine Chemistry*, 41:5–10.

Berg, G. M., P. M. Glibert, M. W. Lomas & M. A. Burford (1997) Organic nitrogen uptake and growth by the chrysophyte *Aureococuus anophagefferens* during brown tide event. *Marine Biology*, 129:377–387.

Berman, T., C. Béchemin & S. Y. Maestrini (1999) Release of ammonium and urea from dissolved organic nitrogen in aquatic ecosystems. *Aquatic Microbial Ecology*, 16:295–302.

Berman, T. & D. A. Bronk (2003) Dissolved organic nitrogen: a dynamic participant in aquatic ecosystems. *Aquatic Microbial Ecology*, 31:279–305.

Blackburn, T. H. (1979) Method for measuring rates of NH_4^+ turnover in anoxic marine sediments, using a ^{15}N-NH_4^+ dilution technique. *Applied and Environmental Microbiology*, 37:760–765.

Boss, S. (1996) A comparison between pCO_2 and dissolved oxygen in the Test, Itchen and Southampton Water estuaries. Master's thesis, Department of Oceanography, Faculty of Science, University of Southampton. 65 pp.

Bronk, D. A. (1999) Rates of NH_4^+ uptake, intracellular transformation and dissolved organic nitrogen release in two clones of marine *Synechococcus* spp. *Journal of Plankton Research*, 21(7):1337–1353.

Bronk, D. A. (2002) Dynamics of DON. In: Hansell, D. A. & C. A. Carlson (eds.), Biogeochemistry of marine dissolved organic matter, chap. 5, pp. 153–247. Accademic Press. USA.

Bronk, D. A. & P. M. Glibert (1991) A ^{15}N tracer method for the measurement of dissolved organic nitrogen release by phytoplankton. *Marine Ecology Progress Series*, 77:171–182.

Bronk, D. A. & P. M. Glibert (1993a) Aplication of a ^{15}N tracer method to the study of dissolved organic nitrogen uptake during spring and summer in Chesapeake Bay. *Marine Biology*, 115:501–508.

Bronk, D. A. & P. M. Glibert (1993b) Contrasting patterns of dissolved nitrogen release by two size fractions of estuarine plankton during a periond of rapid NH4+ consumption and NO2- production. *Marine Ecology Progress Series*, 96:291–299.

Bronk, D. A., P. M. Glibert, T. C. Malone, S. Banahan & E. Sahlsten (1998) Inorganic and organic nitrogen cycling in Chesapeake Bay: autotrophic heterotrophic processes and relationships to carbon flux. *Aquatic Microbial Ecology*, 15:177–189.

Bronk, D. A., P. M. Glibert & B. B. Ward (1994) Nitrogen uptake, dissolved organic nitrogen release, and new production. *Science*, 265:1843–1846.

Bronk, D. A., M. W. Lomas, P. M. Glibert, K. J. Schukert & M. P. Sanderson (2000) Total dissolved nitrogen analysis: comparisons between persulfate, UV and High temperature oxidation methods. *Marine Chemistry*, 69:163–178.

Bronk, D. A. & B. B. Ward (1999) Gross nitrogen uptake and DON release in the euphotic zone of Monterey Bay, California. *Limnology and Oceanography*, 44(3):573–585.

Bronk, D. A. & B. B. Ward (2000) Magnitude of dissolved organic nitrogen release relative to gross nitrogen uptake in marine systems. *Limnology and Oceanography*, 45(8):1879–1883.

Burris, R. H. & C. E. Miller (1941) Application of N15 to the study of biological nitrogen fixation. *Science*, 93(2405):114–115.

Bury, A. J., N. Owens & T. Preston (1995) ^{13}C and ^{15}N uptake by phytoplankton in the marginal ice zone of the Bellingshausen Sea. *Deep-Sea Research Part II*, 42(4-5):1225–1252.

Bury, S. J., P. W. Boyd, T. Preston, G. Savidge & N. J. P. Owens (2001) Size-fractionated primary production and nitrogen uptake during a North Atlantic phytoplankton bloom: implications for carbon export estimates. *Deep-Sea Research Part I*, 48:689–720.

Butcher, S. S. (1992) Equilibrium, Rate, and Natural Systems. In: Butcher, S. S., R. J. Charlson, G. H. Orians & G. V. Wolfe (eds.), Global Biogeochemical Cycles, chap. 5. Academic Press LTD.

Caperon, J., D. Schell, J. Hirota & E. Laws (1979) Ammonium excretion in Kaneohe Bay, Hawaii, measured by 15N isotope dilution technique. *Marine Biology*, 54:33–40.

Capone, D. G., J. P. Zher, H. W. Paerl, B. Bergman & E. J. Carpenter (1997) Trichodesmium, a globally significant marine cyanobacterium. *Science*, 276:1221–1229.

Carpenter, E. J. & S. Dunham (1985) Nitrogenous nutrient uptake, primary production, and species composition of phytoplankton in the Carmans River estuary, Long Island, New York. *Limnology and Oceanography*, 30(3):513–526.

Cebrián, J. & I. Valiela (1999) Seasonal patterns in phytoplankton biomass in coastal ecosystems. *Journal of Plankton Research*, 21(3):429–444.

Christian, G. D. (1994) Analytical Chemistry. JOHN WILEY AND SONS, INC, 5th ed., 812 pp.

Cloern, J. E. (1996) Phytoplankton bloom dynamics in coastal ecosystems: a review with some general lessons from sustained investigation of San Francisco Bay, California. *Reviews of Geophysics*, 34(2):127–168.

Cloern, J. E. (2001) Our evolving conceptual model of the coastal eutrophication problem. *Marine Ecology Progress Series*, 210:223–253.

Cochlan, W. P. (1986) Seasonal study of uptake and regeneration of nitrogen on the Scotian Shelf. *Continental Shelf Research*, 5:555–577.

Cochlan, W. P., P. J. Harrison & K. L. Denman (1991) Diel periodicity of nitrogen uptake by marine phytoplankton in nitrate-rich environments. *Limnology and Oceanography*, 36(8):1689–1700.

Cohen, J. E., C. small, A. Mellinger, J. Gallup & J. Sachs (1997) Estimates of coastal populations. *Science*, 278:1211–1212.

Conley, D. J., C. L. Schelske & E. F. Stoermer (1991) Modification of the biogeochemical cycle of silica with eutrophication. *Marine Ecology Progress Series*, 101:179–192.

Copin-Montégut, G. (1996) Chimie de l'eau de mer, chap. 6: Le système des carbonates, pp. 165–213. Institut océanographique, Paris.

Costanza, R., R. d'Arge, R. de Groot, S. Farber, M. Grasso, B. Hannon, K. Limburg, S. Naeem, R. V. O'Neill, J. Paruelo, R. G. Raskin, P. Sutton & M. van den Belt (1997) The value of the world's ecosystem services and natural capital. *Nature*, 387:253–260.

Crawford, D. W. (1992) The Physiological Ecology of the Red-Water Ciliate *Mesodinium rubrum*. Ph.D. thesis, Faculty of Science, Department Oceanography, University of Southampton. 240 pp.

Crawford, D. W., D. A. Purdie, A. M. Lockwood & P. Weissman (1997) Recurrent red tides in the Southampton Water Estuary caused by the phototrophic ciliate *Mesodinium rubrum*. *Estuarine, Coastal and Shelf Science*, 45:799–812.

Culberson, C. H. & R. M. Pytkowicz (1973) Inonization of water in seawater. *Marine Chemistry*, 1:309–316.

Currie, L. A. (1997) Detection: International update, and some emerging di-lemmas involving calibration, the blank, and multiple detection decisions. *Chemometrics and Intelligent Laboratory Systems*, 37:151–181.

Del Amo, Y., O. L. Pape, P. Tréguer, B. Quéguiner, A. Ménesguen & A. Aminot (1997) Impacts of high-nitrate freshwater inputs on macrotidal ecosystems. I. Seasonal evolution of nutrient limitation for the diatom-dominated phytoplankton of the Bay of Brest (France). *Marine Ecology Progress Series*, 161:213–224.

DeManche, J. M., C. J. Herbert & C. Douglas (1973) An Automated Analysis for Urea in Seawater. *Limnology and Oceanography*, 18(4):686–689.

Dickson, A. G. (1990) Thermodynamics of the dissociation of boric acid in synthetic seawater from 273.15 to 318.15 °K. *Deep-Sea Research*, 37(5):755–766.

Dickson, A. G. & J. P. Riley (1979) The estimation of acid dissociation constants in seawater media from potentiometric titrations with strong base. I. The ionic product of water-K_W. *Marine Chemistry*, 7:89–99.

Dong, L. F., D. C. O. Thorton, D. B. Nedwell & G. J. C. Underwood (2000) Denitrification in sediments of the River Colne estuary, England. *Marine Ecology Progress Series*, 203:109–122.

Dortch, Q. (1990) The interaction between ammonium and nitrate uptake in phytoplankton. *Marine Ecology Progress Series*, 61(1-2):183–201.

Dugdale, R., V. Dugdale, J. Neess & J. Goering (1959) Nitrogen fixation in lakes. *Science*, 130(3379):859–860.

Dugdale, R. C. & J. J. Goering (1967) Uptake of new and regenerated forms of nitrogen in primary productivity. *Limnology and Oceanography*, 12:196–206.

Dugdale, R. C., D. W. Menzel & J. H. Ryther (1961) Nitrogen fixation in the Sargasso Sea. *Deep-Sea Research*, 7:297–300.

Dugdale, R. C. & F. Wilkerson (1986) The use of ^{15}N to measure nitrogen uptake in eutrophic oceans; experimental considerations. *Limnology and Oceanography*, 31(4):673–689.

Dyer, K. R. (1997) Estuaries: a physical introduction. John Willey and Sons Ltd, 2^{nd} ed., 195 pp.

Eppley, R. W. & B. J. Peterson (1979) Particulate organic matter flux and planktonic new production in the Deep ocean. *Nature*, 282:677–680.

Eppley, R. W., E. H. Renger & W. G. Harrison (1979) Nitrate and phytoplankton production in Southern California coastal waters. *Limnology and Oceanography*, 24(3):483–494.

Falkowski, G., R. J. Scholes, E. Boyle, J. Canadell, D. Canfield, J. Elser, N. Gruber, K. Hibbard, P. Högberg, S. Linder, F. T. Mackenzie, B. M. III, T. Pedersen, Y. Rosenthal, S. Seitzinger, V. Smetacek & W. Steffen (2000) The global carbon cycle; a test of our knowledge of Earth as a system. *Science*, 290:291–296.

Falkowski, P. G. & J. A. Raven (1997) Aquatic Photosynthesis. Blackwell Science, Ltd, 375 pp.

Fiedler, R. & G. Proksch (1975) The determination of nitrogen-15 by emission and mass spectrometry in biochemical analysis: a review. *Analytical Chimica Acta*, 78:1–62.

Fifield, F. W. (2000) Analytical environmental data: assessment and interpretation. In: Fifield, F. W. & P. J. Haines (eds.), Environmental Analytical Chemistry, p. 490. Blackwell Science Ltd. U.K.

Fisher, T. R. & E. B. Haines (1979) A comment on the calculation of atom percent enrichment for stable isotopes. *Limnology and Oceanography*, 24(3):593–595.

Fluck & Heumann (2002) Periodic table of the elements, with IUPAC recommendations 2002. WILEY-VCH GmbH and Co. KGaA, Weinheim, Germany, 3rd ed.

Fuhrman, J. (1990) Dissolved free amino acid cycling in an estuarine outflow plume. *Marine Ecology Progress Series*, 66:197–203.

Furnas, M. L. (1983) Nitrogen dynamics in lower Narragansett bay, Rhode Island. I. Uptake by size-fractionated phytoplankton populations. *Journal of Plankton Research*, 5:657–676.

Galloway, J. N. & E. B. Cowling (2002) Reactive Nitrogen and The World: 200 Years of Change. *Ambio*, 31(2):64–71.

Galloway, J. N., E. B. Cowling, S. P. Seitzinger & R. H. Socolow (2002) Reactive Nitrogen: Too Much of a Good Thing? *Ambio*, 31(2):60–63.

Galloway, J. N., W. H. Schlesinger, H. Levy H, A. Michaels & J. L. Schnoor (1995) Nitrogen fixation: Anthropogenic enhancement-environmental response. *Global Biogeochemical cycles*, 9(2):235–252.

Garcia, C. A. E., D. A. Purdie & I. S. Robinson (1993) Mapping a bloom of the photosynthetic ciliate *Mesodinium rubrum* in an estuary from airborne thematic data. *Estuarine, Coastal and Shelf Science*, 37:287–298.

Garside, C. (1981) Nitrate and ammonia uptake in the apex of the New York Bight. *Limnology and Oceanography*, 26:731–739.

Garside, C. & P. M. Glibert (1984) Computer modelling of ^{15}N uptake and remineralization experiments. *Limnology and Oceanography*, 29(1):199–204.

Gattuso, J. P., M. Frankignoulle & R. Wollast (1998) Carbon and carbonate metabolism in coastal aquatic ecosystems. *Annual Review of Ecology and Systematics*, 29:405–434.

Glibert, P. M. (1982) Regional studies of dialy, seasonal and size fraction variability in ammonium remineralizaton. *Marine Biology*, 70:209–222.

Glibert, P. M. (1988) Primary producivity and pelagic nitrogen cycling. In: Blackburn, T. H. & J. Sørensen (eds.), Nitrogen cycling in coastal marine environments, SCOPE 33, chap. Part I, Ch. 1, pp. 3–31. JOHN WILEY AND SONS.

Glibert, P. M. & D. G. Capone (1993) Mineralization and Assimilation in Aquatic, Sediment and Wet Land Systems. In: Knowles, R. & T. H. Blackburn (eds.), Nitrogen isotope techniques, chap. 9, pp. 243–272. Academic Press, New York.

Glibert, P. M. & C. Garside (1989) Discussion on "Spring recycling rates of ammonium in turbid continental shelf waters off the southeastern United States". *Continental Shelf Research*, 9(2):197–200.

Glibert, P. M. & C. Garside (1992) Diel variability in nitrogenous nutrient uptake by phytoplankton in the Chesapeake Bay plume. *Journal of Plankton Research*, 14(2):271–288.

Glibert, P. M., C. Garside, J. A. Fhurman & M. R. Roman (1991) Time-dependent coupling of inorganic nitrogen uptake and regeneration in the plume of the Chesapeake Bay estuary and its regulation by large heterotrophs. *Limnology and Oceanography*, 36(5):895–909.

Glibert, P. M., F. Lipschultz, J. J. McCarthy & M. A. Altabet (1982) Isotope dilution models of uptake and remineralization of ammonium by marine plankton. *Limnology and Oceanography*, 27(4):639–650.

Glibert, P. M., C. A. Miller, C. Garside, M. R. Roman & G. B. McManus (1992) NH_4^+ regeneration and grazing: interdependent processes in size-fractionated $^{15}NH_4^+$ experiments. *Marine Ecology Progress Series*, 82(5):895–909.

Goeyens, L., N. Kindermans, M. A. Yusuf & M. Elskens (1998) A room temperature procedure for the manual determination of urea in seawater. *Estuarine, Coastal and Shelf Science*, 47(415–418).

Goosen, N. K., J. Krompkamp, J. Peene, P. van Rijswijk & P. van Breugel (1999) Bacterial and phytoplankton production in the maximum turbidity zone of three European estuaries: the Elbe, Westerschelde and Gironde. *Journal of Marine Systems*, 22:151–171.

Grelowski, A., M. Astuszak, S. Sitek & Z. Witek (2000) Budget calculations of nitrogen, phosphorus and BODs passing through the Oder estuary. *Journal of Marine Research*, 25:221–237.

Grenz, C., J. M. Cloern, S. W. Hager & B. E. Cole (2000) Dynamics of nutrient cycling and related benthic nutrient and oxygen fluxes during a spring phytoplankton bloom in South San Francisco Bay (USA). *Marine Ecology Progress Series*, 197:67–80.

Hama, T., T. Miyasaki, Y. Ogawa, T. Iwakuma, M. Takahashi, A. Otsuki & S. Ichimura (1983) Measurement of photosynthetic production of a marine phytoplankton population using a stable ^{13}C isotope. *Marine Biology*, 73:31–36.

Hansen, H. P. & F. Koroleff (1999) Nutrient Analysis. In: Grasshoff, K., K. Kremling & M. Ehrhardt (eds.), Methods of seawater analysis, chap. 10, pp. 159–228. WILEY-VCH, Germany, 3rd, completely rev. and extended ed ed.

Harrison, W. G. (1973) Nirtate reductase activity during a dinoflagellate bloom. *Limnology and Oceanography*, 5:457–465.

Harrison, W. G. (1978) Experimental measurements of nitrogen remineralization in coastal waters. *Limnology and Oceanography*, 23(4):684–694.

Hasegawa, T., I. Koije & H. Mukai (2000a) Dissolved organic nitrogen dynamics in coastal waters and the effect of copepods. *Journal of Experimental Marine Biology and Ecology*, 244:219–238.

Hasegawa, T., I. Koije & H. Mukai (2000b) Estimation of dissolved organic nitrogen release by micrograzers in natural planktonic assemblages. *Plankton Biology and Ecology*, 47(1):23–30.

Hasegawa, T., I. Koije & H. Mukai (2000c) Release of dissolved organic nitrogen by size-fractionated natural planktonic assemblages in coastal waters. *Marine Ecology Progress Series*, 198:43–49.

Herbert, R. A. (1999) Nitrogen cycling in coastal marine ecosystems. *Federation of European Microbiological Societies, Microbiology Reviews*, 23:563–590.

Herman, P. M. J. & C. H. R. Heip (1999) Biogeochemistry of the Maximum TURbidity Zone of Estuaries (MATURE): some conclusions. *Journal of Marine Systems*, 22:89–104.

Hoch, M. P. & D. L. Kirchman (1995) Ammonium uptake by heterotrophic bacteria in the Delaware estuary and adjacent coastal waters. *Limnology and Oceanography*, 40(5):886–897.

Holley, S. E. & D. J. Hydes (2002) Ferry-boxes and data stations for improved monitoring and resolution of eutrophication-related processes: application in Southampton Water UK, a temperate latitude hypernutrified estuary. *Hydrobiologia*, 475/476:99–110.

Holligan, P. M. & H. de Boois (1993) Land-Ocean Interactions in the Coastal Zone. Science Plan. Tech. Rep. 25, IGBP Stockholm.

Holmes, R. M., A. Aminot, R. Kérouel, B. A. Hooker & B. J. Peterson (1999) A simple and precise method for measuring ammonium in marine and freshwater ecosystems. *Canadian Journal of Fisheries and Aquatic Science*, 56:1801–1008.

Homewood, J. (2003) Dissolved organic nitrogen in the Upper Test estuary and River Test. MPhil/PhD transfer report, SOC Graduate School of Ocean and Earth Science, University of Southampton. 47 pp.

Hopkinson, C., L. Cifuentes, D. Burdige, S. Fitzwater, D. Hansell, S. Henrichs, P. Käler, I. Koike, T. Walsh & B. Bergamaschi (1993) DON subgrup report. *Marine Chemistry*, 41:23–36.

Horrigan, S. G., J. P. Montoya, J. L. Nevins, J. J. McCarthy, H. Ducklow, R. Goericke & T. Malone (1990) Nitrogenous nutrient transformation in the spring and fall in the Chesapeake Bay. *Estuarine, Coastal and Shelf Science*, 30:369–391.

Howard, A. G., S. D. W. Comber, D. Kifle, E. E. Antai & D. A. Purdie (1995) Arsenic speciation and seasonal changes in nutrient availability and micro-plankton abundance in Southampton Water, U.K. *Estuarine, Coastal and Shelf Science*, 40:435–450.

Howarth, R. W. (1998) An assesment of human influences on fluxes of nitrogen from the terrestrial landscape to the estuaries and continental shelves of the North Atlantic Ocean. *Nutrient Cycling in Agroecosystems*, 52:213–223.

Howarth, R. W., G. Billen, D. Swaney, A. Townsend, N. Jaworski, K. Lajtha, V. A. Downing, R. Elmgren, N. Caraco, T. Jordan, F. Berendse, J. Freney, V. Kudeyarov, P. Murdoch & Z. Zhao-Liang (1996) Regional nitrogen budgets and riverine N and P fluxes for the drainages to the North Atlantic Ocean: natural and human influences. *Biogeochemistry*, 35:75–139.

Hu, S. & W. O. Smith (1998) The effects of irradiance on nitrate uptake and dissolved organic nitrogen release by phytoplankton in the Ross Sea. *Continental Shelf Research*, 19:971–990.

Humborg, C. (1997) Primary productivity regime and nutrient removal in the Danube Estuary. *Estuarine, Coastal and Shelf Science*, 45:579–589.

Hydes, D. (2000) Nutrients in the Solent. In: Collins, M. & K. Ansell (eds.), Solent Science: a review, pp. 1135–148. Elsevier Science B. V.

Hydes, D. J. (1984) A manual of methods for the continuos flow determination of ammonia, nitrate-nitrite, phosphate and silicate in seawater. Tech. Rep. 177, Institute of Oceanographic Sciences.

Hydes, D. J. & P. N. Wright (1999) SONUS: the Southern Nutrients Study 1995-1997. Tech. Rep. 7, Southampton Oceanography Centre.

Iriarte, A. (1991) Picophytoplankton: Ecological and Physiological Studies in Culture and in Natural Coastal and Estuarine Waters. Ph.D. thesis, Faculty of Science, Department of Ocenography, University of Southampton. 362 pp.

Iriarte, A. (1993) Size-fractionated chlorophyll a biomass and picophytoplankton cell density along a longitudinal axis of a temperate estuary (Southampton Water). *Journal of Plankton Research*, 15(5):485–500.

Iriarte, A. & D. A. Purdie (1994) Size distribution of chlorophyll a biomass and primary production in a temperate estuary (Southampton Water): the contribution of photosynthetic picoplankton. *Marine Ecology Progress Series*, 115:283–297.

Iriarte, A. & D. A. Purdie (in press) Factors controlling the timing of major spring bloom events in a UK south coast estuary. *Estuarine, Coastal and Shelf Science.*

Jaffe, D. A. (1992) The Nitrogen Cycle. In: Butcher, S. S., R. J. Charlson, G. H. Orians & G. V. Wolfe (eds.), Global Biogeochemical Cycles, chap. 12, pp. 263–284. Academic Press LTD.

Jickells, T. D. (1998) Nutrient biogeochemistry of the coastal zone. *Science*, 281:217–222.

Joint, I., A. Rees, E. Malcolm & S. Woodward (2001) Primary production and nitrogen assimilation in the Iberian upwelling in August 1998. *Progress in Oceanography*, 51:303–320.

Jorgensen, N. O. G., N. Kroer, R. B. Coffin & M. P. Hoch (1999a) Relations between bacterial nitrogen metabolism and growth efficiency in an estuarine and an open-water ecosystem. *Aquatic Microbial Ecology*, 18:247–261.

Jorgensen, N. O. G., L. J. Tranvik & G. M. Berg (1999b) Ocurrence and bacterial cycling of dissolved nitrogen in the Gulf of Riga, The Baltic Sea. *Marine Ecology Progress Series*, 191:1–18.

Josefson, A. B. & B. Rasmussen (2000) Nutrient retention by benthic macrofaunal biomass of Danish estuaries: importance of nutrient load and residence time. *Estuarine, Coastal and Shelf Science*, 50:205–216.

Kanda, J., E. A. Laws, T. Saino & A. Hattori (1987) An evaluation of isotope dilution effect from conventional data sets of ^{15}N uptake experiments. *Journal of Plankton Research*, 9(1):79–90.

Kanda, J., D. A. Ziemann, L. D. Conquest & P. K. Bienfang (1990) Nitrate and ammonium uptake by phytoplankton populations during the spring bloom in Auke bay, Alaska. *Estuarine, Coastal and Shelf Science*, 30:509–524.

Karl, D. M. & A. F. Michaels (2001) Nitrogen cycle. In: Steele, S. A., S. A. Thorpe & K. K. Turekian (eds.), Encyclopedia of Ocean Sciences, vol. 4, N-R, pp. 1876–1884. Academic Press, San Diego, CA.

Kérouel, R. & A. Aminot (1997) Fluorometric determination of ammonia in sea and estuarine waters by direct segmented flow analysis. *Marine Chemistry*, 57:265–275.

Kifle, D. & D. A. Purdie (1993) The seasonal abundance of the phototrophic ciliate *Mesodinium rubrum* in Southampton Water, England. *Journal of Plankton Research*, 15(7):823–833.

Kirchman, D. L. (2000) Uptake and regeneration of inorganic nutrients by marine heterotrophic bacteria. In: Kirchman, D. L. (ed.), Microbial Ecology of the Oceans, chap. 9, pp. 261 288. Wiley-Liss, Inc.

Kirchman, D. L. & N. H. Borch (2003) Fluxes of dissolved combined neutral sugars (polysaccharides) in the Delaware estuary. *Estuaries*, 26(894–904).

Kirchman, D. L. & J. H. Rich (1997) Regulation of growth rates by dssolved organic carbon and temperature in the Equatorial Pacific Ocean. *Microbial Ecology*, 33:11–20.

Kirchman, D. L. & P. A. Wheeler (1990) Carbon limitation of ammonium uptake by heterotrophic bacteria in the subartic Pacific. *Limnology and Oceanography*, 35(6):1258–1266.

Kirk, J. T. O. (1994) Light and Photosyntesis in aquatic ecosystems. Cambridge University Press, 2^{nd} ed., 509 pp.

Kudela, R. M. & R. C. Dugdale (2000) Nutrient regulation of phytoplankton productivity in Monterey Bay, California. *Deep-Sea Research Part II*, 47:1023–1053.

Lalli, C. M. & T. M. Parsons (1997) Biological Oceanography: an introduction. Oxford: Butterworth-Heinemann for the Open University, 2^{nd} ed., 314 pp.

Lauria, M. L., D. A. Purdie & J. Sharples (1999) Contrasting phytoplankton distributions controlled by tidal turbulence in an estuary. *Journal of Marine Systems*, 21:189–197.

Laws, E. (1984) Isotope dilution models and the mystery of the vanishing ^{15}N. *Limnology and Oceanography*, 29(2):379–386.

Laws, E. (1985) Analytic models of NH_4^+ uptake and regeneration. *Limnology and Oceanography*, 30(6):1340–1350.

Leakey, R. J. L., P. H. Burkill & M. A. Sleigh (1992) Planktonic ciliates in Southampton Water: abundance, biomass, production, and role in pelagic carbon flow. *Marine Biology*, 114:67–83.

Legendre, L. & M. Gosselin (1996) Estimation of N or C uptake rates by phytoplankton using ^{15}N or ^{13}C: revisiting the usual computational formulae. *Journal of Plankton Research*, 19(2):263–271.

Levin, S. A. (1992) The problem of pattern and scale in ecology. *Ecology*, 73(6):1943–1967.

L'Helguen, S., C. Madec & P. L. Corre (1996) Nitrogen uptake in permanently well-mixed temperate coastal waters. *Estuarine, Coastal and Shelf Science*, 42:803–818.

Libes, S. M. (1992) An introduction to marine biogeochemistry. JOHN WILEY AND SONS, USA, 734 pp.

Lomas, M. W. & P. M. Glibert (1999a) Interactions between NH_4^+ and NO_3^- uptake and assimilation: comparison of diatoms and dinoflagellates at several growth temperatures. *Marine Biology*, 133:541–551.

Lomas, M. W. & P. M. Glibert (1999b) Temperature regulation of nitrate uptake: A novel hypothesis about nitrate uptake and reduction in cool-water diatoms. *Limnology and Oceanography*, 44(3):556–572.

Lomas, M. W., C. J. Rumbley & P. M. Glibert (2000) Ammonium release by nitrogen sufficient diatoms in response to rapid increases in irradiance. *Journal of Plankton Research*, 22(12):2351–2366.

Lomas, M. W., T. M. Trice, P. M. Glibert, D. A. Bronk & J. J. McCarthy (2002) Temporal and spatial dynamics of urea uptake and regeneration rates and concentrations in Chesapeake Bay. *Estuaries*, 25(3):469–482.

Maguer, J. F., S. L'Helguen & P. L. Corre (1996) Sources d'azote pour le phytoplancton dans le système brassé peu profond de la Manche Occidentale. Importance de la production régénérée: bilan annuel. *Journal de la Recherche Océanographique*, 21(3-4):103–108.

Maguer, J. F., S. L'Helguen & P. L. Corre (2000) Nitrogen uptake by phytoplankton in a shallow water tidal front. *Estuarine, Coastal and Shelf Science*, 51:349–357.

McCarthy, J. J., W. R. Taylor & J. L. Taft (1977) Nitrogenous nutrition of the plankton in the Chesapeake Bay. 1. Nutrient availability and phytoplankton preferences. *Limnology and Oceanography*, 22(6):996–1011.

McClelland, J. W. & I. Valiela (1998a) Changes in food web structure under the influence of increased anthropogenic nitrogen inputs to estuaries. *Marine Ecology Progress Series*, 168:259–271.

McClelland, J. W. & I. Valiela (1998b) Linking nitrogen in estuarine producers to land-derived sources. *Limnology and Oceanography*, 43(4):577–585.

Meybeck, M. (1982) Carbon, nitrogen, and phosphorus transport by world rivers. *American Journal of Science*, 282:401–450.

Meyer-Reil, L. A. & M. Köster (2000) Eutrophication of marine waters: effects on benthic microbial communities. *Marine Pollution Bulletin*, 41(1-6):255–263.

Middelburg, J. J., G. Kaver, J. Nieuwenhuize & T. Vlug (1995) Carbon and nitrogen cycling in intertidal sediments near Doel Scheldt estuary. *Hydrobiologia*, 311:57–69.

Middelburg, J. J. & J. Nieuwenhuize (2000a) Nitrogen uptake by heterotrophic bacteria and phytoplankton in the nitrate-rich Thames estuary. *Marine Ecology Progress Series*, 203:13–21.

Middelburg, J. J. & J. Nieuwenhuize (2000b) Uptake of dissolved inorganic nitrogen in turbid, tidal estuaries. *Marine Ecology Progress Series*, 192:79–88.

Millero, F. J. (1979) The thermodynamics of the carbonate system in seawater. *Geochimica et Cosmochimica Acta*, 43:1651–1661.

Millero, F. J., R. H. Byrne, R. Wanninkhof, R. Feely, T. Clayton, P. Murphy & M. Lamb (1993) The internal consistency of CO_2 measurements in the equatorial Pacific. *Marine Chemistry*, 44:269–280.

Morel, F. M. M. (1983) Principles of aquatic chemistry, chap. 4, Acids and Bases: alkalinity and pH in natural waters, pp. 127–177. JOHN WILEY AND SONS.

Morris, A. W., J. I. Allen, R. J. M. Howland & R. G. Wood (1995) The estuary plume zone: source or sink for land-derived nutrient discharges? *Estuarine, Coastal and Shelf Science*, 40:387–402.

Mortazavi, B., R. L. Iverson, W. Huang, F. G. Lewis & J. M. Caffrey (2000a) Nitrogen budget of Apalachicola Bay, a bar-built estuary in the northeastern Gulf of Mexico. *Marine Ecology Progress Series*, 195:1–114.

Mortazavi, B., R. L. Iverson, W. M. Landing & W. Huang (2000b) Phosphorus budget of Apalachicola Bay: a river-dominated estuary in the northeastern Gulf of Mexico. *Marine Ecology Progress Series*, 198:33–42.

Mulholland, M. R. & D. G. Capone (2000) The nitrogen physiology of the marine N_2-fixing cyanobacteria *Trichodesmium* spp. *Trends in Plant Science*, 5(4):418–153.

Mulvaney, R. L. (1993) Mass Spectrometry. In: Knowles, R. & T. H. Blackburn (eds.), Nitrogen Isotope Techniques, chap. 2, pp. 11–57. Academic Press, INC.

Mulvenna, P. & G. Savidge (1992) A modified manual method for the determination of urea in seawater using diacetylmonoxime reagent. *Estuarine, Coastal and Shelf Science*, 34:429–438.

Murphy, J. & J. P. Riley (1962) A modified single solution method for the determination of phosphate in natural waters. *Analytical Chimica Acta*, 27:31–36.

Nees, J. C., R. C. Dugdale, V. A. Dugdale & J. Goering (1962) Nitrogen metabolism in lakes. I. Measurements of fixation with ^{1}5N. *Limnology and Oceanography*, 7:163–169.

Newell, B. S., B. Morgan & J. Cundy (1967) The determination of urea in seawater. *Journal of Marine Research*, 25:201–202.

Nixon, S. W. (1995) Coastal marine eutrophicaton: a definition, social causes, and future concerns. *Ophelia*, 41:199–219.

Nixon, S. W., J. W. Ammeran, L. P. Atkinson, V. M. Berounsky, G. Billen, W. C. Boicourt, W. R. Boynton, T. M. Church, D. M. Ditoro, R. Elmgren, J. H. Garber, A. E. Giblin, R. A. Jahnke, N. J. P. Owens, M. E. P. Pilson & S. P. Seitzinger (1996) The fate of nitrogen and phosphorus at the land-sea margin of the North Atlantic Ocean. *Biogeochemistry*, 34:141–180.

Nixon, S. W., S. L. Granger & B. L. Nowicki (1995) An assessment of the annual mass balance of carbon, nitroegn, and phosphorus in Narragansett Bay. *Biogeochemistry*, 31:15–61.

Owens, J. P. & A. P. Rees (1989) Determination of nitrogen-15 at sub-microgram levels of nitrogen using automated continuous-flow isotope ratio mass spectrometry. *Analyst*, 114:1655–1657.

Owens, N. J. P. (1988) Rapid and total automation of shipboard ^{15}N analysis: examples from the North Sea. *Journal of Experimental Marine Biology and Ecology*, 122:163–171.

Paasche, E. & S. Kristiansen (1982) Nitrogen nutrition of the phytoplankton in the Oslofjord. *Estuarine, Coastal and Shelf Science*, 14:237–249.

Pakulski, J. D., R. Benner, T. Whitledge, R. Amon, B. Eadie, L. Cifuentes, J. Ammerman & D. Stockwell (2000) Microbial metabolism and nutrient cycling in the Mississippi and Atchafalaya river plumes. *Estuarine, Coastal and Shelf Science*, 50:173–184.

Parsons, T. R., Y. Maita & C. M. Lalli (1984) A manual of chemical and biological methods for seawater analysis. Pergamon, Oxford, 173 pp.

Pennock, J. R. (1987) Temporal and spacial variability in phytoplankton ammonium and nitrate uptake in the Delaware estuary. *Estuarine, Coastal and Shelf Science*, 24:841–857.

Peperzak, L. (1993) Daily irradiance governs growth rate and colony formation of *Phaeosystis* (Prymnesiophyceae). *Journal of Plankton Research*, 15(7):809–821.

Peperzak, L., F. Colin, W. W. C. Gieskes & C. H. Peeters (1998) Development of the diatom Phaeosystis spring bloom in the Dutch coastal zone of the North Sea: the silicon depletion versus the daily irradiance threshold hypothesis. *Journal of Plankton Research*, 20(3):517–537.

Pernetta, J. C. & J. D. Milliman (1995) Land-Ocean Interactions in the Coastal Zone. Implementation Plan. Tech. Rep. 33, IGBP Stockholm.

Preston, T. & N. J. P. Owens (1983) Interfacing an automatic elemental analyser with an isotope ratio mass spectrometer: the potential for fully automated total nitrogen and nitrogen-15 analysis. *Analyst*, 108:971–977.

Proença, L. (1994) Phytoplankton biomass, organic matter sedimentation, and nutrient remineralization in a macrotidal estuary- Southampton Water. Ph.D. thesis, University of Southampton.

Raimbault, P., G. Slawyk & N. Garcia (2000) Comparison between chemical and isotopic measurements of biological nitrate utilisation: further evidence of low new-production levels in the Equatorial Pacific. *Marine Biology*, 136:1147–1155.

Raven, J. A. (2001) Primary production processes. In: Steele, J. H., S. A. Thorpe & K. K. Turekian (eds.), Encyclopedia of Ocean Sciences, vol. 4, N-R, pp. 2284–2288. Academic Press, San Diego, CA.

Rendell, A. R., T. M. Horrobin, T. D. Jickells, H. M. Edmunds, J. Brown & S. J. Malcolm (1997) Nutrient cycling in the Great Ouse Estuary and its impact on nutrient fluxes to The Walsh, England. *Estuarine, Coastal and Shelf Science*, 45:653–668.

Richardson, K. & B. B. Jorgensen (1996) Eutrophication: definition, history and effects. In: Jorgensen, B. B. & K. Richardson (eds.), Eutrophication in coastal marine ecosystems, Coastal and Estuarine Studies, 52., pp. 1–19. Washington, DC: American Geophysical Union.

Riley, G. A. (1957) Phytoplankton of the North Central Sargasso Sea. *Limnology and Oceanography*, 24(3):252–270.

Rivkin, R. B. & M. R. Anderson (1997) Inorganic limitation of oceanic bacterioplankton. *Limnology and Oceanography*, 42(4):730–740.

Roche, J. L. (1983) Ammonium regeneration: its contribution to phytoplankton nitrogen requirements in a eutrophic environment. *Marine Biology*, 75:231–240.

Roy, R. N., L. N. Roy, K. M. Vogel, C. Porter-Moore, T. Pearson, C. E. Good, F. J. Millero & D. M. Campbel (1993) The dissociation constants of carbonic acid in seawater at salinities 5 to 45 and temperatures 0 to 45°C. *Marine Chemistry*, 44:249–267.

Roy, R. N., L. N. Roy, K. M. Vogel, C. Porter-Moore, T. Pearson, C. E. Good, F. J. Millero & D. M. Campbel (1994) Erratum: The dissociation constants of carbonic acid in seawater at salinities 5 to 45 and temperatures 0 to 45°C. *Marine Chemistry*, 45:337.

Schlesinger, W. H. (1997) Biogeochemistry; an analysis of global change. Academic Press, USA, 2^{nd} ed., 588 pp.

Seitzinger, S. P. (1988) Denitrification in freshwater and coastal marine ecosystems: ecological and geological significance. *Limnology and Oceanography*, 33(4-2):702–724.

Seitzinger, S. R. & R. W. Sanders (1997) Contribution of dissolved organic nitrogen from rivers to estuarine eutrophication. *Marine Ecology Progress Series*, 159:1–12.

Shalovenkov, N. (2000) Scales of ecological processes and anthropogenous loads on the coastal ecosystems of the Black Sea. *Estuarine, Coastal and Shelf Science*, 50:11–16.

Sharp, J. H. (2002) Analytical methods for total DOM pools. In: Hansell, D. A. & C. A. Carlson (eds.), Biogeochemistry of marine dissolved organic matter, chap. 2, pp. 35–58. Academic press. USA.

Sharp, J. H., K. R. Rinker, K. B. Savidge, J. Abell, J. Y. Benaim, D. Bronk, D. J. Burdige, G. Cauwet, W. Chen, M. D. Doval, D. Hansell, C. Hopkinson, G. Kattner, N. Kaumeyer, K. J. McGlathery, J. Merriam, N. Morley, K. Nagel, H. Ogawa, C. Pollard, M. Pijo-Pay, P. Raimbault, R. Samborotto, S. Seitzinger, G. Spyres, F. Tirendi, T. W. Walsh & C. S. Wong (2002) A preliminary methods comparison for measurement of dissolved organic nitrogen in seawater. *Marine Chemistry*, 78:171–184.

Sharples, J. (2000) Water circulation in Southampton Water and the Solent. In: Collins, M. & K. Ansell (eds.), Solent Science: a review, pp. 45–53. Elsevier Science B. V.

Shaw, J., C. Charon, D. A. Purdie & A. P. Rees (1998a) Impacts of phytoplankton activity on dissolved nitrogen fluxes in the tidal reaches and estuary of the Tweed, UK. *Marine Pollution Bulletin*, 37(3-7):280–294.

Shaw, J., D. A. Purdie, P. S. D. Frietas, A. P. Rees & I. Joint (1998b) Nutrient uptake in a highly turbid estuary (the Humber, United Kingdom) and adjacent coastal waters. *Estuaries*, 21(4A):507–517.

Sigman, D. M. & K. L. Casciotti (2001) Nitrogen isotopes in the ocean. In: Steele, J. H., S. A. Thorpe & K. K. Turekian (eds.), Encyclopedia of Ocean Sciences, 1884–1894. Academic Press, San Diego, CA.

Slawyk, G., Y. Collos & J.-C. Auclair (1977) The use of ^{13}C and ^{15}N isotopes for the simultaneous measurement of carbon and nitrogen turnover rates in marine phytoplankton. *Limnology and Oceanography*, 22:925–932.

Slawyk, G., Y. Collos & J.-C. Auclair (1979) Reply to comment by Fisher et al. *Limnology and Oceanography*, 24(3):595–597.

Slawyk, G. & P. Raimbault (1995) Simple procedure for simultaneous recovery of dissolved inorganic and organic nitrogen in ^{15}N-tracer experiments and improving the isotopic mass balance. *Marine Ecology Progress Series*, 124:289–299.

Slawyk, G., P. Raimbault & N. Garcia (1998) Measuring gross uptake of ^{15}N-labeled nitrogen by marine phytoplankton without particulate matter collection: evidence of low ^{15}N losses to the dissolved organic nitrogen pool. *Limnology and Oceanography*, 43(7):1734–1739.

Slawyk, G., P. Raimbault & N. Garcia (2000) Use of ^{15}N to measure dissolved organic nitrogen release by marine phytoplankton (reply to comment by Bronk and Ward). *Limnology and Oceanography*, 45(8):1884–1886.

Smith, V. H., G. D. Tilman & J. C. Nekola (1999) Eutrophication: impacts of excess nutrient inputs on freshwater, marine, and terrestrial ecosystems. *Environmental Pollution*, 100:179–196.

Solorzano, L. (1969) Determination of ammonia in natural waters by the phonolhypochlorite method. *Limnology and Oceanography*, 14(5):799–801.

Stumm, W. & J. J. Morgan (1996) Aquatic Chemistry; chemical equilibria and rates in natural waters. JOHN WILEY AND SONS, INC, 3rd ed., 1022 pp.

Suttle, C. A., J. A. Fuhrman & D. G. Capone (1990) Rapid ammonium cycling and concentration-dependent partitioning of ammonium and phosphate: Implications for carbon transfer in planktonic communities. *Limnology and Oceanography*, 35:424–432.

Tremblay, J. E., L. Legendre, B. Klein & J. C. Therriault (2000) Size-differential uptake of nitrogen and carbon in a marginal sea (Gulf of St. Lawrence, Canada): significance of diel periodicity and urea uptake. *Deep-Sea Research Part II*, 47:489–518.

Tyrrell, T. (2001) Redfield Ratio. In: Steele, J. H., S. A. Thorpe & K. K. Turekian (eds.), Encyclopedia of Ocean Sciences, vol. 4, N-R, pp. 2377–2387. Academic Press, San Diego, CA.

Utermöhl, H. (1958) Zur Vervollkommnung der Phytoplankton-Methodik. *Mitteilungen-Internationale Vereiningung für Limnologie*, 9:1–38.

Vitousek, P. M. (1994) Beyond global warming: ecology and global change. *Ecology*, 75(7):1861–1876.

Vitousek, P. M., J. D. Aber, R. W. Howarth, G. E. Likens, P. A. Matson, D. W. Schindler, W. H. Schlesinger & D. G. Tilman (1997a) Human alteration of the global nitrogen cycle: sources and consequences. *Ecological Applications*, 7(3):737–750.

Vitousek, P. M., H. A. Mooney, J. Lubchenco & M. Melillo (1997b) Human domination of earth's ecosystems. *Science*, 277:494–499.

Walsh, T. W. (1989) Total dissolved nitrogen in seawater: a new High-temperature combustion method and a comparison with Photo-oxidation. *Marine Chemistry*, 26:295–311.

Ward, B. B. & D. A. Bronk (2001) Net nitrogen uptake and DON release in surface waters: importance of trophic interactions implied from size fractionation experiments. *Marine Ecology Progress Series*, 219:11–24.

Watts, L. J. & N. J. P. Owens (1999) Nitrogen assimilation and the *f*-ratio in the northwestern Indian Ocean during an intermonsoon period. *Deep-Sea Research Part II*, 46:725–743.

Weiss, R. F. (1974) Carbon dioxide in water and seawater: the solubility of a non-ideal gas. *Marine Chemistry*, 2:203–215.

Welschmeyer, N. A. (1994) Fluorometric analysis of chlorophyll *a* in the presence of chlorophyl *b* and pheopigments. *Limnology and Oceanography*, 29(8):1985–1992.

Weston, K., T. D. Jickells, L. Fernand & E. R. Parker (2004) Nitrogen cycling in the southern North Sea: consequences for total nitrogen transport. *Estuarine, Coastal and Shelf Science*, 59:559–573.

Wheeler, P., P. M. Glibert & J. J. McCarthy (1982) Ammonium uptake and the incorporation by Chesapeake Bay phytoplankton:short term uptake kinetics. *Limnology and Oceanography*, 27(6):1113–1128.

Wood, E. D., F. A. J. Armstrong & F. A. Richards (1967) Determination of nitrate in seawater by cadmium copper reduction to nitrite. *Journal of Marine Biological Association UK*, 47:23–31.

Wright, P. N., D. J. Hydes, M. L. Lauria, J. Sharples & D. A. Purdie (1997) Data buoy measurements of phytoplankton dynamics in Southampton Water, UK, a temperate latitude estuary with high nutrient inputs. *Deutsches Hydrographisches Zeitschrift*, 49:201–210.

Zehr, J. P., E. J. Carpenter & T. A. Villareal (2000) New perspectives on nitrogen-fixing microorganisms in tropical and subtropical oceans. *Trends in Microbiology*, 8:68–73.

Zehr, J. P., M. T. Mellon & S. Zani (1998) New nitrogen-fixing microorganisms detected in oligotrophic ocean by the amplification of nitrogenase (*nifH*) genes. *Applied and Environmental Microbiology*, 64:3444–3450.

Zehr, J. P. & B. B. Ward (2002) Nitrogen cycling in the ocean: new perspectives on processes and paradigms. *Applied and Environmental Microbiology*, 68(3):1015–1024.

Zehr, J. P., J. B. Waterbury, P. J. Turner, E. Omoregie, G. F. Steward, A. Hansen & D. M. Karl (2001) Unicellular cyanobacteria fix N_2 in the subtropical North Pacific Ocean. *Nature*, 412:635–638.